PREDICTIVE AND ADAPTIVE EXTREMAL CONTROL

BY

I. KIMMEL

SEPTEMBER 1976

Presented to the Faculty of Engineering of the University of Cape Town in fulfilment of the M.SC. (Eng.) degree.

SYNOPSIS

The time-optimal predictive control strategy for second order relay or bang-bang control systems is investigated along with modifications of this strategy for third order systems.

One basis of this strategy is the utilization of a model, a replica of the plant run in a fast-time mode so as to obtain the future output of the plant under the present input. Based upon these measurements, corrections to the plant may be implemented to achieve the desired response.

The concept of the fast model is a useful one in that it falls into the synthesis of the more general time-optimal trajectory and switching functions for various second, third and higher order plants. However the difficulties in providing the exact time-optimal control for these plants result in the generation of acceptable sub-optimal and near time-optimal strategies. The nature of plant sensitivity, parameter variation and identification are investigated as well as a novel self-adoptive controller which dispenses with the identification phase but

identifies a certain surface in the state space and establishes a stable sub-optimal control strategy. These control techniques are applied to a small DC motor with responses close to time-optimal.

ACKNOWLEDGEMENTS

To Mr. S.G. McLaren, my supervisor for his guidance, encouragement and patience.

To the Council for Scientific and Industrial Research for their research grant.

To the University of Cape Town for its facilities and general assistance.

SUMMARY

The technique of predictive control offers a heuristic approach to the theory and application of Extremal or Relay Control also called Bang-Bang control on second and higher order plants and processes. The very nature of extremal control implies maximal effort in one direction or the other and this progresses to the notion of minimal time or time-optimal control strategy.

The basic idea of the fast model predictive control technique can be briefly described as follows:

A fast model is set up which corresponds to the plant, but with all time constants reduced by some factor (typically 50 to 1 000). At the start of each computation, the state of the model is set to correspond to the present state of the plant and the model is then allowed to run, predicting the future behaviour of the plant under some given input. From this behaviour, a logical decision is made, determining the required present plant input, and the model is then reset to commence iteration.

Plants which take the form of a number of cascaded integrators, where the input to the first integrator is limited in magnitude are considered in this paper. From Pontryagin's

maximum principle[2] it may be shown that, for time-optimal control of such a system, the input must always take on an extreme value at either the positive or negative limit. Since for time-optimal control the input to the plant is bang-bang, the input to the fast model will also be bang-bang and the purpose of the controller is to answer the question, 'In which direction must full plant drive be applied now?'

The performance of the predictive control system is dependent on the accuracy with which the fast model represents the plant. When the parameters of the plant (gain, time-constants) vary appreciably with time both in the transient and steady state conditions, the use of a fixed parameter model results in a non time-optimal response. However, by employing an adaptive scheme in which the parameters of the plant are continuously identified and the parameters of the fast model are continuously updated, the response remains generally time-optimal.

The method used to achieve this adaptation is a scheme of a type known in the literature[3] as 'model reference adaptive systems'.

This scheme can be briefly described as follows:

The desirable characteristics of the plant are specified in a

reference model and the input signal or the controllable parameters of the plant are adjusted, continuously or discretely, so that its response will duplicate that of the model as closely as possible. The plant transient state need not be identified and hence a fast adaptation can be achieved.

The above paragraph is specific for what is called in the literature[3,4] 'adaptive control', viz. getting the plant to behave like the pre-determined model. However in this thesis the dual, viz. that of 'Identification' is utilized. The identification problem consists in specifying a suitable model and in developing a scheme for dynamically adjusting its parameters so that they converge to those of the plant.

The problem of identification, in the model reference framework, is essentially that of adaptive control. In this case, the roles of the plant and model are interchanged so that the parameters of the model track those of the plant. While the two problems are mathematically equivalent, it is worth noting that the identification problem is somewhat simpler since the structure of the model (whose parameters are adjusted) unlike that of the plant, can be chosen freely by the designer.

Put simply, the plant consists of a set of partially known parameters and the model consists of a set of initial

parameters. The difference between the system's output and the model's output is called the identification or tracking error and is used as a measure of the 'goodness' of the model. The parameter adjustment procedures are such that they will minimize the magnitude of this error and in many cases the error approaches zero and the model parameters then match those of the plant.

Two other techniques are described in this paper both concerned with optimal and sub-optimal relay or bang-bang control of second, third and higher order systems.

The adaptive relay control developed by A.S.I. Zinober[5,24] is a strategy that does not organize itself through adaptive correction, i.e. it dispenses with the parameter identification phase but identifies a certain surface[+] in the state-space. This surface is associated with sliding motion[++] and is found by rotating a switching hyperplane[+++] in the state space whenever the system is in a sliding mode. The controller is easily implemented and the resulting system response is close to the desired time-optimal trajectory.

[+] In the case of a second order system the surface is a curve

++ Sliding motion is also referred to as chatter, gliding and after-endpoint motion

+++ The hyperplane is a line in the case of a second-order system

The nominal-$\underline{y}$ control developed by E.P. Ryan[6,31] with predictive strategy is a method for optimal and sub-optimal relay control by state-variable transformation which permits the application of relatively simple time-optimal feedback control laws for the double and triple intergrator plants to a wide range of more general second and third order plants having real non positive eigenvalues. The method, which is based on a state-variable transformation technique, gives near time-optimal control for certain plants with eigenvalues in a simple ratio, for other cases the control is sub-optimal but yields settling times close to time-optimal. In this way one may avoid the difficulty of synthesizing the logarithmic, exponential or other complicated functions of state variables which are generally present in the exact time optimal control laws (where known) for such plants.

By combining the properties of the $\underline{y}$ controller with a fast model, a predictive strategy may be generated which gives near time-optimal control for third and fourth order plants. It is also shown that the $\underline{y}$ controller is to some degree

insensitive to plant parameter changes and investigation has shown it to be practical for third-order plants with complex eigenvalues.

Finally the approach taken in this thesis is heuristic and of a practical nature.

Mathematical derivations and proofs where required are featured in the text and the appendix but stress is put on the physical realization of the various techniques especially the use of a digital computer - analogue computer combination thus avoiding only pure digital simulations.

Furthermore the control of a DC motor by both analogue and digital computer derived control laws underscored the application of these techniques.

NOMENCLATURE

A	plant coeffecient matrix
A^T	transpose of A
a	nominal plant gain parameter
B	plant input or driving matrix
b	actual plant gain parameter
$e, \dot{e}, \ldots$	general system output or state error, error rate etc.
H	Hamiltonian
I	identity matrix
J	performance criterion
K_p	plant gain
K_m	model gain
n	order of system, number of variations of samples
p	differential operator $\frac{d}{dt}$
P_i	ith co-state variable
P, Q	positive definite symmetric matrices
q	control variable
r	reference
s	Laplace transform variable
T	time constant or lower triangular matrix
t	time
u	input or control signal (scalar)
$\underline{u}$	input or control vector
V	Liapunov function

$\underline{y}$	transformed state vector
$\underline{x}$	state vector
$\underline{x}^T$	$\underline{x}$ transposed
α_p	plant lag (inverse of plant time constant)
Γ	adaptive loop gain
γ	adaptive loop damping factor
δ, ϵ	small positive numbers
λ	auxiliary variables
λ_i	ith eigenvalue
τ	fast model time or speeded-up time
ϕ	switching function

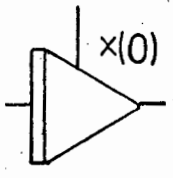

integrator with initial condition

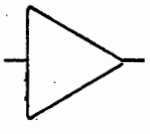

inverter or summer

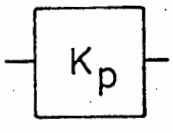

gain element

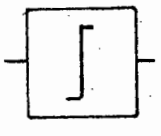

ideal relay (signum function)

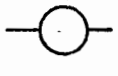

potentiometer

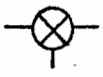

summing junction

Note: Not all the symbols used appear in the above list. Unless specifically defined to have other meanings, all the symbols used take on the above nomenclature.

CONTENTS

CHAPTER 1

INTRODUCTION

This chapter (and the introductions to the various other chapters) is devoted to the theory behind time-optimal control strategies, and therefore, is concerned with the underlying mathematical analysis and development for these strategies. The whole essence of time-optimality is the utilization of minimal-time techniques offered by the calculus of variations, the Hamiltonian, and Pontryagin's maximum principle for a class of amplitude limited input signals. It is felt that without some understanding of this theoretical background, it would be difficult to derive meaningful and useful results from the strategies examined in this thesis.

1.1 Investigations

In this thesis the step function relay control of single-input, single output nominally linear plants with some parameter uncertainty are considered. Noise disturbances are assumed absent or of secondary importance.

The input to the relay is a function of the state variables of the fast model or plant, and controllers

are designed to yield a near-minimal value of the settling time, i.e. the time for the state trajectory to go from a set of initial conditions to the desired end point.

Cases are considered when the plant parameters (by plant parameters we refer to the plant gain and time constants) are known but changes in these parameters occur during the transient motion and steady state. To realise the time-optimal controller we need to identify the plant dynamics, to design the time-optimal controller when our ignorance of the plant structure is minimal and to implement the optimal-control laws.

There are difficulties in applying these procedures. The identification techniques require a finite computing time which for certain plants might be insufficient for time-optimal performance. The time-optimal switching function whether synthesized by a fast model or generated directly from the plant parameters and state co-ordinates, is usually a non-linear and mathematically unwieldy function to manipulate. Even for certain second order plants, the derivation of the synthetic fast model equations are complicated and require excessive computing time for their execution. The effort required to execute the exact time-optimal

control laws are often not justified and several methods of sub-optimal control are therefore employed.

The problem of plant parameter variations on systems with nominally time-optimal controllers, i.e. the time-optimal controller calculated for a nominal set of plant parameters, is one of great importance, and research workers[7] in this field have shown that for higher order systems, remarkably small deviations of the plant parameter from the nominal value, give greatly increased settling time and even instability. Hence a robust controller, insensitive to plant parameter variations and disturbances but able to maintain its design conditions, or a self-adapting controller which requires neither the precise plant dynamic structure or identification of the plant parameters, or a rapid identification scheme to maintain a closely matched plant to model pair, must be utilized and simple to implement, if the desired design goals are to be attained.

For all these cases, the resulting state trajectory was found to be close and in some cases equal to the time-optimal trajectory, and the increase in settling time over the optimal settling time is small.

1.2. The System

The control systems to be considered are shown in Fig. 1.2.1 and Fig. 1.2.2.

The plant has the transfer function

$$G(p) = \frac{1}{b} \cdot \frac{1}{g(p)} \qquad (1.2.1)$$

between its (scalar) input u(t) and its output x_1 ; g(p) is a polynomial with degree n, and b(b > 0) is the plant gain parameter for this case.

The nominal plant has the transfer function

$$G(p) = \frac{1}{a} \cdot \frac{1}{g(p)} \qquad (1.2.2)$$

where a (a > 0) is the nominal plant gain parameter.

Note: In more conventional terms, the nominal plant gain $Kp(nom) = \frac{1}{a}$, while the actual plant gain $K_p = \frac{1}{b}$ as defined.

The relay has an (scalar) input ϕ and output u which satisfy

$$u = \text{sgn}(\phi) \qquad (\phi \neq 0) \qquad (1.2.3)$$

$$= \frac{\phi}{|\phi|}$$

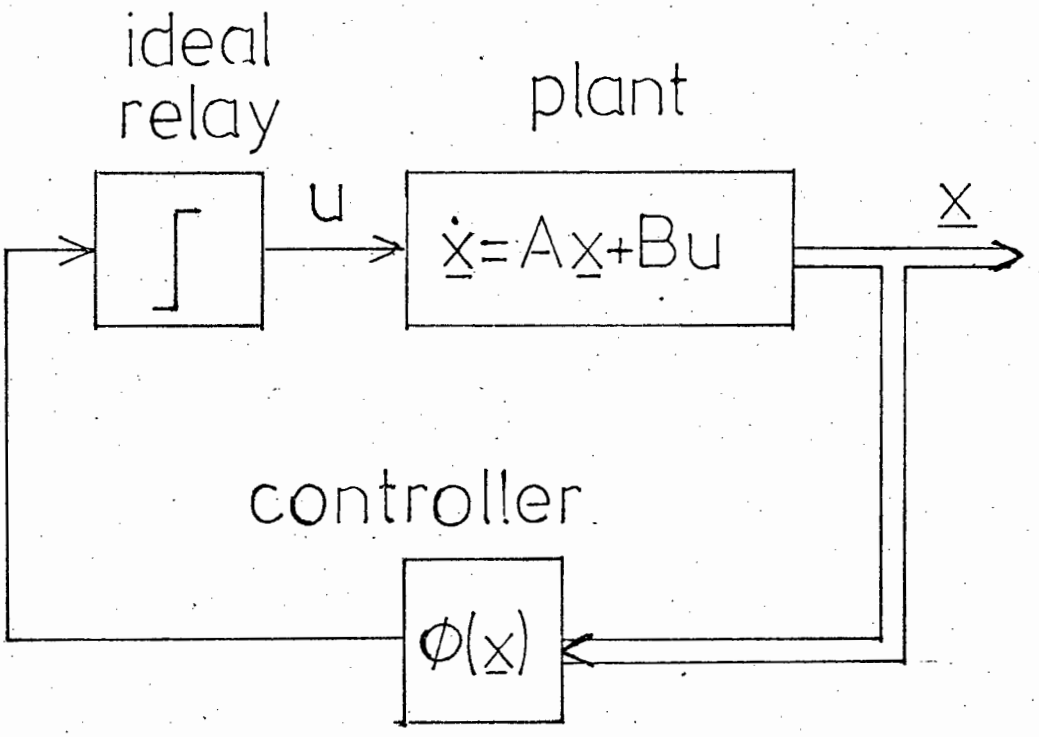

FIGURE: 1.2.1 VECTOR FEEDBACK CONTROL SYSTEM

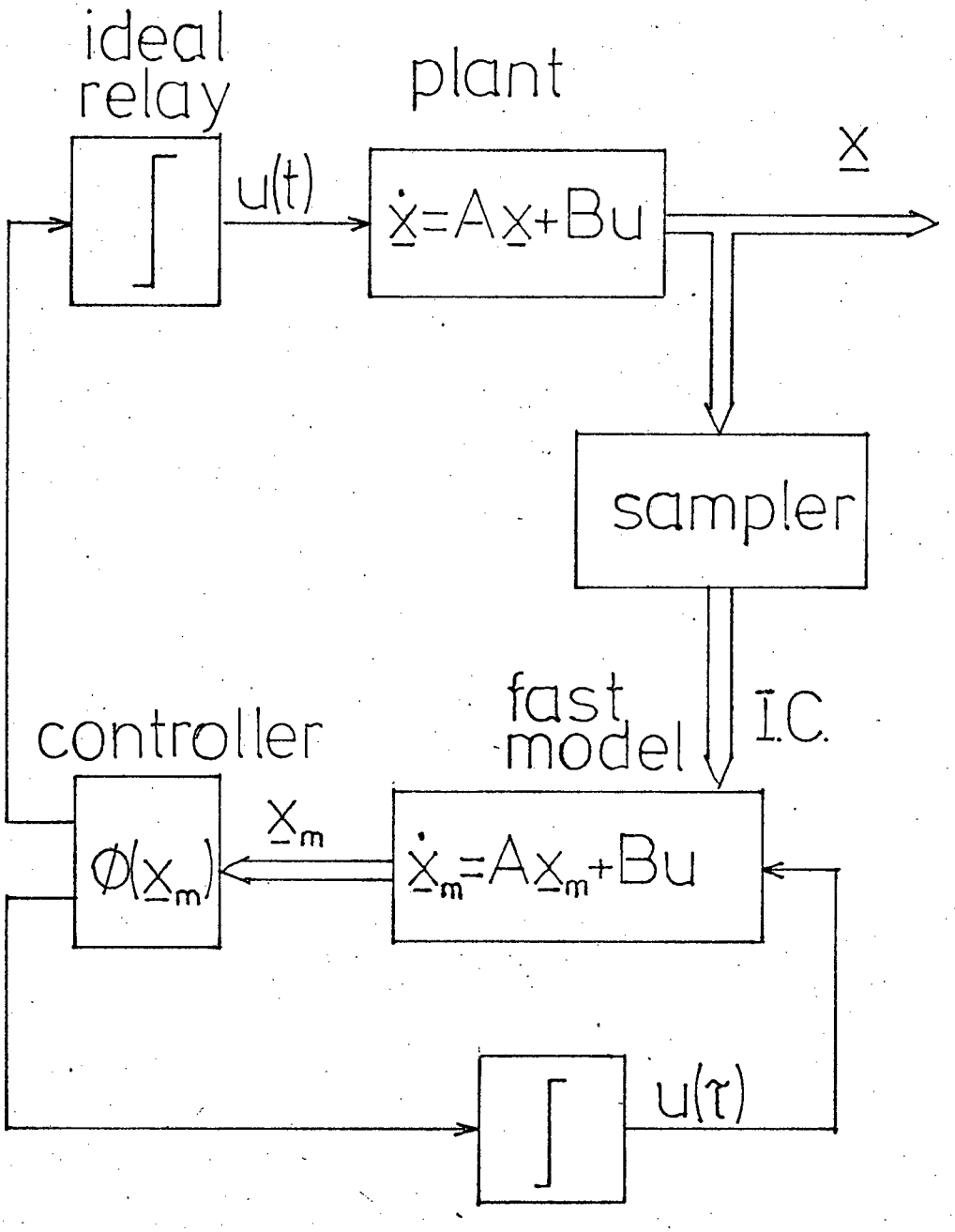

FIGURE 1.2.2 FAST MODEL PREDICTIVE CONTROL SYSTEM

The state co-ordinates are

$$x_1, x_2 = \dot{x}_1 \ldots \quad , x_n = \frac{d^{n-1}}{dt^{n-1}} \cdot x_1 \quad (1.2.4)$$

Using matrix notation the plant can be described by the differential equations

$$\dot{\underline{x}} = A\,\underline{x} + Bu \quad (\,|u| \leq 1) \qquad (1.2.5)$$

where A is an (n x n) system matrix and B and $\underline{x}$ are n-vectors.

The control which minimises the time of transition from the initial condition to the desired state, either the state origin or error state origin is of the form

$$u(t) = \text{sgn}\ \phi\ (x_1, x_2, \ldots, x_n, b) \qquad (1.2.6)$$

where $\phi\ (x_1, x_2, \ldots, x_n, b)$ is the time-optimal switching function. The system with the control

$$u(t) = \text{sgn}\ \phi\ (x_1, x_2, \ldots, x_n, a) \qquad (1.2.7)$$

is simultaneously investigated where

$\phi\ (x_1, x_2, \ldots, x_n, a)$ is the time-optimal switching function of the nominal plant (1.2.2)

The boundary between the region of the state space where $\phi\ (\underline{x}, a)$ is negative and the region where $\phi\ (\underline{x}, a)$ is positive is called the switching surface and is given by

$$\phi\ (x_1, x_2, \ldots, x_n, a) = 0 \qquad (1.2.8)$$

(in the case of second order systems the switching

surface is a switching curve or switching line).

The Laplace transformation enables us to express the transfer function of the nominal plant as

$$Gp(s) = \frac{1}{a(s^n + \alpha_{n-1}s^{n-1} + \cdots + \alpha_1 s + \alpha_0)} \quad (1.2.9)$$

between its scalar input u and output x_1.

In this thesis attention will be focussed on second order and third order systems and the eigenvalues of the matrix A (or the poles of $G_p(s)$) will be assumed non positive.

With the assumption that the system (1.2.5) is controllable, there is no loss in generality in assuming A and B to be of the canonical forms

$$A = \begin{bmatrix} 0 & 1 & \cdots & 0 \\ 0 & 0 & \cdots & \\ \cdots & \cdots & \cdots & \\ \cdots & \cdots & \cdots & \\ \cdots & \cdots & 1 & 0 \\ 0 & 0 & \cdots & 0 \ 1 \\ -\alpha_0 & -\alpha_1 & \cdots & -\alpha_{n-1} \end{bmatrix} \qquad B = \begin{bmatrix} 0 \\ 0 \\ \cdot \\ \cdot \\ \cdot \\ \frac{1}{a} \end{bmatrix} \quad (1.2.10)$$

Where á = a for the nominal plant gain parameter or á = b for the actual plant gain parameter corresponding to (1.2.5)

1.3. Basis for Extremal Control

More than 40 years ago[8] relay switched controls became common and led to the concept of optimal bang-bang control of a process with bounded inputs described by the differential equations

$$\frac{dx_i}{dt} = f_i\,(x_1, x_2, \ldots, x_n, u_1, \ldots, u_r)$$

$$(i = 1,2, \ldots, n) \qquad (1.3.1)$$

where $\underline{x} \triangleq (x_1, x_2, \ldots, x_n)^T$ defines the process state and $u_i(t)$ comprises the control inputs.

This was to a great degree intuitive as for example to get a motor to run up as fast as possible from rest; maximum current had to be applied to achieve this condition and conversely, to return it to rest. Mathematical optimal-control theory showed that under certain conditions, the bang-bang control, $u_i = 1$ or -1, optimises a performance criterion: $\int f(\underline{x}, \underline{u})dt$, which can represent the time, energy and mean square error over a manoeuvre.

Pontryagin's maximum principle[2] is used to study the optimal control of systems in which there is a constraint or limitation of some kind on the instantaneous value of the control input.

Suppose we consider a system whose behaviour is governed by the equation (1.3.1)

The typical problem which can be solved by the maximum principle is one in which the control vector $\underline{u}$, with components $u_1, u_2, \ldots, u_r$ is constrained so as to lie in a closed bounded region U in the r-dimensional vector space of the control inputs.

For example for r=2, a closed bounded region U may be specified by the inequality

$$u^2_1 + u^2_2 \leq R^2 \qquad (1.3.2)$$

The region U in this case is illustrated in Fig. 1.3.1 and the control vector $\underline{u}$ is constrained to lie in or on the boundary of the circle as shown.

In this thesis we consider U to be fixed and any control vector $\underline{u}$ which satisfies the requirement that $\underline{u}$ lies in the closed bounded region U at every instant will be called an admissible control input.

Pontryagin's maximum principle can be considered as an extension or generalization of the calculus of variations to enable us to take account of systems whose input signals have constraints of certain types.

In order to apply the maximum principle, the Hamiltonian formulation in the calculus of variations is utilized. The derivation of the Hamiltonian is found in the Appendix A.1.

To illustrate the use of the maximum principle we have the following problem:

'How do we find the optimal-control vector u(t) applied to a system whose differential equations are in the form of equations 1.3.1 in order to achieve a transition of the system state from a given initial state $\underline{x}^0$ at a time to a specified point $\underline{x}^1$ in <u>minimum time</u> ?'

The performance criterion (a specified functional) can be expressed as

$$J = \int_{to}^{ti} fo\ (\underline{x},\ \underline{u})\ dt \qquad (1.3.3)$$

provided that the integrand is defined as

$$fo\ (\underline{x},\ \underline{u}) = 1 \qquad (1.3.4)$$

The Hamiltonian H, as defined in Appendix A1 therefore becomes

$$H = p_o + \sum_{i=1}^{n} p_i\ f_i\ (\underline{x},\ \underline{u}) \qquad (1.3.5)$$

where the notation p_o, p_i, ..., p_n refer to the auxiliaries variables

The p notation is more commonly used in the study of the maximum principle than the λ notation.

For equation 1.3.5 p_o is constant and is equal to -1. We define a new Hamiltonian H, by omitting p_o in equation 1.3.5 and we obtain the relationship

$$H = \sum_{i=1}^{n} p_i f_i(\underline{x}, \underline{u}) \qquad (1.3.6)$$

The differential equations governing the behaviour of the auxiliary variables and the system state variables can now be written the forms

$$\frac{dp_i}{dt} = -\frac{\partial H}{\partial x_i} \quad (i = 1,2, \ldots, n) \qquad (1.3.7)$$

$$\frac{dx_i}{dt} = \frac{\partial H}{\partial p_i} \quad (i + 1,2, \ldots, n) \qquad (1.3.8)$$

We can therefore say that a necessary condition for the control input $\underline{u}$ to be a time optimal control is that $\underline{u}$ must be chosen from the admissible region, at every instant of time during the process, in such a way that the Hamiltonian H, achieves its maximum possible value. If the two end points $\underline{x}^o$ and $\underline{x}^1$ are prescribed, we have the 2n boundry conditions required for the complete solution of the 2n first-order differential equations 1.3.7 and 1.3.8. Because the final time t_1 is free, the transversality condition tells us that the final value of H is generally a positive value.

As a first example consider the time-optimal control of a double integrator plant as shown in Fig. 1.3.2.

The differential equations governing the behaviour of the system are

$$f_1(\underline{x}, \underline{u}) = \frac{dx_1}{dt} = x_2$$

$$f_2(\underline{x}, \underline{u}) = \frac{dx_2}{dt} = u \qquad (1.3.9)$$

We desire to find the control input function u(t) which will transfer the state from an initial condition $\underline{x}^0$ to a specified final state $\underline{x}^1$.

The input u(t) is subject to the following condition

$$|u| \leq 1 \qquad (1.3.10)$$

The Hamiltonian H, as defined in 1.3.6 has the following form

$$H = p_1 x_2 + p_2 u \qquad (1.3.11)$$

(Since $\dot{\underline{x}} = f(\underline{x}, \underline{u})$)

For a given set of values of p_1, p_2 and x_2 H takes on a maximum when $u = \pm 1$.

So the optimal value of u(t) denoted by $u^*(t)$ is given by

$$u^*(t) = \text{sgn}(p_2(t)) \qquad (1.3.12)$$

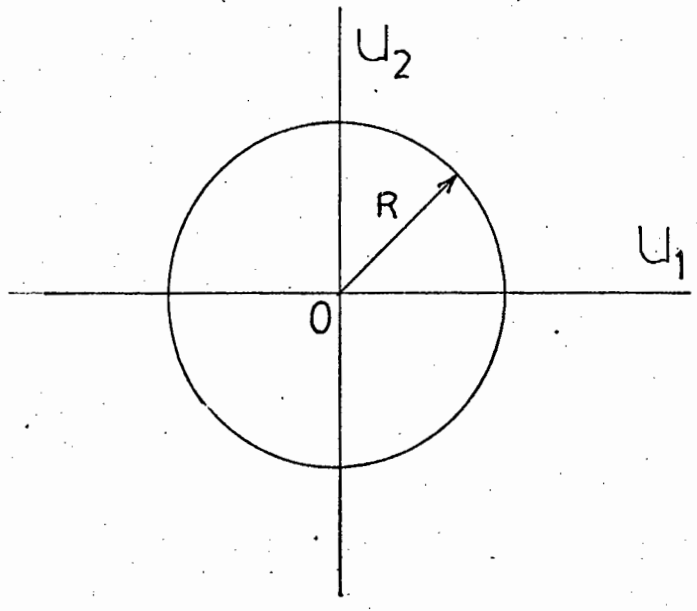

FIGURE 1.3.1 THE CLOSED BOUNDED REGION (EQUATION 1.3.2)

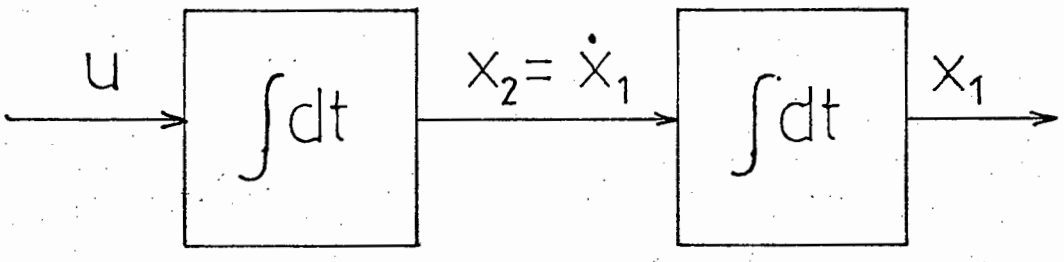

FIGURE 1.2.1 A DOUBLE INTEGRATOR

The differential equations for p_1 and p_2 are derived from equations 1.3.7 and have

$$\frac{dp_1}{dt} = 0$$

$$\frac{dp_2}{dt} = - p_1 \qquad (1.3.13)$$

Integrating the above equations with respect to time yields

$$p_1 (t) = c_2$$

$$P_2 (t) = - c_1 t + c_2 \qquad (1.3.14)$$

where c_1 and c_2 are constants

Equation 1.3.14 tells us that $p_2 (t)$ can change sign not more than once as t increases from t_o to t_1, therefore $u^x (t)$ changes sign not more than once during the transition.

For equations 1.3.12 and 1.3.14, the following possibilities are considered in turn:

(a) If $c_1 = 0$, and $c_2 < 0$, then $p_2(t) < 0$ for $t > 0$, and the corresponding control signal will always be - 1.

(b) If $c_1 = 0$, and $c_2 > 0$, then $p_2(t) > 0$ for $t > 0$, and the corresponding control signal will always be + 1.

(c) If $c_1 > 0$, then $p_2(t) < 0$ for $t > \frac{c_2}{c_1}$ and otherwise $p_2(t) > 0$.

Hence the corresponding control signal will be - 1 for $t > \frac{c_2}{c_1}$ and otherwise it will be + 1.

(d) If $c_1 < 0$, then $p_2(t) > 0$ for $t > \frac{c_2}{c_1}$ otherwise $p_2(t) > 0$.

Hence the corresponding control signal will be + 1 for $t > \frac{c_2}{c_1}$ and otherwise it will be - 1.

This shows that the only possible types of optimal trajectory in the state space are:

(i) A first arc with u=+ 1 followed by a second arc with u = -1

(ii) A first arc with u=- 1 followed by a second arc with u = +1

(iii) A single arc with u=+ 1 throughout

(iv) A single arc with u=- 1 throughout

Cases (iii) and (iv) represent isolated types of solution for special starting conditions and, in general, the optimal control action will be a period of time with the control variable at the maximum permissible value with one sign, then an instantaneous switch to maximum permissible value of opposite sign with the control remaining at this value till the target is reached.

In this simple case, a knowledge of the nature of the

optimal trajectories to be constructed.

Integrating equations 1.3.9 for $u^* = u = \text{sgn } p_2 = +1$ gives

$$\begin{aligned} x_1(t) &= \tfrac{1}{2} t^2 + x_2(0)\, t + x_1(0) \\ x_2(t) &= t + x_2(0) \end{aligned} \qquad \text{Field 1 (1.3.15)}$$

and for $u^* = u = \text{sgn } p_2 = -1$ gives

$$\begin{aligned} x_1(t) &= \tfrac{1}{2} t^2 + x_2(0)t + x_1(0) \\ x_2(t) &= t + x_2(0) \end{aligned} \qquad \text{Field 2 (1.3.16)}$$

where the initial conditions $\underline{x}^0 = x_1(0), x_2(0)$ at $t = 0$ and field 1 is positive drive, field 2 negative drive.

An examination of the corresponding trajectories in Figures 1.3.3, 1.3.4 and 1.3.5 shows that if the target is the phase plane origin the optimal control is specified by a switching curve separating the regions of positive and negative drive. For release from any arbitrary value of initial state, the system state is driven along a parabolic arc under one sign of drive to the appropriate place on the switching curve at which point the sign of the drive is reversed, and the state point travels along the appropriate parabolic trajectory to the target, the origin in this case.

The equations of curves 1 and 2 are

$$\begin{aligned} &\text{curve 1 : } x_1 + \tfrac{1}{2} x_2^2 = 0 \\ &\text{curve 2 : } x_1 + \tfrac{1}{2} x_2^2 = 0 \end{aligned} \qquad (1.3.17)$$

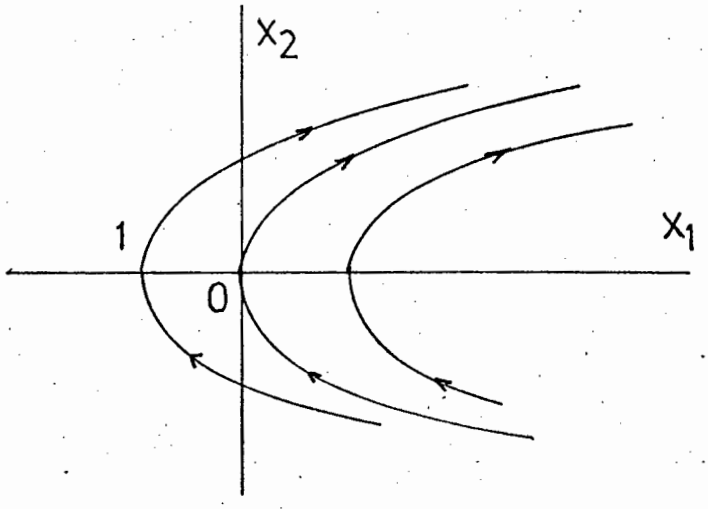

FIGURE 1.3.3 STATE TRAJECTORIES FOR u= +1

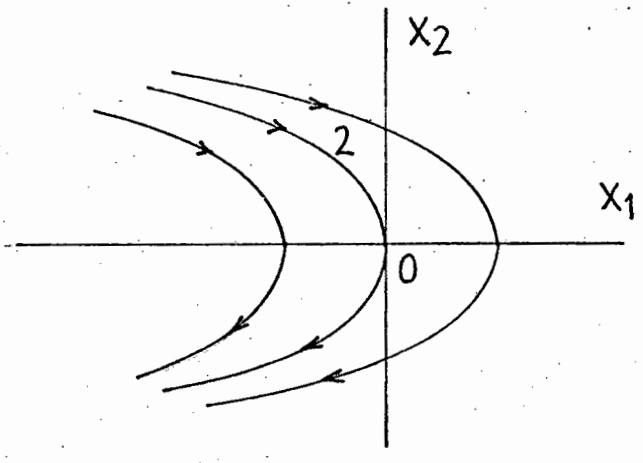

FIGURE 1.3.4 STATE TRAJECTORIES FOR u= -1

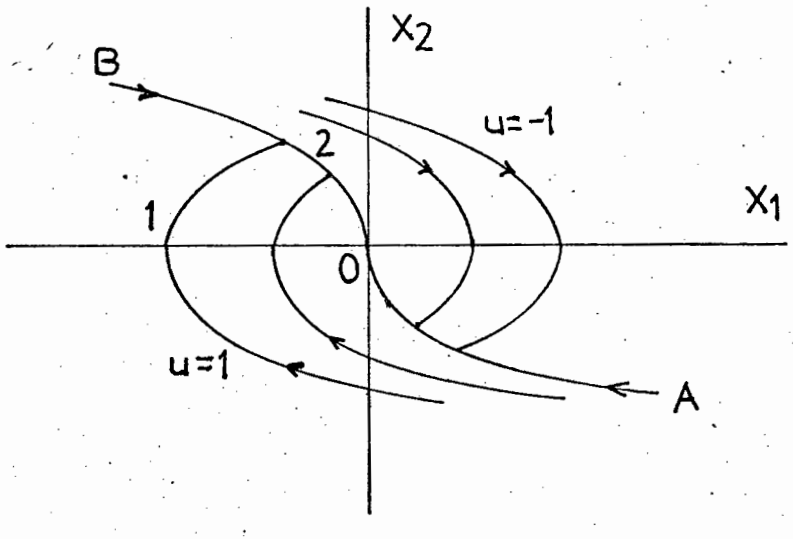

FIGURE 1.3.5 FAMILY OF TIME OPTIMAL TRAJECTORIES FOR A DOUBLE INTEGRATOR

from which it follows that the equation of the switching curve (AOB) is

$$x_1 + \tfrac{1}{2} x_2 |x_2| = 0 \qquad (1.3.18)$$

A time-optimal controller shown in Fig. 1.3.6 is required to choose u^* in accordance with the following logical rules:

$u^* = +1$ if $\underline{x}$ is below AOB or on AO

$u^* = -1$ if $\underline{x}$ is above AOB or on BO

Hence $\phi = -(x_1 + \tfrac{1}{2} x_2 |x_2|) \quad (x_1 + \tfrac{1}{2} x_2 |x_2| \neq 0)$ (1.3.19)

and $\phi = -x_2 \quad (x_1 + \tfrac{1}{2} x_2 |x_2| = 0)$ (1.3.20)

Pontryagin et al also proved the very important fact that, for the general non-order linear system of the kind

$$\dot{\underline{x}} = A\underline{x} + Bu \qquad (1.3.21)$$

if the eigenvalues of A are all <u>real</u> and if the system is controllable by each component of the input vector $\underline{u}$ along (a normal system) and if the admissable control region U is a parallelepiped of the form

$$M_i \leq u_i \leq N_i \ (i = 1,2, \ldots, r) \qquad (1.3.22)$$

then each control input u_i is peicewise constant, takes on only the values M_i and N_i and has at most n-1 switchings (n periods of constant value) during a time-optimal transition from one specified state to another.

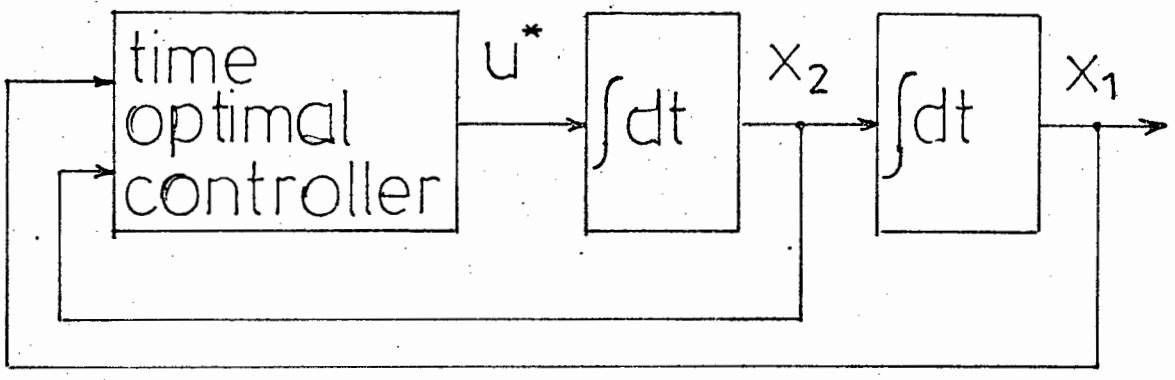

FIGURE 1.3.6 TIME-OPTIMAL CONTROLLER OPERATING ON STATE-VARIABLES

Put simply, for a system of order k and real eigenvalues a minimum of k-1 switchings are required to bring the system state trajectory to its target in minimal-time.

1.4. Aspects on Plant Sensitivity

The effect of plant parameter variations on systems with nominally time-optimal feedback controllers profoundly modify the behaviour and response of the plant being controlled. For higher ordered systems and for very small deviations of the plant parameter from its nominal value the plant response can become unstable.

Several research workers in this field as indicated by Zinober and Fuller (1973) have investigated the double integrator plant with closed and open loop control. The fact that double integrator and triple integrator plants are so highly sensitive to plant parameter variations, some method of sub-optimal control must be applied, to negate excessive overshoots and instability.

A double-integrator plant is investigated for sensitivity analysis but only results for a triple-integrator plant are stated. The sensitivity analysis of a triple integrator plant is complex and the "reduced state space" technique of Fuller[10] (1971) has to be employed.

1.4.1 Sliding Motion

The term 'sliding motion' plays an extremely important role in the behaviour of time-optimal controlled systems and as such is analysed in detail by Weissenberger[11] (see Appendix A9).

Sliding motion was also the term used by Weissenberger in dealing with stability problems in relay controlled systems, and sliding motion can be briefly described as follows:

A switch in the control variable u occurs when the state trajectory approaches, crosses and leaves the switching surface, $\phi = 0$, on the opposite side. The control then changes sign and, if certain conditions are fulfilled, the state trajectory attempts to recross the switching surface and reach the other side. In practice the state point oscillates about the switching surface at a high frequency dependent upon parasitic delays in the switching elements and tends to move on the switching surface. This type of motion is termed sliding, gliding, chattering or after-end point motion. The term sliding is used in this thesis.

Mathematically the dynamic behaviour is no longer well

defined by the differential equations

$$\dot{\underline{x}} = A\underline{x} + Bu \quad (|u| \leq 1) \qquad (1.4.1.)$$

The motion of the state point is governed during sliding motion by the equation of the switching surface

$$\phi (x_1, x_2, \ldots, x_n, a) = 0 \qquad (1.4.2)$$

which is independent of the plant numerator dynamics. In other words the system (Billingsley and Coates[12]) is thus insensitive to changes in the plant parameters, and has the attributes at an adaptive system, furthermore, if the plant has the most general linear form

$$\underline{x} = \frac{N(P)}{D(P)} u \qquad (1.4.3)$$

it is sufficient to control the related system

$$\underline{y} = \frac{1}{D(P)} u \qquad (1.4.4)$$

for when $\underline{y}$ and all the derivates of $\underline{y}$ have been brought to zero, $\underline{x}$ will equally be zero, providing there exists a region of the state-space containing the origin, such that for any initial conditions within this region, the behaviour of the controlled system will after the first switch be the same as that of the double or triple integrator plant respectively. This notion of sliding motion is taken up further in Chapter Four.

1.5. Sensitivity of a Double Integrator[7]

The effect of plant parameter variation on a nominally time-optimal double integrator plant is described and the behaviour of a plant with one integrator and one lag.

For a double integrator (from equation 1.2.1)

$$G(p) = \frac{1}{ag(p)} = \frac{1}{ap2} \qquad (1.5.1)$$

The well known time-optimal switching function for the nominal plant is (from equations 1.3.19 and 1.3.20)

$$\phi = -x_1 - \tfrac{1}{2}a\, x_2\, |x_2| \quad (x_1 + \tfrac{1}{2}a\, x_2\, |x_2| = 0) \qquad (1.5.2)$$

and

$$\phi = -x_2 \quad (x_1 + \tfrac{1}{2}\, ax_2\, |x_2| = 0) \qquad (1.5.3)$$

The initial conditions $(x_1(0);\ x_2(0))$ are written as

$$x_1(0) = x_1^{\,0} \quad \text{and} \quad x_2(0) = x_2^{\,0} \qquad (1.5.4)$$

Consider the region in the phase-plane $\phi(x_1^{\,0}, x_2^{\,0}, a) < 0$. Since the regions are symmetrical the results apply for the region $\phi(x_1^{\,0}, x_2^{\,0}, a) \geq 0$.

The cases b=a, b > a and b < a (see equations 1.2.1 and 1.2.2) will be considered separately as follows.

Case (i) b=a. This case corresponds to time-optimal control. The initial control, u= -1, yields the

trajectory from (x_1^0, x_2^0) to (x_1^1, x_2^1), which lies on the switching surface (a curve for a double integrator). See Figure 1.5.1.

The control then switches to the value + 1 and the state moves along the switching surface to the origin.

The settling time is the time taken for the plant to go from its initial conditions to the phase-plane origin. This may be conveniently expressed as T_{ba} for the control system when the plant parameter is b and the switching function parameter is a (for a nominal plant b = a).

T_e is the fractional increase in settling time with plant parameter b and switching function parameter a over the optimal settling time with plant parameter b.

Thus $T_e = \frac{T_{ba} - T_{bb}}{T_{bb}}$ (1.5.5)

Thus T_e is used also for the fractional increase in settling time, of a sub-optimal control system over the optimal settling time.

The settling time is $T_{bb} = T_{aa}$ and satisfies (see Appendix A4).

$T_{bb} = T_{aa} = ax_2^0 + (2ax_1^0 + a^2(x_2^0)^2)^{\frac{1}{2}}\, 2^{\frac{1}{2}}$ (1.5.6)

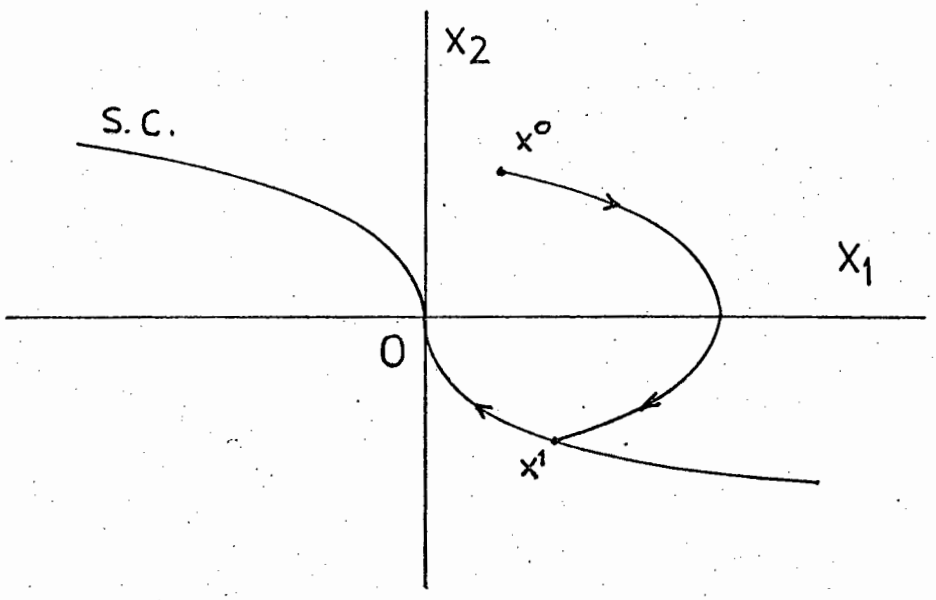

FIGURE 1.5.1 SWITCHING CURVE AND TRAJECTORY FOR THE DOUBLE INTEGRATOR PLANT ($\ddot{x}_1=\frac{u}{b}$) WITH THE SWITCHING FUNCTION $\phi(x_1,x_2,a)$ b=a

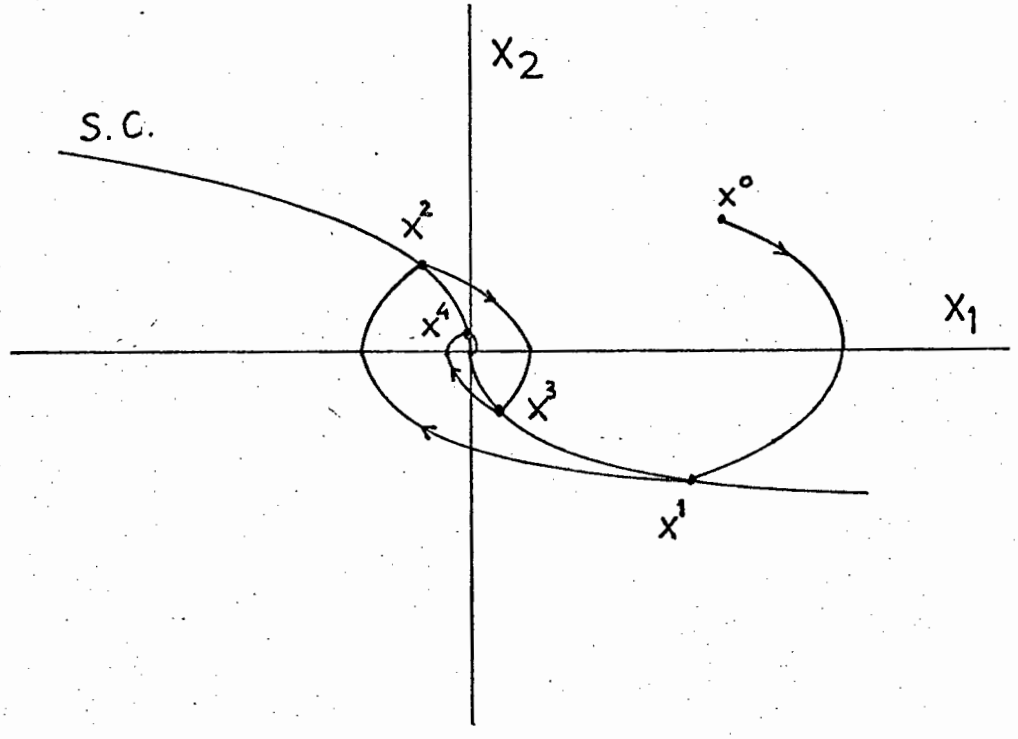

FIGURE 1.5.2 SWITCHING CURVE AND TRAJECTORY FOR THE DOUBLE INTEGRATOR PLANT ($\ddot{x}_1=\frac{u}{b}$) WITH THE SWITCHING FUNCTION $\phi(x_1,x_2,a)$ b > a

Case (ii) $b > a$. With $u=-1$, the state is transferred from (x_1^o, x_2^o) to (x_1^1, x_2^1) which lies on the switching surface (Fig. 1.5.2). The control then switches to the value +1 and the motion overshoots, the state trajectory missing the origin and reaching the switching surface at the point (x_1^2, x_2^2), where the control switches to -1. This behaviour is successively repeated and the state spirals in to the origin.

It is shown (see Appendix 4) that the time intervals between successive switches decrease in constant ratio, so that the total settling time is represented by a geometric series and is finite. The expression for the settling time turns out to be (see Appendix 4)

$$T_{ba} = bx_2^o + (2bx_1^o + b^2(x_2^o)^2)^{\frac{1}{2}} \; 2\left((1+\tfrac{a}{b})^{\frac{1}{2}} - (1-\tfrac{a}{b})^{\frac{1}{2}} \right)^{-1} \qquad (1.5.7)$$

Case iii : $b < a$. As before the control, $u = -1$, transfers the state to the point (x_1^1, x_2^1) which lies on the switching surface (Figures 1.5.3 and 1.5.4). The plant then slides along the switching surface to the state origin. During this sliding motion, the trajectory is that of the optimal system with parameter value a and therefore u has magnitude b/a.

The total settling time is (see Appendix A4)

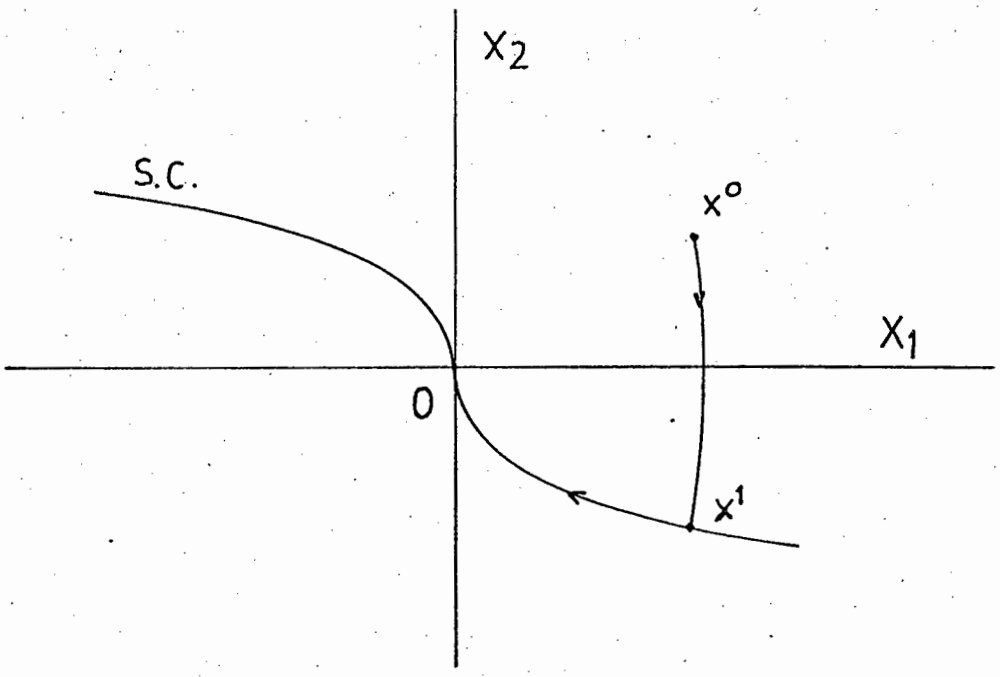

FIGURE 1.5.3 SWITCHING CURVE AND TRAJECTORY FOR THE DOUBLE INTEGRATOR PLANT ($\ddot{x}_1=\frac{u}{b}$) WITH THE SWITCHING FUNCTION $\phi(x_1,x_2,a)$ $b < a$

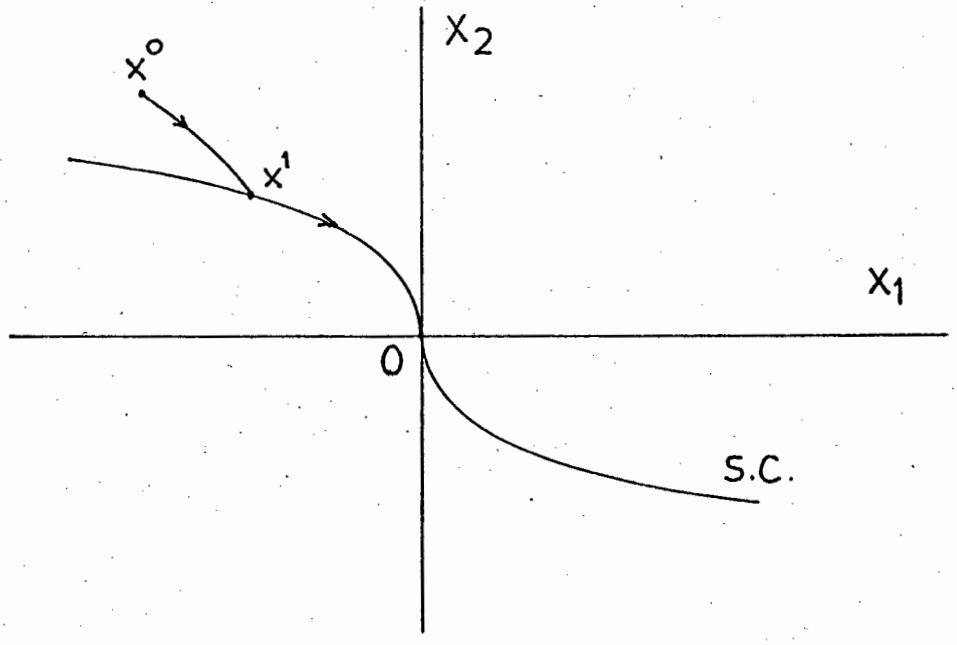

FIGURE 1.5.4 SWITCHING CURVE AND TRAJECTORY FOR THE DOUBLE INTEGRATOR PLANT ($\ddot{x}_1=\frac{u}{b}$) WITH THE SWITCHING FUNCTION $\phi(x_1,x_2,a)$ $b < a$

$$T_{ba} = bx_2^o + (2bx_1^o + b^2(x_2^o)^2)^{\frac{1}{2}} \left(\frac{a}{b} + 1\right)^{\frac{1}{2}} \quad (1.5.8)$$

for

$$x_1^o + \tfrac{1}{2}bx_2^o \quad |x_2^o| \geq 0 \text{ and}$$

$$T_{ba} = bx_2^o + (-2bx_1^o - b^2(x_2^o)^2)^{\frac{1}{2}} \left(\frac{a}{b} - 1\right)^{\frac{1}{2}} \quad (1.5.9)$$

for

$$x_1^o + \tfrac{1}{2}bx_2^o \quad |x_2^o| \leq 0$$

Zinober and Fuller[7] show that an approximate expression for T_e can be derived from equations 1.5.7, 1.5.8 and 1.5.9. Values of T_e are calculated for a step input viz. $x_1^o = A$, $x_2^o = 0$ and the 'worst case' initial conditions where

$$x_1^o + \tfrac{1}{2}bx_2^o \quad |x_2^o| = 0 \qquad b > a \qquad (1.5.10)$$

or $$x_1^o + \tfrac{1}{2}bx_2^o \beta_o |x_2^o| = 0 \qquad b < a \qquad (1.5.11)$$

where $\beta_o = f(\beta)$ $\beta = a/b$

These values are shown in Figure 1.5.5 in which T_e is plotted against b/a. The overshoot trajectory (case $b > a$ or $K_b < K_a$; plant gain reduced) yields larger settling times than the sliding trajectory (case $b < a$ or $K_b > K_a$; plant gain increased) for a comparable parameter variation. Some typical values are given in table 1.5.1.

b/a	T_e (Step input) %	T_e ('worst case' initial conditions) %	Motion
.5	22,5	38	Sliding
.8	6,1	11,5	Sliding
.95	1,3	2,6	Sliding
1.05	19,9	39,9	Overshoot
1.20	49,5	99,1	Overshoot
1.50	98,2	196,3	Overshoot

Table 1.5.1 System with double integrator plant.

The sensitivity, S, of the settling time, T_s, of the system to a variation δb in the parameter b, is, for $b = a$, from 1.5.10

$$S = \lim_{\delta b \to 0} \left(\frac{\frac{\delta T_s}{T_s}}{\frac{\delta b}{b}} \right)_{b = a} = \lim_{\Delta \to 0} \left(\frac{T_e}{\Delta} \right) \quad b = a \qquad (1.5.12)$$

. where $\Delta = \left|1 - \frac{a}{b}\right|$, the magnitude of the fractional change of plant parameter and is used in the approximate expressions for T_e.

For $\delta b > 0$ (i.e. $b > a$) and substituting the approximate T_e into equation 1.5.12 yields

$$S = \lim_{\Delta \to 0} \frac{1}{(2\Delta)^{\frac{1}{2}}} = \infty \qquad (1.5.13)$$

i.e. the sensitivity is infinite. This fact illustrates

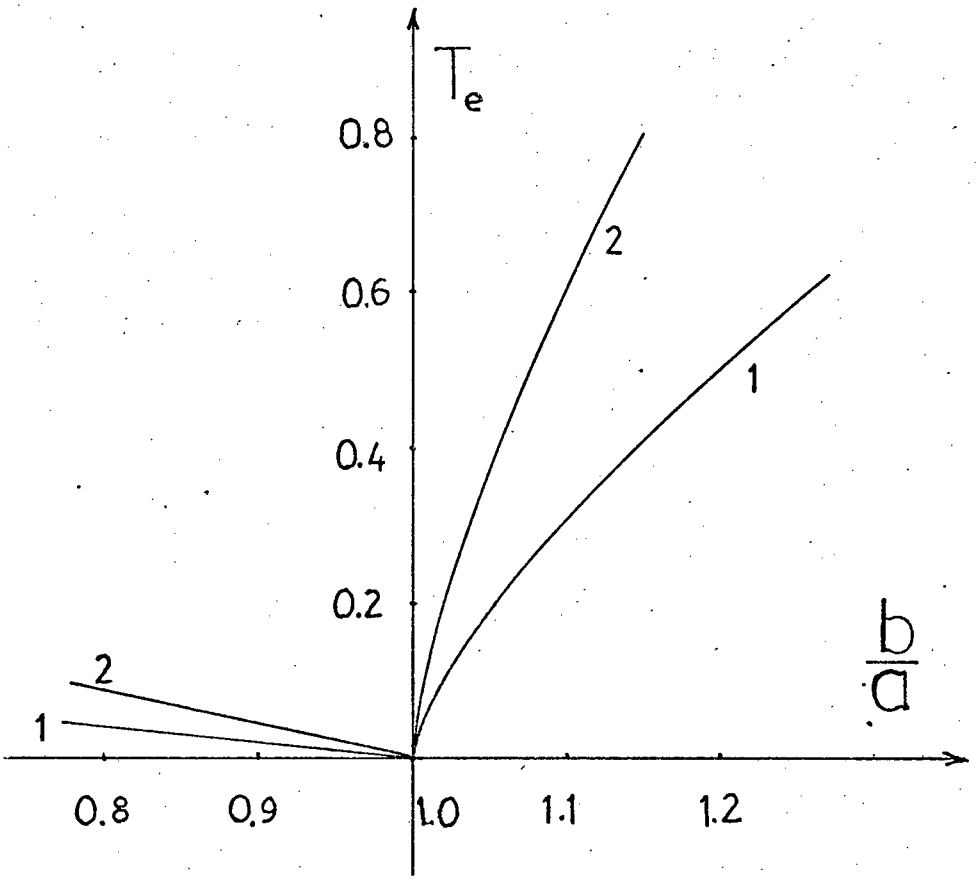

FIGURE 1.5.5 FRACTIONAL INCREASE IN SETTLING TIME AGAINST NORMALIZED PLANT PARAMETER FOR A DOUBLE INTEGRATOR PLANT

1. STEP INPUT
2. WORST CASE INITIAL CONDITIONS

the complexity of the sensitivity analysis of non-linear systems in contrast to that of linear systems.

These results were referred to by the author for verification from results obtained on a real system.

The control system with the plant having $g(p)=p(p+d)$ $d>0$ (1.5.14) ie. one integrator and one lag is also considered. The time constant of the lag is $\frac{1}{d}$. The time optimal switching function of the nominal plant is:

$$\phi = -x_1 - \frac{x_2}{d} - \frac{\operatorname{sgn} x_2}{ad^2} \operatorname{Ln}(1+ ad\,|x_2|) \qquad (1.5.15)$$

and if the RHS of (1.5.15) is zero,

$$\phi = -x_2 \qquad (1.5.16)$$

The cases $b=a$, $b > a$ and $b < a$ give trajectories having a form similar to the double integrator plant. For $b=a$ we obtain the time-optimal control, $b > a$ yields overshoot motion and $b < a$ give sliding motion.

The effect of plant parameter d variations are investigated. It is found that if the nominal plant parameter is d_{nom} then when $d=d_{nom}$ the response is time optimal. For $d > d_{nom}$ sliding motion occurs after the first switch and for $d < d_{nom}$ overshoot motion results.

The triple integrator plant where $g(p)=p^3$ and the time-optimal switching function given by equation A 3.11, A 3.12 and A 3.13 has been fully investigated by Zinober and Fuller[7]. Their method of analysis involves the use of the 'reduced state space' developed by Fuller for a two dimensional graphical analysis of a system having three state variables. The analysis is tedious, however, the results show that if b is increased by 44% over its nominal value a, it is sufficient to cause instability.

For values of $b < a$ sliding motion results with a reasonable increase in settling time, however the plant is extremely sensitive for values of $b > a$.

1.6. Summary and Comments

Relay switching of second order (and higher order) plants is considered. The role of the switching function $\phi(\underline{x})$ and the switching surface $\phi(\underline{x})=0$ is stressed. The use of Pontryagin's maximum principle in which there is a constraint or limitation of some kind on the control input, and with the use of the calculus of variations (the derivation of the Hamiltonian formulation) enable us to find the optimal control vector $u^*(t)$ to the plant in question, to achieve a time-optimal transition from an initial state to a specified

state.

It is shown that a time-optimal trajectory for a specific plant is highly sensitive, in that relatively small deviations of the plant parameter causes large increases in settling times over the nominal. The notion of sliding motion is introduced and its very practical and important use in extremal control is demonstrated.

Finally equations are derived for a double integrator plant yielding the settling times for a step input, for the nominal parameters and variations in the plant parameters. The theory in this chapter (and to the Appendices where referred) provides the basis for extremal control whether the controller is based upon the fast model predictor, adaptive-relay or $\underline{v}$ transformation method, and the following chapters aptly demonstrate the concepts.

CHAPTER 2

PREDICTIVE CONTROL

2.1 Background

One of the first reports on the idea of predictive control was a paper published by Ziebolz and Paynter[1] in 1954, entitled 'Possibilities of a two-time dynamic systems'. Basically they proposed a repetitive type of computer whose initial conditions are watched with the plant variables at a given time. Since the computer establishes the resultant response under the assumption of no additional disturbances during the projected interval, and provides information about the future state of the plant, this information can be used to apply the correct control to bring the plant to the desired target.

Three important points were singled out and are still valid;

(a) The necessary repetition and computation rates are a function of the process time constants.

(b) The repetition rate depends on the relative certainty or probable accuracy of the future prediction.

(c) A high repetition and computation rate permits comparison between alternate modes of action making possible a choice of strategy.

In 1955 Coales and Noton[13] published a paper titled 'An on-off servo mechanism with predicted changeover' where the principles of a predictive controller were investigated along with an actual test conducted on a servo-motor.

The method used to achieve the predicted change-over point was as follows:

A double integrator is considered where $\ddot{x} = u$ and $u = \pm 1$. The state of the system at any time is given by x and $\dot{x}$ written as (x_0, x_1). The desired trajectory has only one switching and takes the state from the initial value (a_0, a_1) to the origin and can be found using only two iterations for a double integrator and several for a general second order system, by the following strategy: (See Figures 2.1.1 and 2.1.2).

For the first run the model is set to (a_0, a_1) and u is set to $-\text{sgn}(a_1)$. The model is allowed to run until $x_1 = 0$ and at this point E is set equal to x_0 (E is a parameter).

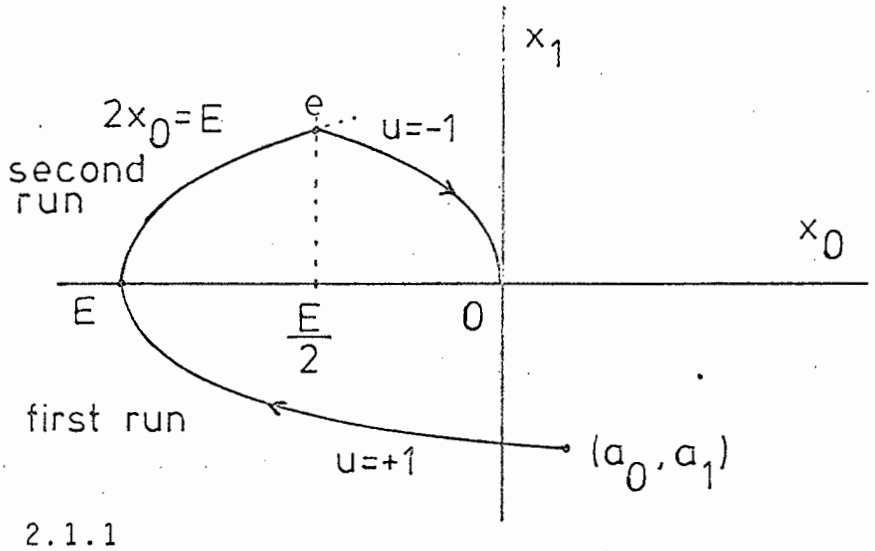

FIGURE 2.1.1
METHOD OF COALES AND NOTON
ILLUSTRATION OF CASE (i)

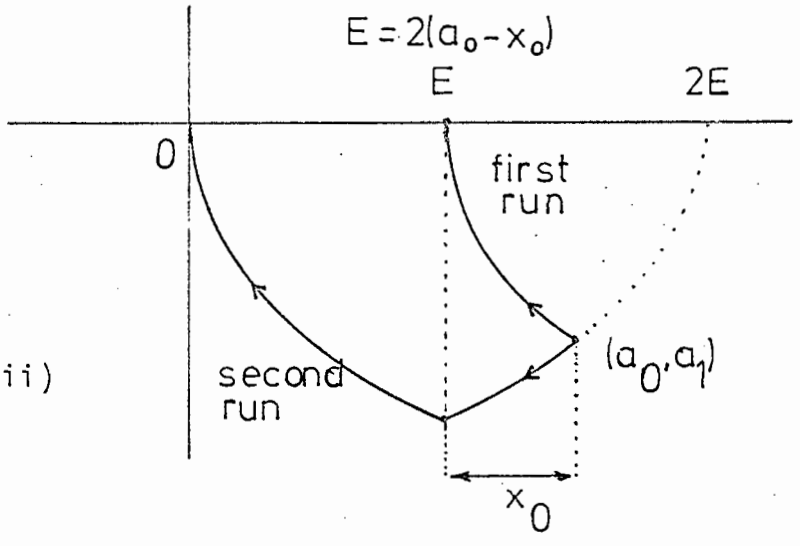

FIGURE 2.1.2
ILLUSTRATION OF CASE (ii)

NOTE: The technique here is to first have a trial run and locate point E, second the fast model is reset to the previous position and the same drive applied and switch at point e in Fig. 2.1.1 according to $x_0 = E/2$ or in Fig. 2.1.2 merely switch at point E on the second run where $E = 2(a_0 - x_o)$. (If the trajectory at point (a_0, a_1) is reversed it will meet the x_o axis at a point 2E).

For the second run the model is reset to (a_0, a_1) and u set to -sgn(E). The model is allowed to run and the sign of $\dot{U}$ reversed according to the appropriate following conditions:

(i) If $sgn(E) = sgn(a_1)$ switch when both $sgn(x_1) = -sgn(E)$ and $2x_0 = E$ (see Fig. 2.1.1)

(ii) If $sgn(E) = -sgn(a_1)$ switch when $2(a_0-x_0) = E$ (See Fig. 2.1.2)

This trajectory will now pass through the origin as shown in Fig. 2.1.1 and 2.1.2.

One of the shortcomings of this method of prediction is that it assumes the plant parameters are invariant and ideally watch that of the fast model. If the plant parameters do change during the transient state, this change will not be detected by the fast model as only the initial conditions are used to detect the switch-over point. However both step and varying imputs were used in this case.

In 1961 Chestnut, Sollecito and Troutman[14] published a paper titled 'Predictive-Control System Application'. The method used here was different to that of

Coales and Noton in that repeated estimations of the future error and hence the changeover point are obtained by projecting from the fast model that trajectory which passes through the phase plane origin. The initial conditions for the fast model are obtained from the plant on a sampled-data basis.

The method of this operation is explained as follows:

The error phase portrait for a double integrator with a constant negative reference -r, is shown in Fig. 2.1.3.

Since the reference is negative, the polarity of the actuating signal is such that the direction of the plant error trajectory moves to the origin. The starting point is at a (= -r). At point b the first prediction is made to observe the value of $e(\tau)$ (τ is the fast model or speeded-up time) when $\dot{e}(\tau)$ remains zero in the event of a polarity reversal in the actuating signal. Successive predictions are made until finally, at point g, the predicted error changes sign from minus to plus when $\dot{e}(\tau)$ reached zero. This information is used by the control logic to switch the signal polarity at point g.

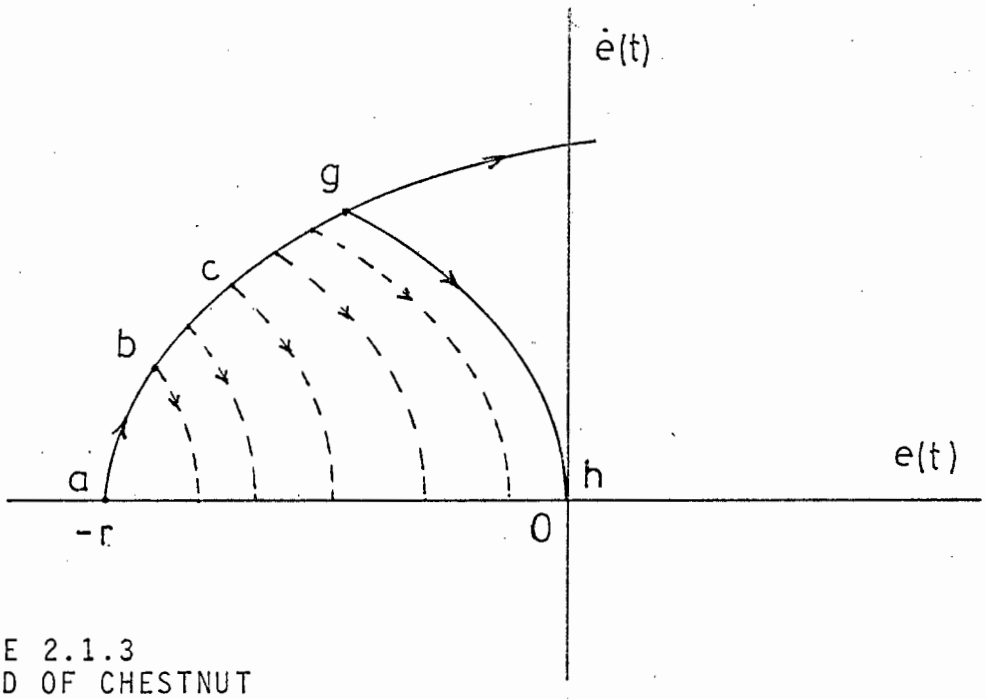

FIGURE 2.1.3
METHOD OF CHESTNUT
TRAJECTORIES IN THE ERROR-ERROR RATE PHASE PLANE

The actual error phase-plane trajectory passes from point a through b, c, ..., g and h. Along this curve time takes on real-time dimensions. The predicted trajectories shown dotted in Fig. 2.1.3 are obtained from the fast time model and along these trajectories time takes on computer-time dimensions.

It will be noted that the predicted trajectory starting at b is much shorter than the one starting at c. This occurs because the next prediction is started when the previous predicted error rate reached zero. This results in a variable-frequency prediction rate which was born out during experimentation using relays and analogue computing equipment. This means that for large error rates, the prediction rate is slowest and for small error and error rates, the prediction rate is fastest. This situation is desirable because it results in tightest control when it is needed most.

Beyond point h there exists a limit cycle about the origin, the magnitude and frequency of this limit cycle depends in large part upon the prediction repetition rate. If this rate is relatively high, the magnitude of oscillation can be small and the frequency high depending on the nature of the controlled system and the speed of the equipment to perform the switching functions.

Several important aspects arose from this fast model prediction technique, as listed below:

(a) The removal of the bang-bang motion of the relay to the plant when the errors are in close proximity to the phase-plane origin.
(b) The effect of noise and random disturbances on the system and reference signal.
(c) The behaviour of plant and model mismatch both in order, gain and time constants.
(d) The stability of the system.
(e) The minimal rate of the sampled data interval.

Subsequent publications (12, 15, 19, 20, 21, 22, 23) deal with higher ordered systems, plant parameter variations and methods to compensate for these variations, plant and model mismatch, stability considerations as well as same practical applications. Of note was the application and analysis of analogue computer control employing a predictive fast model of a chemical batch type process[18], the application of a fast model with an adaptive scheme for a batch reaction[17] and similar application for voltage control of a synchronous generator[16].

The use of a fast model for predictive control as a time-optimal controller (this term makes real sense only in those controllable systems which are called upon to respond to a step-input) was only really given a mathematical basis soon after Pontryagin's principle was made known and all the advantages that had accrued to switching systems now held a firm mathematical basis.

A suitable definition of predictive control is therefore a control technique that employs a fast time model of the time-optimal trajectory which provides the correct switching criteria to the plant actuator based upon the values of the instantaneous state variables of the plant.

Put another way, predictive control describes a form of automatic control in which the manipulated variable operating the controlled system is actuated by the estimate of the error that will exist at some future time.

Repeated estimations of the future error are obtained by predicting ahead on a fast-time base the controlled variable as well as some lower order derivatives.

It is shown that an exact model of the plant is not always necessary as a second order model can in certain circumstances provide control for a third and fourth order plant provided some overshoot can be tolerated.

2.2 Stability Analysis of a second order fast model predictor

The use of a low order model to determine the approximate time-optimal switching function for a given plant has been experimentally investigated. Liapunov's second method is used to determine (see Appendix 5) asymptotic stability in the large (globally) or in some cases boundedness[+] of the states. The basis model transfer function is:

$$G_m(s) = \frac{K}{s(1+Ts)} \quad (K,T>0) \qquad (2.2.1)$$

[+] Boundedness is meant by obtaining boundaries in the error-error rate phase-plane through which the trajectories cannot pass and then proving these boundaries ultimately contract into some closed curve.

This model transfer function was found to be versatile in controlling plants of various forms. Systems with stable, controllable second-order plants will be asymptotically stable globally as the results shown and systems with no more than two free integrators will have ultimately bounded error and error rates.

It was observed that controlling a plant with a fast model whose transfer function was $G_m(s) = \frac{K_m}{s(1+T_m s)}$ yielded virtually zero steady-state error and error-rate (apart from the limit cycles) for the step response of several of the following types of plants; $\frac{K_p}{s(1+T_p s)}$, $\frac{K_p}{s^2}$, $\frac{K_p}{(1+T_{p1}s)(1+T_{p2}s)}$ as well as third and fourth order plants and where all parameters are positive.

Overshoot was seen to be reduced or eliminated through the use of a slower (larger T_m, smaller K_m) model, sometimes at the expense of a small increase in rise time. The step response of higher order plants having negative poles and no more than two integrations was observed to have a steady state limit cycle, the size of which was decreased by a slower model at the expense of a longer rise time. Liapunov's second or direct method of

determining stability was chosen, as the closed loop transfer function for a bang-bang system is highly non-linear and complex to treat, using the more traditional methods for ascertaining stability.

$$\text{The model transfer function} = \frac{K_m}{s(1+T_m s)} = \frac{K_d}{s(s+d)} \quad (2.2.2)$$

where $\frac{1}{T_m} = d$, $K_d = \frac{K_m}{T_m}$

$$\text{The plant transfer function} = \frac{K_p}{s(1+T_p S)} = \frac{K_q}{s(s+q)} \quad (2.2.3)$$

where $\frac{1}{T_p} = q$, $K_q = \frac{K_p}{T_p}$

Figure 2.2.1 shows the general predictive control system arrangement while Figure 2.2.2 shows the equivalent block diagram for the closed loop system with a reference step input.

It is convenient to use the error and error-rate such that:

$$\begin{cases} e = x_1 \\ \dot{e} = x_2 \end{cases} \quad (2.2.4)$$

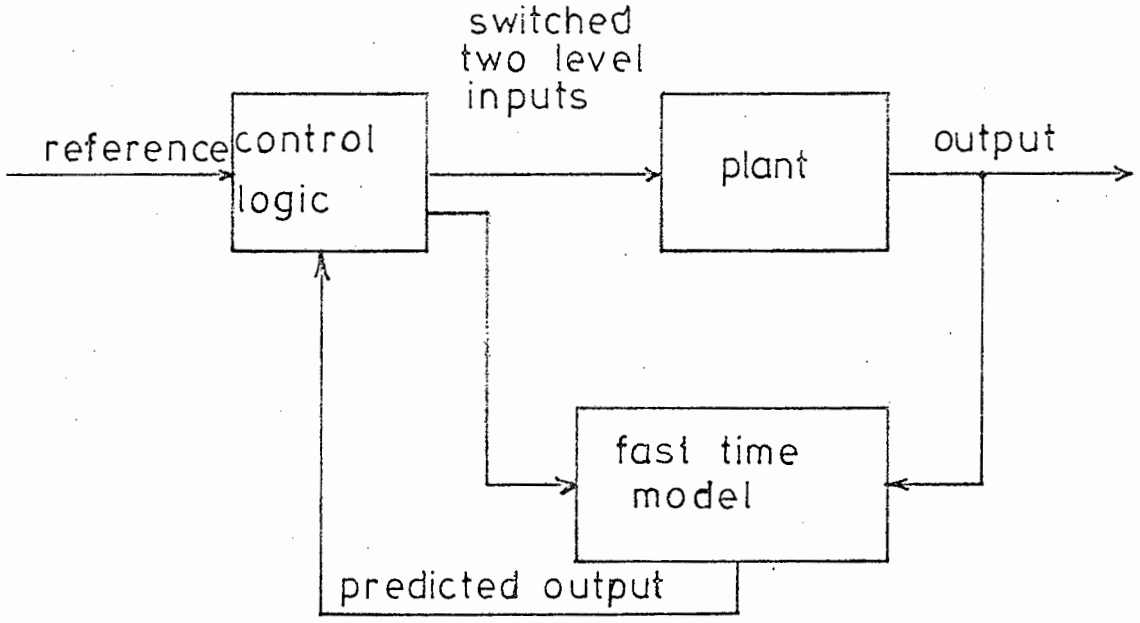

FIGURE 2.2.1
PREDICTIVE CONTROL SYSTEM

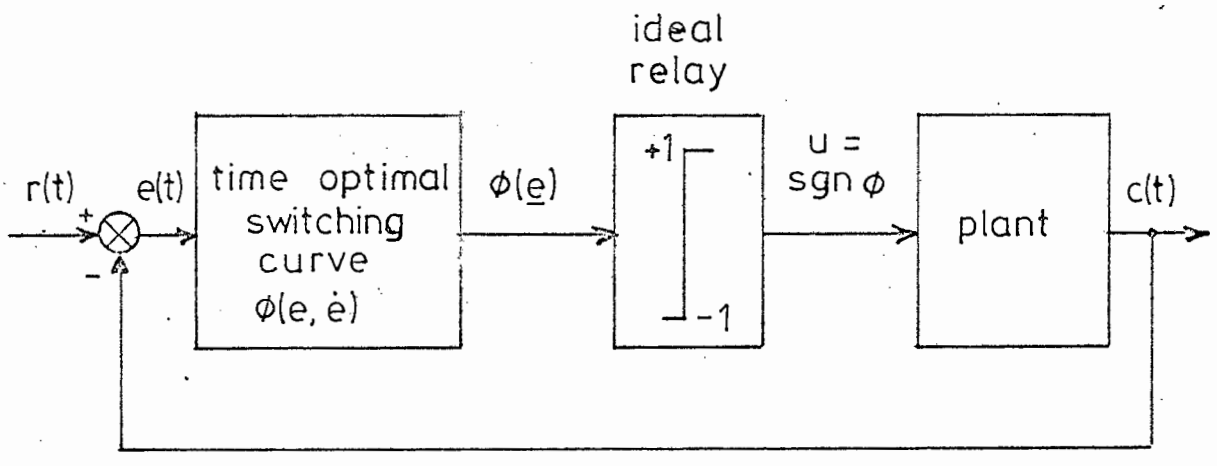

FIGURE 2.2.2
TIME-OPTIMAL CONTROL SYSTEM

The plant actuating signal is determined from

$$u = \text{sgn}(\phi) \quad (2.2.5)$$

where $\phi\ (x_1, x_2)$ is the time optimal switching curve for the model as is given as:

$$\phi = -\left(x_1 + \frac{x_2}{d} + \frac{K_d \text{ sgn } x_2}{d^2} \text{ Ln } \left(1 + \frac{d\,|x_2|}{K_d}\right)\right) \quad (2.2.6)$$

or $\phi = -x_2$ if the r.h.s of 2.2.6 is zero.

Figure 2.2.3. represents in the error-error rate phase plane the time-optimal switching curve for the model.

The curves in quadrant II and IV serve to define the switching functions for the various plants investigated. For appropriate values of d and K_d, certain systems can be made asymptotically stable and some higher ordered systems to yield bounded responses.

We have (see Figure 2.2.2)

$$r - c = e$$

$$r - \frac{K_q}{s(s+q)} \text{ sgn } \phi = e$$

$$\ddot{r} + q\dot{r} - K_q \text{ sgn } \phi = \ddot{e} + q\dot{e} \quad (2.2.7)$$

Since $\dot{r}$, $\ddot{r}$, ... = 0 we obtain

$$\ddot{e} + q\dot{e} + K_q \text{ sgn } \phi = 0 \qquad (2.2.8)$$

This can be expressed as:

$$\begin{cases} \dot{e}_1 = e_2 \\ \dot{e}_2 = -qe_2 - K_q \text{ sgn } \phi \end{cases} \qquad (2.2.9)$$

Using equations 2.2.4 we obtain

$$\begin{cases} \dot{x}_1 = x_2 \\ \dot{x}_2 = - qx_2 - K_q \text{ sgn } \phi \end{cases} \qquad (2.2.10)$$

For the purpose of determining a Liapunov function[22], consideration of the undamped system

$$\begin{cases} \dot{x}_1 = x_2 \\ \dot{x}_2 = K_q u \end{cases} \qquad (2.2.11)$$

where $u = \text{sgn } x_1$ yields

$\frac{dx_2}{dx_1} = \frac{-K_q \text{ sgn } x_1}{x_2}$ which after integration yields

$$\tfrac{1}{2} x_2^2 = - K_q x_1 \quad x_1 > 0 \qquad (2.2.12)$$

$$\tfrac{1}{2} x_2^2 = K_q x_1 \quad x_1 < 0 \qquad (2.2.13)$$

Thus 2.2.12 and 2.2.13 suggest that

$$V(x_1, x_2) = \frac{x_2^2}{2} + K_q \, |x_1| = c \quad (2.2.14)$$

where $V(x_1,x_2)$ is the Liapunov function and c is a constant. This is shown in Figure 2.2.4.

Since K_q and $q>0$, $V(x_1, x_2)$ will be positive definite and continuous in the entire x_1 - x_2 plane.

Taking the time derivative of $V(x_1, x_2)$ yields:

$\dot{V}(x_1, x_2) = \frac{\partial V}{\partial x_1} \dot{x}_1 + \frac{\partial V}{\partial x_2} \dot{x}_2$ and using equations 2.2.10 yields:

$$\begin{aligned} \dot{V}(x_1, x_2) &= K_q \operatorname{sgn} x_1 \, \dot{x}_1 + x_2 \, \dot{x}_2 \\ &= K_q \, x_2 \operatorname{sgn} x_1 + x_2 \, (- q x_2 - K_q \operatorname{sgn} \phi) \\ &= - q \, x_2^2 - K_q \, x_2 \, (\operatorname{sgn} \phi - \operatorname{sgn} x_1) \end{aligned} \quad (2.2.15)$$

where $\operatorname{sgn} x_1 = \frac{x_1}{|x_1|}$ and $u = \operatorname{sgn} \phi$

Inspection of Figure 2.2.4. shows $\dot{V}$ to be equal to $- q \, x_2^2$ in regions 2, 3, 5, 6 and $- q \, x_2^2 - 2K_q \, |x_2|$ in regions 1 and 4.

Along the switching curve; $\dot{V} = - q \, x_2^2 - mK_q \, |x_2|$

where m = 0, 1, 2 depending if u is assumed to be +1, 0, -1 respectively.

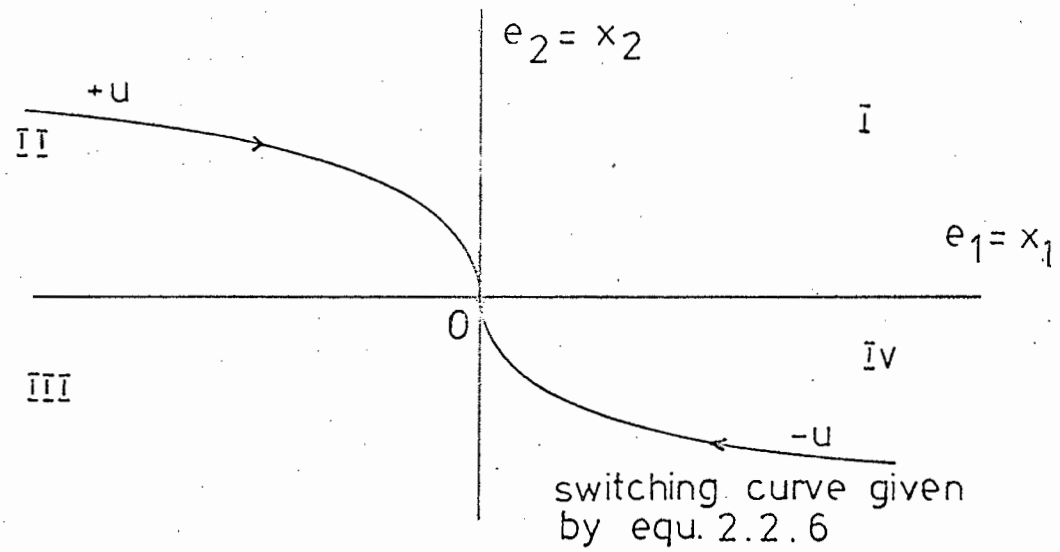

FIGURE 2.2.3
TIME-OPTIMAL SWITCHING CURVE FOR $\frac{K_d}{s(s+d)}$

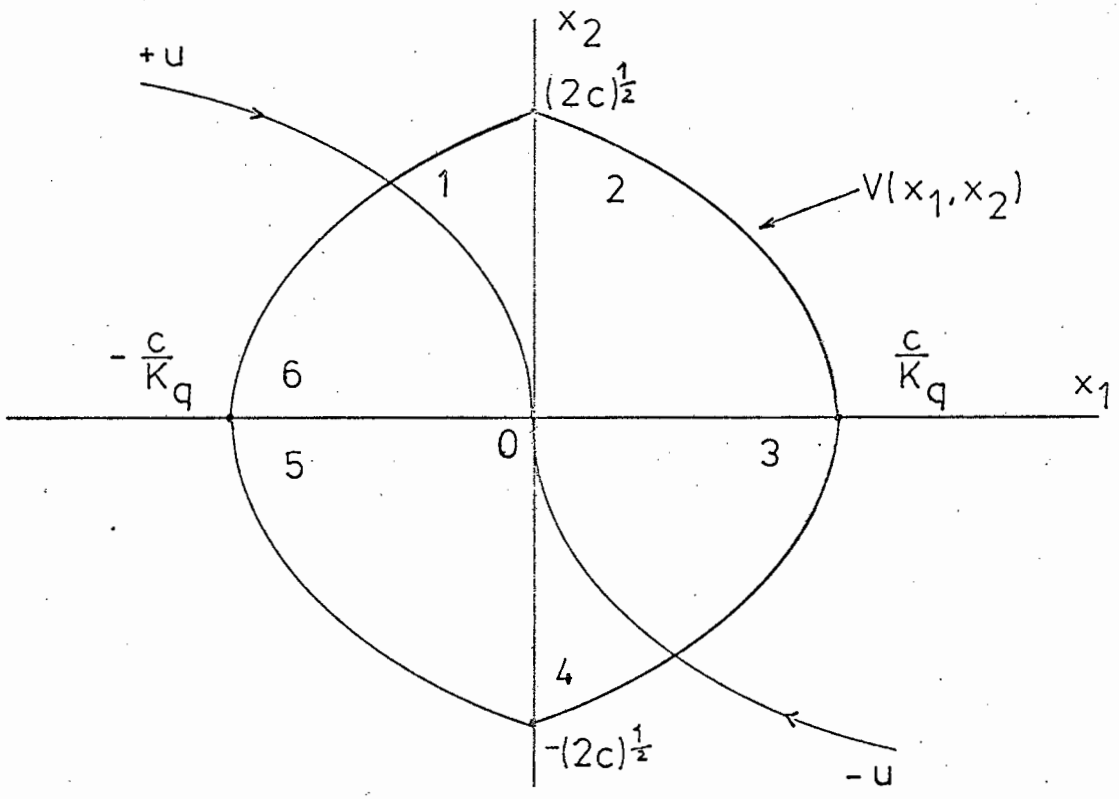

FIGURE 2.2.4
ERROR-ERROR RATE PHASE PLANE WITH SWITCHING CURVE AND LIAPUNOV FUNCTION

$$V(x_1, x_2) = \frac{x_2^2}{2} + K_q |x_1| - c = 0$$

Therefore $\dot{V}$ is negative everywhere in the x_1-x_2 plane except along the x_1 - axis where $\dot{V} = 0$, and along the x_2 - axis where $\dot{V}$ is undefined.

However, when $x_2 = 0$

$$\left.\frac{dx_2}{dx_1}\right|_{x_2 = 0} = \left.\frac{-K_q \ \text{sgn}\ x_1}{x_2}\right|_{x_2=0} = \pm\infty$$

In other words no portion of the solution curve lies along the x_1 - axis.

Furthermore, because of the magnitude constraints on u, it is seen from equation 2.2.10 that since $\frac{dx_2}{dx_1}$ is infinite only when $x_2 = 0$ no trajectory lies along the x_2-axis except at the origin.

Consequently since trajectories which cross the x_2-axis have a finite slope and since $V(x_1, x_2)$ is continuous across and decreasing on both sides of the x_2-axis, $V(x_1, x_2)$ does indeed decrease everywhere along the trajectories crossing $x_1 = 0$.

These results imply that the concentric curves $V(x_1, x_2) = c$ of Figure 2.2.4 constantly shrink into the origin along the solution trajectories of the system.

In this way one can conclude that for the given system, global asymptotic stability results from a step reference input provided that K_m, T_m, K_p and T_p are all positive.

These results demonstrate that if the plant parameters K_p and T_p were positive but not properly identified, the overall system is still asymptotically stable in the large, even if the model parameters remain invariant. This has been borne out by experimental results.

Kaufman and De Russo[22] have demonstrated that asymptotic stability can be obtained also for ramp inputs, non-linear second-order plants of the form;

$\ddot{c} + g(c)h(\dot{c})+f(c) = K_p m$, disturbances and fluctuating inputs provided they are small or of a short duration. Finally the error-error rate states of the nth order plant $\frac{K_p}{s(1+T_1 s)(1+T_2 s) \ \ldots\ (1+T_n s)}$ controlled by the model $\frac{K_m}{s(1+T_m s)}$ will be unstable at the origin of the phase plane, but ultimately bounded provided that initially all error derivatives of order greater than one are zero. Again this has been demonstrated experimentally to be valid for n = 2 and 3.

2.3 Experimental Procedures

Four separate stages of system simulation development took place and they were:

Stage 1 : The use of an analogue computer and relays to simulate the entire system operation.

Stage 2 : The digital simulation of the system on a minicomputer.

Stage 3 : The use of hybrid control (the combination of an analogue computer and minicomputer via the necessary signal converters) to simulate system operation.

Stage 4 : Direct digital control (DDC) of a small DC Motor using the minicomputer as the fast model.

2.3.1. Stage One. Description of the predictor-control Logic and switching network.

The heart of the analogue predictive control system is the logic section and switching network. In its simplest form the control logic is only a means of mechanizing the switching criteria that were introduced in section 2.1.

This procedure is summarized in the flow chart shown in Figure 2.3.1(b) and for ease of description, reference is made to the symbols in Figure 2.3.1(a).

From the flow chart it can be seen that the first step in applying the logic is to compute the present values of $e(t)$, $\dot{e}(t)$ from the present values of $r(t)$, $c(t)$ and $\dot{c}(t)$. After determining the signs of $e(t)$ and $\dot{e}(t)$, they are compared in sign to determine in which quadrant of the phase plane the start of the trajectory is located.

Hence if $e(t).\dot{e}(t) > 0$ the start of the trajectory is either in quadrant I or III of the phase-plane (see Figure 2.3.2) and must be driven into quadrant II or IV.

The choice of polarity of $u(t)$ is dependent on the sign of $e(t)$ and is quite apparent.

For $e(t).\dot{e}(t) < 0$ the initial trajectory is already in quadrant II or IV and $u(t)$ is set according to the sign of $e(t)$.

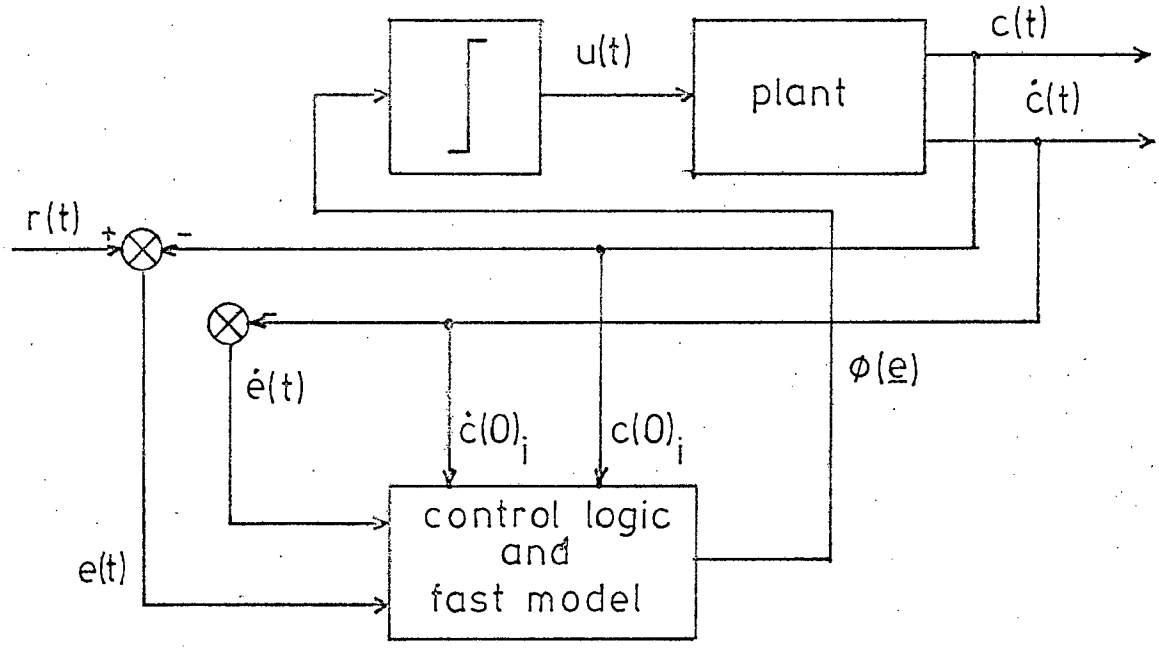

FIGURE 2.3.1(a)
BLOCK DIAGRAM OF FAST MODEL PREDICTOR

$r(t)$ = Reference (Step)
$c(t)$ = Output
$\dot{c}(t)$ = Output rate
$e(t)$ = Error
$\dot{e}(t)$ = Error rate
$c(0)_i$ = Sampled output as initial conditions to fast model
$\dot{c}(0)_i$ = Sampled output rate as initial conditions to fast model
$e(\tau)$ = Fast model output (not shown in diagram)
$\dot{e}(\tau)$ = Fast model output rate (not shown in diagram)
$u(t)$ = Actuating signal to plant
$\phi(\underline{e})$ = Switching function of plant and fast model states
$u(\tau)$ = Actuating signal to fast model (not shown in diagram)

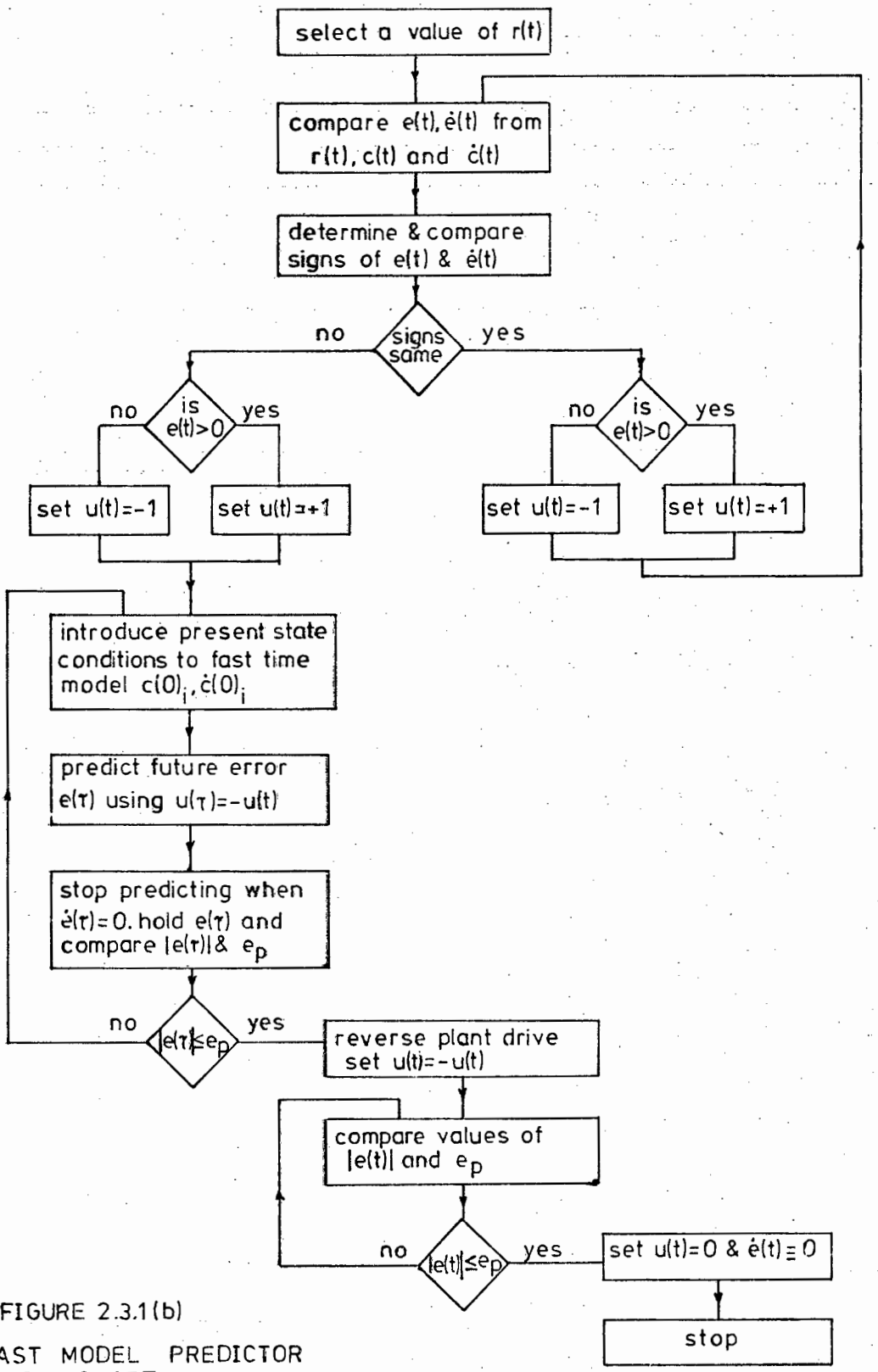

FIGURE 2.3.1(b)

FAST MODEL PREDICTOR FLOW CHART

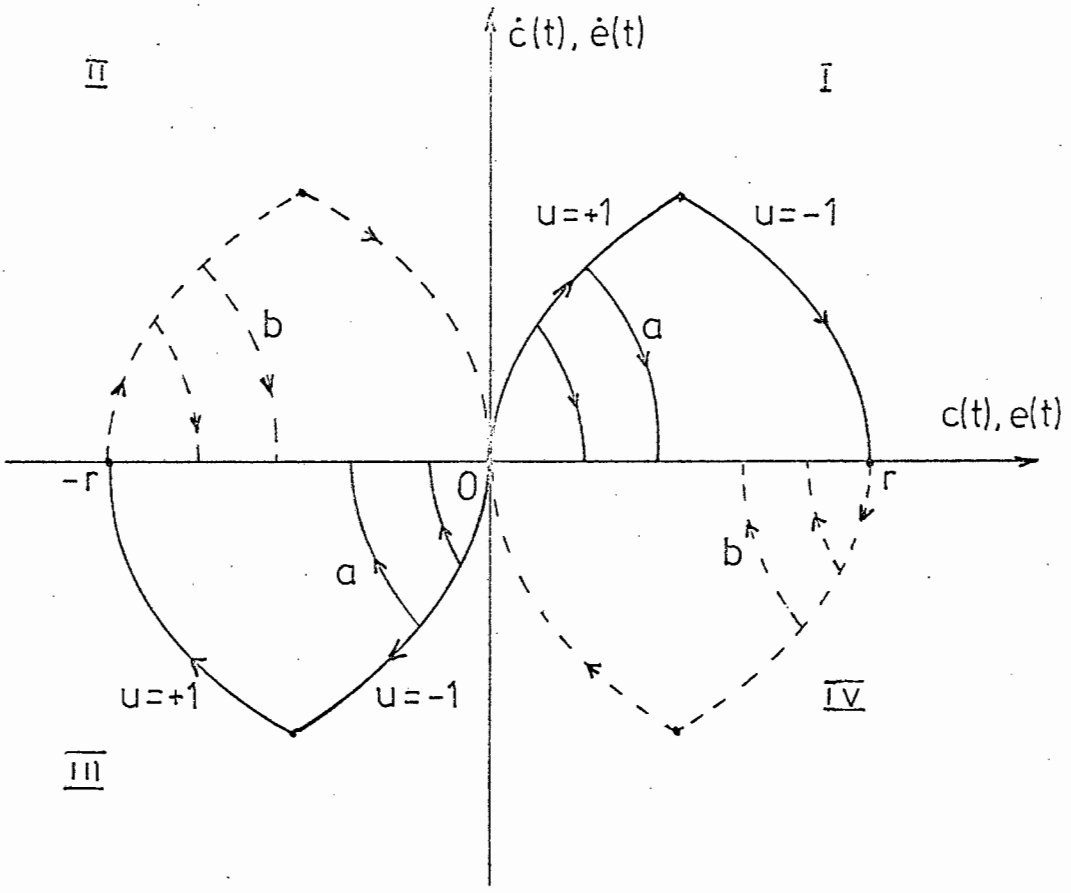

FIGURE 2.3.2
PHASE PLANE REPRESENTATION OF STATES AND ERROR-STATES

——→ STATE (OUTPUT) TRAJECTORIES
- - →- - ERROR STATE TRAJECTORIES
a FAST MODEL STATE TRAJECTORIES
b FAST MODEL ERROR STATE TRAJECTORIES

Once this is implemented the plant present states are introduced as initial conditions to the fast model and $u(\tau)$ the fast model input is set so that $u(\tau) = -u(t)$.

The future error $e(\tau)$ is then predicted and as soon as $\dot{e}(\tau) = 0$ (or crosses the abcissa) the fast model is 'held' and stops predicting and the current absolute value of $e(\tau)$ is compared with a small positive predetermined number e_p $(0 < e_p << 1)$.

If $|e(\tau)| > e_p$, the fast model is reset to a pair of new initial conditions obtained from the plant (the plant having moved an amount Δ along its trajectory) and allowed to run with $u(\tau) = -u(t)$. This process is iterated until $|e(\tau)| \leq e_p$.

At that point the plant drive is reversed i.e. $u(t) = -u(t)$ and the absolute plant output error $e(t)$, is compared with e_p. As long as $|e(t)| > e_p$ the plant error trajectory continues towards the error phase-plane origin.

When $|e(t)| \leq e_p$, $\dot{e}(t)$ is checked for $\dot{e}(t) \leq e_p$ and $u(t)$ is set to zero. The process is then halted.

The above procedure assumes a dead-beat trajectory i.e. one with neither overshoot nor undershoot.

To take undershoot and overshoot into consideration i.e. early switching or late switching, a minor modification takes place in the logic. Figure 2.3.3. shows this modification and Figure 2.3.4 depicts the new trajectories.

For trajectory -a (early switch) the plant drive is reversed and the fast model predicts the new trajectory for the plant error to go to zero.

Similarly for trajectory - b (late switch) the plant continues with its current drive while the fast model predicts the new trajectory for the plant error to go to zero.

Hence for multiple overshoots or for limit cycles the process iterates until the input u(t) is set to zero or an alternative control course of action is taken.

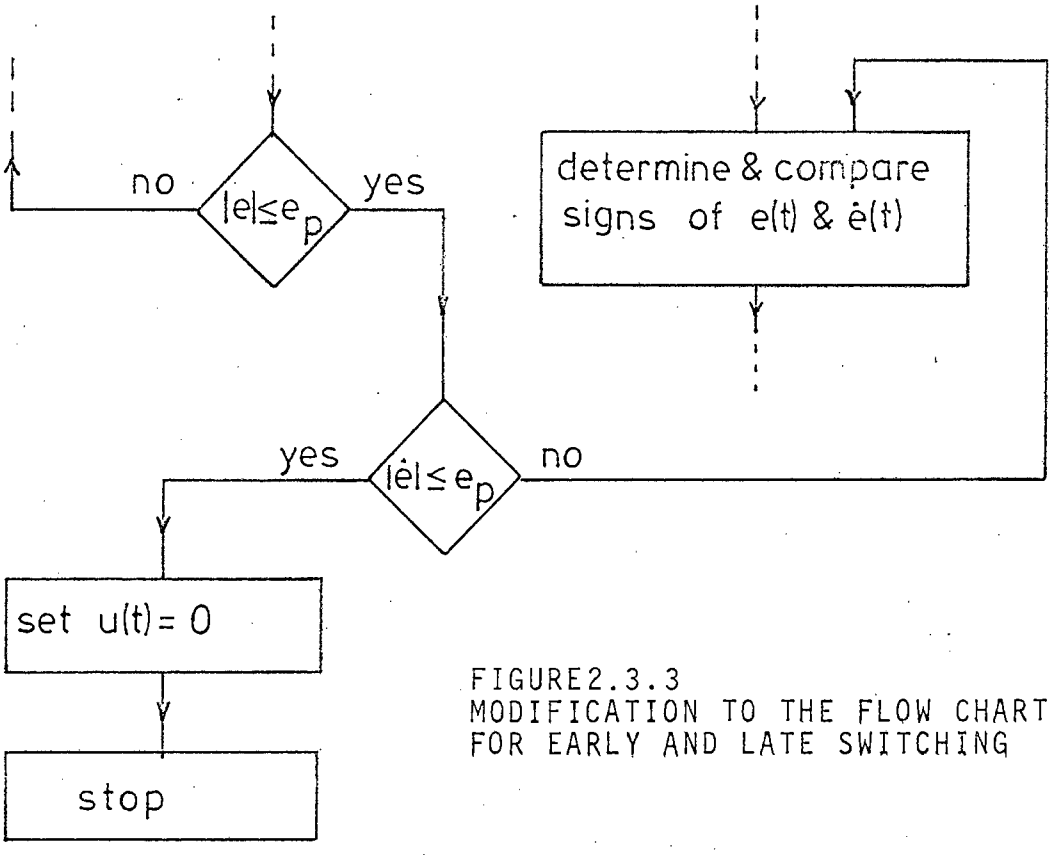

FIGURE2.3.3
MODIFICATION TO THE FLOW CHART
FOR EARLY AND LATE SWITCHING

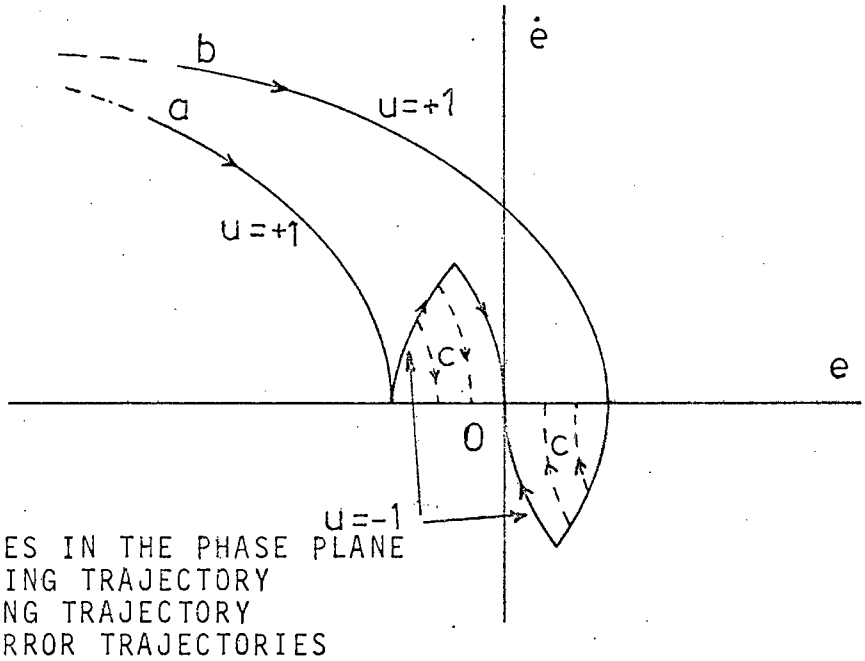

FIGURE 2.3.4
ERROR TRAJECTORIES IN THE PHASE PLANE
a - EARLY SWITCHING TRAJECTORY
b - LATE SWITCHING TRAJECTORY
c - FAST MODEL ERROR TRAJECTORIES

Generation of the Analogue Computer Diagram. From the flow chart it is evident that some means of setting the initial conditions for the fast model as well as a variable iteration rate has to be maintained. For the TR-48 analogue computer external relays were used to reset the fast model and reverse the plant and fast model drive.

The logic for determining the switching criteria was implemented through threshold detectors (signum functions) and comparators easily implemented on the computer while the remainder of the system followed conventional analogue computer practice.

The reference signal r(t), was taken as 5 volts while the inputs u(t) and u(τ) were taken $\pm$ 5 volts e_p took on valued $0 \leq e_p \leq .2$ volt.

In Appendix A6.1 is a complete block diagram for a double integrator plant (and fast model) with the external relays.

2.3.2. Stage 2. Description of a digital simulation of the fast model predictor control system.

The flow chart of Figure 2.3.1(b) can be easily transformed for implementation on a digital computer both for simulation and control purposes. The plant (or fast model) differential equations are used to obtain the trajectory equations in the phase plane and the state variable (output) response in the time domain. Both the phase plane representation and time response were used for demonstration and observation of system behaviour.

A second-order plant and model were used and Appendix A6.2 contains the necessary derivations and a programme actually used for a simulation.

2.3.3 Stage 3. Hybrid control for the simulation of a second-order system.

The methods of stage one and two of the previous sections are combined and a method of hybrid control is evolved to simulate a second-order fast model predictor system.

The TR-48 analogue computer is used to simulate the plant, i.e. a suitable second-order system is patched with the state variables conveniently arranged for connection to the Varian 600i digital computer and for recording on an X-Y plotter (see Figure 2.3.5).

The Varian 600i is used for the 'synthetic' fast model and the decision making for plant control. The signal conversions were implemented by the A to D and D to A converters installed on the Varian 600i and under direct control of the computer. There exists a sub-routine for instructing and calling the A to D and D to A converters in the "Basic" language.

In Appendix A6.3 is a description of the method and a programme for control of a second-order system.

2.3.4. Stage 4. Direct Digital control for a small D.C. motor.

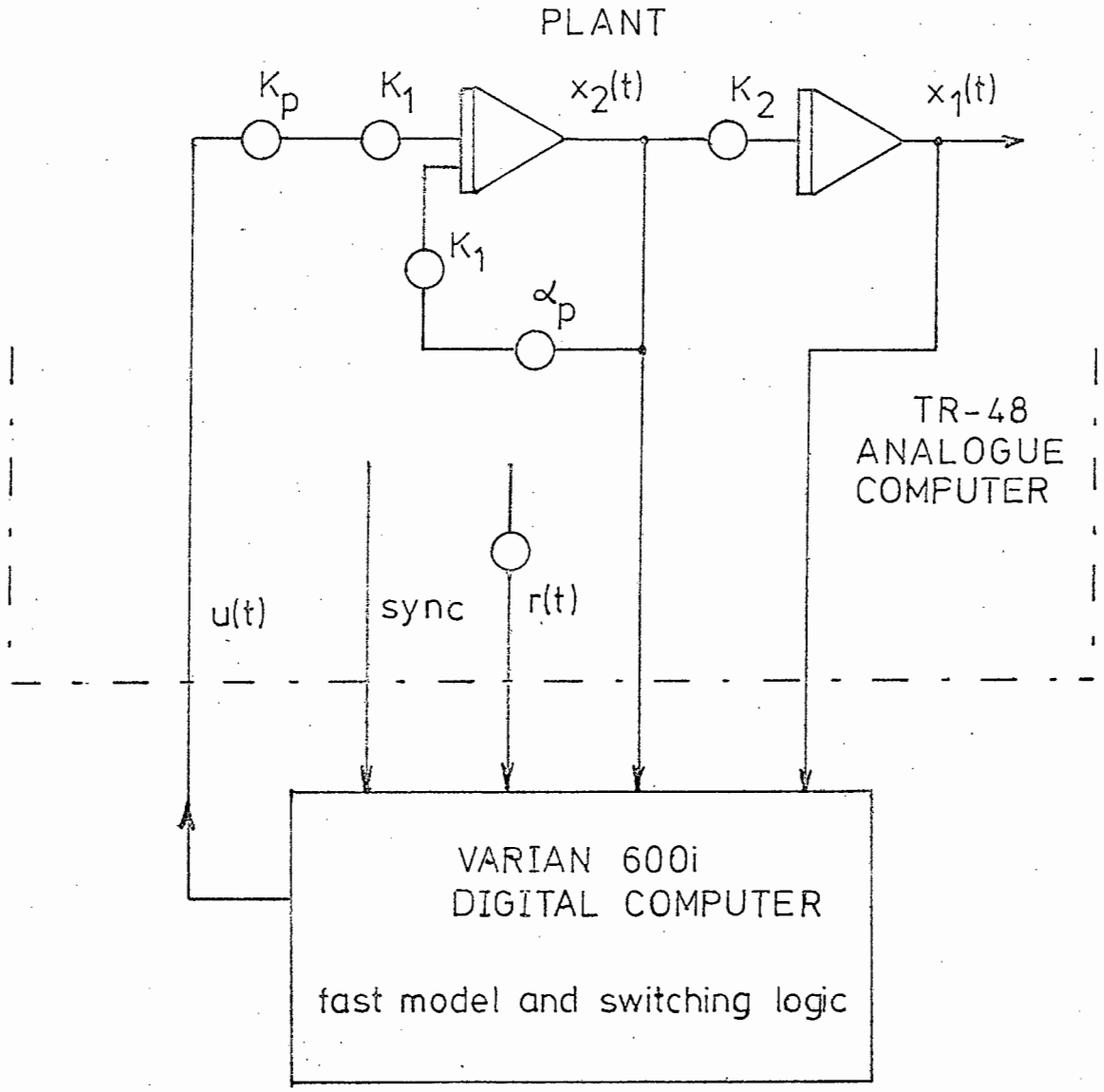

FIGURE 2.3.5
BLOCK DIAGRAM OF HYBRID CONTROL OF A SECOND-ORDER SYSTEM

In section 2.3.3 a programme was developed for controlling a second order plant simulated on an analogue computer. A real plant, viz. a small DC motor used for teaching purposes was selected as a suitable candidate to test the fast model predictor control.

The transfer function of this motor can be approximated to $\frac{K}{s(1+Ts)}$ since the motor was operated under no load conditions. This transfer function is identical to that used in the programme in section 2.3.3 and allowances were made for the plant gain and time constant.

A plotter was used to record the output position in response to a step input. In Appendix A6.4 is an account of this procedure and a block diagram of the system.

2.4. Simulation results

2.4.1. Analogue computer simulations.

In its simplest form the plant transfer function was taken as

$$G_p(s) = \frac{K_p}{s(s+\alpha_p)} \qquad (2.4.1)$$

and the fast model transfer function as

$$G_m(s) = \frac{K_m}{s^2} \quad \text{for a double integrator} \qquad (2.4.2)$$

or

$$G_m(s) = \frac{K_m}{s(s+\alpha_m)} \quad \text{for one integrator and one lag} \qquad (2.4.3)$$

Since the plant parameters will in general not be known exactly, consideration was given to the effects of inaccuracies in the gain and time constant parameters of the second order control system. Consideration was also given to the problems of time-lags and the non-ideal behaviour of the relays. The analogue computer was also prone to drift and thermal effects, hence required constant 'tuning' for satisfactory operation. There were also deficiencies in the non-linear elements.

Figure 2.4.1 compares the error and error-rate responses of the plant (equation 2.4.1) for a double integrator fast model, a step reference of -5 volts was applied. The time constant $\frac{1}{\alpha_p}$, was varied for

curves 1 : $\alpha_p = .2$

curves 2 : $\alpha_p = .14$

curves 3 : $\alpha_p = .04$

For this run the model to plant time ratio was 30:1 and for the following runs was subsequently increased to 50:1.

As can be observed the plant output settled with slight overshoot for $\alpha_p = .2$, while for $\alpha_p = .04$ the overshoot was much increased. Although in curves 3 the model approximates the plant and one would anticipate a dead-beat type response, relay switching delays and even a 50% difference in the model and plant gains can cause a 100% increase in settling time (see table 1.5.1).

From equation 1.5.6, the settling time for a double integrator plant is (for the above example)

$$T_{aa} = (2a\, x_1^o)^{\frac{1}{2}}\, 2^{\frac{1}{2}} \qquad (2.4.4)$$

where $x_1^o = 5v$ and $a = \frac{1}{5x(.0282)^2} = 251.5$

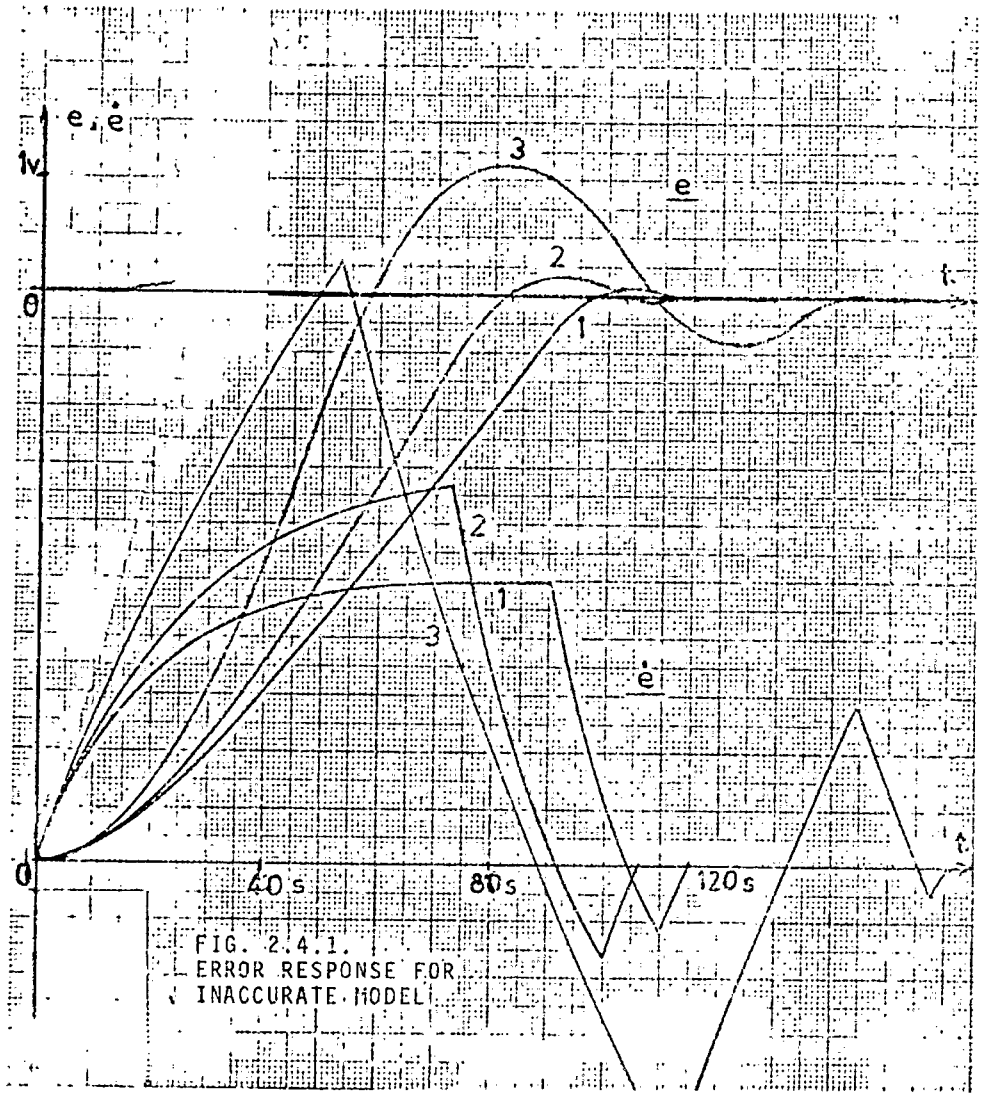

FIG. 2.4.1.
ERROR RESPONSE FOR
INACCURATE MODEL

.0282 was a scale factor introduced to slow down the integration rates in the plant, while the input was $\pm$ 5 volts. Substituting these values into equation 2.4.4 yields T_{aa} = 71 seconds. The measured value of settling time was 160 seconds, a 125% increase in settling time over the optimal.

Prior experimentation had shown that the relays used were limited to a slow switching rate and there were obvious bounds on the lower and upper fast model to plant time ratios. By suitably 'tuning' the computer, an increase in the settling time over the optimal of $< 10\%$ for the double integrator was achieved.

Figure 2.4.2 is the phase-plane representation of Figure 2.4.1 for both positive and negative references.

Figure 2.4.3 represents the error and error-rate responses for a step reference when the plant and model were matched. Here $G_p(s) = \frac{1}{s(s+.2)}$ and $G_m(s) = \frac{K_m}{s(s+\alpha_m)}$ and both K_m and α_m are varied.

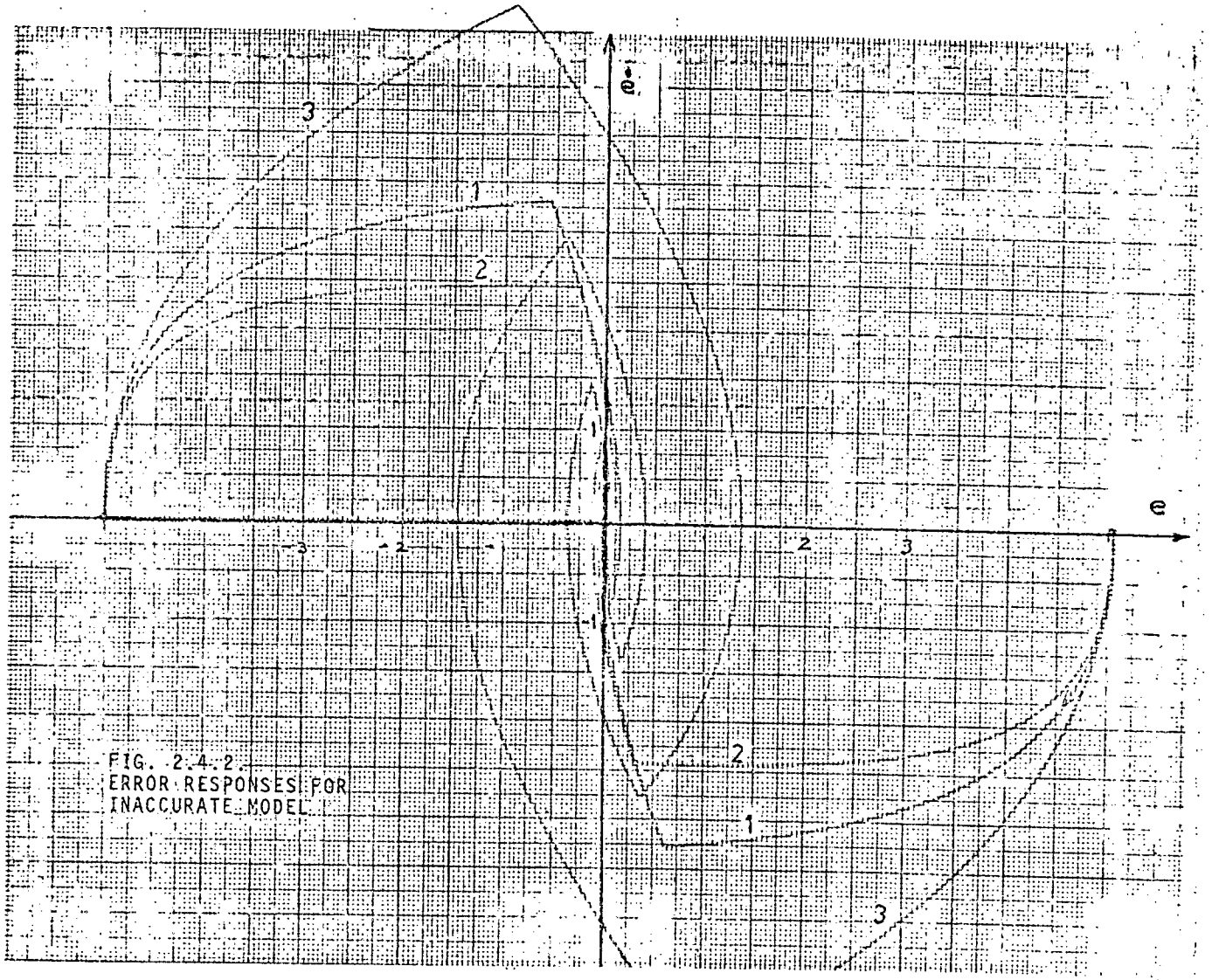

FIG. 2.4.2.
ERROR RESPONSES FOR
INACCURATE MODEL

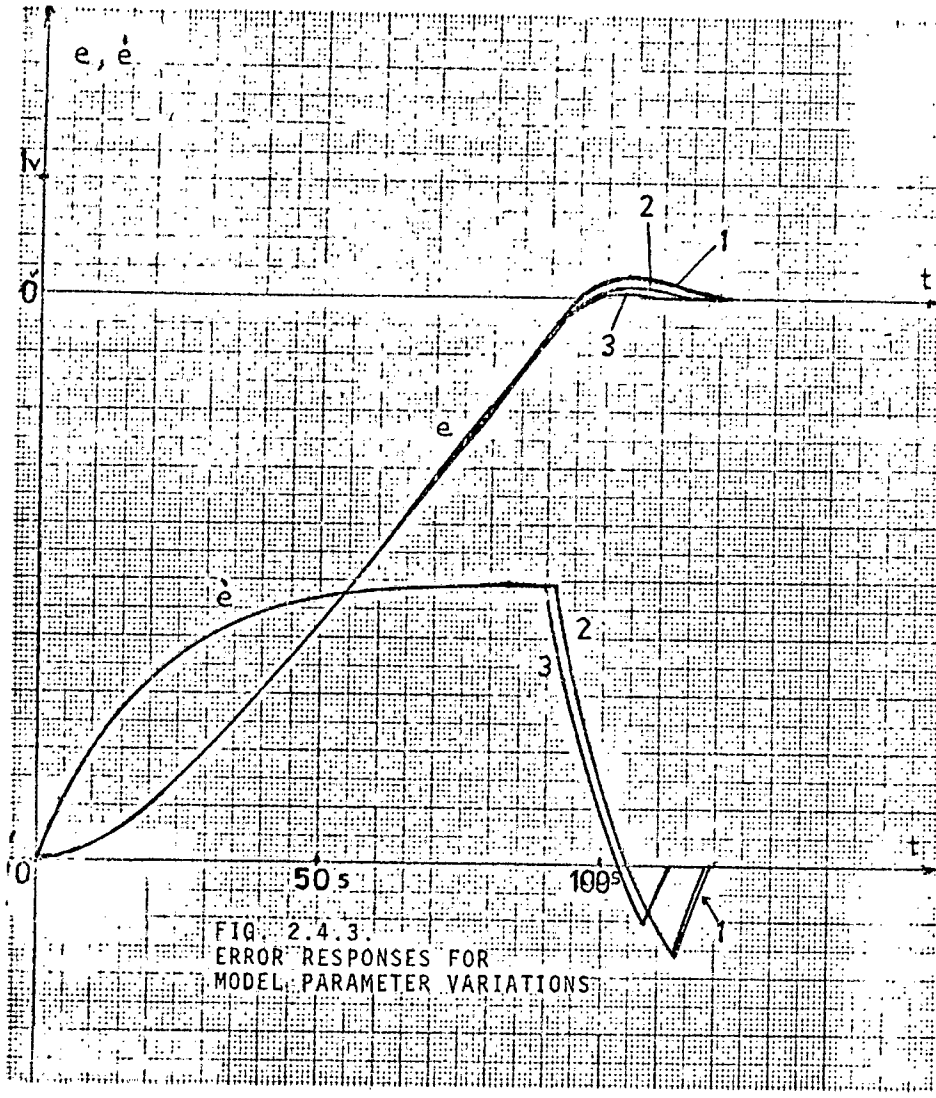

FIG. 2.4.3.
ERROR RESPONSES FOR
MODEL PARAMETER VARIATIONS

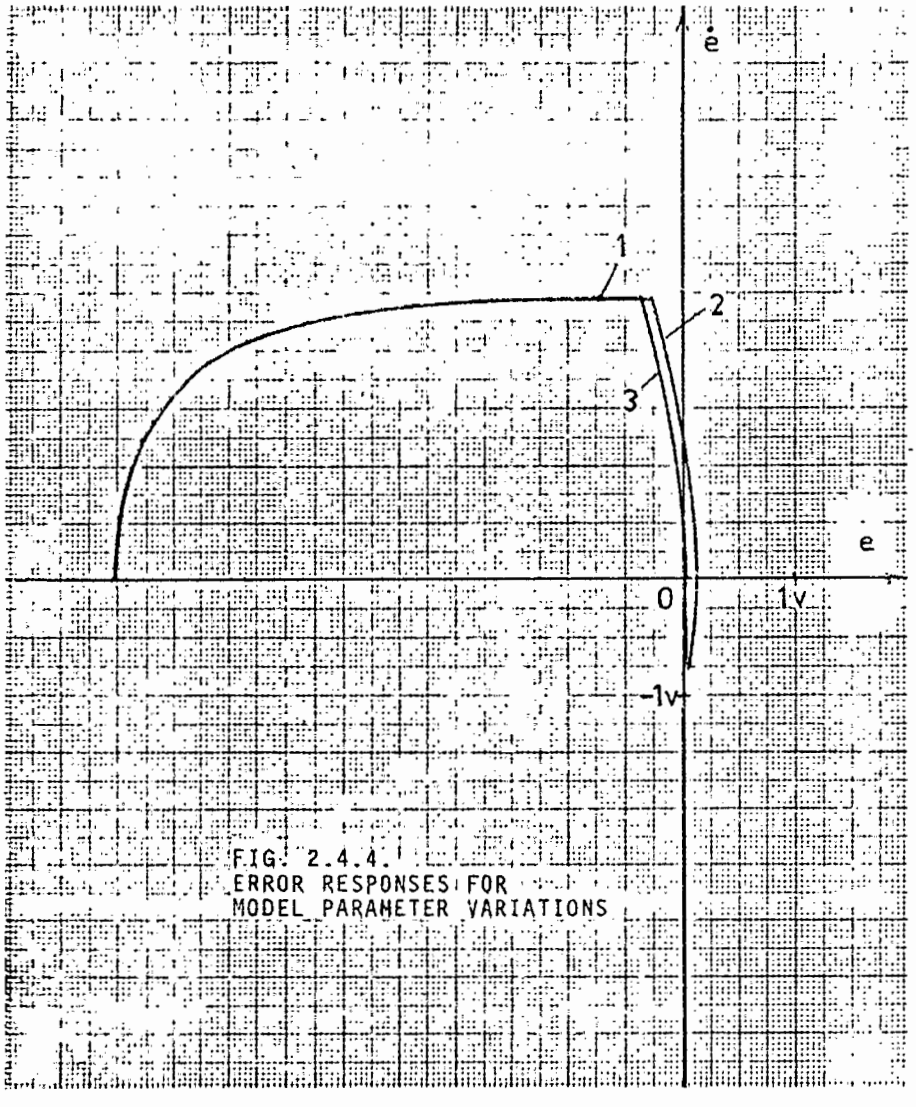

FIG. 2.4.4.
ERROR RESPONSES FOR
MODEL PARAMETER VARIATIONS

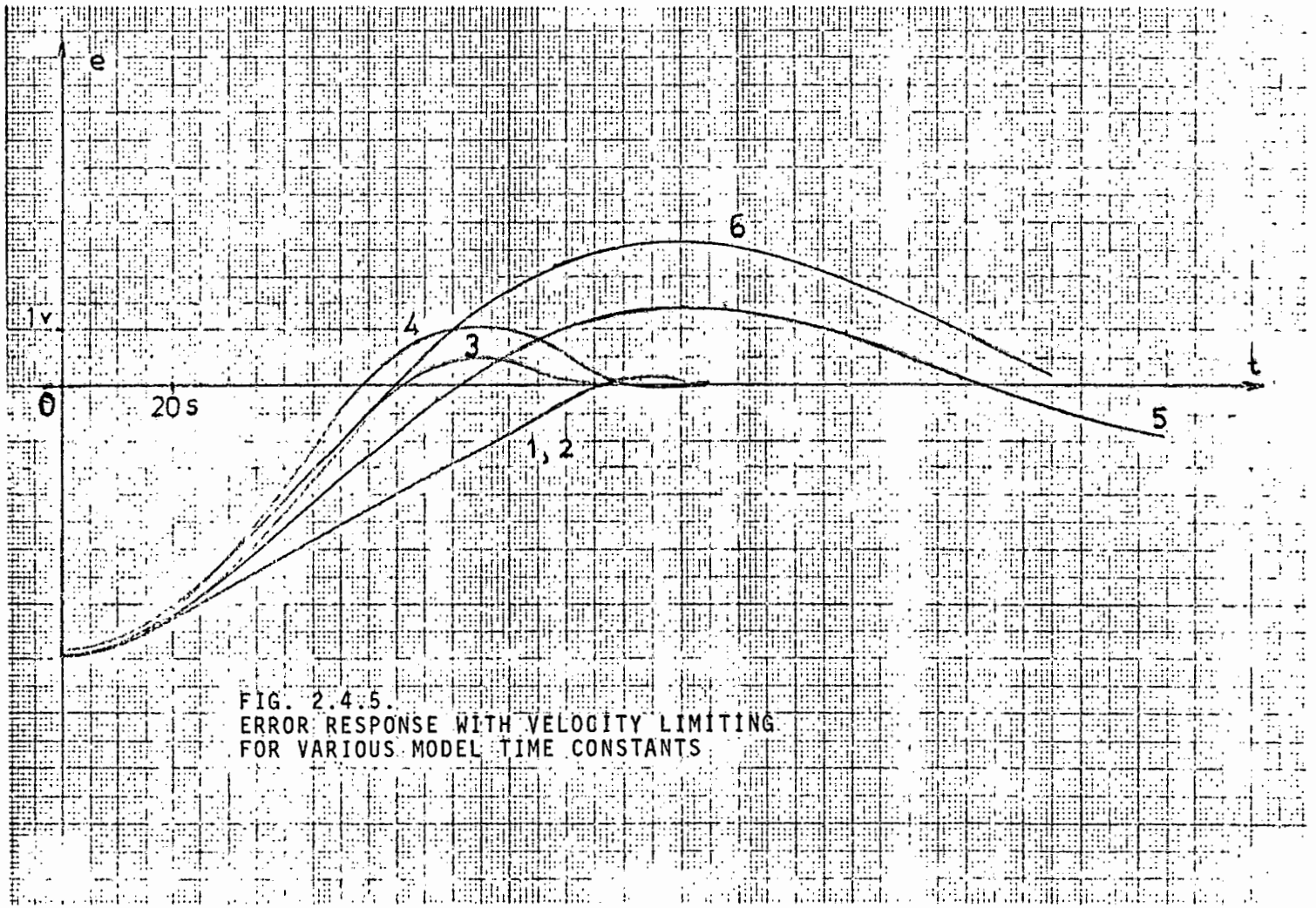

FIG. 2.4.5.
ERROR RESPONSE WITH VELOCITY LIMITING
FOR VARIOUS MODEL TIME CONSTANTS

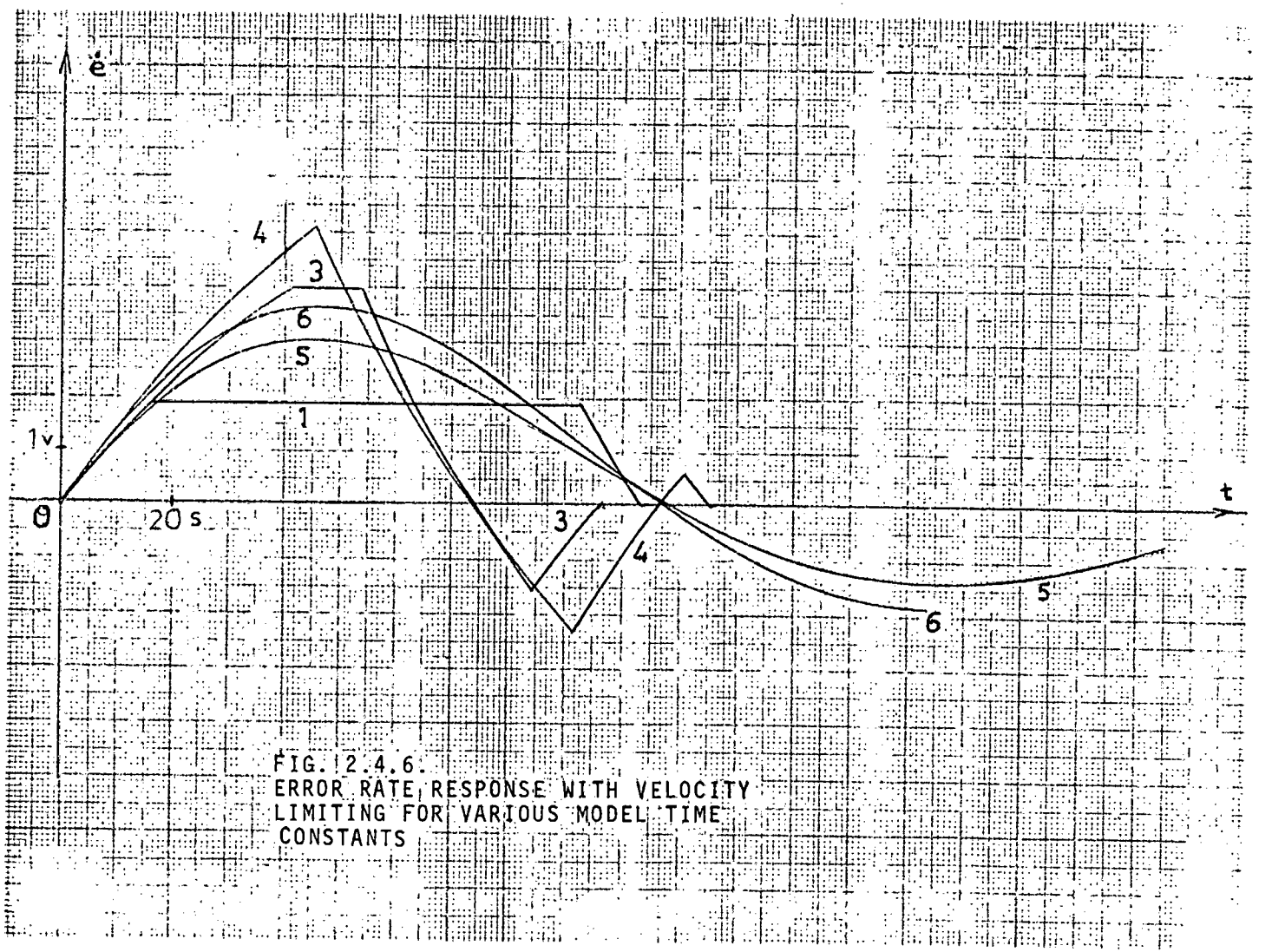

FIG. 12.4.6.
ERROR RATE RESPONSE WITH VELOCITY LIMITING FOR VARIOUS MODEL TIME CONSTANTS

For these curves both α_p and α_m were varied as listed below. Furthermore curves 5 and 6 represent proportional control to illustrate the different characteristics.

Curves No.	α_p	α_m	Limiting
1 :	.5	.05	1.9 volts
2 :	.5	3	1.9 volts
3 :	.5	.05	4.0 volts
4 :	.5	.05	No velocity limiting
5 :	.5	proportional plus differential control, w = 1 and	limiting = 3.0 volts
6 :	.5	proportional plus differential control, w = 1 and no velocity limiting.	

As can be seen, heavy velocity limiting of the plant (similar in behaviour to a heavily damped system) resulted in a virtually time-optimal response (curves 1 and 2) while moderate limiting effectively reduced the overshoot hence settling time (curves 3 and 4). The settling time for proportional control is seen to be much longer as anticipated. Again a 'livelier' fast model mini-

mized the plant settling time except for a heavily velocity limited plant when variation of the fast model time constant had little effect on the overall response.

The representation of a controlled system as a second-order system is often a simplified assumption. In the results that follow, the plants considered had transfer functions of the form.

$$G_p(s) = \frac{K_p}{s(s+\alpha_1)(s+\alpha_2)} \qquad (2.4.5)$$

$$G_p(s) \quad \frac{K_p}{s(s+\alpha_p\ s+1)} \qquad (2.4.6)$$

$$G_p(s) = \frac{K_p}{s(s+\alpha_1)(s+\alpha_2)(s+\alpha_3)(s+\alpha_4)} \qquad (2.4.7)$$

It is possible to control in a sub-optimal manner certain third or fourth-order systems with only a second-order model. Obviously for third or higher ordered systems (see Chapters four and five) the switching logic is far more complex. However it was decided to investigate what the penalties were by keeping the simple second-order switching logic controller.

The effect of adding significant time constants to the plant was to increase the initial overshoot and settling time, and if carried to extremes, caused sustained oscillation of the system in its steady-state, and even instability.

Figure 2.4.7 represents the error response of a third-order system and a second order model to a step reference for variations in α_1 and α_2. The plant transfer function has the form of equation 2.4.5 and the fast model transfer function is $G_m(s) = \frac{1}{s(s+.2)}$ and $K_p = 1$. The responses are listed as follows:

Curve No.	α_1	α_2
1 :	1	2
2 :	2	2
3 :	1	5

As can be seen from curves 1, 2 and 3, the significance of the time-constants had precisely the abovementioned effects.

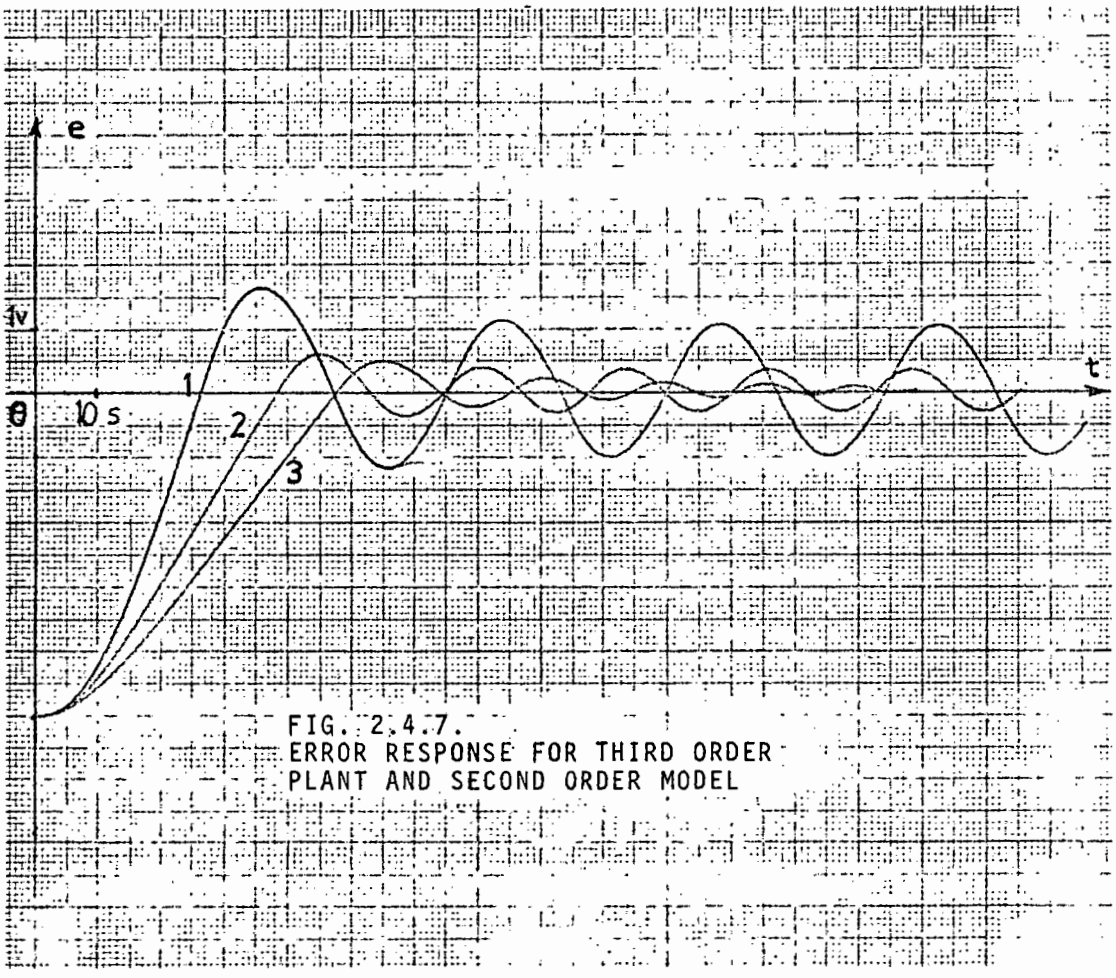

FIG. 2.4.7.
ERROR RESPONSE FOR THIRD ORDER
PLANT AND SECOND ORDER MODEL

For the third-order plant corresponding to equation 2.4.6, Figures 2.4.8. and 2.4.9. display the error and error-rate responses respectively for a second-order model $G_m(s) = \frac{1}{s(s+.2)}$ under a step reference, and $K_p = 1$. The responses are listed as follows:

Curve No.	α_p
1 :	1
2 :	2
3 :	4
4 :	10

As can be seen for α_p $(= \frac{1}{T_p}) = 1$, the plant response in unstable. For values of $\alpha_p > 1$ the response is oscillatory but damped and the settling time is greatly increased. Third order plants that have complex poles are generally more difficult to control than those with pure lags.

Figure 2.4.10 is the error response of a fourth-order plant described by equation 2.4.7 and a second-order model $G_m(s) = \frac{1}{s(s+.5)}$ and $K_p = 1$ for a step reference. The responses are

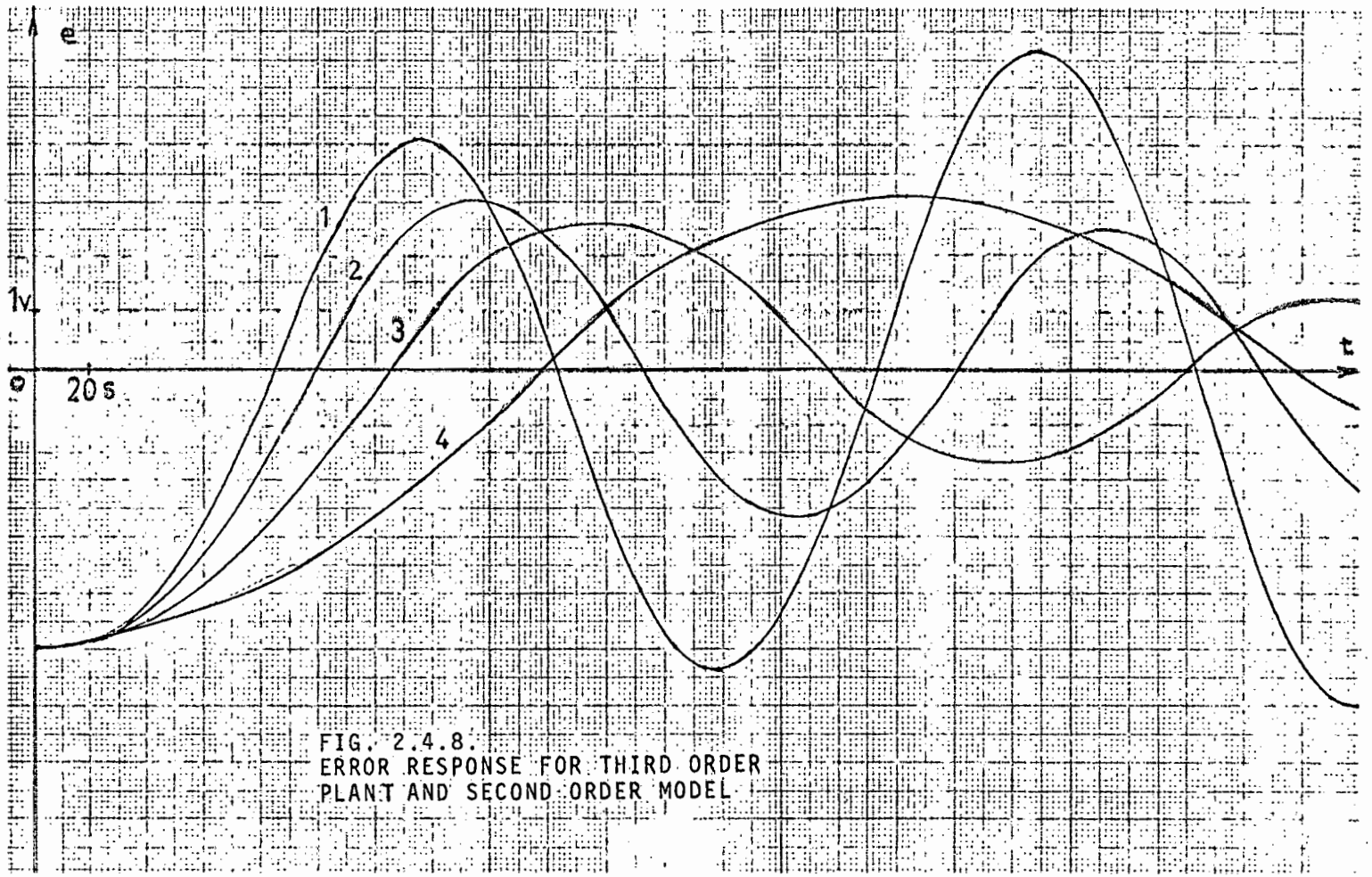

FIG. 2.4.8.
ERROR RESPONSE FOR THIRD ORDER
PLANT AND SECOND ORDER MODEL

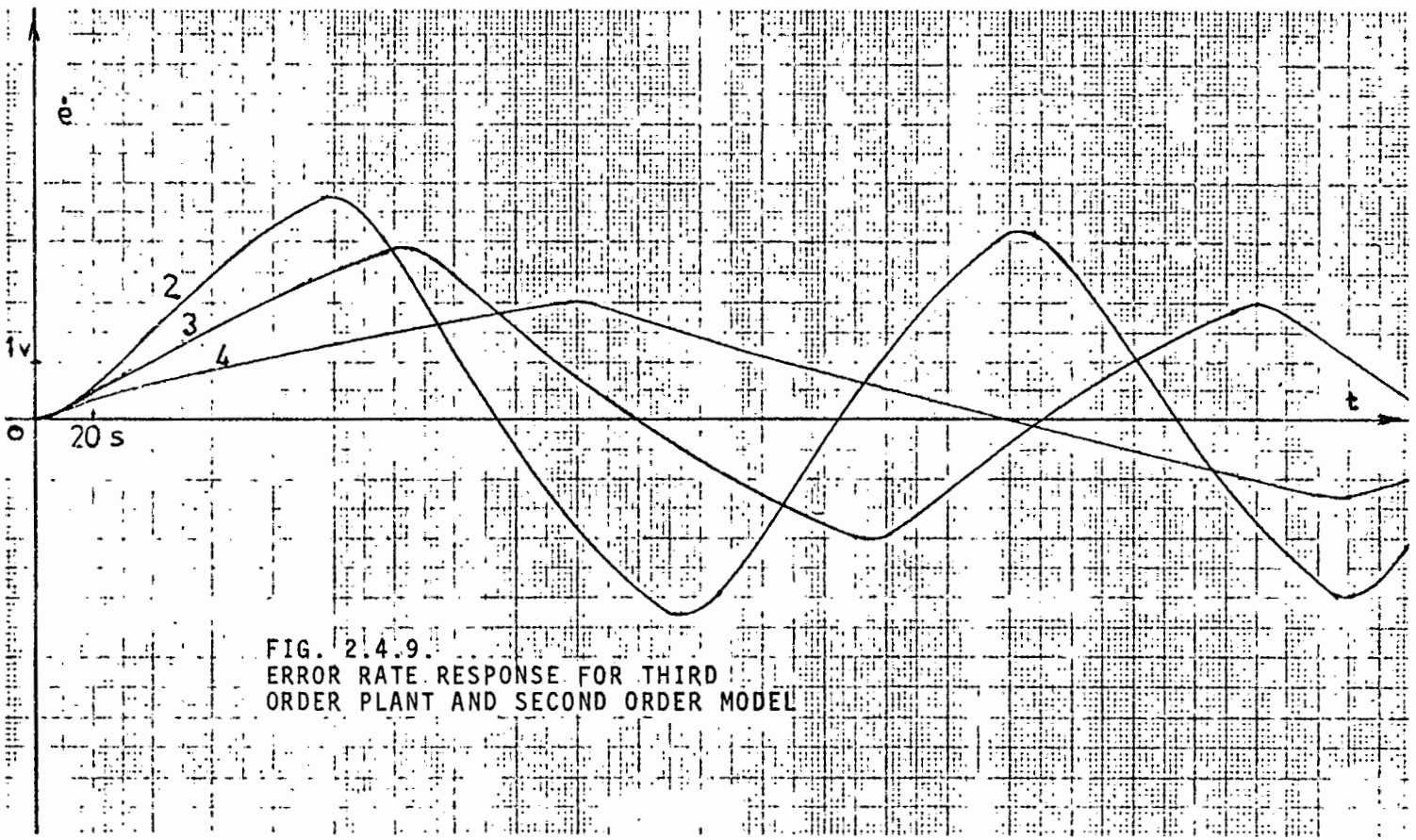

FIG. 2.4.9.
ERROR RATE RESPONSE FOR THIRD ORDER PLANT AND SECOND ORDER MODEL

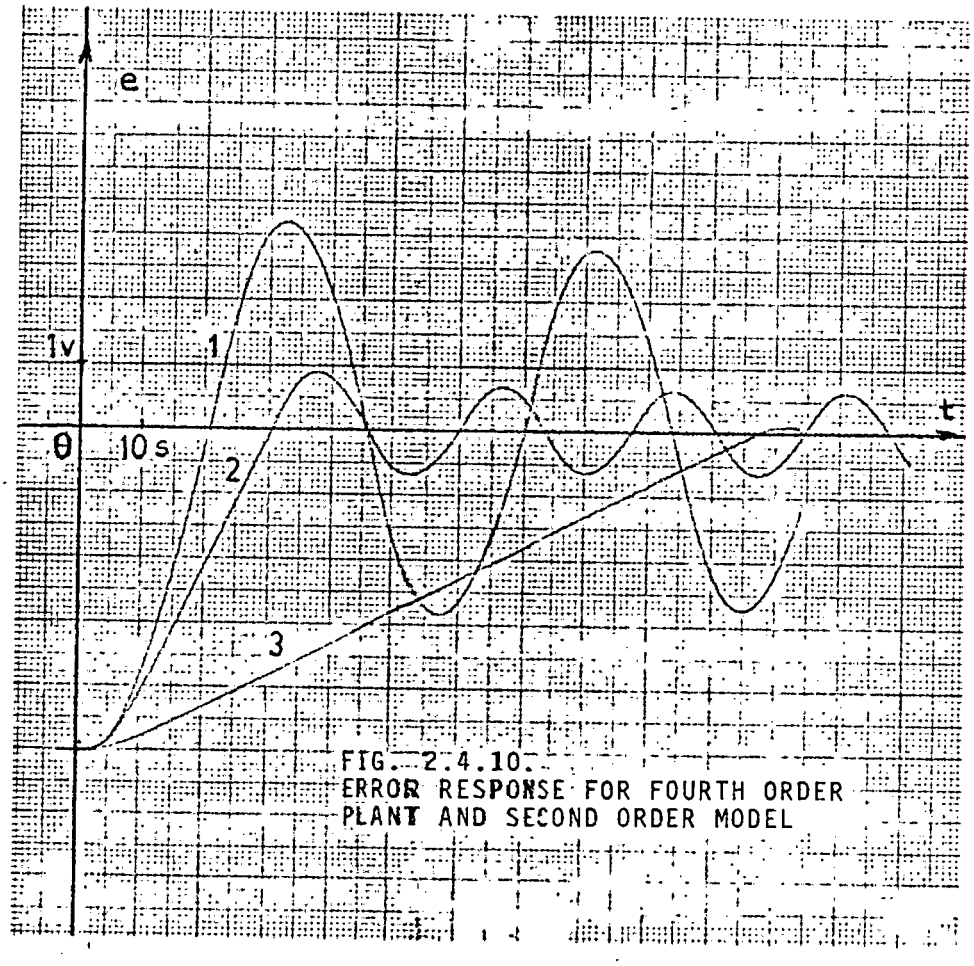

FIG. 2.4.10.
ERROR RESPONSE FOR FOURTH ORDER PLANT AND SECOND ORDER MODEL

Curve No.	α_1	α_2	α_3
1 :	1	5	.5
2 :	1	2	3
3 :	1	10	3

The responses (1, 2 and 3) serve to augment the remarks made concerning Figure 2.4.7 for the third order plant.

Figure 2.4.11 is a comparison of the responses of a fourth-order plant (as in equation 2.4.7), a third-order plant (as in 2.4.5) and a second order plant (as in equation 2.4.1), the model transfer function is $G_m(s) = \frac{1}{s(s+.5)}$ and $K_p = 1$.

The reference is a step of -5 volts. The responses are

Curve No.	α_1	α_2	α_3
1 :	1	3	2
2 :	1	3	
3 :	1		

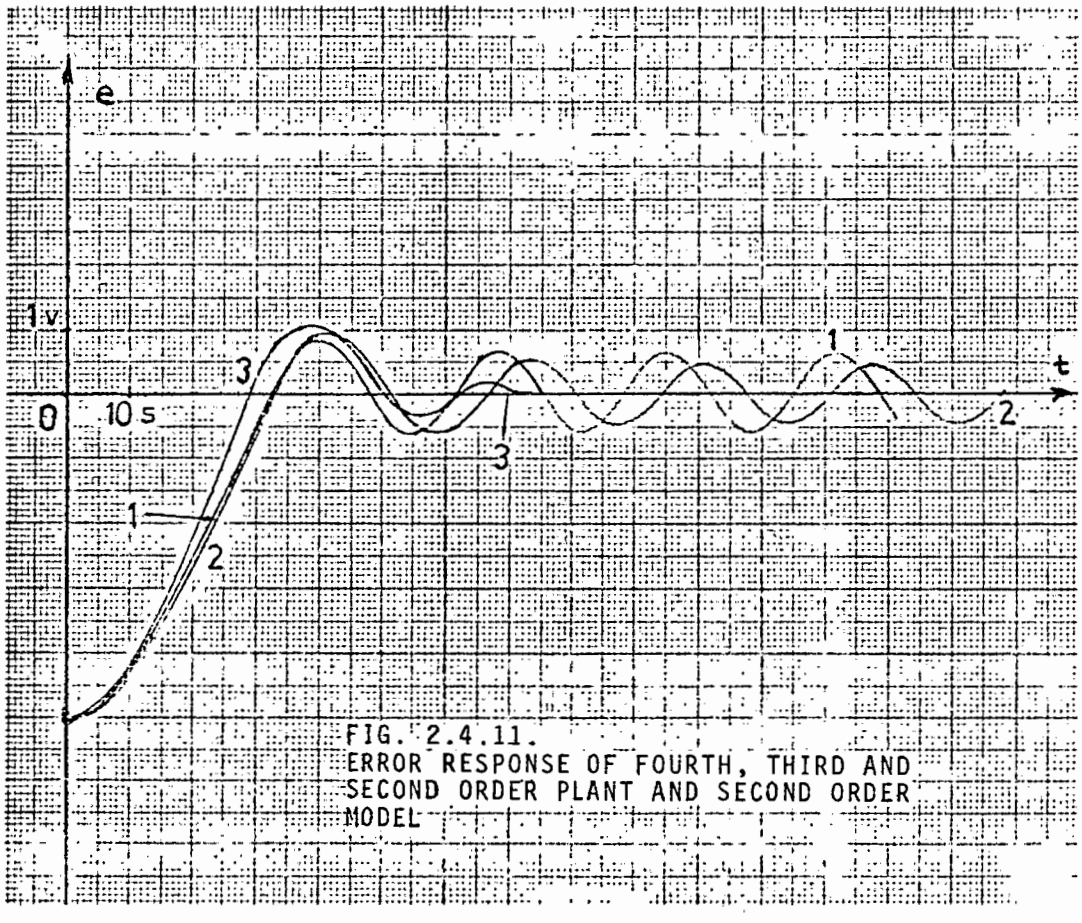

FIG. 2.4.11.
ERROR RESPONSE OF FOURTH, THIRD AND SECOND ORDER PLANT AND SECOND ORDER MODEL

As can be seen the fourth and third order plant responses are similar, with sustained oscillation about the steady-state, whereas the second-order plant has a short oscillatory response before reaching steady-state for this particular model to plant match.

2.4.2. Digital Simulation.

The digital simulations were performed in order to analyse the parameter variations of the equations governing the system behavious in a systematic manner and with a view to hybrid control. With the computing facilities available, the graphical response of a second-order plant (similar to equation 2.4.1) was obtained on a VDU and hardcopied.

A fast model to plant ration of 50:1 was used and the nominal plant and model gain was set to unity. The plant transfer function used was

$$G_p(s) = \frac{K_p K_1 K_2}{s(s+\alpha_p)} \qquad (2.4.8)$$

and the model transfer used was

$$G_m(s) = \frac{K_m K_3 K_4}{s(s+\alpha_m)} \qquad (2.4.9)$$

where $K_p = K_m = 1$ (nominal) and $K_1 = .12$, $K_2 = .6667$, $K_3 = 6.00$ and $K_4 = 33.333$. In all examples considered the reference is a step of magnitude 5 units.

Figure 2.4.12. represents the output position response for variation in K_1 about the nominal value and $\alpha_p = \alpha_m = .2$, $K_p = K_m = 1$. The values of K_1 and the curves are listed below;

Curve 1 : K_1 = nominal (=.12)

Curve 2 : K_1 = decrease of 20% (=.096)

Curve 3 : K_1 = increase of 20% (=.144)

The decrease in K_1 may be expressed in the ratio "$\frac{a}{b}$" of section 1.5 viz. $\frac{K_1(\text{nom})}{K_1} = 1{,}2$ and the overshoot of curve 2 results, thus confirming the sensitivity assertions in section 1.5. Similarly for $\frac{K_1(\text{nom})}{K_1} = .8$ the undershoot of curve 3 results. Curve 1 is the nominal time-optimal curve.

Figure 2.4.13. has the same format as for Fig. 2.4.12. except K_2 is the parameter being varied. In this case the response is quite different.

Curve 1 : K_2 = nominal (=.6666)

Curve 2 : K_2 = decrease of 20% (= .5334)

Curve 3 : K_2 = increase of 20% (= .7998)

For a decrease in the position integrator gain the response is reduced and undershoots with the maximum settling time. For an increase in the position integrator gain the response is enhanced with the fastest rise time and with some overshoot. From Figure A.6.2.1 of Appendix A.6.2 and is easily seen that variations in K_2 would produce the above response curves. Curve 1 is the nominal time-optimal curve.

Figure 2.4.14. is the response for the variations in the plant gain parameter K_p, and it follows the same pattern as for K_1. The curves are;

Curve 1 : K_p = nominal (=1)

Curve 2 : K_p = decrease of 20% (=0,8)

Curve 3 : K_p = increase of 20% (=1,2)

Hence for curve 2 $\frac{K_p(nom)}{K_p}$ = 1,2 and for curve 3 $\frac{K_p(nom)}{K_p}$ = 0,8. Curve 1 is the nominal time-optimal curve.

Figure 2.4.15. is the response for the variations in the plant time constant parameters or lags α_p.

Curve 1 : $\alpha_p = \alpha_m = .2$

Curve 2 : $\alpha_p = .1$ $\alpha_m = .2$ (α_p decreased by 50%)

Curve 3 : $\alpha_p = .4$ $\alpha_m = .2$ (α_p increased by 100%)

It can be seen that all three responses are similar. For the more 'livelier' plant the rise time is slightly shorter than the less livelier plant viz. curve 3. This result has bearing in Chapter 3.

Figure 2.4.16. is the same as Figure 2.4.15. except α_m is the variable and has large variations.

Curve 1 : $\alpha_m = \alpha_p = 1$

Curve 2 : $\alpha_m = .01$ $\alpha_p = 1$

Curve 3 : $\alpha_m = 5$ $\alpha_p = 1$

For a 'lively model i.e. close to the double integrator model the switching is early and there is some undershoot as seen in curve 2. For a 'sluggish' model the switching is late and the overshoot of curve 3 results. Curve 1 is the nominal time optimal curve.

Figure 2.4.17. is the error phase-plane representation of curve 3 in Figure 2.4.16.

2.4.3. Hybrid simulation.

The hybrid simulation is a logical follow-up of section 2.4.2. Additional experimentation consisted of velocity limiting, a second-order plant of two lags and a third-order plant.

The plant transfer function is the same as equation 2.4.8. and the model transfer function is the same as 2.4.9. The reference is a step of 5 volts, $K_p = K_m = 1$ (nominal), $K_1 = K_3 = .03$ and $K_2 = K_4 = .166$.

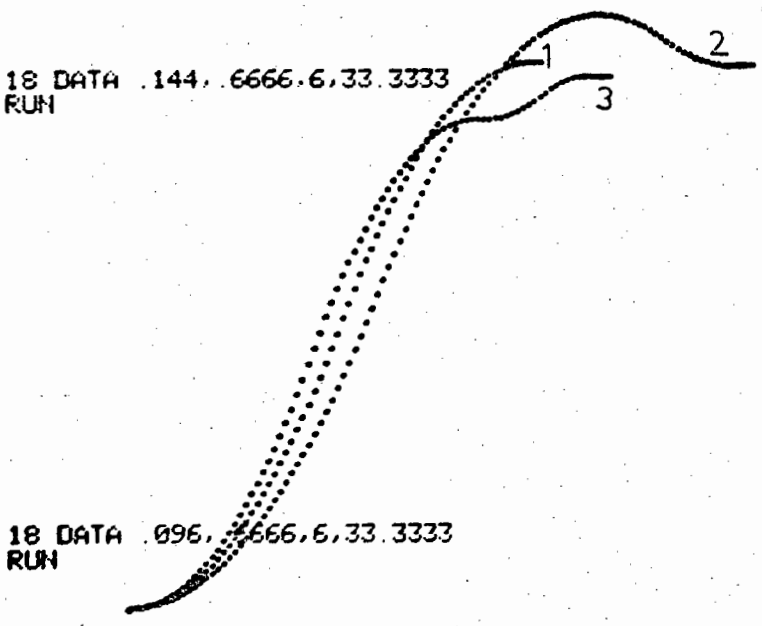

FIG. 2.4.12.
POSITION RESPONSE OF A SECOND ORDER PLANT WITH A FAST MODEL CONTROLLER FOR VARIATION IN K_1

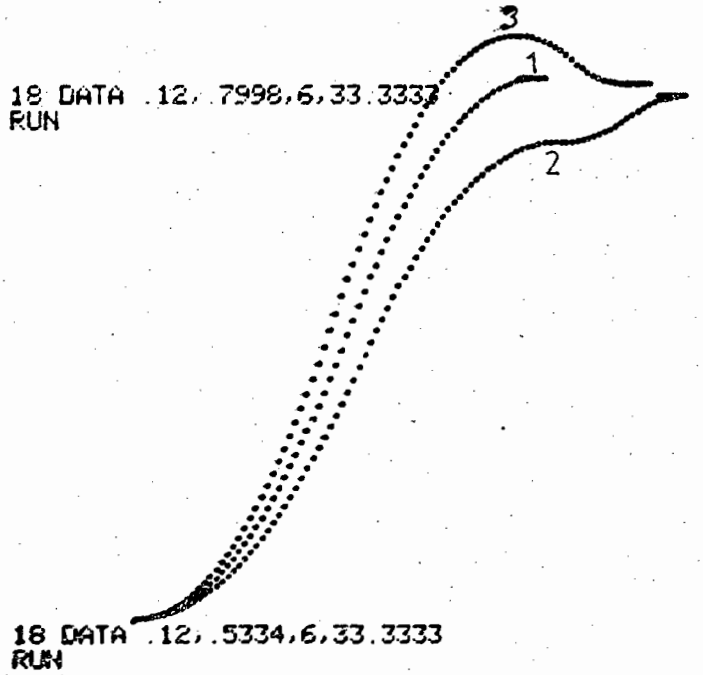

FIG. 2.4.13.
POSITION RESPONSE OF A SECOND ORDER PLANT WITH A FAST MODEL CONTROLLER FOR VARIATION IN K_2

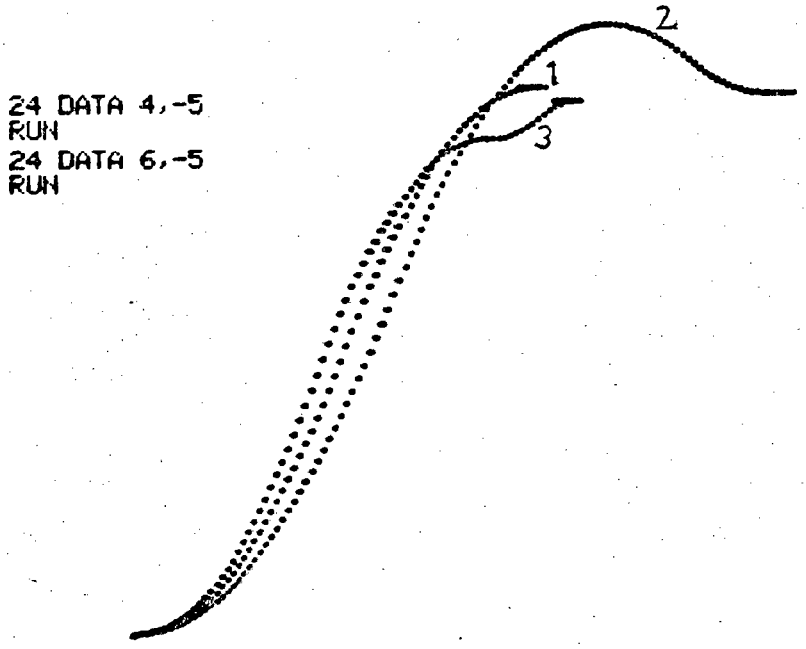

FIG. 2.4.14.
POSITION RESPONSE OF A SECOND ORDER PLANT AND A FAST MODEL CONTROLLER FOR VARIATION IN K_p

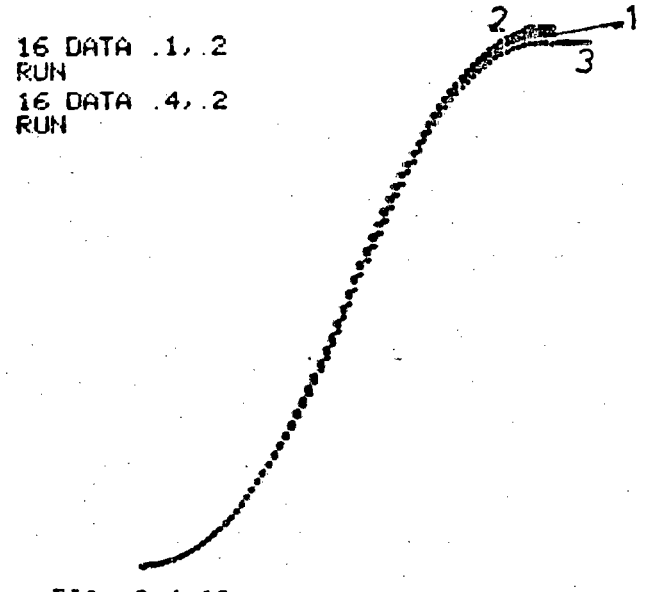

FIG. 2.4.15.
POSITION RESPONSE OF A SECOND ORDER PLANT AND FAST MODEL CONTROLLER FOR GROSS VARIATION IN α_m

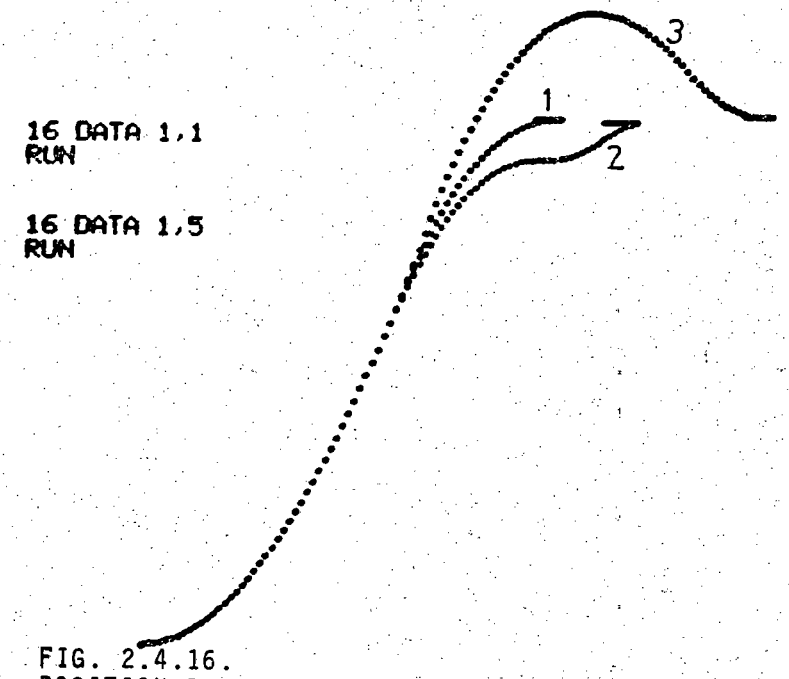

FIG. 2.4.16.
POSITION RESPONSE OF A SECOND ORDER PLANT AND FAST MODEL CONTROLLER FOR GROSS VARIATION IN α_m

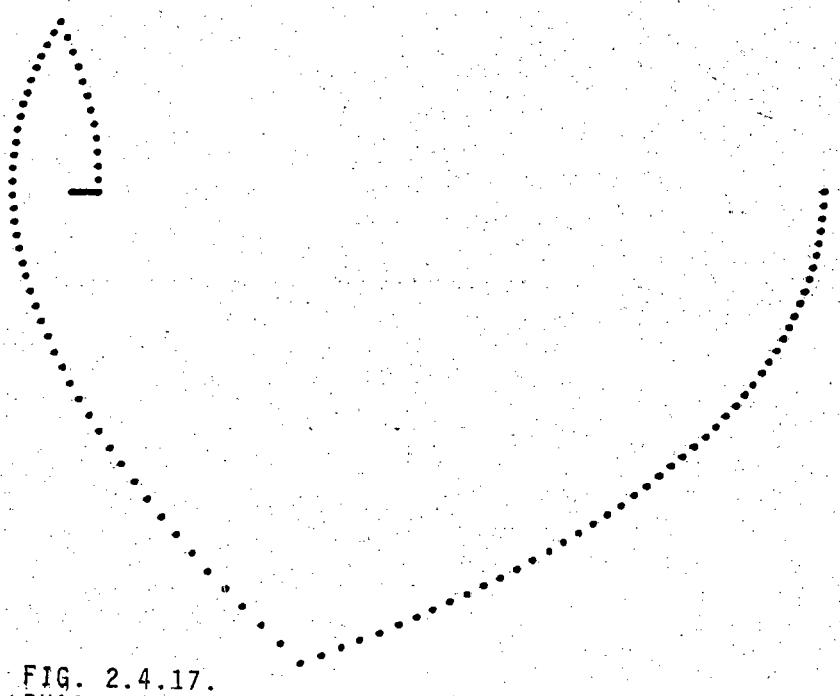

FIG. 2.4.17.
PHASE-PLANE REPRESENTATION OF CURVE 3 IN FIGURE 2.4.16.

Figure 2.4.18. is the position response of a second-order plant where $G_p(s)$ is given by equation 2.4.8. which is $G_p(s) = \frac{K_p K_1 K_2}{s(s+.5)}$ and $G_m(s) = \frac{K_m K_3 K_4}{s(s+.5)}$. The plant gain parameter K_p is varied.

Curve 1 : K_p = Nominal (=1)

Curve 2 : K_p = 20% increase (=1.2)

Curve 3 : K_p = 20% decrease (=.8)

The responses of all the three curves were virtually identical to that in Figure 2.4.14. of the digital simulation, as was expected.

Figure 2.4.19. displays the responses for variations in the plant lag for the same basic set of conditions as above.

Curve 1 : $\alpha_p = \alpha_m = .5$

Curve 2 : $\alpha_p = .1 \quad \alpha_m = .5$

Curve 3 : $\alpha_p = 1 \quad \alpha_m = .5$

The responses were as expected and were virtually identical to those examined in Figure 2.4.16. of the digital simulation. The conclusion drawn here

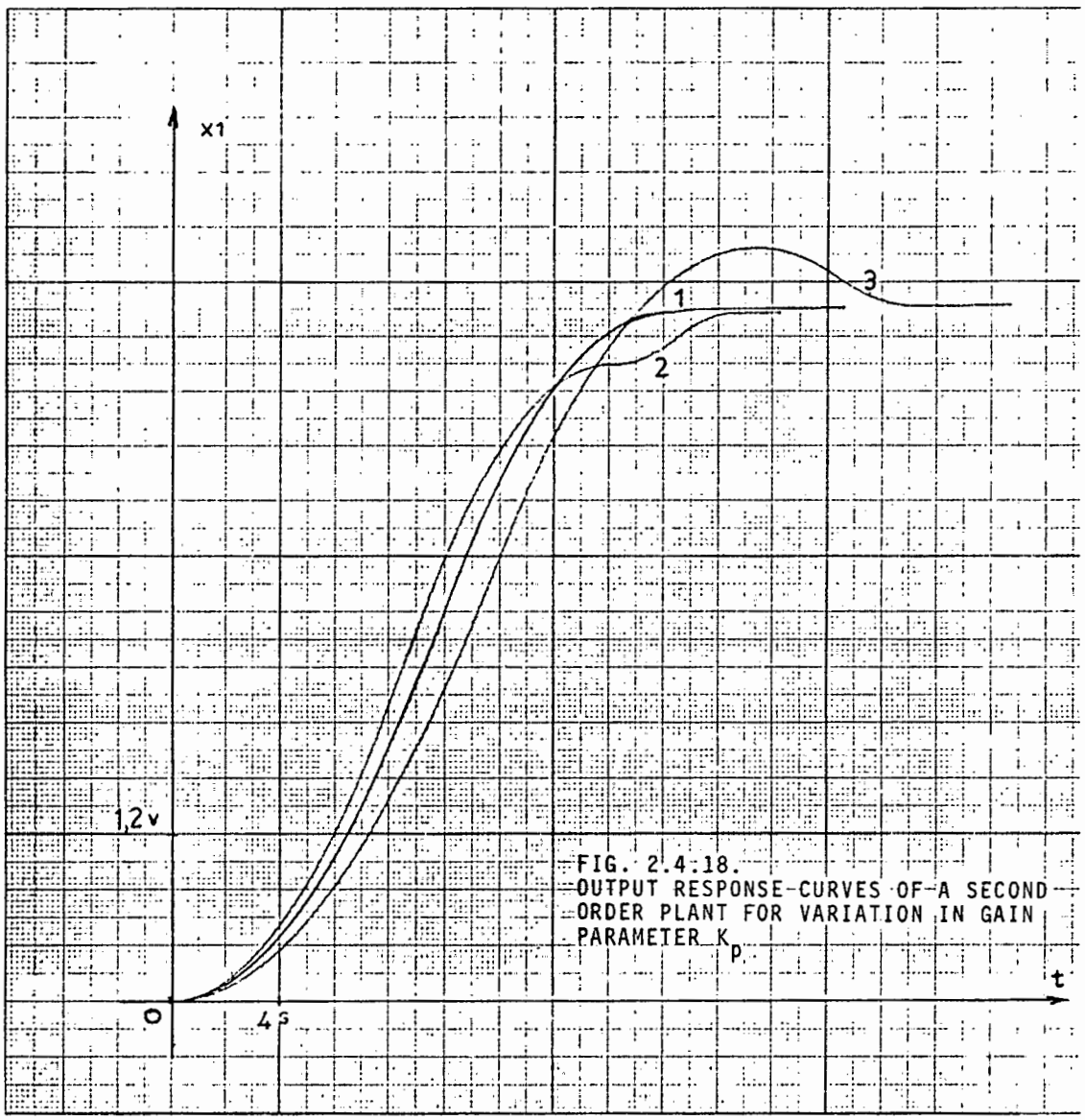

FIG. 2.4.18.
OUTPUT RESPONSE-CURVES OF A SECOND-ORDER PLANT FOR VARIATION IN GAIN PARAMETER K_p

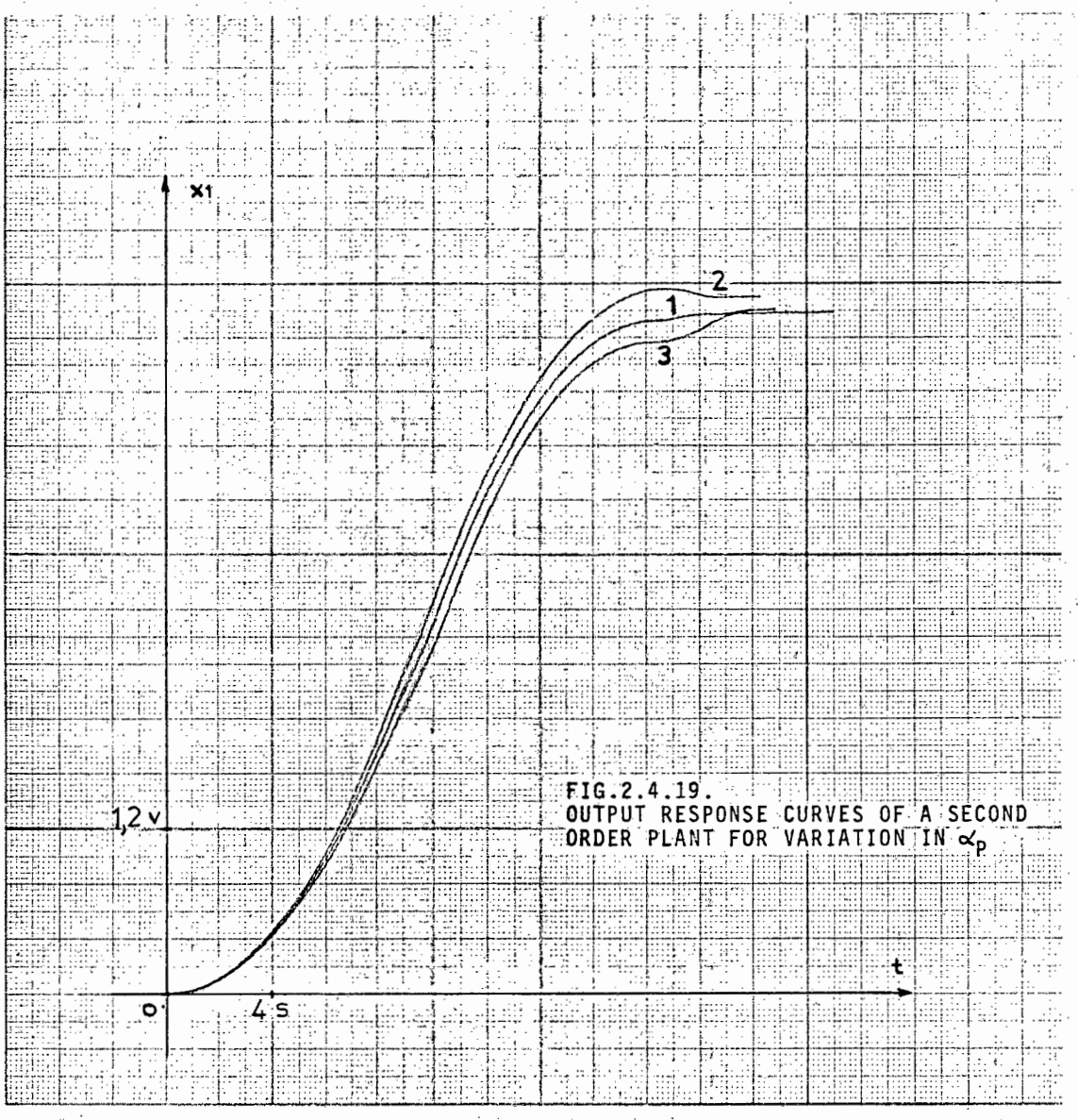

FIG.2.4.19.
OUTPUT RESPONSE CURVES OF A SECOND ORDER PLANT FOR VARIATION IN α_p

and used in chapter three was that the effects of moderate variations in the plant time constant were small compared to moderate variations in plant gain. Zinober[24] published similar results.

Figure 2.4.20 displays the response for variations in K_1 and applying limiting to the velocity integrator.

Here $\alpha_p = \alpha_m = .1$ and $K_1(\text{nom}) = .03 = K_3$

Curve 1 : nominal time-optimal response

Curve 2 : velocity limit set at .7 volt ($.33 \cdot \dot{x}_1$ max.)

Curve 3 : velocity limit set at $.33\dot{x}_2$ max.

Curve 4 : $K_1 = .02$ (33% decrease) velocity limiting set at $.33\dot{x}_1$ max.

Curve 5 : $K_1 = .04$ (33% increase) velocity limiting set at $.33\dot{x}_1$ max.

Curve 6 : $K_1 = .01$ (67% decrease) velocity limiting set at $.33\dot{x}_1$ max.

The effects of velocity limiting were similar in respects to a heavily damped plant. However with limiting and an increase and decrease in plant gain the overshoots were virtually non-existant or very small and the settling time was

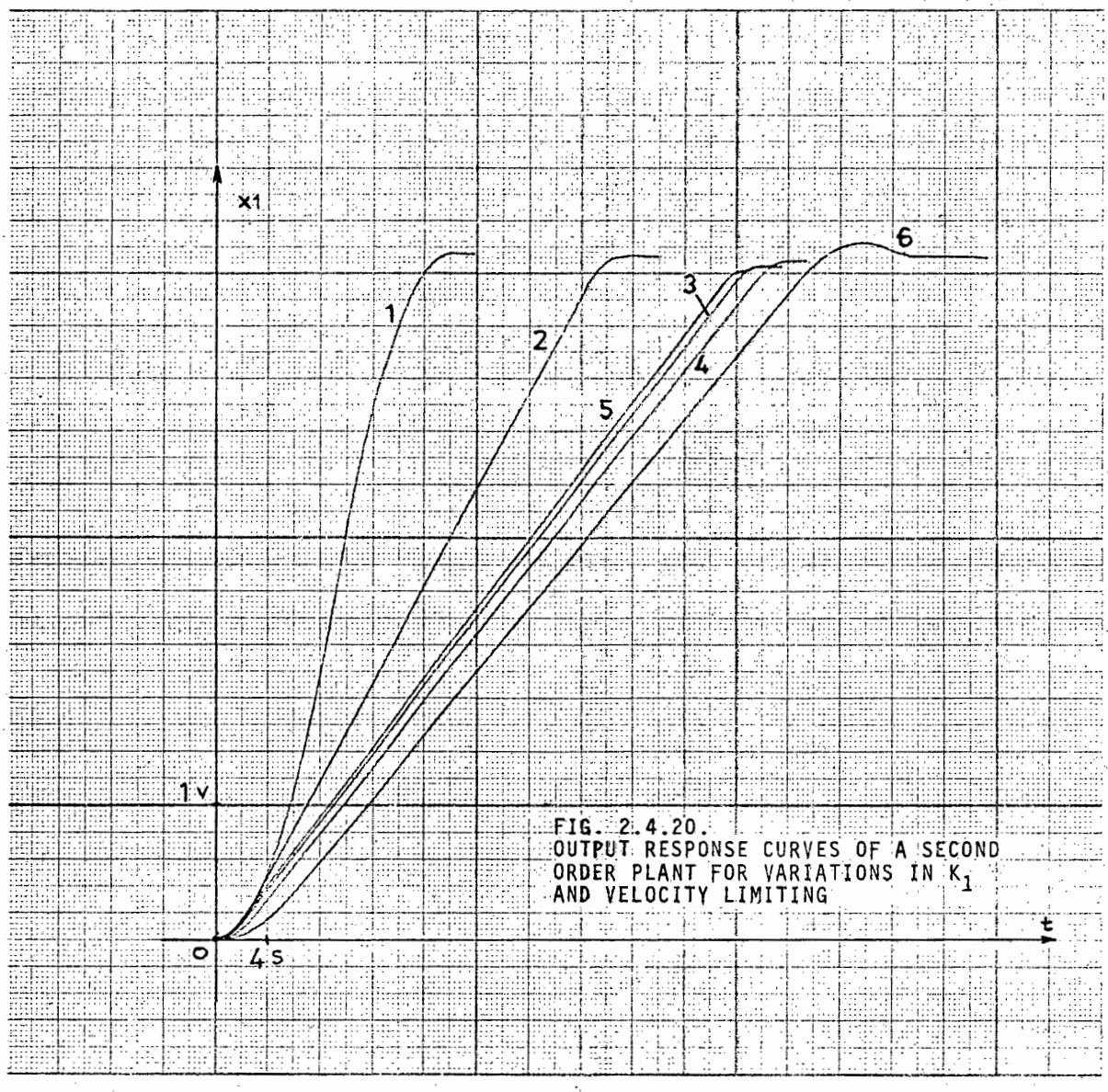

FIG. 2.4.20.
OUTPUT RESPONSE CURVES OF A SECOND ORDER PLANT FOR VARIATIONS IN K_1 AND VELOCITY LIMITING

minimized. Hence a non-linearity such as velocity limiting (a common feature in any electric motor) can be easily contained when using a linear fast model. For example, when $\frac{K_p(nom)}{K_p}$ = 3 with limiting, curve 6 had an increase in settling time over the nominal (curve 3) of approximately 28%, while in Figure 2.4.18. for curve 3 where $\frac{K_p(nom)}{K_p}$ = 1.2, the increase in settling time over the nominal is approximately 40%.

Figure 2.4.21. displays the response of a second-order plant with two lags with a transfer function of $G_p(s) = \frac{K_p K_1 K_2}{(s+\alpha_1)(s+\alpha_2)}$ and the model $G_m(s) = \frac{K_m K_3 K_4}{s(s+\alpha_m)}$ where the K's have the values defined as previously.

$\alpha_m = \alpha_1 = .1$ and $\alpha_2 \geq \alpha_1$. α_2 is the variable.

Curve No.	α_2
1	0
2	.1
3	.5
4	1
5	2

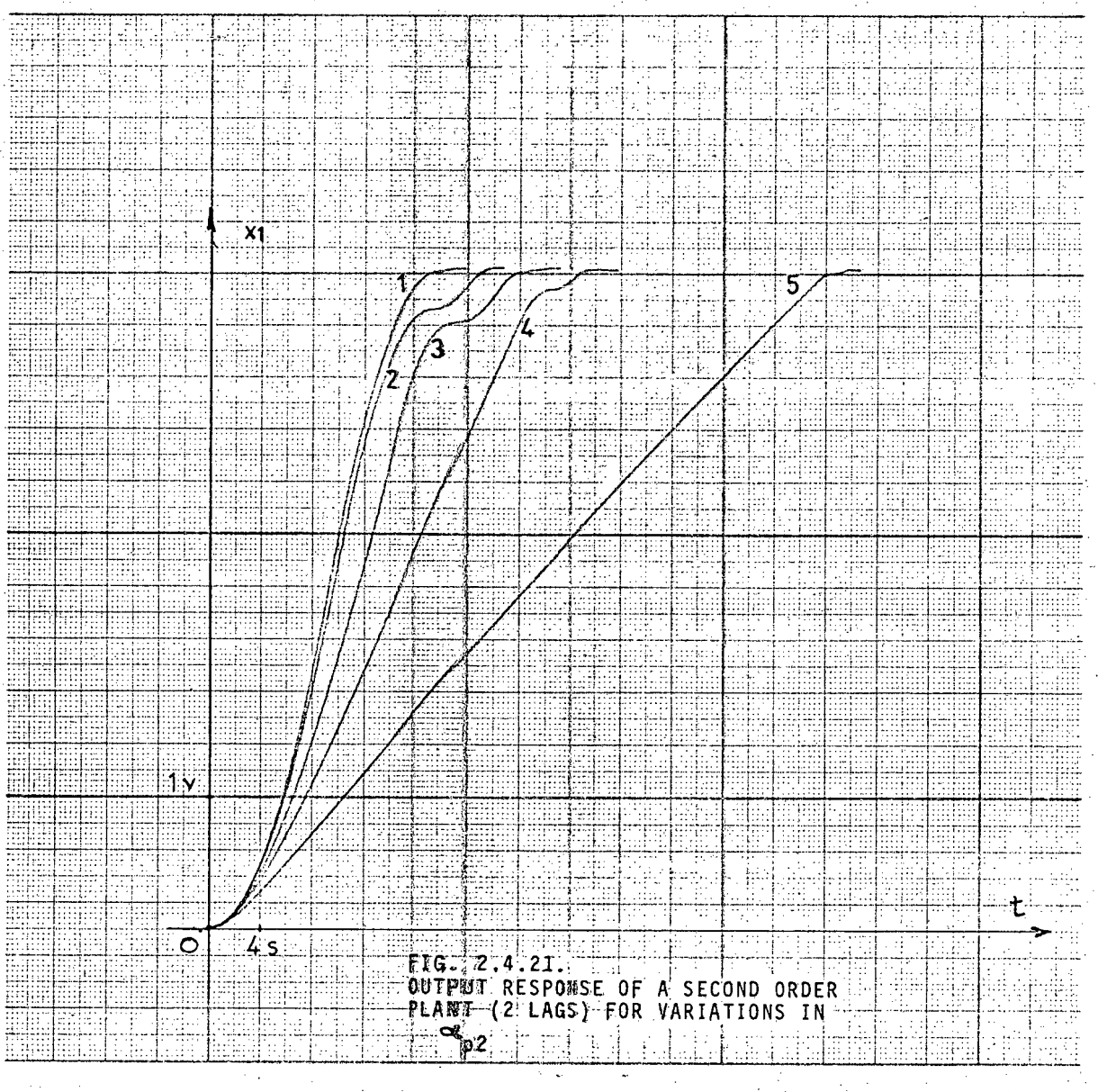

FIG. 2.4.21.
OUTPUT RESPONSE OF A SECOND ORDER PLANT (2 LAGS) FOR VARIATIONS IN α_{p2}

Curves 2, 3, 4 and 5 show an undershoot or early-switching response. The additional lag in the plant responsible for this mismatch is not serious as the settling times do not differ by much over their nominal settling times. When $\alpha_2 >> \alpha_1$ as for curve 5, this lag dominates and the plant behaves similar to the velocity limited plant described in Figure 2.4.20.

Figure 2.4.22 displays the response of a third-order plant for variations in α_2 where the transfer function of the plant is

$$G_p(s) = \frac{K_p K_1 K_2}{(s+\alpha_1)(s^2+\alpha_2 s+1)}$$

where $K_p = K(\text{nom}) = 1$, $K_1 = K_2 = .2 = K_3 = K_4$.

The model transfer function is $G_m(s) = \frac{K_m K_3 K_4}{s(s+\alpha_m)}$ and $\alpha_m = .1$.

Curve No.	α_1	α_2
1	0	2
2	1	2
3	1	1
4	1	1.41

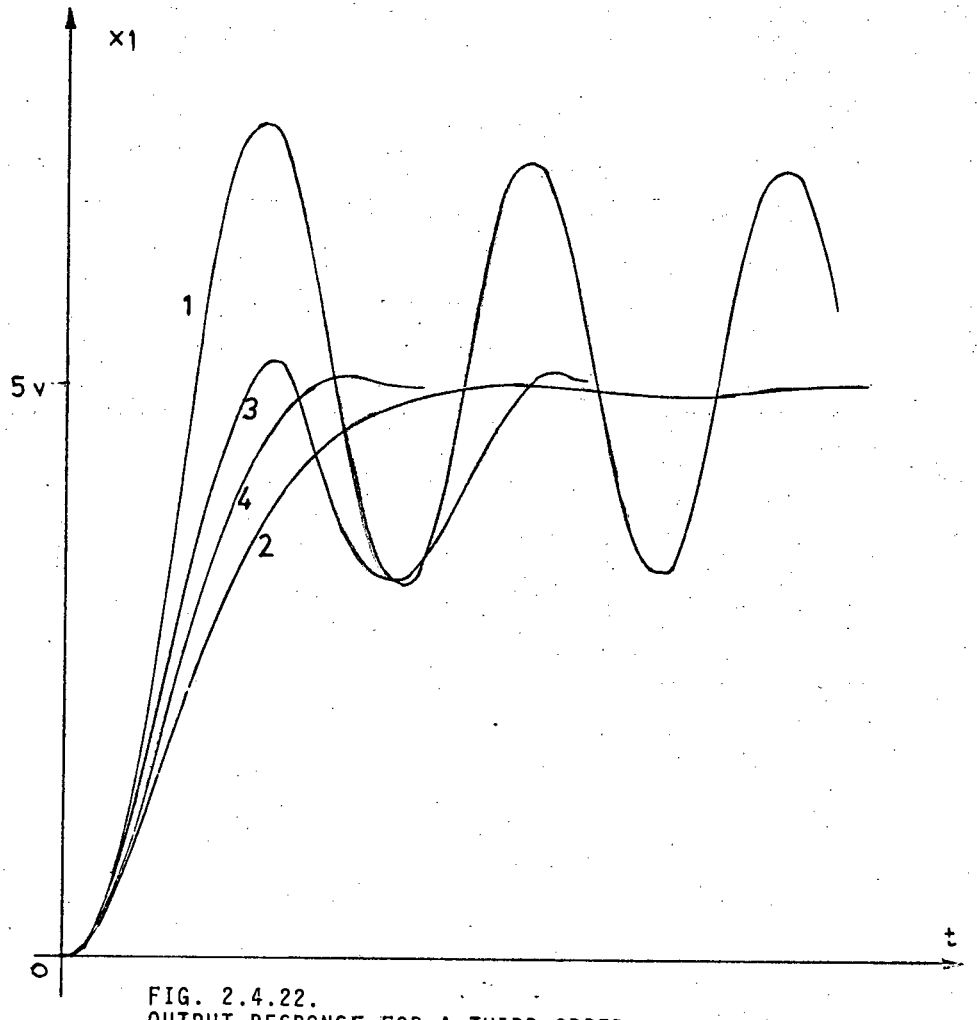

FIG. 2.4.22.
OUTPUT RESPONSE FOR A THIRD ORDER
PLANT FOR VARIATIONS IN α_2

Curve 1 is similar to those recorded in Figures 2.4.7 and 2.4.8 in section 2.4.1. Curves 2 and 4 reached the steady-state with very little overshoot. For curve 3 (as with curve 4) the plant has complex poles and the plant response is interesting in that the steady-state was also reached in spite of the sustained oscillation not about the steady-state value as in Curve 1.

The near time-optimal control of a third-order plant with complex poles by a second-order fast model is very difficult in general to achieve however by empirical methods, values of α_m for given values of α_p can be found to yield responses close to time-optimal.

2.4.4. Direct digital control of a DC Motor.

The fast model transfer function used in the programme was $G_m(s) = \frac{K_m}{s(s+\alpha_m)}$ where $K_m = 5$.

Figure 2.4.23. represents the motor output potentiometer response for a step initial condition of 100 degrees angular rotation.

Curve 1 represents the response when using the fast model predictor controller while curve 2

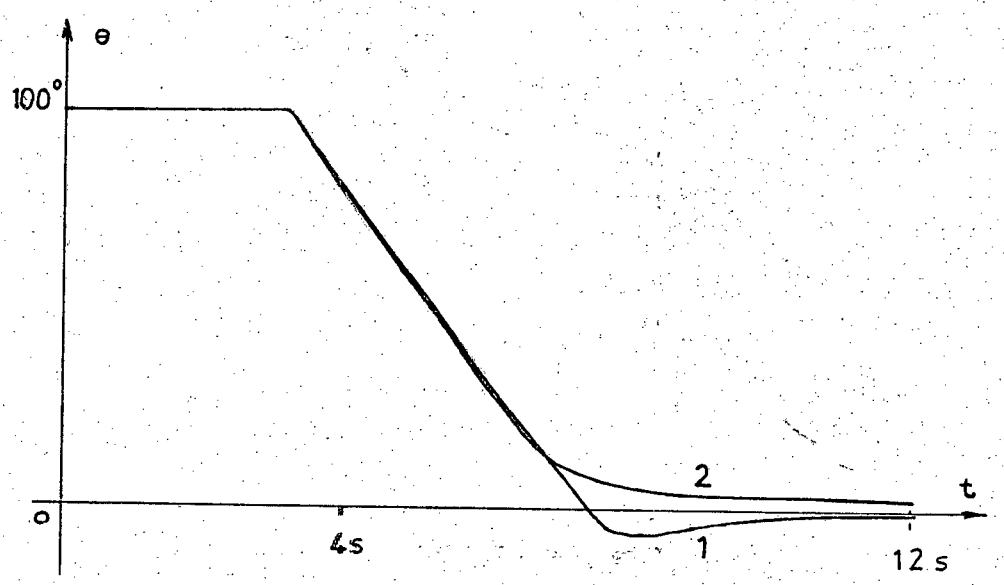

FIG. 2.4.23.
ANGULAR DISPLACEMENT OF DC MOTOR FOR
FAST MODEL PREDICTION AND P & D
RELAY CONTROL

represents the response for a 'proportional plus differential' relay controller. The value of α_m selected for the fast model was 0,5.

In spite of the mismatch between the plant (motor) and the model, the fast model controller brought the plant to rest in about 8 seconds.

Figure 23.2.24. represents the response for a v-controller,, an adaptive relay controller and a fast model predictor controller.

Curve 1 : v-controller
Curve 2 : adaptive relay controller
Curve 3 : fast model predictor controller

The adaptive relay controller and the v-controller are discussed in chapters four and five respectively. α_m was adjusted to 0,1 and the response time was improved to about 6 seconds with less overshoot as compared with curve 1 of Figure 2.4.23.

Figure 2.4.25. represents the response for a y-controller curve 2, and a fast model predictor controller curve 1. α_m was adjusted to 0,05 and the response time was improved to about 5 seconds with no overshoot, and was virtually identical to the response from the v-controller.

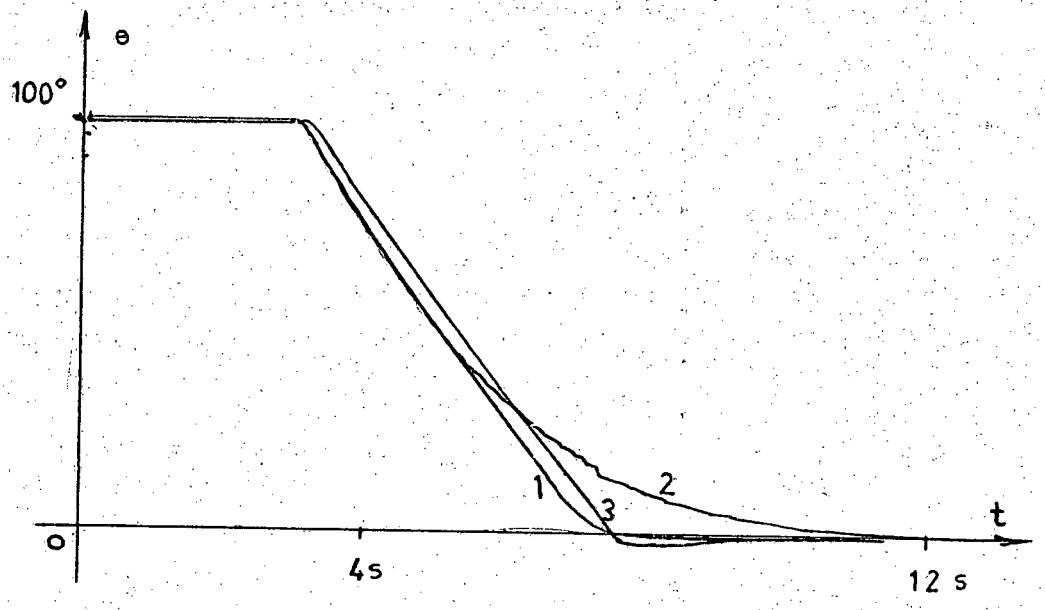

FIG.2.4.24.
ANGULAR DISPLACEMENT OF A DC MOTOR FOR THE V-CONTROLLER, ADAPTIVE RELAY CONTROLLER AND FAST MODEL PREDICTOR

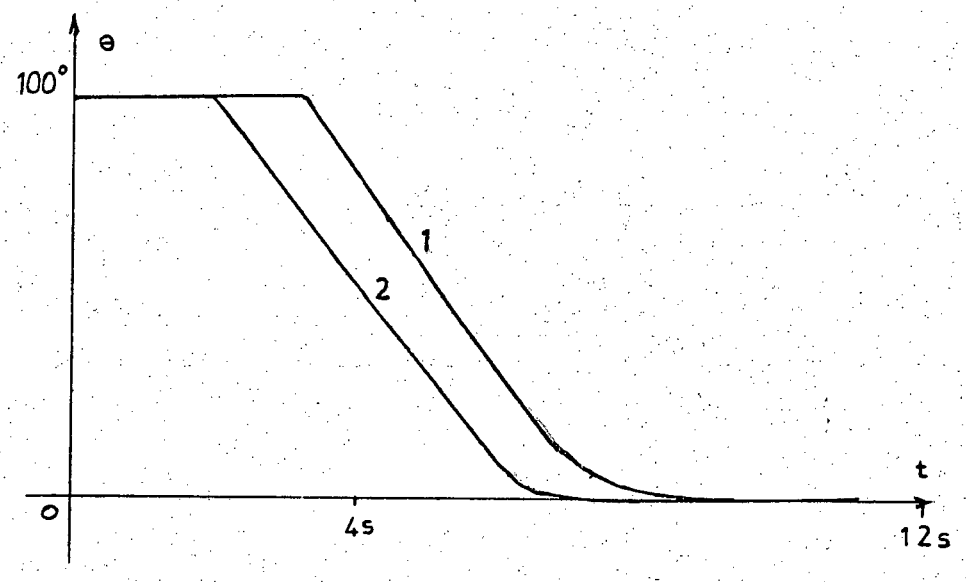

FIG. 2.4.25.
ANGULAR DISPLACEMENT OF A DC MOTOR
FOR FAST MODEL PREDICTION AND
NOMINAL-V CONTROL

It must be remembered that the fast model transfer function is only an approximation of the (unloaded) motor transfer function but the performance is reasonably adequate as seen from curve 1.

2.5 Summary of results and comments

In stage one an analogue computer with external relays for the 'reset' and 'changeover drive' elements were used, to simulate a fast model predictor system, for second-order; third-order; and fourth-order plants and using a second-order fast model.

Practical problems arose and are listed for convenience:

(1) The relays used had severe deadband, backlash and contact bounce.

(2) Drift in the computer became significant.

(3) The existance of severe non-linearities in the electronic switching elements (comparators and signum function generators).

(4) The existance of upper and lower limits of the model to plant run-time ratios.

However in spite of these shortcomings, the curves obtained were quite satisfactory and demonstrated the utility of this method. Despite severe mismatch between plant and model (in section 2.2 a stability analysis was undertaken to determine the bounds for stable operation) successful control was brought to bear on plants with real poles for step references or disturbances. Plants with complex poles are in general difficult to control and each case has to be evaluated independently.

It was found that a model to plant time ratio of 20:1 was about the lowest usuable ratio, below 20:1 the control became hopelessly inaccurate. The relays could not be energized at high switching rates ($\leq$50 milliseconds switching rate) hence the upper bound was of a practical one and depended on the type of plant under control. It was inconvenient and impractical to slow the plant (computer solution) down such that the model to plant time ratio was, for example 1000:1, and the model run time was of the order of several seconds. This was, however, demonstrated but the improvement in accuracy and performance was small when compared with the 50:1 ratio commonly used throughout.

To improve and enhance the method both for system performance and accuracy and for use on plants with rapid run-times, the use of a small digital computer as a digital controller was a logical choice.

Stage two evolved around developing a programme to simulate system behaviour for variations in the plant and model parameters, not only to confirm and augment the analogue computer results but to utilize the digital simulations for the generation of a suitable programme for direct digital control. The curves derived in the digital simulation clearly demonstrated the effective use of this technique for a systematic analysis of system behaviour, provided of course, the mathematical equations describing the system are reasonable approximations to the real system and are amenable for manipulation.

One obvious limitation in the digital simulation is that the computer can only do what is written in the programme i.e. the effects of non-linearities, random disturbances and noise, drift and other factors have to be included in the programme. The inclusion of these factors is a very difficult task.

Stage three was the development of hybrid system; in that a minicomputer was used to provide control to an analogue computer, i.e. the minicomputer was the decision making element in the plant control loop. The programme developed in stage two was modified to accommodate analogue-to-digital and digital-to-analogue channels and the results obtained were virtually identical to those derived in the digital simulation, and in no way did they contradict any of the results obtained through the analogue computer-relay simulation.

The theory developed in chapters one and two indicate the problems of sensitivity (to plant parameter variations), stability and the derivations of the time-optimal control law, especially for higher order plants. Plants whose characteristic equation has complex roots are especially troublesome and much work remains to be done for this particular case.

Stage four was a practical test and application of the fast model predictor method to a real plant. A small DC motor was used as a position controller and as the curves indicated, the response to a step input was close to time-optimal in spite of the saturation or velocity limit of the motor.

In conclusion it can be stated that the fast model predictive control method is a useful and practical approach to the minimal-time control problem of single-variable second-order plants, and in certain cases for third and fourth-order plants, where the degree of plant to model mismatch although severe, is of no serious consequence as satisfactory performance is generally obtained.

CHAPTER 3

ADAPTIVE CONTROL

3.1. Introduction

The interest in adaptive control systems has been largely motivated by a sizable class of problems for which conventional techniques for synthesising the controller have proven inadequate.

Specifically, a controller having fixed parameters may not be capable of achieving the desired system performance with a given plant. Such a situation may occur when the parameters which describe the plant vary over a wide range of values during the operation of the system (i.e. when the dynamic characteristics of the plant change markedly).

In spite of the proliferation of adaptive techniques (see Eveleigh[25], Gibson[26], Landau[3]) that have been proposed, there are many difficulties in applying such methods to real problems[4]. These difficulties may be attributed to a variety of reasons among which are:

i) The large number of parameters that may have to be adjusted simultaneously while assuring the

stability of the overall adaptive system.

ii) The lack of exact information or partial ignorance regarding the variations of the plant parameters.

iii) The noise present in the measurements of the plant outputs.

Recent developments in model reference adaptive control using Lyapunov's direct or second method (4,27,28,29,30) have overcome some of these difficulties and have resulted in schemes that may be attractive in practical situations.

In particular, it is quite evident that the model reference adaptive control system abbreviated as MRAS, was the method selected to improve the performance of the systems dealt with in Chapter 2. The heart of the fast model prediction is the "fast model", hence if we introduce a real-time model (of the plant) besides the fast model, there now exists the basis for identifying the unknown or partially known plant parameters. Once this is achieved the real time model and fast time model parameters are updated (adapted) to that of the plant and the control can now approach the time-optimal situation.

3.2. Liapunov Synthesis and the Identification Scheme

This adaptive scheme applied to the predictive control problem is the dual of the "adaptive control" namely that of "parameter identification" as is discussed in the following:

3.2.1. Adaptive Control

Consider a linear plant described by the vector differential equation:

$$\dot{\underline{x}}_p = A_p \underline{x}_p + B_p u \qquad (3.2.1)$$

where the elements of the (nxn) matrix A_p and those of the (nxm) matrix B_p are unknown or only partially known.

The behaviour desired of the plant is prescribed by the model:

$$\dot{\underline{x}}_m = A_m \underline{x}_m + B_m u \qquad (3.2.2)$$

where A_m is a (nxn) stable matrix and B_m is a (nxm) matrix.

We employ a feedforward (mxm) matrix Q, and a feedback (mxn) matrix F to control the plant (see Figure 3.2.1) so that the plant together with the controller, is characterised by

$$\dot{\underline{x}}_p = (A_p + B_p Q F)\, \underline{x}_p + (B_p Q) u \qquad (3.2.3)$$

The problem, then, consists of specifying a scheme that continuously adjusts the elements of the matrices F(t) and Q(t) such that the norm of the error between the plant and the model states is reduced.

Under certain conditions, it is possible to reduce this error to zero and it is this case that is of interest in this thesis.

3.2.2. Identification

The identification problem, on the other hand, consists in specifying a suitable model and in developing a scheme for dynamically adjusting its parameters so that they converge to those of the plant (3.2.1) so in equation 3.2.3 if we substitute m for p we have the identification scheme (see Figure 3.2.1). Hence the roles of the plant and model are interchanged so that the parameters of the model track those of the plant.

While the two problems are mathematically equivalent, it is worth noting that the identification problem is somewhat simpler since the structure of the model (whose parameters are

adjusted) unlike that of the plant, can be chosen freely by the designer.

3.2.3 Liapunov Synthesis

A basic necessity of the adaptive controller is a good compromise between the stability and speed of adaptation, and it is found that the Liapunov synthesis approach is the most successful. The adaptive rule is obtained by selecting the design equation to satisfy conditions derived from Liapunov's direct method, so that system stability is guaranteed for all inputs.

The main disadvantage of the Liapunov method is that all the state variables must be available for measurement, which for many real plants is not always possible.

The Liapunov synthesis is based on the use of the Liapunov function (see Appendix A5). Successful forms of this V function are discussed by Hang and Parks[30], Narendra and Kudva[4] and Landau[3].

Appendix A7 contains a short development and

summary of the adaptive control laws as well as the identification law used. In chapter two it was found that large changes in the plant time constant caused a small degradation in system performance while moderate changes in the plant gain caused large system deviations from the normal. Hence it was felt that only the model input matrix B_m, need be given attention, while the model and plant A matrices could be considered identical for all practical purposes.

From Appendix A7 the plant gain parameter identification law is:

$$K_y = \gamma\Gamma_2\underline{e}^T P b u + \int_0^\infty \Gamma_2\underline{e}^T P b u \, dt \cdot \quad (3.2.4)$$

where K_y = additional gain parameter determined by the adaptive loop

γ = adaptive loop damping factor

Γ_2 = adaptive loop gain

P = positive definite symmetric matrix

$\underline{e}$ = state or output generalized error vector

$\underline{e}^T$ = transpose of $\underline{e}$

b = input matrix

u = input

Figure 3.2.2 represents the block diagram of an actual system.

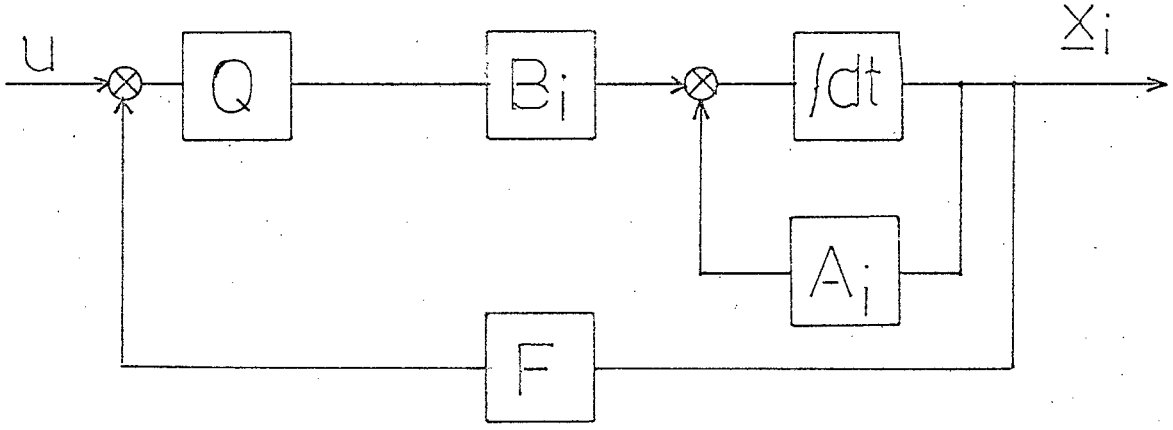

FIGURE 3.2.1 : CONFIGURATION OF PLANT OR MODEL WITH FEEDFORWARD AND FEEDBACK GAIN MATRICES

For Plant i = p
For Model i = m

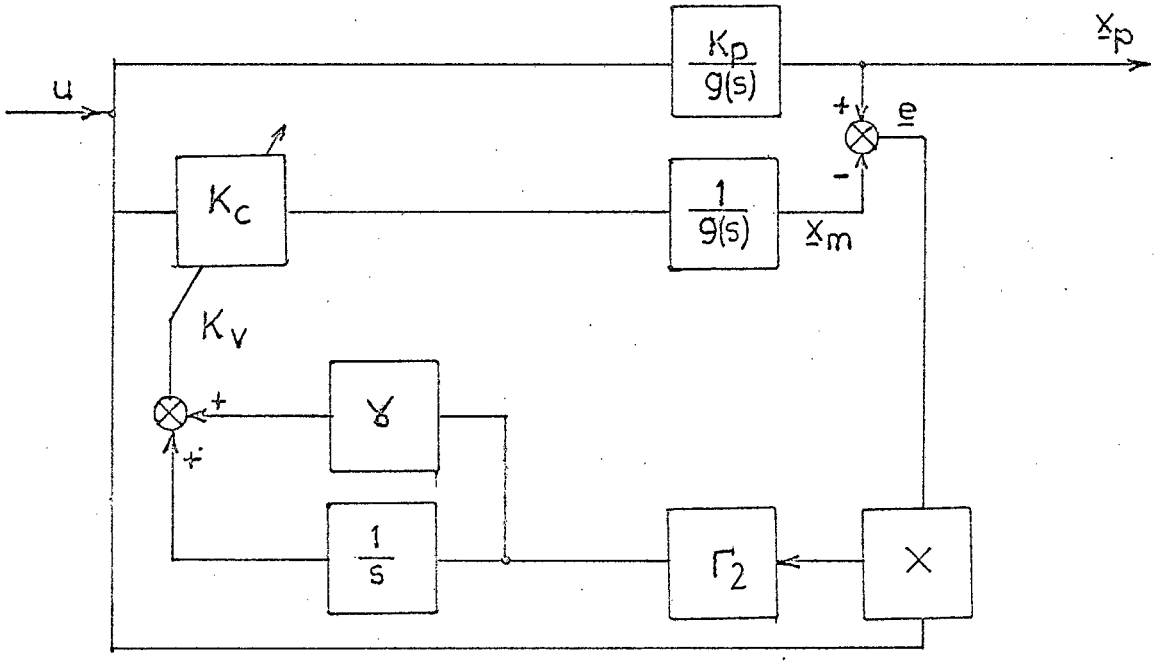

FIGURE 3.2.2 : BLOCK DIAGRAM OF PARAMETER IDENTIFICATION VIA AN ADJUSTABLE MODEL

3.3. Experimental Procedures

3.3.1 Analogue Computer Simulations

The block diagram in Figure 3.2.2 was used to demonstrate the feasibility of parameter identification via an adjustable model. The patching on the computer required no special or additional equipment to implement this method, and the procedure followed standard analogue computer practice.

Several types of second order models were selected but the curves depicted in Figures 3.4.1 and 3.4.2 represent a plant with a transfer function:

$$G_p(s) = \frac{K_p}{s^2 + \alpha s + 1} \qquad (3.3.1)$$

and a real-time model with transfer function

$$G_m(s) = \frac{(K_m + \tilde{K})}{s^2 + \alpha s + 1} \qquad (3.3.2)$$

when $K_c = (K_m + \tilde{K})$ and $\tilde{K} = f(K_y)$

The reference used was a step input of 5 volts magnitude.

In Figure 3.4.2 a square wave was used to perturbate the input, to investigate whether the

model could continue to track the plant successfully in spite of these disturbances. This was also performed using sine and triangular wave disturbances of various magnitudes and frequencies (these curves are not shown here) but in all cases the model continued to track the plant with virtually no tracking error. The adaptive loop dynamics in some respects behaves as a low pass filter, in that the high frequency components are ignored, while for the low frequency terms, the adaptive loop responds rapidly to these variations.

The ease with which the parameters Γ_2, γ, e_1 and e_2 could be changed made the analogue computer approach very practical and direct.

3.3.2. Hybrid Simulations

One of the primary objectives of this section was to develop an algorithm to provide the adaptation to the synthetic fast model so as to maintain time-optimal performance. Initially a program was written that represented an algorithm of equation 3.2.4. Appendix A8.1 contains this program and a diagram (Figure

A8.1.1) showing the actual system structure.

What was of interest in this program was the integral term in equation 3.2.4. The numerical integration method used was the trapezoidal rule and extremely rapid convergence resulted as seen in Figures 3.4.3 and 3.4.4. It was difficult to calculate the truncation error (see Scheid[33]) as the variables involved in the computation converge towards zero extremely rapidly but a rough calculation showed the truncation error to be less than 0.0001. Hence the simple trapezoidal rule was found to be reasonably adequate.

The methods derived for the digital simulation in chapter two for synchronization and control were also used in this procedure and no real problems arose. After some experimentation, nominal values of γ, Γ_2 and h were established for the system under test.

The final stage in the simulation was the inclusion of the parameter identification algorithm into the program developed for the fast model predictor hybrid controller in chapter two.

The preparation of the program presented little difficulty (see Appendix A8.2 for a description of this program and a diagram of the system set-up) although there arose definite practical limitations in regard to device limitations and to the method of control.

A description of this is simplified by referring to Figures 3.3.1 and 3.3.2. The c.p.u. (central processing unit) of the minicomputer can only handle instructions sequentially and tasks are therefore performed serially in time(there is no facility at the time of writing, of multi-task sharing of programs, written in Basic). Hence it is physically impossible for the c.p.u. to be simultaneously occupied with the predictor mode and the parameter identification mode. A multiplication in Basic takes about 1 milli-second while a Logarithmic calculation takes about 10 milliseconds which is slow by contempo-rary computer standards.

Hence the time allotted (t_1 and t_3 in Figure 3.3.1) for identification, prediction and fast model parameter adjustment, and the sampling of the plant vectors(t_2 and t_4 in Figure 3.3.1) had

available to adjust K_y and hence to hold the plant and fast model in a close match. This would result in gross mismatch and ultimate deterioration of plant control.

The introduction of a high speed c.p.u. with special priority interrupts could go a long way to improve this situation or even two parallel processors for a plant operating under these control laws. This is an area where much investigation still has to be done.

3.4. Simultation Results

In section 3.3.1, a description of the plant and real-time model was given. Figure 3.4.1 represents the plant identification and convergence of a model parameter.

The curves may be listed as:

Curve No.

1 · plant output

2 model output

3 $(K_m+\tilde{K}) = K_c$

4 $\dot{e}(t)$ system error rate

with $r(t)$= 5 volts(a step function), α= 1, w=1, K_m=.4 K_p=1, γ= 1, Γ_2= 5 and τ = .1

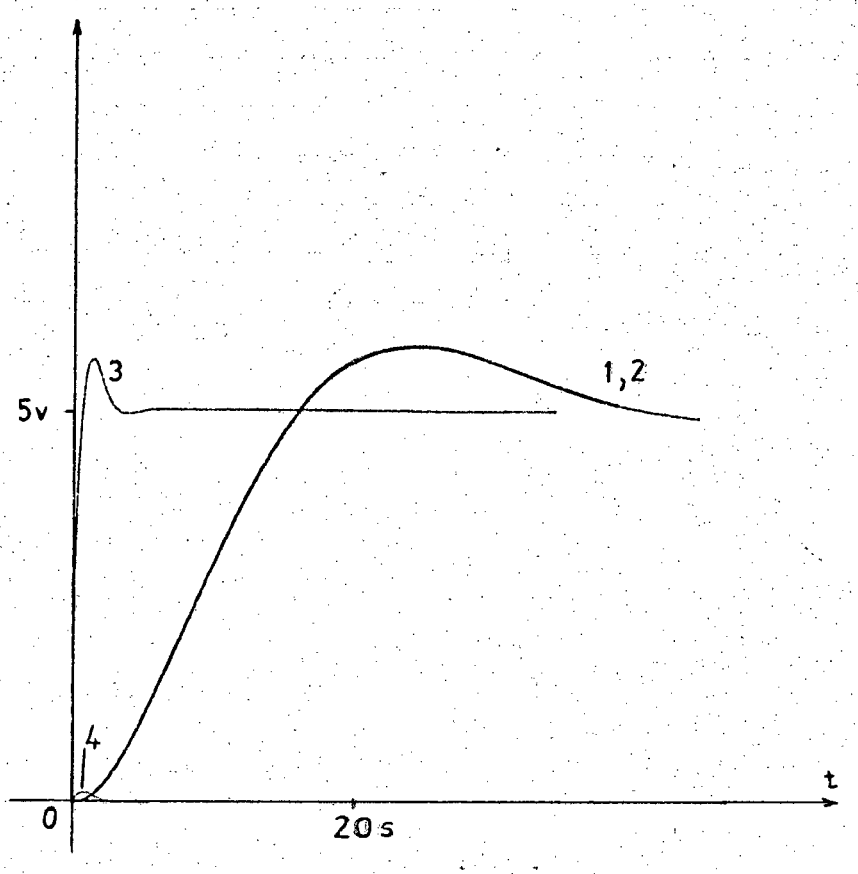

FIGURE 3.4.1 : PLANT IDENTIFICATION AND CONVERGENCE OF A MODEL PARAMETER

The rapid convergence of K_c to K_p is quite astonishing although some overshoot occurred (curve 3). It is virtually impossible to differentiate between Curves 1 and 2 in spite of the plant having complex poles. As seen the system error rate is small.

Figure 3.4.2 represents the plant identification and convergence of a model parameter with a step-like disturbance of the plant input. In this case the plant damping was reduced to $\alpha = .4$, $w = 1$, $K_m = .6$, $K_p = 1$, $\gamma = 1$, $\Gamma_2 = 5$ and $= .1$.

The disturbance was a square wave of a 5 second period and 2,5 volt amplitude. $r(t) = 5$ volts.

Curve No.

1	plant output
2	model output
3	$(K_m + \tilde{K})$

As in Figure 3.4.1 the parameter convergence is very rapid while the parameter tracking errors are virtually zero in spite of the perturbations applied to the plant input.

The small errors between curves 1 and 2 were caused by poor synchronization when repeating the recording for

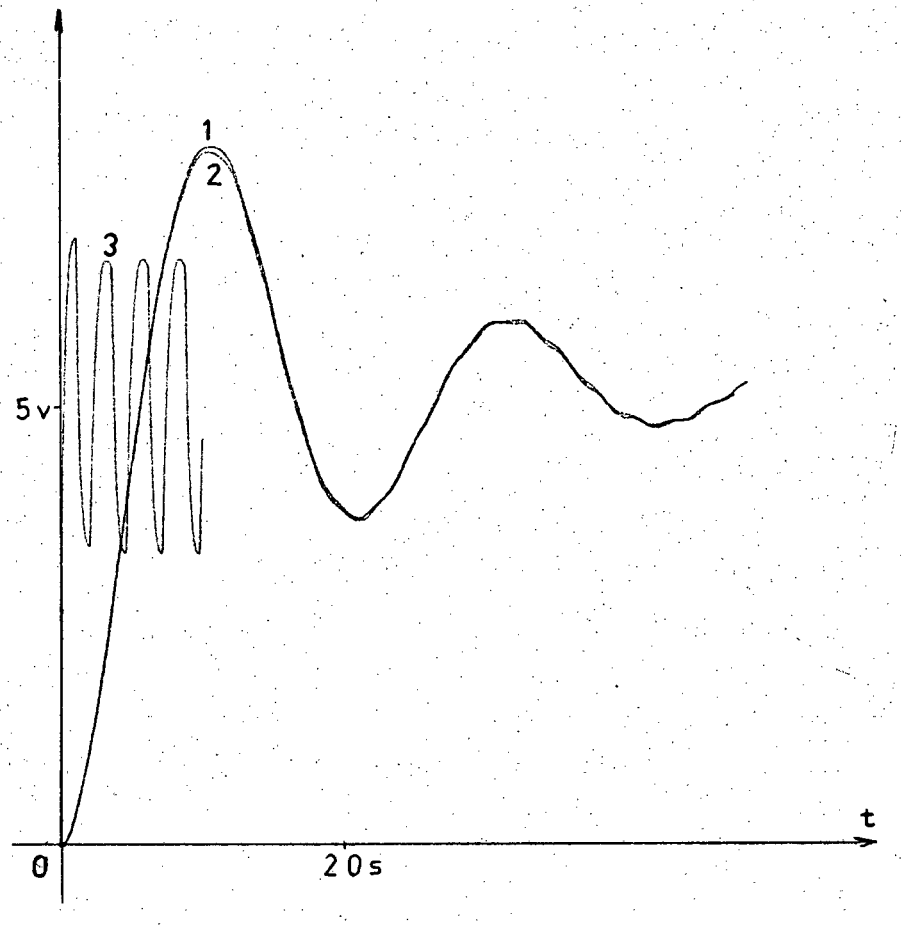

FIGURE 3.4.2 : PLANT IDENTIFICATION AND CONVERGENCE OF A MODEL PARAMETER WITH A DISTURBANCE OF THE PLANT INPUT

curve 2.

Figure 3.4.3 represents the adaptive gain parameter K_y, for various Γ_2, γ and h. Figure 3.4.4 represents the Liapunov parameter identification method applied to plant with transfer function as in equation 3.3.1 with $\alpha=2$ and w=1. Both these figures display data derived from the digital computer. In both examples $K_m=.4$, $r(t)= + 5$ volts and $e^T Pb=(e+10\dot{e})$.

For Figure 3.4.3

Curve No	Γ_2	γ	h
1	5	.5	.01
2	1	.5	.01
3	.5	.5	.01
4	.5	.1	.01
5	.5	1	.01

For Figure 3.4.4

Curve No	$\Gamma_2 = 5$, $\gamma = .5$, $h = .05$
1.1	Plant output
1.2	Model output
1.3	system error with X100 amplification
1.4	K_y

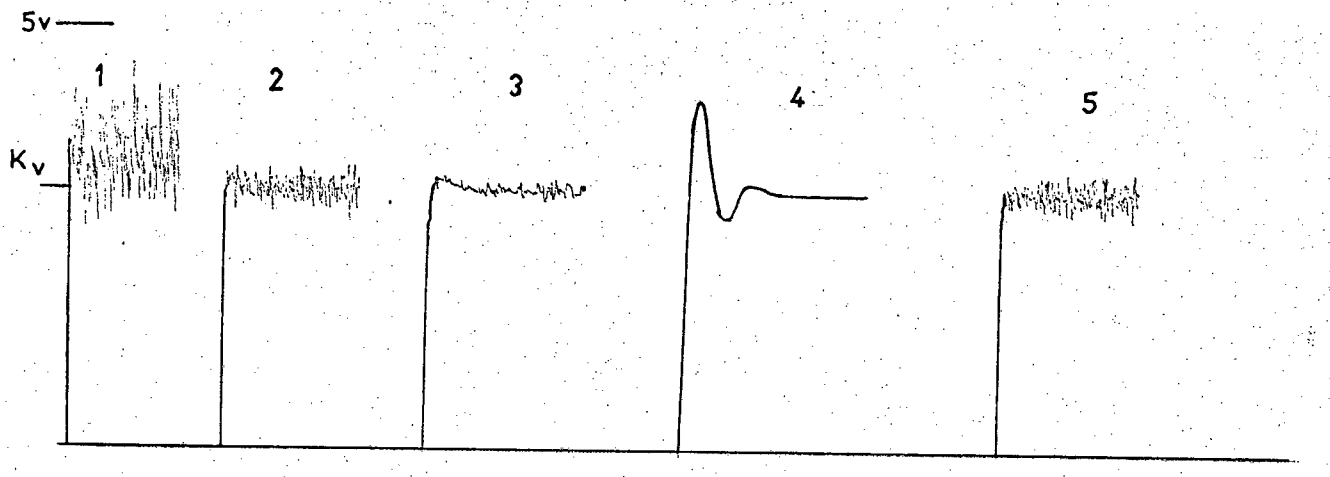

FIGURE 3.4.3 : ADAPTIVE GAIN PARAMETER K FOR VARIOUS γ, Γ_2 AND h

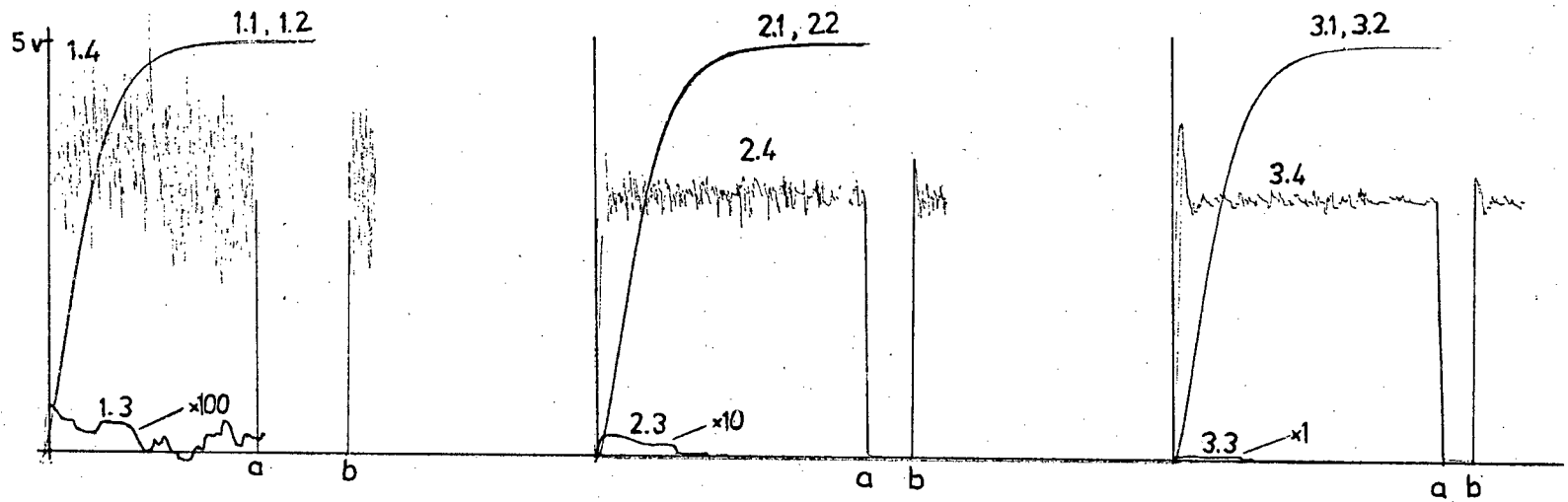

FIGURE 3.4.4 : LIAPUNOV ADAPTIVE LOOP CONTROLLER

Curve No	$\Gamma_2 = 1,\ \gamma = .5,\ h = .05$
2.1	Plant output
2.2	model output
2.3	system error with x 10 amplification
2.4	K_v

	$\Gamma_2 = .5,\ \gamma = .5,\ h = .05$
3.1	plant output
3.2	model output
3.3	system error with x 1 amplification
3.4	K_v

As seen in Figure 3.4.3, a decrease in Γ_2 (i.e. loop gain) results in a reduced amplitude of K_v. Variations in Γ_2 and γ result in minor variations of the response curves for K_v but they all converge to K_v=0,6 (since $(K_v+K_m) = (.6 + .4) = 1 = K_p$).

These various values were tried as indicated in Figure 3.4.4. Again the convergence was extremely rapid as it was virtually impossible to differentiate the plant output from the model output.

The rapid oscillations in K_v were caused by the output of the D to A channel which is not continuous but whose voltage is renewed after every iteration in the

integration loop. The oscillations caused no difficulties as the two integrators in the plant merely responded to the dc components in K_v.

Point 'a' represents where the input r is set to zero and point 'b' represents where the input r is restored to 5 volts. In all cases, the value of K_v=.6 was stored in the 'memory' of the integration loop.

These tests demonstrate the simplicity of using this method for parameter identification and tracking.

Figures 3.4.5 to 3.4.8 depict the output response of a second-order plant for a step reference with the method of fast model predictive control with and without parameter identification and tracking. For all these curves the plant transfer function is

$$G_p(s) = \frac{K_p}{s(s + .1)}$$

The real time model transfer function is

$$G_m(s) = \frac{(K_m + \tilde{K})}{s(s + .1)}$$

The fast model transfer function is the same as the real time model except the gain $(K_m+\tilde{K})$ is updated at the end of an 'identification' run.

K_p= 1 (nominal), K_m = .8 and r(t)= 5 volts

Figure 3.4.5 illustrates the response when K_p in increased by 20% (K_p = 1.2).

Curve No

1	plant output with adaptation
2	real time model output
3	plant output without adaptation

The results are as anticipated, a dramatic improvement in system performance. There was a small tracking error between the plant output and real time model output due to the control action that was allotted in the time slot t_4 (see section 3.3.2)

Figure 3.4.6 illustrates the response when K_p is decreased by 20% (K_p = 0.8)

Curve No

1	plant output with adaptation
2	real time model output
3	plant output without adaptation

Again the same remarks as above apply.

Figure 3.4.7 illustrates the response when K_p is now

increased by 40% (K_p = 1.4).

Curve No

1	plant output with adaptation
2	real time model output
3	plant output without adaptation

Again the response with adaptation is close to time - optimal and the same remarks as in Figure 3.4.5 apply.

Figure 3.4.8 illustrates the response when K_p is now decreased by 40% (K_p = .6).

Generally the settling time of the plant is greatly increased (see section 1.5) when the plant gain parameter K_p, is reduced below the nominal gain parameter. And this is observed to be the case as in Curve 3. However the tracking error has also increased as compared to Figure 3.4.6 although by a small amount. Hence for large decreases in K_p the maximization of the time slot for t_3 i.e. the identification and tracking becomes more critical. Nevertheless the response of Curve 1 as compared with Curve 3 is still a great improvement. In fact the settling time has been reduced by approximately 100%.

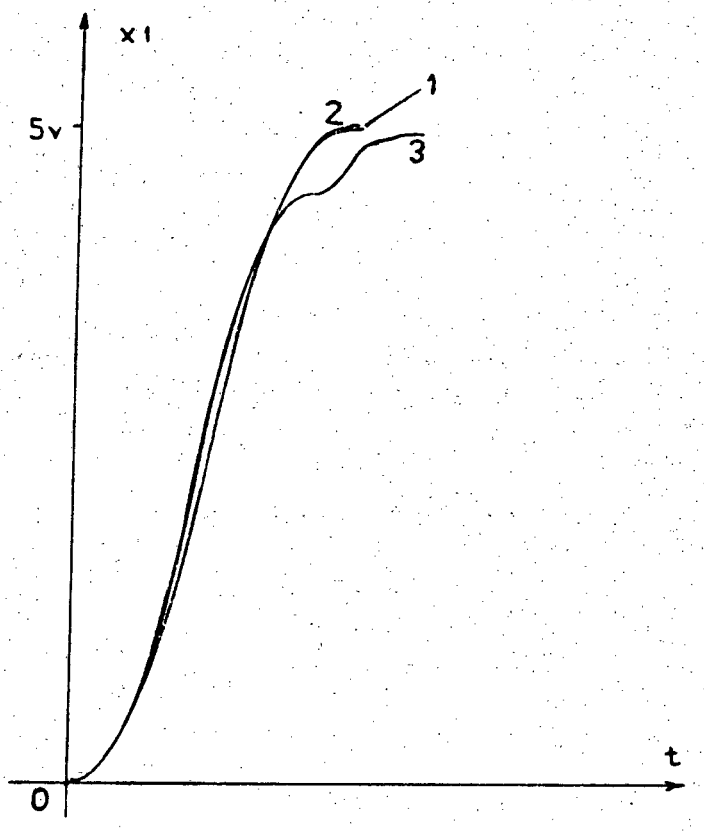

FIGURE 3.4.5 : ADAPTIVE FAST MODEL PREDICTION WITH INCREASED GAIN PARAMETER

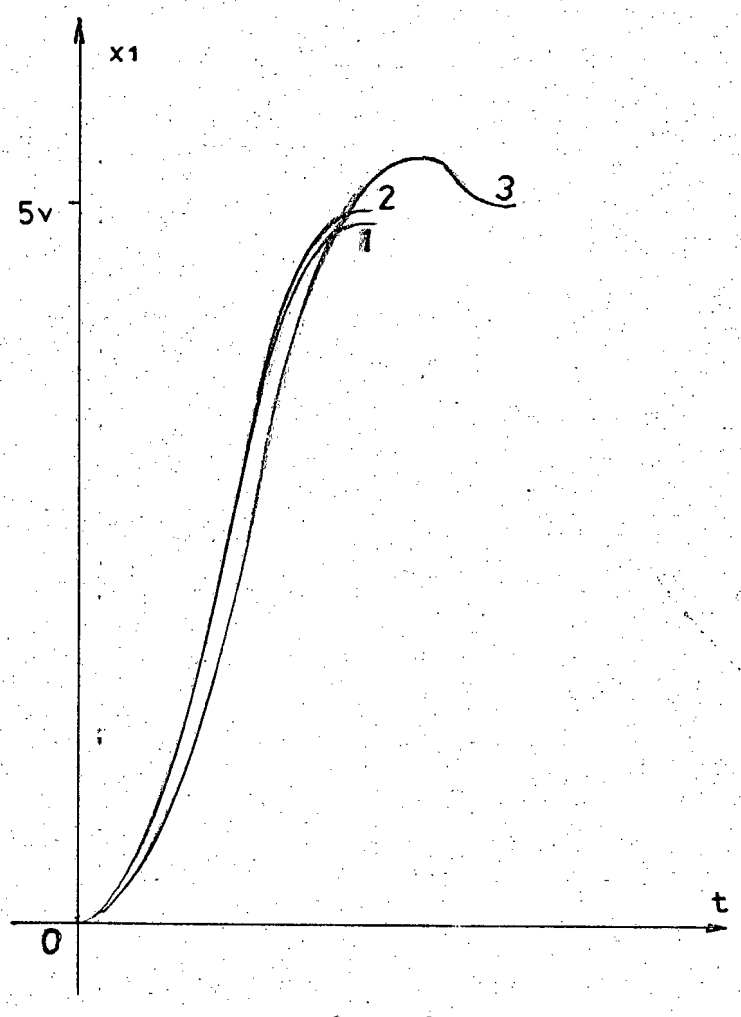

FIGURE 3.4.6 : ADAPTIVE FAST MODEL PREDICTOR WITH DECREASE IN PLANT GAIN

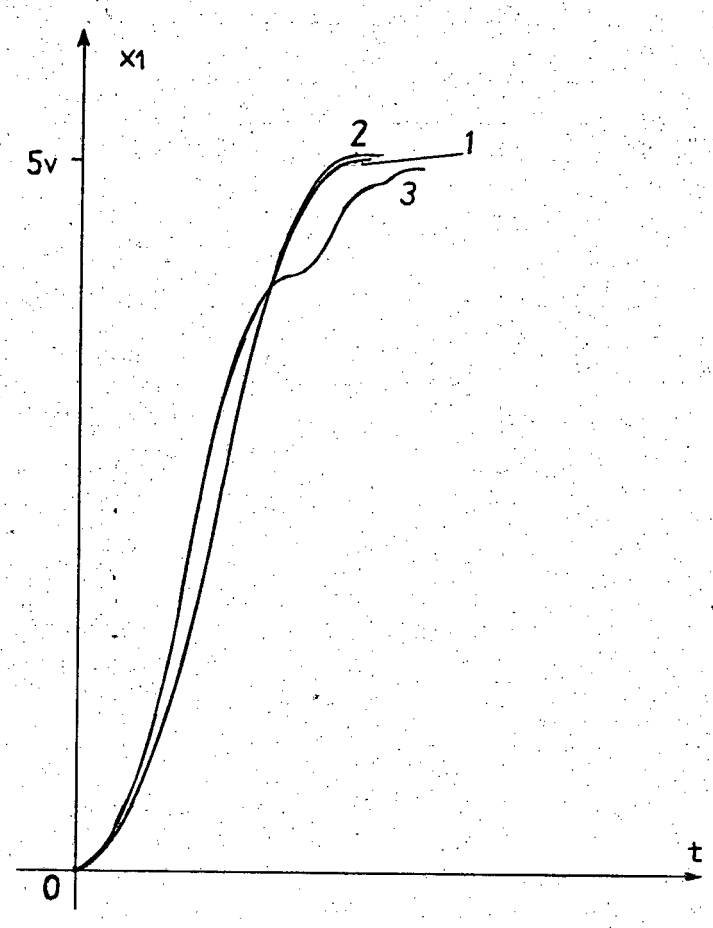

FIGURE 3.4.7 : ADAPTIVE FAST MODEL PREDICTOR WITH AN INCREASE IN PLANT GAIN

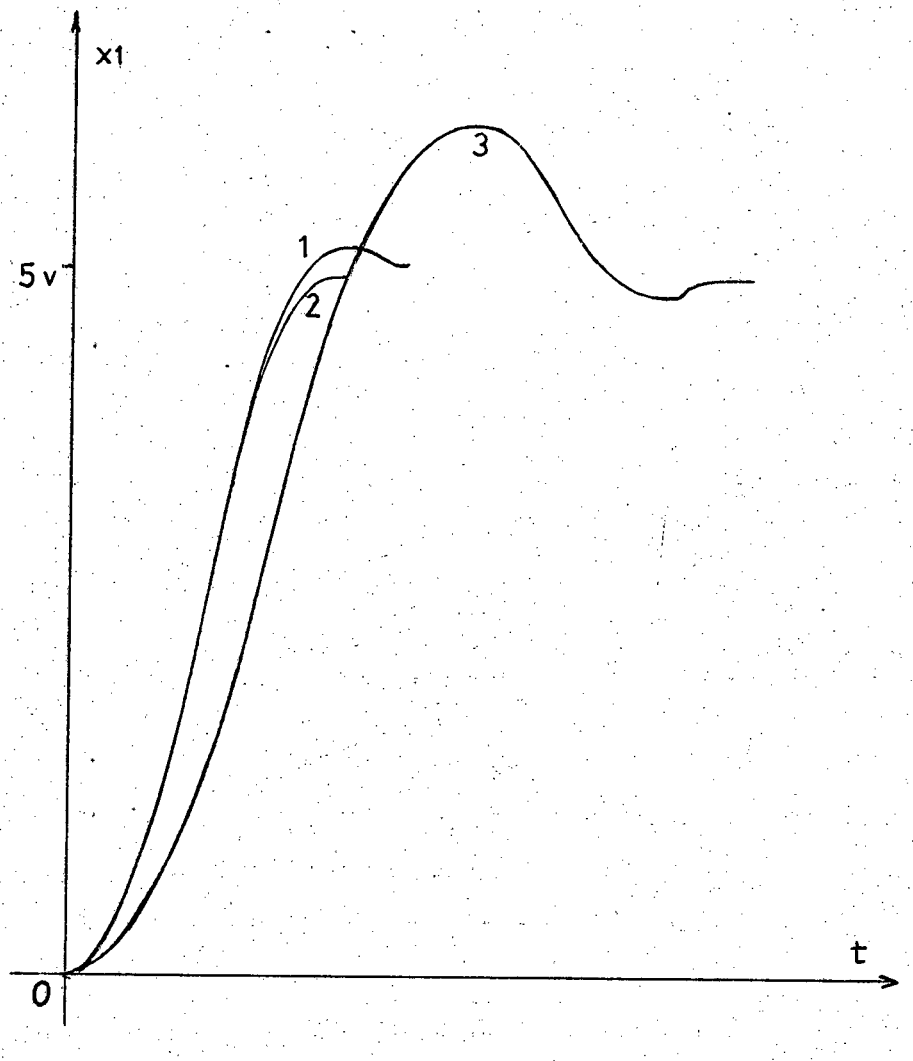

FIGURE 3.4.8 : ADAPTIVE FAST MODEL PREDICTION WITH DECREASE IN PLANT GAIN

3.5. Summary of Results and Comments

The goal of this chapter was to augment and improve the performance of the fast model predictor controller, for a plant to model mismatch, through the utilization of an adaptive technique known as parameter identification and tracking. The method employs a real time model of the plant which parameters may be adjusted to match those of the plant.

By developing a set of equations known as the adaptive or identification laws based upon Liapunov stability considerations, a means of guaranteeing the stable performance of the adaptive loop during the updating or adjusting period (when the tracking error is the greatest) was demonstrated.

A suitable solution of the expression $(e^T Pb)$ yields the necessary form of $e(t)$ and $\dot{e}(t)$ for a second order plant where P (and Q) is a positive symmetric matrix such that $A^T P + PA = -Q$.

There are several parameters; Γ_2, γ, h and the selection of Q which in some respects can be optimized with respect to the plant to be controlled. This was demonstrated to some degree in Figures 3.4.3 and 3.4.4.

Howeyer some practical difficulties arose from these tests. There was the problem of the lack of a high speed processor or some means of a high speed priority interrupt and the second problem was that of the nature of the bang-bang input. It has been demonstrated that for one or two sign reversals, the convergence of the identification algorithm was sufficiently rapid so as to minimize the tracking error but for a sliding input this would not be the case any longer.

This technique attempts to maintain a close model to plant match and hence to maintain the time-optimal or close to time-optimal switching trajectory, and so, avoid any sliding of the input. However, sudden or dramatic changes on or in the system could very well cause rapid deterioration of system performance. Neyertheless the curves in Figures 3.4.5 to 3.4.8 demonstrate convincingly the power of this technique.

CHAPTER 4

ADAPTIVE RELAY CONTROL

4.1. Introduction

The adaptive relay control[5,24] of single-input second-order plants with parameter uncertainty is considered in this section. It is assumed that the plant parameters (plant gain and time constant) remain constant but initially unknown, during motion from the initial conditions to the desired endpoint, taken here to be the state origin or error state origin where indicated.

The controller is designed to yield a near-minimal value of settling time, The state variables are assumed to be accessible and that noise disturbance is not present or of secondary importance.

Adaptive control of uncertain systems plays a large role in control engineering and the structure of an adaptive control system generally has the form shown in Figure 4.1.1.

The plant parameters are identified and the parameters of the controller are adjusted accordingly.

In the time-optimal control problem we desire to transfer the plant state from an initial condition to the state or error state origin.

As shown in this thesis the time-optimal controller is complex and nominally time-optimal systems are highly sensitive to parameter variation.

For certain systems the accurate identification of the plant dynamics can prove difficult and the computation speed may not be sufficiently fast for the adaptive scheme in Fig 4.1.1. to be feasible or insufficiently fast if reasonable system response is to be obtained.

The adaptive strategy described in the following sections dispenses with the learning or identification phase and the arrangement of this control system is given in Figure 4.1.2.

Unlike most adaptive schemes the control strategy does not organize itself through adaptive correction, but identifies a certain surface (for a second-order system the surface is a curve) in the state space.

This surface is associated with sliding motion, and is found by rotating or slewing a switching hyperplane (for

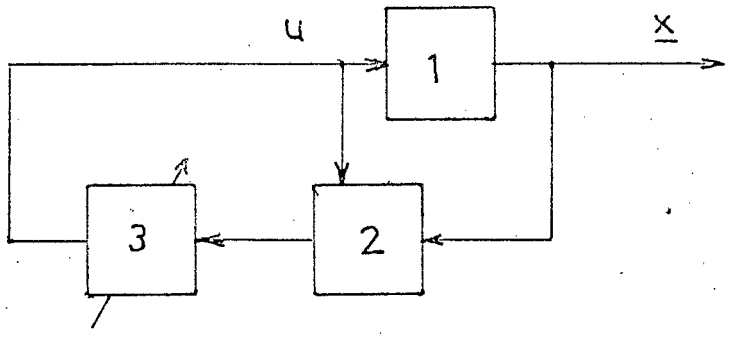

FIGURE 4.1.1 : TYPICAL ADAPTIVE CONTROL SYSTEM

1 : Plant

2 : Plant Identification

3 : Controller

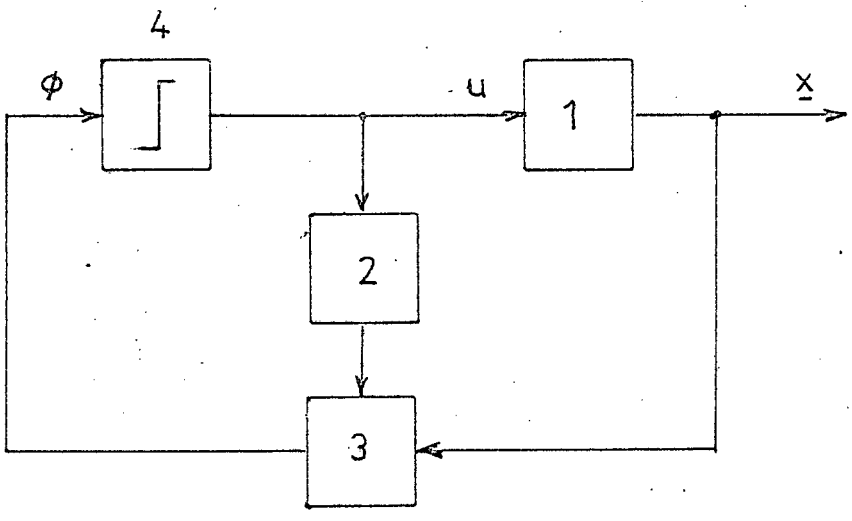

FIGURE 4.1.2 : ADAPTIVE RELAY CONTROL SYSTEM

1 : Plant

2 : Sliding Motion Detector

3 : Linear Switching Function

4 : Ideal Relay

a second-order system the hyperplane is a line) in the state space whenever the system is in a sliding mode. The controller is easily implemented and the resulting system response is close to desired time-optimal trajectory.

4.2. Background

Since the switching function $\phi(x_1,x_2)$ operates a (ideal) relay, the switching hyperplane (a line in the x_1-x_2 plane) corresponding to the relay change-over can be established in the phase plane. Whenever $\phi(x_1,x_2)$ changes sign the relay switches and at that instant the switching line corresponds to zero error and error rate (x_1 and x_2 are synonymous with error and error rate).

There exists a unique combination of x_1 and x_2, for a well defined plant, which results in that $\phi^*(x_1,x_2)$ such that the plant trajectory to the origin is time-optimal. Hence for the correct 'slew' of the switching line, time-optimality results. This is illustrated in Figure 4.2.1.

For incorrect adjustment of the switching line either an overshoot will occur, or the trajectory will recross and cross the switching line so that sliding motion

commences.

An analysis of sliding motion and the switching hyperplane is conducted in Appendix A9. The results of this are important in demonstrating the usefulness of controlling the rotation of the switching hyperplane, and the motivation now becomes evident in section 4.1.

Before analysing the adaptive control strategy the sliding motion of the plant must be investigated.

4.3. Sliding Motion of the Double Integrator Plant

The state co-ordinates of the double integrator plant, $G(p) = \frac{1}{b\,p^2}$ satisfy;

$$\dot{x}_1 = x_2$$

$$\dot{x}_2 = \frac{u}{b} \qquad (4.3.1)$$

where $|u| \leq 1$ and b is a parameter > 0.

The control is given by

$$u = \text{sgn}\ \phi \qquad (4.3.2)$$

where ϕ is the linear switching function

$$\phi = -qx_1 - x_2 \qquad (4.3.3)$$

where $q > 0$ (is a switching parameter) we may write equations 4.3.1 as

$$\begin{bmatrix}\dot{x}_1\\ \dot{x}_2\end{bmatrix} = \begin{bmatrix}0 & 1\\ 0 & 0\end{bmatrix}\begin{bmatrix}x_1\\ x_2\end{bmatrix} + \begin{bmatrix}0\\ \frac{1}{b}\end{bmatrix} \operatorname{sgn}(-qx_1 - x_2) \quad (4.3.4)$$

From Appendix A 9 we know that for sliding motion to occur at the switching surface, the following conditions must hold

1. $qx_1 + x_2 = 0$. This is the switching line.
2. $|\nabla\phi A\underline{x}| \leq |\nabla\phi B|$ for sliding motion to occur, where $B = \begin{bmatrix}0\\ \frac{1}{b}\end{bmatrix}$
3. $\nabla\phi B < 0$. A condition for sliding motion to occur.

Now $\nabla\phi = \left[\frac{\partial\phi}{\partial x_1}, \frac{\partial\phi}{\partial x_2}\right]$

$= (-q, 1)$ (4.3.5)

Hence $|\nabla\phi A\underline{x}| = |qx_2|$ (4.3.6)

and $|\nabla\phi B| = \frac{1}{b}$ (4.3.7)

so condition 1 holds that

$$|qx_2| \leq \frac{1}{b}$$

or $|x_2| \leq \frac{1}{qb}$ (4.3.8)

and $\nabla\phi B = -\frac{1}{b}$, -ve so condition 3 is satisfied.

Hence the sliding region consists of points on the switching line satisfying:

$$|x_2| \leq \frac{1}{qb}$$

As long as equation 4.3.8 is satisfied the state remains on the switching line $qx_1(t)+x_2(t) = 0$ which lie between points A and A^1 in Figure 4.3.1

Consider the initial conditions at the time t=0 as satisfying:

$$qx_1+x_2= 0 \qquad (4.3.9)$$

From equations 4.3.1 and 4.3.9, the motion on the switching line $qx_1 + x_2 = 0$ satisfies:

$$x_1(t) = x_1(0)\, e^{-qt}$$

$$x_2(t) = x_2(0)\, e^{-qt} \qquad (4.3.10)$$

Thus the system behaves like a linear plant

$$\dot{x}_1 = x_2$$

$$\dot{x}_2 = - qx_2 \qquad (4.3.11)$$

and the state approaches the state origin. The state origin is not attained within a finite time since the state co-ordinates decay exponentially with time.

Suppose the state co-ordinates satisfy

$$\phi = qx_1 + x_2 = 0$$

$$q = \frac{1}{b\,|x_2|} \qquad (4.3.12)$$

The point (x_1, x_2) i.e. A or $\bar{A}$ in Figure 4.3.1 lies on the boundry of the sliding region (equation 4.3.8).

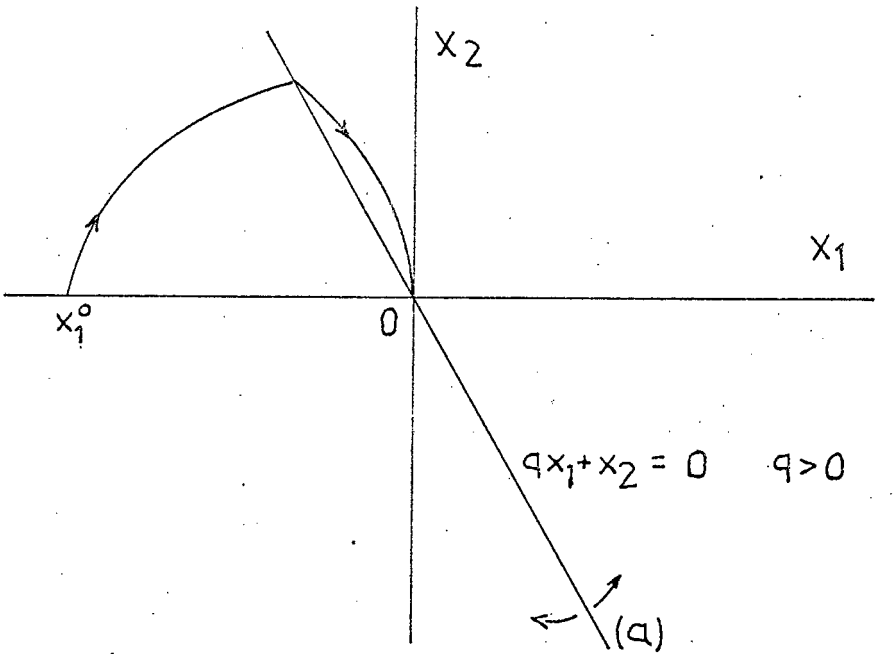

FIGURE 4.2.1 : POSITIONING OF SWITCHING LINE FOR TIME-OPTIMAL SWITCH

(a) Switching Line for Time-optimality

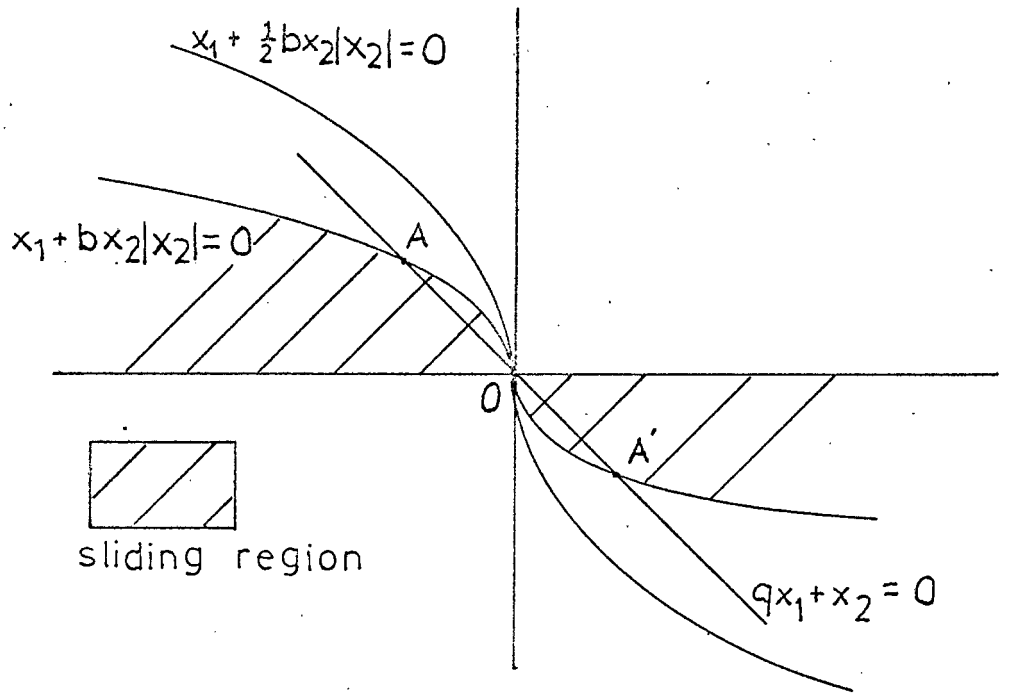

FIGURE 4.3.1 : DOUBLE INTEGRATOR PLANT SWITCHING CURVES

We shall define a point satisfying $\Phi = qx_1+x_2 = 0$ and $q = \frac{1}{b|x_2|}$ a sliding boundry point.

So far we have considered q as fixed. If q varies, the point (x_1,x_2) describes a locus.

From equations 4.3.12 we can derive the sliding boundry locus (see Figure 4.3.1) i.e. $x_1+bx_2\ |x_2| = 0$

or $x_1+\frac{1}{2}(2b)x_2\ |x_2| = 0$ (4.3.13)

We next consider the motion of a state point constrained to lie on this locus.

Consider an initial condition (x_1^0, x_2^0) satisfying $x_1+ bx_2\ |x_2| = 0$

From equation 4.3.12

$$q^0 = \frac{1}{b|x_2^0|} \qquad (4.3.14)$$

Suppose we allow q to vary as a function of time so that the state moves on the locus $x_1+bx_2\ |x_2| = 0$

Then differentiation of $q = \frac{1}{b|x_2|}$ yields

$$\dot{q}(t)\ x_2 + q(t)\dot{x}_2(t) = 0 \qquad (4.3.15)$$

and differentiation of $x_1+ bx_2\ |x_2|$ and use of 4.3.1 yields $x_2 + 2b\ |x_2|\ \dot{x}_2 = 0$ (4.3.16)

From equations 4.3.1 and 4.3.16 the control is

$$u = b\dot{x}_2 = -\tfrac{1}{2}\ \text{sgn}\ x_2 \qquad (4.3.17)$$

where $\text{sgn}\ x_2 = \dfrac{x_2}{|x_2|}$

The state trajectory is therefore identical to that of the double integrator plant with plant gain parameter 2b and full control $|u| = 1$.

Substitution of equation 4.3.17 into 4.3.15 gives

$$\dot{q}(t) = \frac{q(t)}{2b|x_2|} \qquad (4.3.18)$$

and from 4.3.12 and 4.3.18

$$\dot{q}(t) = \tfrac{1}{2}(q(t))^2 > 0 \qquad (4.3.19)$$

The fact that $\dot{q}(t) > 0$ will be used to verify a certain condition in the next section.

The trajectory reaches the origin in a finite time since from equations 4.3.1 and 4.3.17

$$x_2(t) = x_2^{\,o} - \frac{t}{2b}\ \text{sgn}\ x_2^{\,o} \qquad (4.3.20)$$

The state co-ordinates are zero together on the locus $x_1 + bx_2|x_2| = 0$.

Substituting $x_2(t) = 0$ into equation 4.3.20 gives the finite time:

$$t = 2h \left| x_2^{\,o} \right| \qquad (4.3.21)$$

where $\operatorname{sgn} x_2^{\,o} = \dfrac{x_2^{\,o}}{\left| x_2^{\,o} \right|}$

to reach the state origin.

4.4. The Basic Adaptive Controller

The adaptive controller has a (time-variable) linear switching function (see Figure 4.4.1)

$$qu = \operatorname{sgn}(-qx_1 - x_2) \quad q > 0 \qquad (4.4.1)$$

and the switching line is from 4.4.1

$$qx_1 + x_2 = 0 \qquad (4.4.2)$$

At time $t=t_o$ the control parameter q is set to the value

$$q = \varepsilon \qquad \varepsilon > 0 \qquad (4.4.3)$$

Initially ε is small and the initial position of the switching line is, from 4.4.2 and 4.4.3

$$\varepsilon x_1 + x_2 = 0 \qquad (4.4.4)$$

The parameter q is subsequently continually adjusted according to the following rule:

If sliding motion occurs, the current switching line is rotated to be just ahead of the state point, i.e. the control parameter is increased to the value

$$q(t+) = q(t)(1+\epsilon) \quad (\epsilon > 0) \qquad (4.4.5)$$

where ϵ is a small positive number. If the plant is not sliding on the current switching line 4.4.2, the

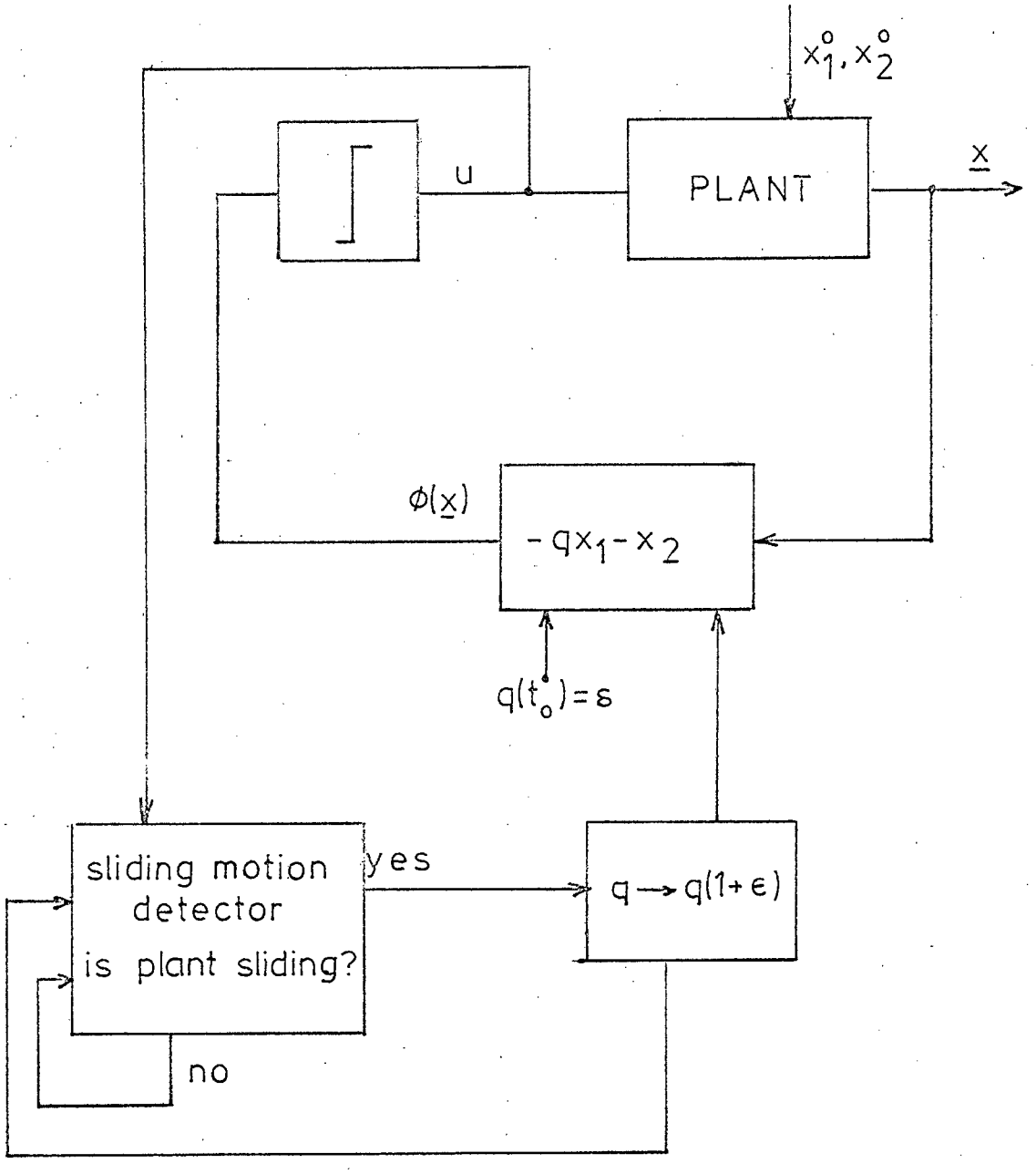

FIGURE 4.4.1 : THE BASIC ADAPTIVE CONTROLLER FOR A SECOND-ORDER PLANT

switching line is kept fixed, i.e. the value of q remains unchanged. The assumption is that sliding motion can be detected in an infinitesimal time interval.

Ideally δ and ϵ are vanishingly small. For this limiting case the following properties have been verified in 4.3:

Property 1: The time taken to reach the state origin is finite

Property 2: The state trajectory approaches the state origin on a certain sliding boundry locus

Property 3: At all points on the sliding boundry locus $\dot{q}(t) > 0$

4.5. Analysis of the Basic Adaptive Controller

The controller 4.4.1 and 4.4.3 drives the state to the point A on the switching line L_1 (see Fig 4.5.1)

$$\delta x_1 + x_2 = 0 \qquad (4.5.1)$$

in a finite time. From 4.3.8, for $q = \delta$ sufficiently small, sliding commences (the state slides on the current switch line from point A to point $\bar{A}$. Assuming that sliding motion can be detected with an infinitesimal time interval, $\bar{A}$ is coincident with A) and the strategy given by 4.4.5 is implemented, i.e. the switching line is rotated.

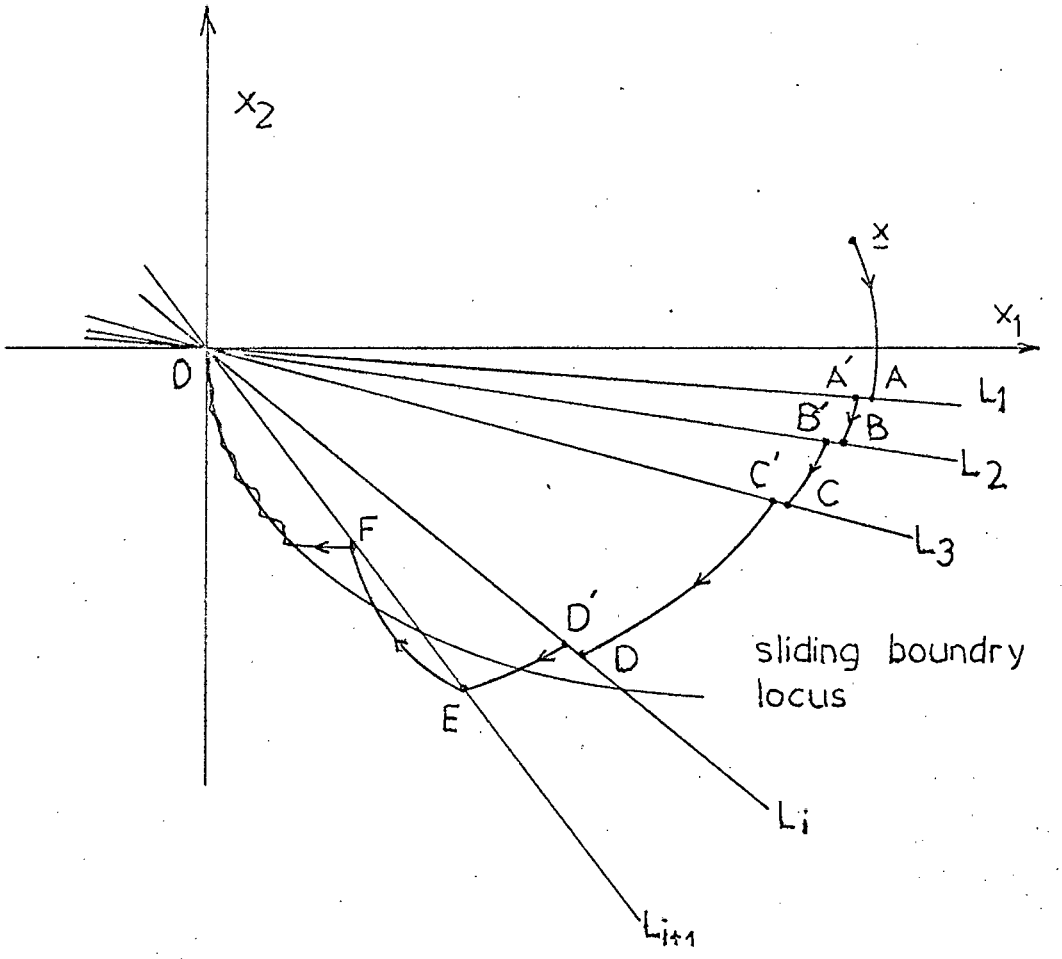

FIGURE 4.5.1 : SECOND-ORDER PLANT ADAPTIVE CONTROL STATE PATH

L_1 : $\varepsilon x_1 + x_2 = 0$

L_2 : $\varepsilon(1+\epsilon)x_1 + x_2 = 0$

L_i : $q_i x_1 + x_2 = 0$

L_{i+1} : $q_i(1+\epsilon)x_1 + x_2 = 0$

In the limit as the time taken to detect sliding motion tends to zero, points A', B', C', D' tend to the points A,B,C,D.

From 4.4.1 and 4.4.5, the control parameter q is changed, and the new control law is

$$u = \text{sgn}(\quad -\varepsilon(1+\epsilon)x_1 - x_2) \qquad (4.5.2)$$

From 4.4.2 and 4.5.2 the control value at point A is now

$$u_{\phi} = \text{sgn}(-x_1) = \text{sgn}(x_2) \qquad (4.5.3.)$$

which drives the state to point B on the current switching line L_2

$$\varepsilon(1+\epsilon)\, x_1 + x_2 = 0 \qquad (4.5.4)$$

Sliding recommences and the swtiching line is rotated further. The control is given by 4.4.1 and after repeated rotation of the switching line whenever sliding occurs, the state reaches the point D in the neighbourhood of the sliding boundry locus in the sliding region (see Figure 4.5.1) within a finite time.

At this point the current switching line L_i

$$q_i x_1 + x_2 = 0 \qquad (4.5.5)$$

is rotated to the line L_{i+1}, viz.

$$q_i(1+\epsilon)\, x_1 + x_2 = 0 \qquad (4.5.6)$$

The control 4.5.3 drives the state to the point E (see Figure 4.5.1) on the line L_{i+1} equation 4.5.6 in the non sliding region. Sliding does not occur at point E.

The state enters the region, from 4.5.6

$$x_1(q_i(1+\epsilon)x_1 + x_2) < 0 \qquad (4.5.7)$$

and the state trajectory returns to the switching line L_{i+1} at point F in the sliding region. Sliding then recommences. As $\epsilon \rightarrow 0$ the overshoot of the sliding boundry locus becomes negligibly small and the states moves effectively on the sliding boundry locus to the state origin.

The motion on the locus to the state origin has been shown in 4.3 to be identical to that of the double integrator plant with plant parameter 2b.

The sliding boundry locus is in fact the time-optimal switching curve of the double integrator plant with plant parameter 2b.

The time taken to reach the state origin has been shown in 4.3 to be finite and on the locus we have $\dot{q} > 0$ (4.3.19) in agreement with requirement 4.4.5 of the adaptive strategy. Properties 1, 2 and 3 have therefore been verified for the double integrator plant (For modifications to the basic strategy see Appendix A.10).

4.6. Performance of the Adaptive System

Only step initial conditions and step reference inputs were used in practical demonstrations for this thesis. However non step inputs or non step initial conditions do often arise as for example the control of a jacketed stirred tank reactor where the initial conditions (the two state co-ordinates (phase variables)) are the temperatures of the outer and inner tank. Here a new situation exists and in Appendix 8 is a short description of the modifications in the basic strategy that are required for these situations.

Practical demonstrations of this method were also successfully performed on a triple integrator plant = $\frac{1}{bp^3}$, a plant of two lags plus one integrator = $\frac{1}{bp(1+T_1p)(1+T_2p)}$ and a plant with one integrator plus the 'second-order servo transfer function' = $\frac{1}{bp(p^2+2\zeta wp + w^2)}$

The analysis of third order controllers and plants with the sliding motion regime is complex but is well documented by Zinober[24]. The control strategy for third-order systems does not differ very much from second-order systems and only a brief description of the third

order strategy is discussed in Appendix A.11.

4.7. Experimental Procedures

The basis of operation of the adaptive relay control is the implementation of the control law, viz. the linear switching function:

$$\phi(\underline{x}) = - q^{n-1} x_1 - a_1 q^{n-2} x_2 - \ldots - a_{n-2} q x_{n-1} - x_n$$

and $q > 0$ (4.7.1)

where the design parameters, a_i, are chosen to be the binomial coefficients

$$a_i = \frac{(n-1)!}{(i+1)!(n-i-2)!}$$

For a second-order plant:

$$\phi(\underline{x}) = - qx_1 - x_2 \text{ and } a_i = a_0 = 1 \qquad (4.7.2)$$

For a third-order plant:

$$\phi(\underline{x}) = - q^2 x_1 - a_1 \, qx_2 - x_3 \text{ where } a_1 = 2 \qquad (4.7.3)$$

However Zinober[24] indicates that a_1 can be modified such that $a_1 d \geq 2 \left(\frac{2}{3} 2^{\frac{1}{2}}\right)$ where d is a damping parameter. For the smallest settling time $d = \frac{2}{3} 2^{\frac{1}{2}}$ (= .943) (see Appendix A.11).

The position of the switching hyperplane is given by:

$$\phi = q^{n-1}x_1 + a_1 q^{n-2}x_2 + \ldots + a_{n-2} qx_{n-1} + x_n = 0 \qquad (4.7.4)$$

Initially the control parameter q is set to the value

$$q = \varepsilon \qquad 1 >> \varepsilon > 0 \qquad (4.7.5)$$

The control parameter q is continually adjusted according to the following rules:

(i) If sliding motion occurs, the current switching hyperplane is roated to be just ahead of the state point, i.e. the control parameter q is increased to the value

$$q(t+) = q(t)(1+\epsilon) \quad (\epsilon > 0) \qquad (4.7.6)$$

where ϵ is a small number

(ii) If the plant is not sliding on the current switching surface (4.7.4), the switching hyperplane is kept fixed, i.e. the value of q remains unchanged.

The assumption is that sliding motion can be detected in an infinitesimal time interval and hence ideally ε and ϵ are vanishingly small.

The state trajectory moves from the initial conditions to the initial position of the switching hyperplane. Sliding motion ensues and the switching surface is incrementally rotated. After repeated rotation of the switching hyperplane whenever sliding motion occurs, the

state reaches a certain non-linear surface, the sliding boundry surface, and then moves on this surface to the state origin (see Figure 4.5.1 where the state trajectory of a second-order system is given).

The first demonstration of the control strategy was implemented on an analogue computer for a second-order plant(a double integrator). Appendix A12.1 contains a diagram of the system and a discussion of the means of detecting sliding motion.

The second stage consisted of writing a program to demonstrate the strategy using hybrid simulation. This proved to be also highly successful. Appendix A12.2 contains a diagram of the system and the programs for a second-order and third-order plant.

Finally the control strategy was used to control a small DC motor as demonstrated in chapter two. The use of an analogue computer as well as hybrid control, were both demonstrated.

4.8. Simulation Results

Figures 4.8.1 and 4.8.2 represent analogue computer simulations of a double integrator plant for variations in the plant gain parameter $K_p = \frac{1}{b}$, and the inclusion of a non-linearity, velocity limiting.

For Figure 4.8.1 $K_p(nom) = \frac{1}{a} = 1$ and the curves are:

Curve No	K_p
1	.3
2	.4
3	.5
4	.7
5	1.0
6	3.0
7	4.0

The ratio $\frac{b}{a}$ varied from $.25 \leq \frac{b}{a} \leq 3.33$, a large variation in plant gain. Only for curve 1 overshoot occurred.

For Figure 4.8.2 the curves are: ($K_p = .4$)

Curve No	
1	no velocity limiting
2	velocity limit set to 1.9 volts
3	velocity limit set to 1.0 volts

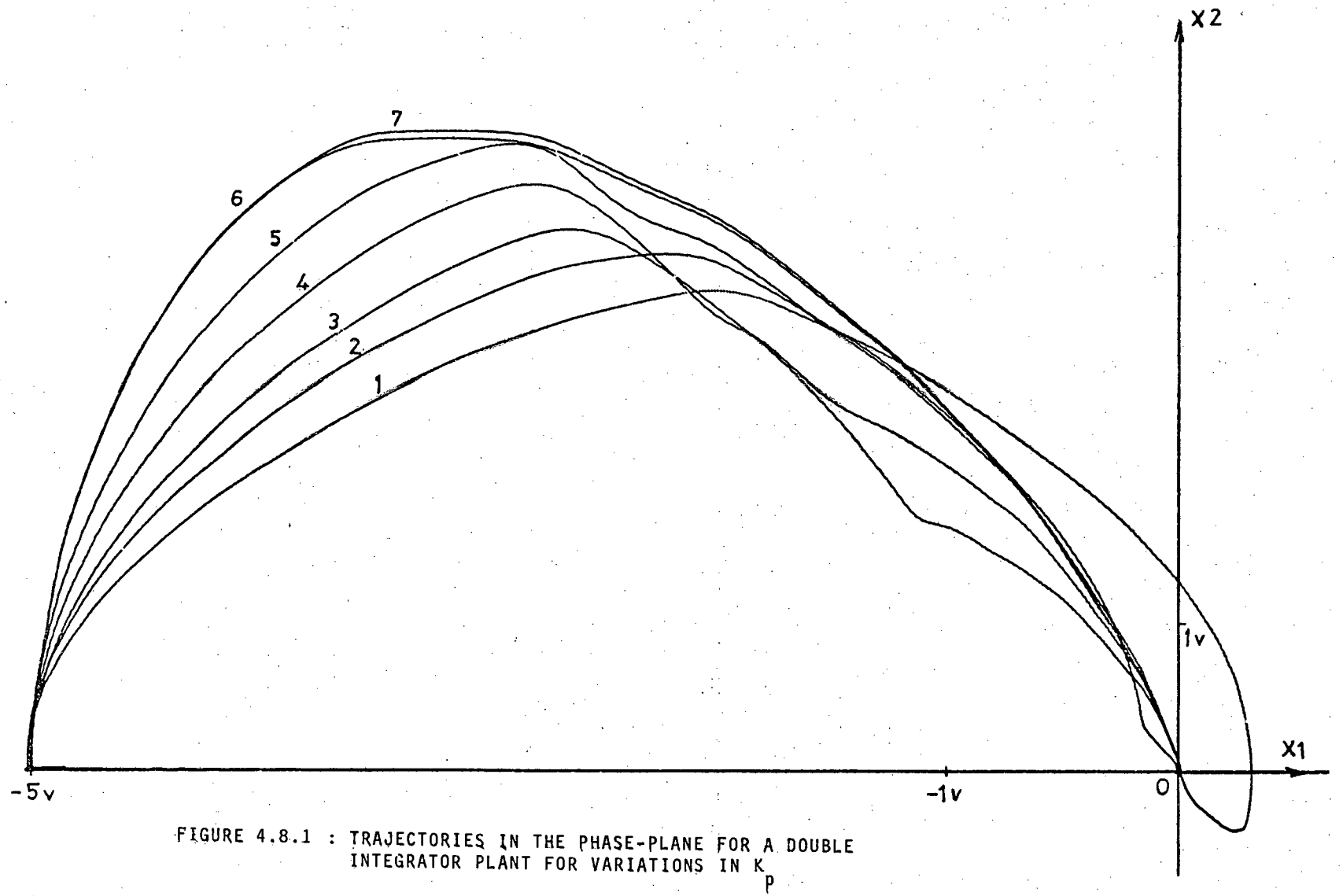

FIGURE 4.8.1 : TRAJECTORIES IN THE PHASE-PLANE FOR A DOUBLE INTEGRATOR PLANT FOR VARIATIONS IN K_p

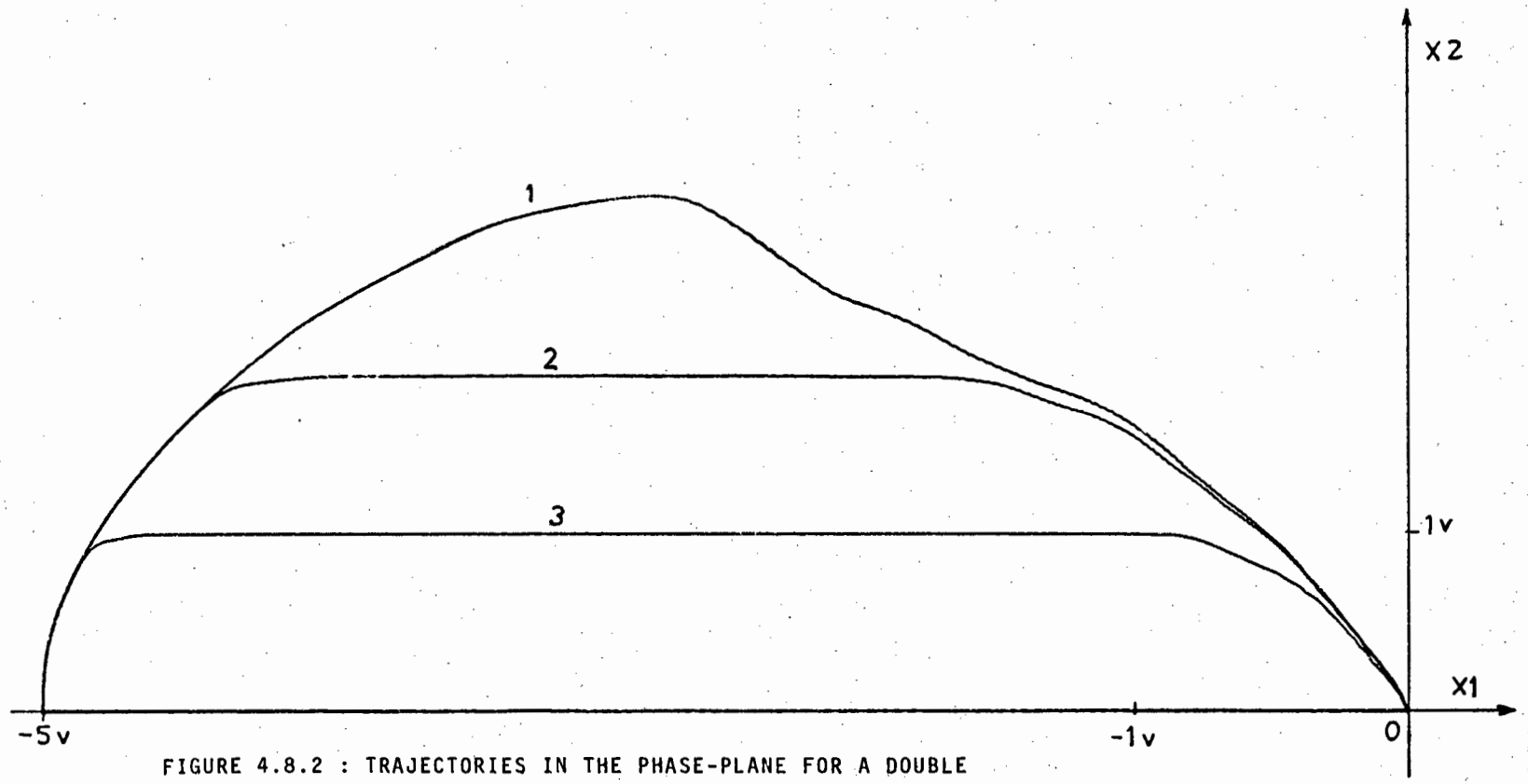

FIGURE 4.8.2 : TRAJECTORIES IN THE PHASE-PLANE FOR A DOUBLE INTEGRATOR PLANT FOR VARIATIONS IN VELOCITY LIMITING

The inclusion of a non-linearity in no way impeded the performance of the strategy.

Figures 4.8.3 and 4.8.4 illustrate the responses of a second-order plant with variations in K_p for a step initial condition and with a non-linearity(velocity limiting).

The second-order plant has a transfer function

$$G_p(s) = \frac{K_p}{s(s+\alpha_p)} \text{ where } K_p = 1(\text{nominal}), \alpha_p = .1.$$

The responses for Figure 4.8.3 are:

Curve No	K_p
1	1
2	1.2 (20% increase)
3	.8 (20% decrease)

The responses are as anticipated. For values of $K_p < K_{nom}$ there is a slight overshoot (curve 3) and for values of $K_p > K_{nom}$ the response is close to nominal (curves 2 and 1).

The responses for Figure 4.8.4 are

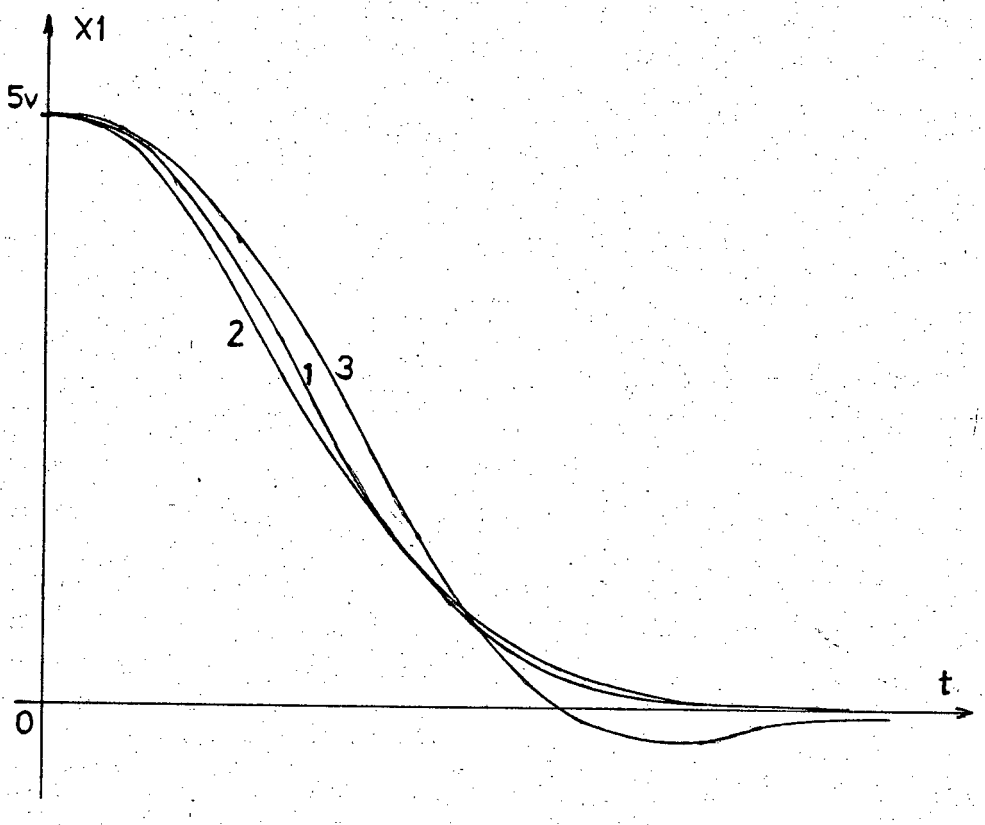

FIGURE 4.8.3 : HYBRID SIMULATION OF A SECOND ORDER PLANT FOR VARIATION IN K_p

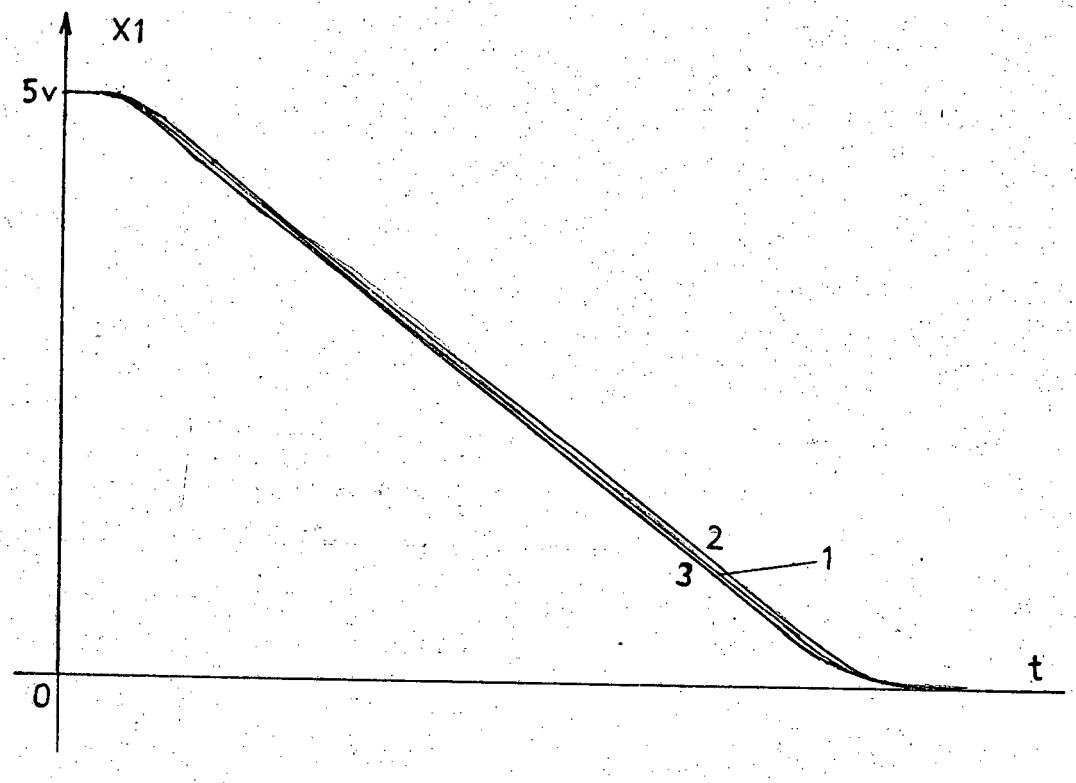

FIGURE 4.8.4 : HYBRID SIMULATION OF A SECOND ORDER PLANT FOR VARIATION IN K_p WITH VELOCITY LIMITING

Curve No	K_p
1	1
2	.9 (10% decrease)
3	1.2 (20% increase)

and the velocity limit was set at $.4\dot{x}_1 max$. The responses follow virtually the same path for even moderate changes in plant gain.

Figure 4.8.5 is a phase-plane representation of the second order plant discussed above but for variations in α_p. K_p = 1(nominal) and the curves are:

Curve No	α_p
1	0
2	.1
3	.5
4	1
5	.1 (with velocity limiting of $.4\dot{x}_1$ max).

There are no overshoots and the behaviour of sliding motion as part of the control strategy is well demonstrated by the trajectories moving towards the state origin.

Figures 4.8.6 and 4.8.7 represent the responses of a triple integrator plant for a step initial condition.

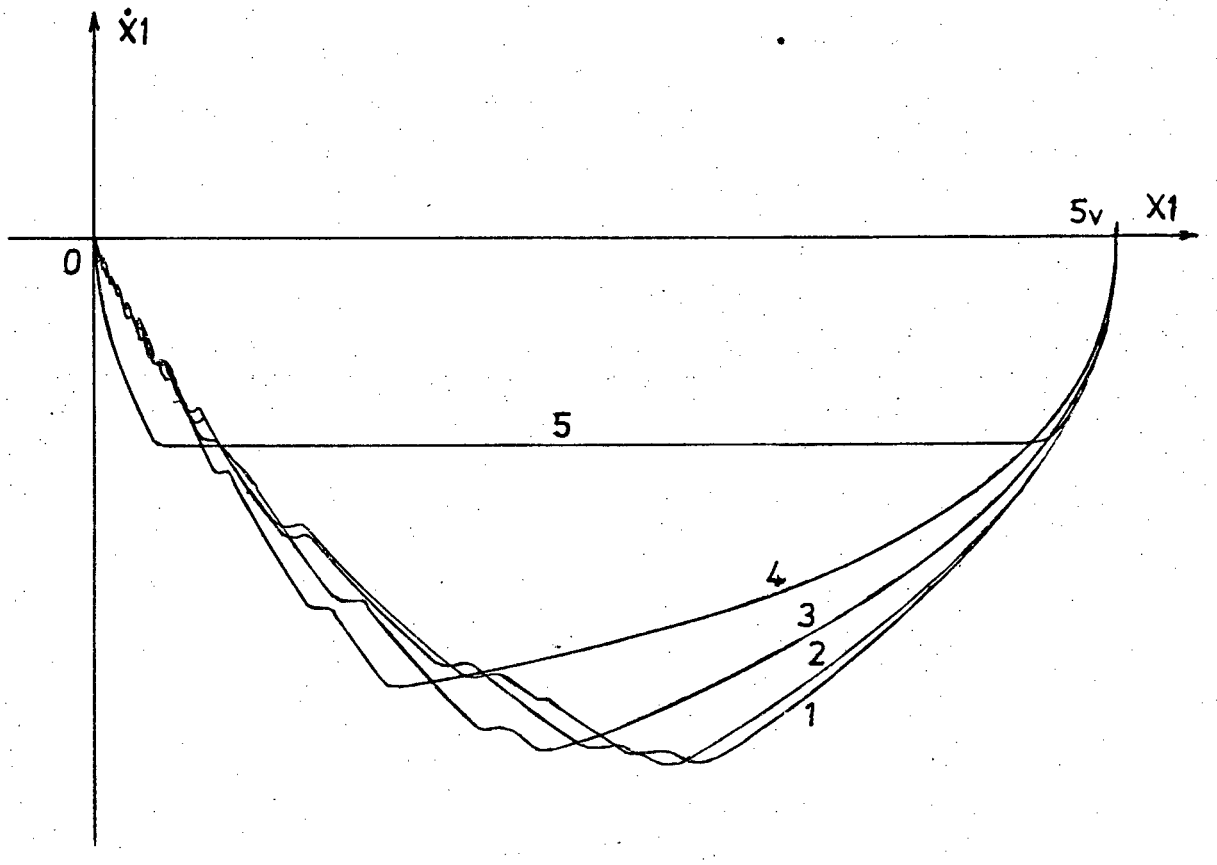

FIGURE 4.8.5 : HYBRID SIMULATION OF A SECOND ORDER PLANT IN VARIATION IN α_p AND VELOCITY LIMITING

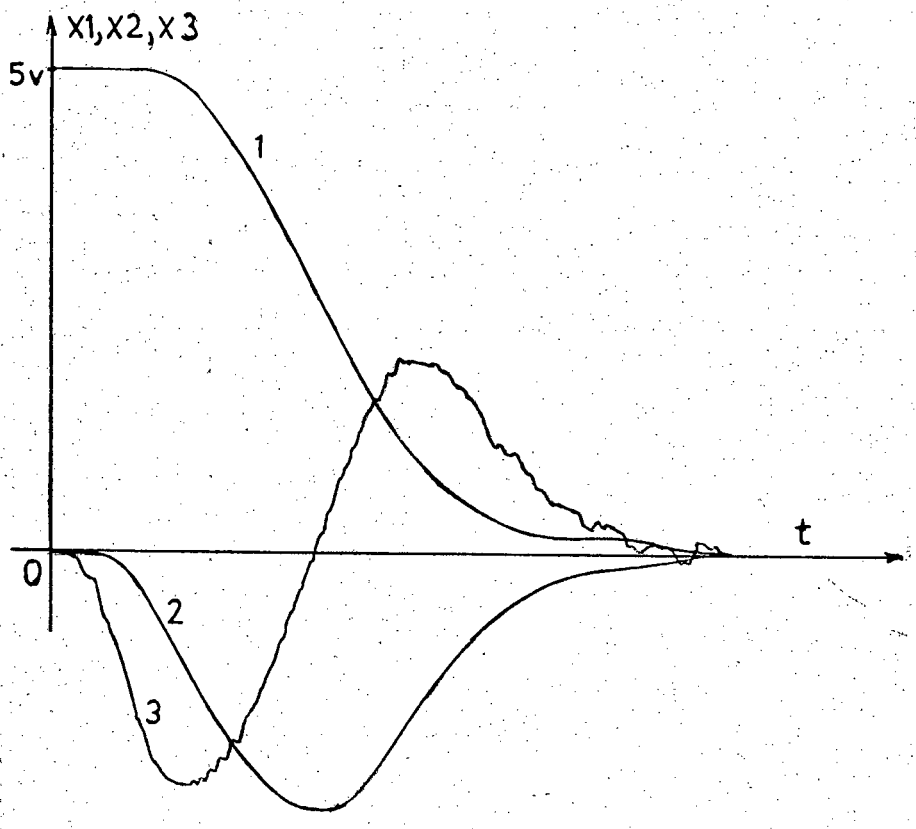

FIGURE 4.8.6 : HYBRID SIMULATION OF A TRIPLE INTEGRATOR PLANT

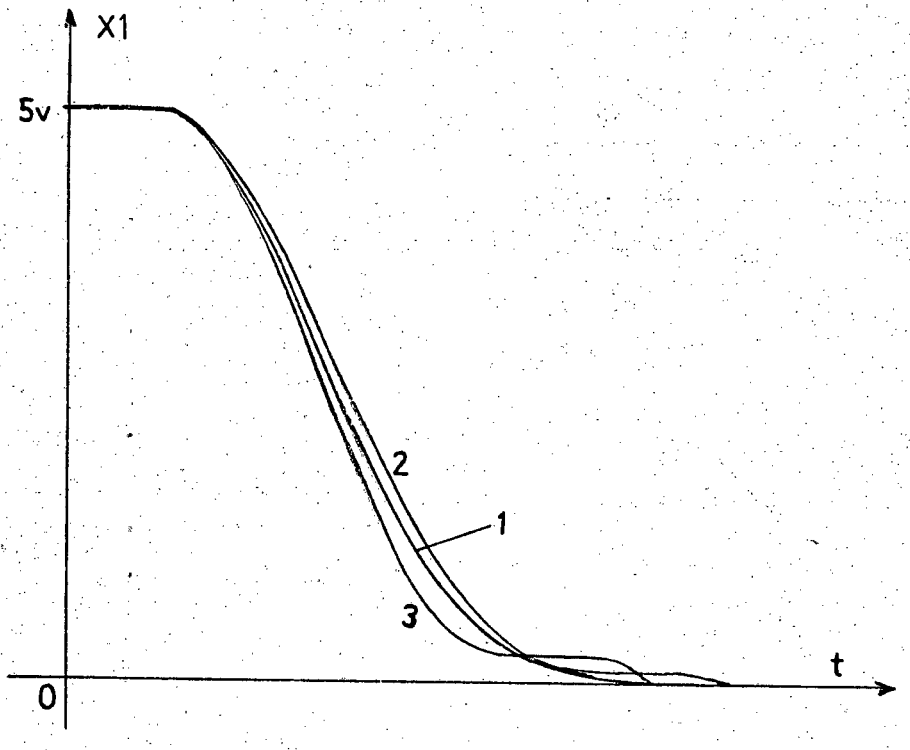

FIGURE 4.8.7 : HYBRID SIMULATION OF A TRIPLE INTEGRATOR PLANT FOR VARIATION IN K_p

The triple integrator has a transfer function $\frac{K_p}{s^3}$ where $K_p = 1$(nominal).

Figure 4.8.6 illustrates the position response curve 1, velocity curve 2 and acceleration curve 3. Although the trajectories were sub-optimal, the curves converged to zero simultaneously.

Figure 4.8.7 illustrates the response when K_p is varied.

Curve No	K_p
1	1 (nominal)
2	1.2(20% increase)
3	.9(10% decrease)

For moderate variations of K_p about the nominal, the settling times are close to nominal.

Figures 4.8.8 and 4.8.9 represent the responses of a third-order plant for variations in α_p and with acceleration limiting. The transfer function of the third order plant is $G_p(s) = \frac{K_p}{s(s^2+\alpha_p s+1)}$ where $K_p = 1$ (nominal) and $s^2+\alpha s+1 = s^2+2\zeta ws+w^2$, hence $\alpha_p = 2\zeta$ and $w = 1$.

The curves in Figure 4.8.8 reflect a variation of α_p

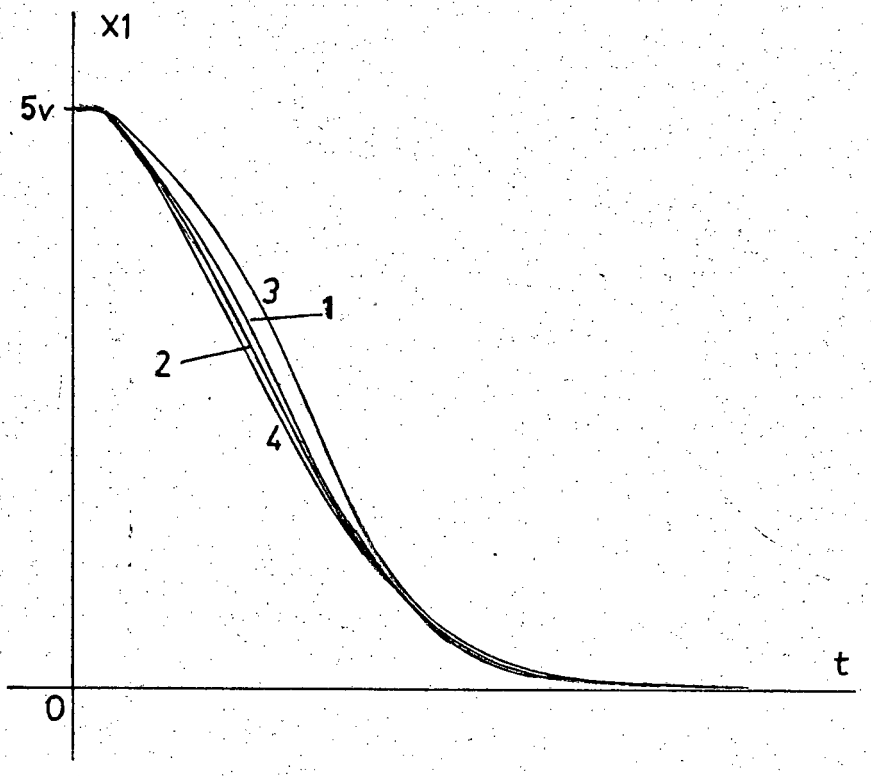

FIGURE 4.8.8 : HYBRID SIMULATION OF A THIRD-ORDER PLANT FOR VARIATION IN α_p

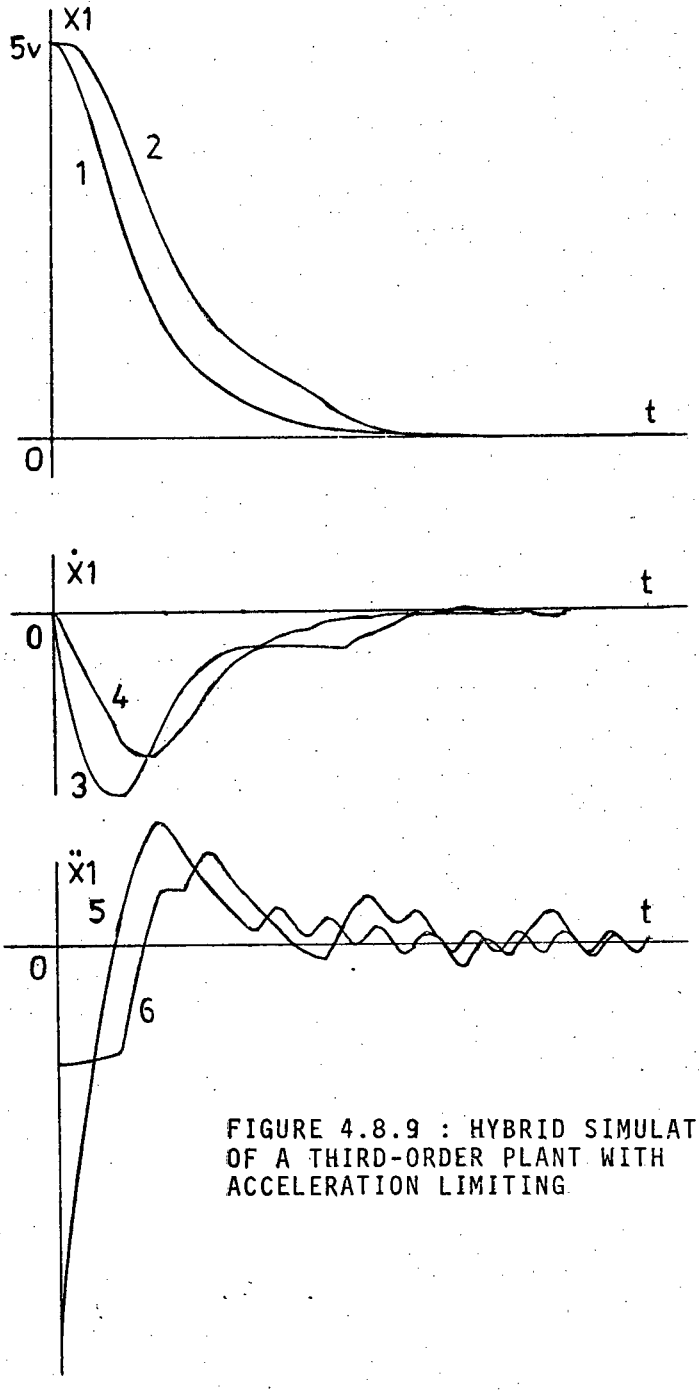

FIGURE 4.8.9 : HYBRID SIMULATION OF A THIRD-ORDER PLANT WITH ACCELERATION LIMITING

such that:

curve No	α_p
1	1
2	.4
3	2
4	0 (triple integrator)

Again the settling times are virtually the same as for the nominal ($\alpha = 0$).

Figure 4.8.9 illustrates the responses for position, velocity and acceleration when acceleration limiting was introduced (a non-linearity). $K_p = 1$ and $\alpha_p = 1$ and the acceleration limit setting was about $.3\ddot{x}_1$ max.

Curves 1,3 and 5 represent the state variables with no acceleration limiting and curves 2,4 and 6 represent the state variables with limiting. It is seen that the introduction of limiting the acceleration does not modify the performance of the plant by any appreciable means.

Finally Figure 4.8.10 represents the response of the output potentiometer of a small DC motor for a step input. The adaptive relay control strategy was synthesized on an analogue computer and is essentially the same as in Figure A12.1.1. This is distinct from the digital control as indicated in Figure 2.4.24 in chapter

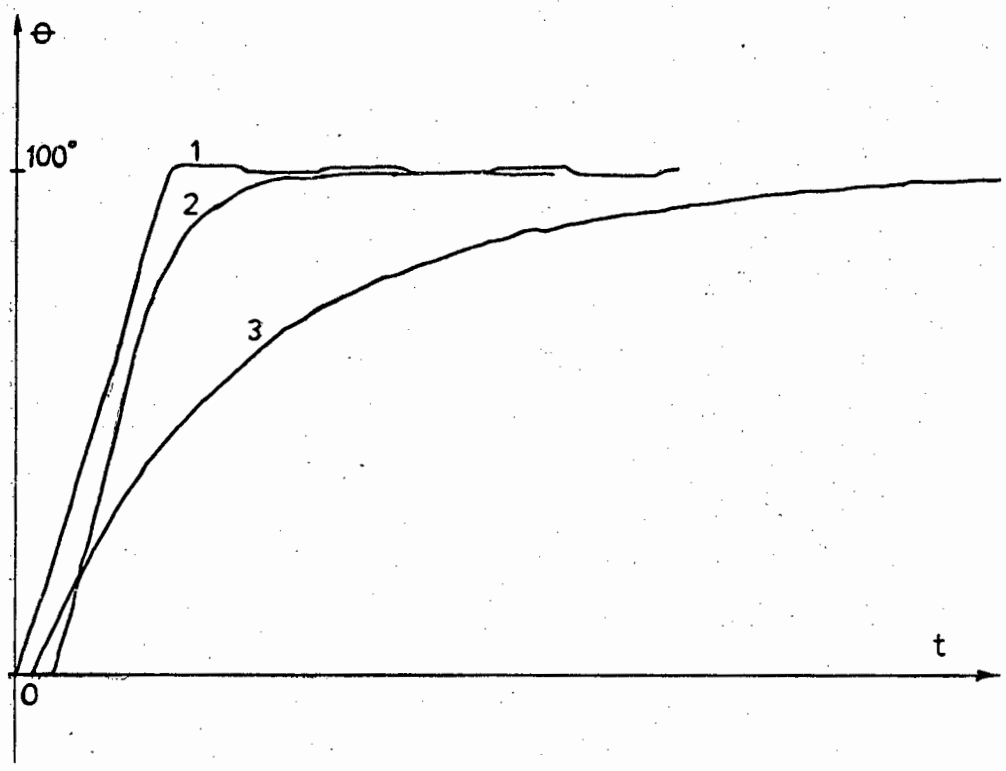

FIGURE 4.8.10 : ANALOGUE COMPUTER CONTROL OF A DC MOTOR
WITH THE ADAPTIVE RELAY STRATEGY

two, but the basic analogue block diagram of Figure A6.4.1 still applies.

Curve 1 represents the output response when there was no velocity feedback present and merely the position feedback provided the switching function to the electronic relay. As can be seen there were limit cycles in the steady state and further augmented by the severe backlash in the gearbox. Curve 3 represented the adaptive relay strategy for a particular velocity feedback constant (the tachogenerator voltage was attenuated through a potentiometer) and curve 2 represented the response when the velocity feedback constant was reduced by a factor of four.

It can be seen from Figures 4.8.10 and 2.4.24 that this method provides good control over a DC motor whose transfer function can be approximated to by a second-order function (note that in Figure 2.4.24 no attempt was made to optimize the velocity feedback constant).

4.9. Summary of Results and Comments

The adaptive relay controller was applied without any modification to second and third order plants, both containing non linearities (velocity and acceleration limiting). Neither the plant parameters nor the precise plant dynamics need be known. In contrast the time-optimal (see chapter two) controller requires an accurate knowledge of the plant dynamics.

The application of the relay adaptive control law is straightforward and is the implementation of a linear algebraic function of the plant state-variables provided of course, that they are accessible. The strategy can be applied for a set of references provided the error state-variables are generated.

In general this method provides satisfactory system response of second-order and third order plants throughout the state-space, and the controller does not require the knowledge of the plant dynamics for its implementation. The effect of the sliding motion of the switching element need not necessarily be a problem as a smoothing network inserted between the relay and the input to the plant, would alleviate the action of the bang-bang control signal upon the plant (similar in respects to

the diode limited integrator used for sliding motion detection, see Appendix A12.1).

The results obtained from the third-order plant with complex eigenvalues in the hybrid simulations and the control of the dc motor indicate a good practical application of this control method to motor position control with large inertial loads.

CHAPTER 5

STATE VARIABLE TRANSFORMATION AND NOMINAL-$\underline{V}$ CONTROL

5.1 INTRODUCTION

One of the difficulties in synthesising the time-optimal expression for a fast model (where known) is it's complicated form which consists of several combinations of exponential, logarithmic and other complicated functions of the state variables (see Appendix A6.2 and A6.5).

A method developed by Ryan[6,31] whereby the time-optimal feedback control laws can be expressed in an explicit algebraic form is presented here. Ryan shows that in certain cases the time-optimal control law for triple integrator plants may be expressed in a form involving merely products and integer powers of state variables together with signum functions. Moreover it has been established that this control law is also precisely optimal for specific third order plants with negative real eigenvalues in a certain ratio and for double integrator plants and negative real eigenvalues in a certain ratio.

This property forms the basis of the nominal-$\underline{y}$ control approach whereby the relatively simple time-optimal control laws for the double and triple integrator plants may be applied, via a special state variable transformation (the nominal-$\underline{y}$ transformation) to more general second and third order real pole plants with little deterioration from optimal system performance.

The use of a fast model predictor whether synthesized as a mathematical model on a computer or otherwise, presents no real difficulties for second order systems so far as the switching logic is concerned. However for third and higher order systems the switching strategy based on a fast model becomes extremely complex and to achieve exact time-optimal response even more so.

For more general third order (and fourth order) systems a simplified sub-optimal predictive control strategy is shown which gives near time-optimal performance. Attention is focussed however on third-order plants with complex eigenvalues during the hybrid simulations.

5.2 The System

The relay control system under consideration is shown in Figure 5.2.1 and is the same as that in section 1.2. However for explanatory purposes a short introduction to the system is felt to be justified. The system in Figure 5.2.1 is described by the vector-matrix equation

$$\dot{\underline{x}} = A\underline{x} + Bu \qquad (5.2.1)$$

Where $\underline{x}$ is the n-dimensional state vector. The nxn system matrix A and the n-dimensional vector B are assumed to be of the canonical forms where

$$A = \begin{bmatrix} 0100 \ldots 0 \\ 0010 \ldots 0 \\ \vdots \quad\quad \vdots \\ -\alpha_1 \ -\alpha_2 \ldots -\alpha_n \end{bmatrix} \text{ and } B = \begin{bmatrix} 0 \\ 0 \\ \vdots \\ \frac{1}{a} \end{bmatrix} \qquad (5.2.2)$$

i = constant (i = 1, 2, ..., n) a = constant >0 $(= \frac{1}{K_p})$. The eigenvalues of the matrix A are assumed real and non-positive.

The components of the state vector $\underline{x}$ are the phase co-ordinates x_i (i = 1, 2, ..., n) which satisfy

$$\dot{x}_i = x_{i+i} \quad (i = 1, 2, \ldots, n-1) \qquad (5.2.3)$$

The controller generates a scaler function of the system state vector, $-\phi(\underline{x})$ at the input to the relay so that

$$u = u(\underline{x}) = -\mathrm{sgn}(\phi(\underline{x})) = \begin{cases} +1 & \phi(\underline{x}) > 0 \\ \sigma \ (-1 \leq \sigma \leq +1) & \phi(\underline{x}) = 0 \\ -1 & \phi(\underline{x}) < 0 \end{cases} \qquad (5.2.4)$$

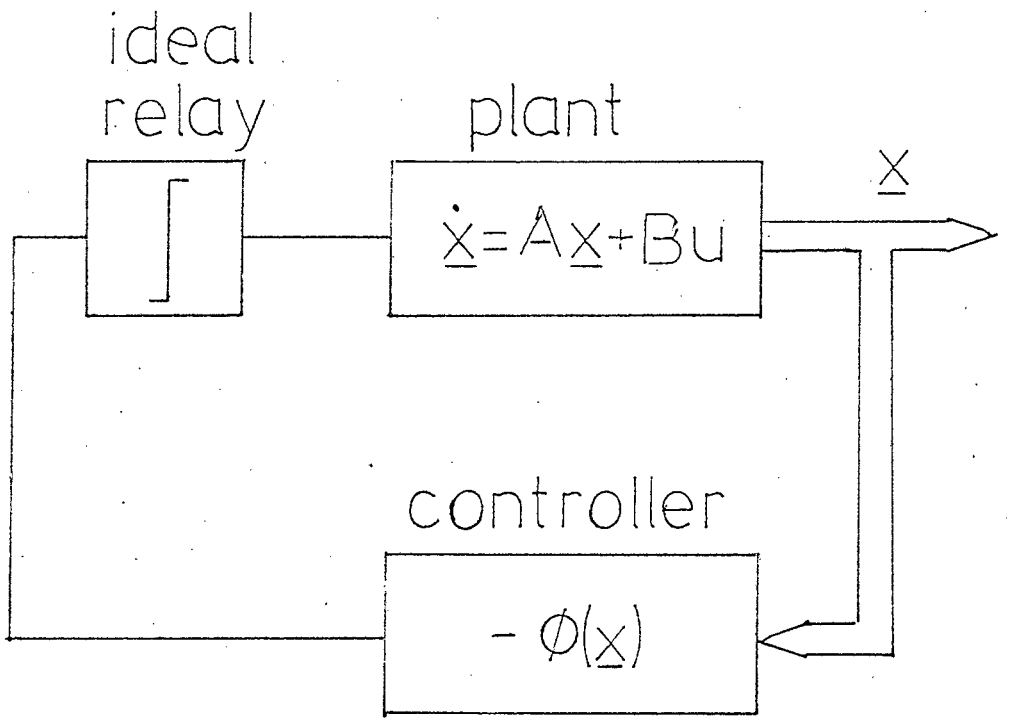

FIGURE 5.2.1.
RELAY CONTROL SYSTEM

The function $\phi(\underline{x})$ will be referred to as the switching function. The set of state points satisfying $\phi(\underline{x}) = 0$ constitutes the switching surface which partitions the state space into two mutually exclusive regions of positive ($u = +1$) and negative ($u = -1$) control effort.

It is required to determine the switching function $\phi(\underline{x})$ such that, under control law 5.2.4, the system is transferred from an arbitrary initial state $x(0) = x^0$ to the state origin in minimum or near minimum time.

For continuous feedback control the switching function $\phi(\underline{x})$ is synthesized directly. For predictive control, the controller generally incorporates a model of the plant simulated on a fast time scale.

The predictive control system operates with sampled data, the plant state being measured at the beginning of each sampled-data interval. This measurement is used to set the initial conditions of the fast model.

During a given sampled-data interval (real time) the response of the fast model to some prescribed control schedule is examined. The control input to the actual plant during the next sampled-data interval (real time) is determined on the basis of the fast model response.

The ideal (but unrealizable) condition for which the sampled-data interval is infinitely small is assumed throughout. Under this idealized condition, the predictive controller may be regarded as generating an equivalent switching function $\phi(\underline{x})$ so that a given predictive control strategy and its equivalent feedback control law are identical in effect, i.e. an idealized predictive strategy and its equivalent feedback control law are synonymous.

5.3 Implementation of predictive control strategies

As indicated in section 5.2, a predictive controller operates with sampled-data (see chapter 2). For the purpose of analysis, the idealized condition, for which the sampled-data interval is infinitely small, was assumed throughout. As this condition is physically unrealizable, practical implementation of both time-optimal and modified sub-optimal predictive control strategies is discussed briefly below.

For an nth order plant the time-optimal predictive control strategy required that, during each sampled-data interval (n-1) state co-ordinates of the nth order fast model be controlled time-optimally to the origin (Billingsley and Coales[12] proposed a sub-optimal predictive strategy

in which the fast model is not controlled but merely observed) of the (n-1) dimensional sub-space; the remaining state co-ordinate is then inspected and the real plant control is set to the opposite polarity.

The (n-1) state co-ordinates of the nth order fast model may in turn be controlled by a complete predictive controller which uses a second 'nested' model, of order (n-1), operating on a still faster time scale. This procedure may be continued yielding a set of (n-1) nested models, each successive model being reduced in order by unity and operating on a progressively faster time scale and culminating in an innermost model of the first order.

In practice this strategy is restricted to low-order plants as the iterative speeds of the inner nested models are difficult to achieve. In chapter two some estimate was made to establish a lower bound of model iteration rate.

The sub-optimal strategy utilized here reduces the number of nested models by unity by requiring that, during each sampled-data interval, only (n-2) state co-ordinates of the fast model be controlled time-optimally to the origin of the (n-2) dimensional sub-space.

An easily synthesized function of the remaining two co-ordinates is then inspected and the real plant control is set the opposite polarity. This decrease in sub-system order affords a considerable reduction in controller complexity and makes practical application of the sub-optimal predictive strategy to third and fourth order plants relatively simple. For example, when applied to a third-order plant, the strategy utilizes a first order sub-system and consequently requires only a single fast model.

The sub-optimal predictive strategy applied to a general third-order plant with real non-positive eigenvalues via the nominal state transformation is shown schematically in Figure 5.3.1. Note that the fast model is not a model of the actual plant but rather a model of the nominal plant with nominal eigenvalues in the ratio 3:2:1.

5.4 Nominal-$\underline{v}$ control

5.4.1 Series Decomposition

Consider the general plant of Figure 5.4.1 with real eigenvalues λ_i ($i = 1, 2, \ldots, n$)

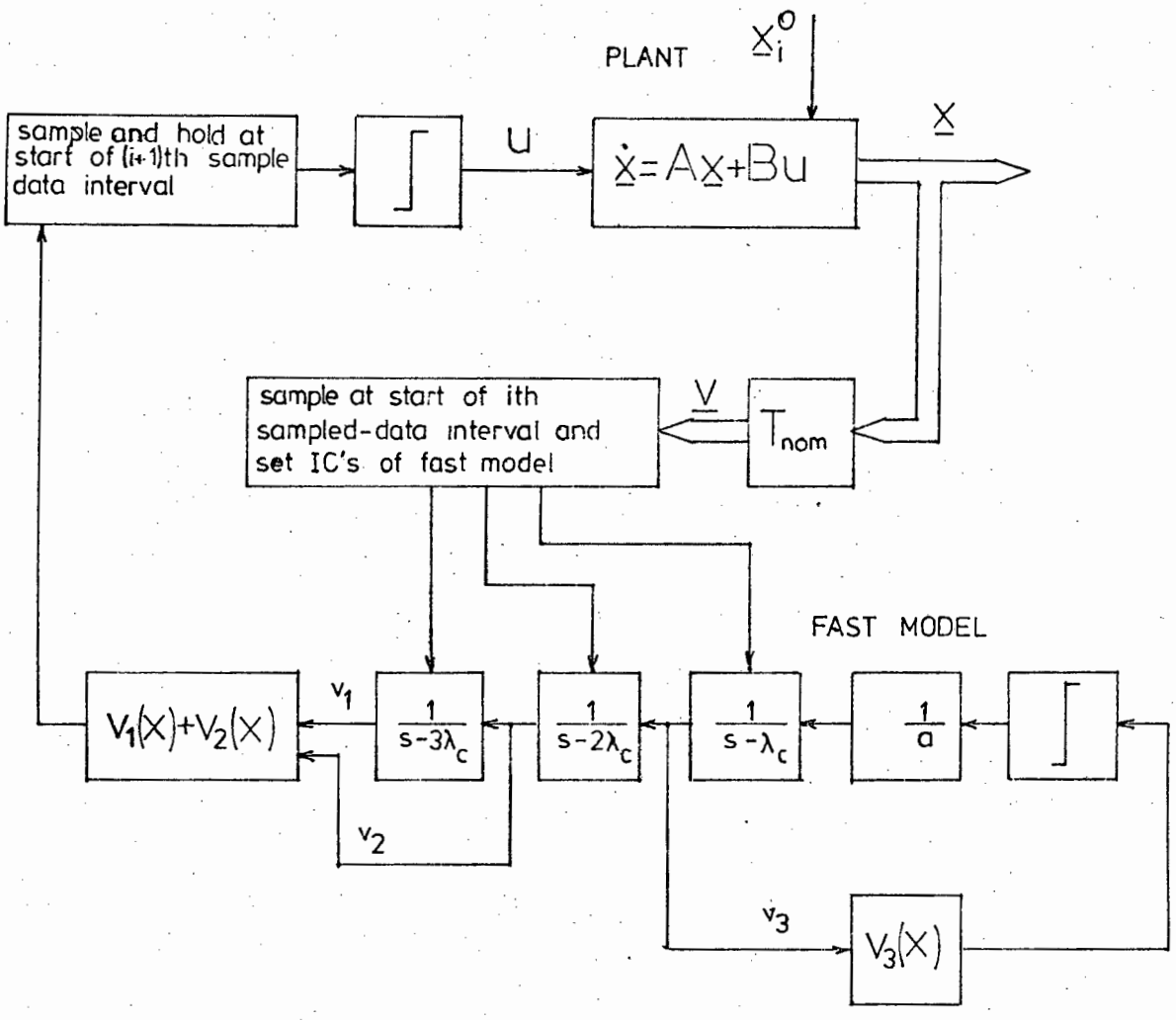

FIGURE 5.3.1

SUB-OPTIMAL PREDICTIVE STRATEGY APPLIED TO A THIRD-ORDER PLANT WITH REAL NON-POSITIVE EIGENVALUES

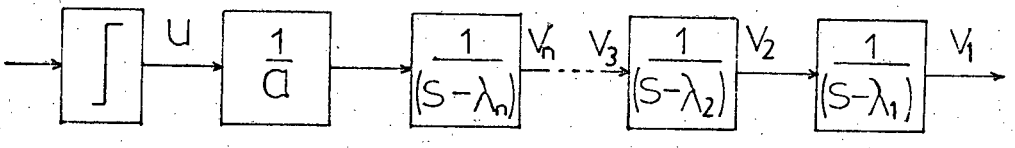

FIGURE 5.4.1
SERIES DECOMPOSITION

It may be shown that the state vector $\underline{v}$ with elements v_i ($i = 1, 2, 3, \ldots, n$) defined by Figure 5.4.1, may be obtained from the $\underline{x}$ state vector by the transformation

$$\underline{v} = T\underline{x} \qquad (5.4.1)$$

where T is the lower triangular matrix of the form

$$T = \begin{bmatrix} 1 & 0 & 0 & \ldots & 0 \\ T_{2,1} & 1 & 0 & \ldots & \\ T_{3,1} & T_{3,2} & 1 & \ldots & \\ \ldots & \ldots & \ldots & 1 & 0 \\ T_{n,1} & T_{n,2} & \ldots & T_{n,n-1} & 1 \end{bmatrix} \qquad (5.4.2)$$

The non-zero off-diagonal elements are determined by the relations

$$T_{i,1} = \prod_{k=1}^{i-1} (-\lambda_k), \quad i = 2, 3, \ldots, n$$

$$T_{i,j} = -\lambda_{i-1} T_{i-1,j} + T_{i-j,j-1} \quad \begin{matrix} (i=2,3,\ldots,n \\ (j=2,3,\ldots,i-1 \end{matrix} \qquad (5.4.3)$$

specifically from 5.4.2. and 5.4.3

(a) for n = 2

$$T = \begin{bmatrix} 1 & 0 \\ -\lambda_1 & 1 \end{bmatrix} \qquad (5.4.4)$$

(b) for n = 3

$$T = \begin{bmatrix} 1 & 0 & 0 \\ -\lambda_1 & 1 & 0 \\ \lambda_1\lambda_2 & -(\lambda_1+\lambda_2) & 1 \end{bmatrix} \qquad (5.4.5)$$

The transformation from $\underline{x}$ into the $\underline{v}$ state vector will be referred to as series decomposition.

5.4.2 Plants with negative real eigenvalues and having a time-optimal control law identical to that of a pure integrator plant of corresponding order.

It is shown (Ryan[6]) that the time-optimal control problem for an nth order plant with negative real eigenvalues given by

$$\lambda_i = (n+1-i)\lambda \ , \quad i = 1,2, \ldots, n \qquad (5.4.6)$$

where λ is a negative constant, may be reduced to the corresponding problem for a plant consisting of n pure integrating elements.

A particular consequence of this property is that the time optimal control law for the plant expressed by 5.4.6., when expressed as a function of the series decomposition state vector $\underline{v}$, is identical to that of a pure integrator plant of the same order.

Referring to Figure 5.4.2., if $u = \text{sgn}(\phi^o(\underline{x}))$ is the time-optimal control law for the pure integrator system of Figure 5.4.2(a), then $u=\text{sgn}(\phi^o(\underline{v}))$ is the time-optimal control law for the negative real-pole system of Figure 5.4.2(b).

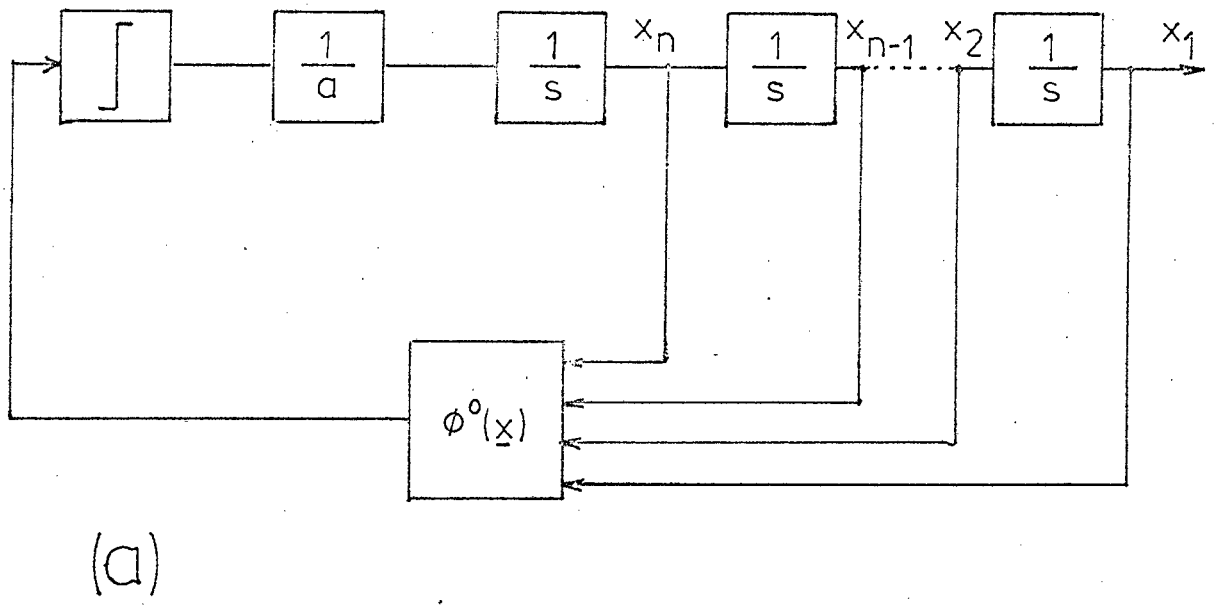

(a)

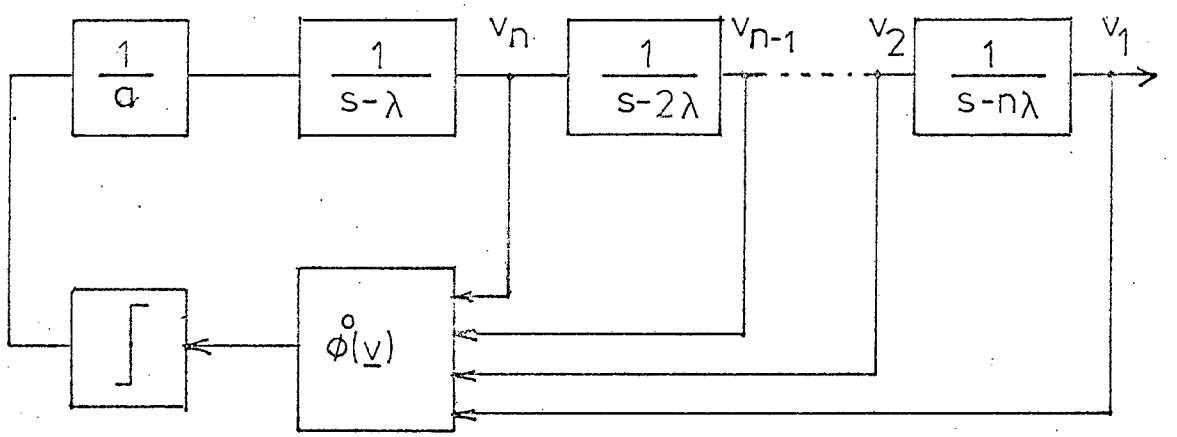

(b)

FIGURE 5.4.2.
(a) TIME-OPTIMAL PURE INTEGRATOR SYSTEM
(b) EQUIVALENT SYSTEM WITH NEGATIVE REAL EIGENVALUES

5.4.3 Nominal-$\underline{y}$ control

In cases of more general second and third order systems, for which the plant eigenvalues are real but no longer in the specific ratio represented by (5.4.6), it is shown that successful application of the relatively simple time-optimal control Laws for second and third order pure integrator plants may be achieved by

(a) assuming a nominal plant with nominal eigenvalues given by 5.4.6 i.e.

$$\lambda_{i(nom)} = (n+1-i)\lambda_c, \quad i=1,2,\ldots,n \quad \lambda_c = \text{constant} \tag{5.4.7}$$

with

(b) the sum of the nominal eigenvalues equal to the sum of the actual eigenvalues, i.e.

$$\sum_{i=1}^{n} \lambda_{i(nom)} = \sum_{i=1}^{n} \lambda_i \tag{5.4.8}$$

or in view of (5.4.7)

$$\lambda_c = \frac{\sum_{i=i}^{n} \lambda_i}{\sum_{i=1}^{n} (n+1-i)} \tag{5.4.9}$$

and

(c) Implementing on the actual system the optimal control law for the nominal system (identical to that of a pure integrator plant of the same order).

Equation 5.4.8. implies that the trace of the nominal system matrix is equal to the trace of the actual system matrix, i.e. in defining the nominal system 5.4.7, the trace of the original system A matrix ($\text{tr } A = \sum_{i-1}^{n} \lambda_i$) is preserved (see Wiberg[32]).

Stated alternatively, the nominal-$\underline{y}$ control approach facilitates near time-optimal control of second and third-order real-pole plants by implementing the easily synthesized control Laws for the double and triple integrator plants, this being achieved by mapping the actual system $\underline{x}$ state vector into the series decomposed $\underline{y}$ vector for the nominal system via the nominal series decomposition transformation.

$$\underline{y} = T_{(nom)}\, \underline{x} \qquad (5.4.10)$$

Here $T_{(nom)}$ is the nominal series decomposition transformation matrix which, from 5.4.4., for a second order system is

$$T_{(nom)} = \begin{bmatrix} 1 & 0 \\ -\lambda_{1(nom)} & 1 \end{bmatrix} \qquad (5.4.11)$$

or from 5.4.7. and 5.4.9. in terms of the actual system eigenvalues

$$T_{(nom)} = \begin{bmatrix} 1 & 0 \\ -\frac{2}{3}(\lambda_1+\lambda_2) & 1 \end{bmatrix} \qquad (5.4.12)$$

and for a third order system, from 5.4.5.

$$T_{(nom)} = \begin{bmatrix} 1 & 0 & 0 \\ -\lambda_{1(nom)} & 1 & 0 \\ \lambda_{1(nom)}\lambda_{2(nom)} & -(\lambda_{1(nom)}+\lambda_{2(nom)}) & 1 \end{bmatrix} \qquad (5.4.13)$$

or, from 5.4.7 and 5.4.8 in terms of the actual system eigenvalues

$$T_{(nom)} = \begin{bmatrix} 1 & 0 & 0 \\ -\frac{1}{2}(\lambda_1+\lambda_2+\lambda_3) & 1 & 0 \\ \frac{1}{6}(\lambda_1+\lambda_2+\lambda_3)^2 & -\frac{5}{6}(\lambda_1+\lambda_2+\lambda_3) & 1 \end{bmatrix} \qquad (5.4.14)$$

The control method outlined above is referred to as 'nominal-$\underline{v}$ control'. The overall nominal-$\underline{v}$ control system is depicted in Figure 5.4.3.

5.4.4 Properties of second order nominal-$\underline{v}$ control systems.

The properties of these systems are well documented by Ryan[6] and only a brief outline is given in Appendix A13. Only the results are stated here, namely

$$\begin{cases} v_1 = x_1 \\ v_2 = \frac{-2}{3}\lambda_1 \frac{(\alpha+1)}{(\alpha)} \dot{x}_1 + x_2 \end{cases} \qquad (5.4.15)$$

Where the eigenvalue ratio $\alpha \triangleq \frac{\lambda_1}{\lambda_2}$ $(0 \geq \lambda_1 \geq \lambda_2)$ (5.4.16)

and the nominal -$\underline{v}$ control law may now be written in the same form as that of the double integrator plant, viz.

$$u = u(\underline{v}) = -\text{sgn}(v_1 + \tfrac{a}{2} v_2 \,|\, v_2 |) \qquad (5.4.17)$$

when (a) $\lambda_1 = \lambda_2 = 0$ (the double integrator plant) and (b) $\lambda_1 = 2\lambda_2$ (when $\alpha = 2$) equation 5.4.17. represents the exact time-optimal control Law, and for other cases the control is sub-optimal.

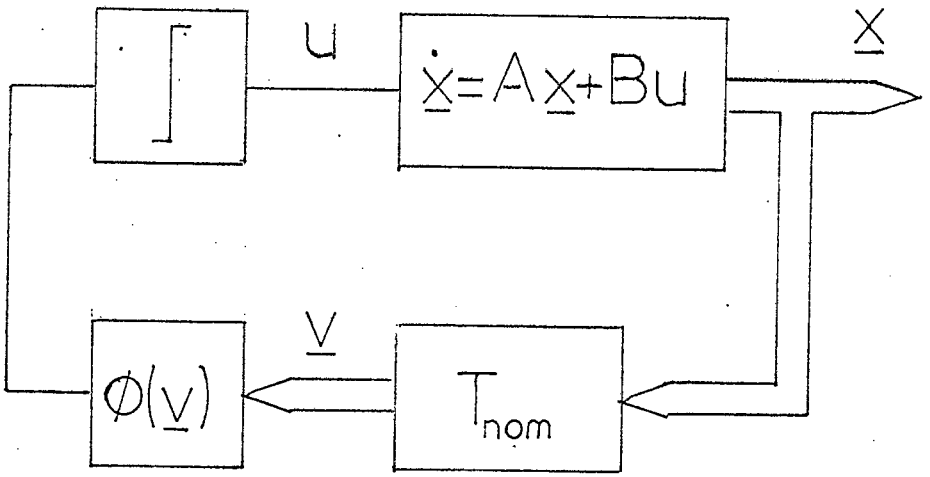

FIGURE 5.4.3.
NOMINAL -$\underline{v}$ CONTROL SYSTEM

It was found however that the very much simplified nominal-$\underline{v}$ switching function provides control that departs very little from the exact time-optimal trajectory.

5.5 Third-Order Sub-Optimal Predictive Strategy

As outlined in Section 5.3 the time-optimal strategy involves the rapid computation of the time-optimal trajectory to the origin of the (n-1) dimensional sub-space with co-ordinates $x_i (i=2, 3, \ldots, n)$; at this (fictitious) point the remaining co-ordinate x_1 is inspected and the control input to the actual plant (henceforth to be called the real plant control) is set to the opposite polarity.

The sub-optimal strategy is as follow:
For an arbitrary initial state
$\underline{x}^A = (x_1^A, x^A, \ldots, x^A)^T$, if the time-optimal trajectory to the $(x_1 - x_2)$ plane meets this plane at a point B satisfying

$$\underline{x}^B = (x_1^B, x_2^B, 0, \ldots, 0)^T \qquad (5.5.1)$$

then the real plant control is given by

$$u = -\text{sgn}\,(\Gamma(x_1^B, x_2^B)) \qquad (5.5.2)$$

In other words, the sub-optimal strategy involves the rapid computation of the time-optimal trajectory to the origin of the (n-2) dimensional sub-space with co-ordinates $x_i (i=3, 4, \ldots, n)$; at this (fictitious) point some function of the remaining two co-ordinates, $\Gamma(x_1, x_2)$ is inspected and the real plant control is set to the opposite polarity.

Thus, by adopting the sub-optimal strategy, the order of the sub-system is reduced by unity (see Figure 5.5.1).

It now remains to select the function $\Gamma(x_1, x_2)$ so that the strategy gives near time-optimal control.

In order to select the function $\Gamma(x_1, x_2)$ a Lemma asserted and proved by Ryan[31] (1976) is stated.

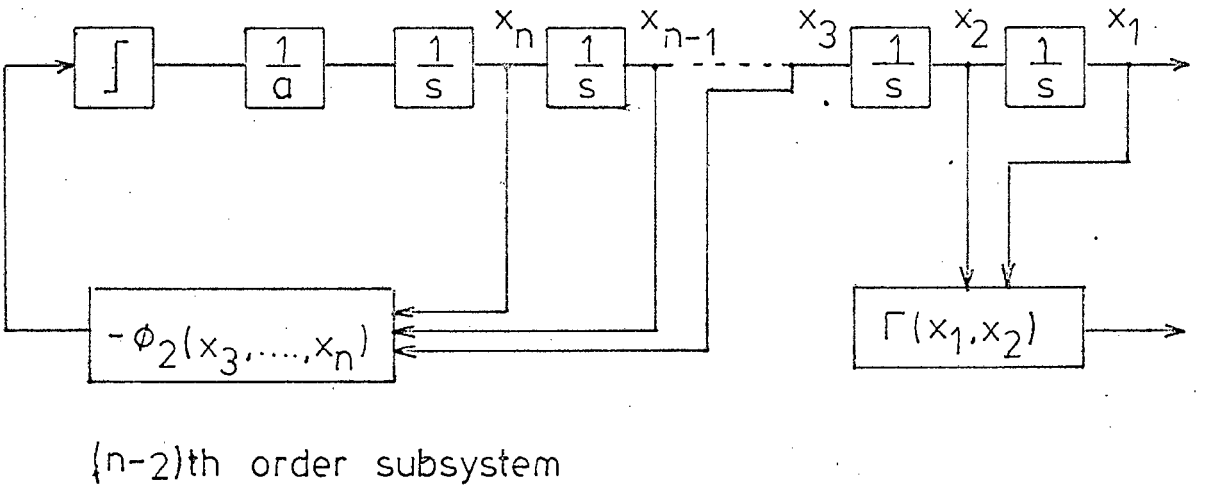

FIGURE 5.5.1
(n-2)TH -ORDER SUBSYSTEM FOR THE SUB-OPTIMAL STRATEGY

Lemma 5.5 :

For the nth order pure integrator system

$$\begin{cases} \dot{x}_i = x_{i+1} \quad (i = 1, 2, \ldots, n-1) \\ \dot{x}_n = \frac{u}{a} \end{cases}$$

the time optimal control at a point

$\underline{x} = (x_1, x_2, 0, \ldots, 0)^T$

in the (x_1, x_2) plane is given by

$u = u(x_1, x_2, 0, \ldots, 0) =$

$-\text{sgn}(|x_1|^{n-1}\text{sgn}(x_1) + \beta |x_2|^n \text{sgn}(x_2))$

$n = 2, 3, \ldots$

where β (> 0) is a constant given by

$\beta = 2^{n-3} (n-2) ! a$

For example,

(i) if $n = 2$ then by Lemma 5.5, $\beta = \frac{a}{2}$ and

$$u = u(x_1, x_2) = -\text{sgn}(x_1 + \frac{a}{2} x_2 |x_2|) \qquad (5.5.3)$$

i.e. the well known time-optimal control Law for the double integrator plant.

(ii) if $n = 3$, then $\beta = a$ and

$$u = u(x_1, x_2, 0) = -\text{sgn}(x_1 |x_1| + a x_2^3) \qquad (5.5.4)$$

By setting

$$\Gamma(x_1, x_2) = |x_1|^{n-1} \operatorname{sgn}(x_1) + \beta |x_2|^n \operatorname{sgn}(x_2) \quad . (5.5.5.)$$

it is established that the sub-optimal strategy gives near time-optimal control for third (and fourth order) plants.

The sub-optimal strategy now involves the rapid computation of the time optimal trajectory from the initial state at a point A to a point B in the $(\ldots, x_2)$ plane.

The real plant control is then set equal to the time optimal control at B.

5.6 Application of the sub-optimal strategy to the triple integrator plant

For the sub-optimal strategy, the first-order sub-system satisfies the equation

$$\dot{x}_3 = \frac{u}{a} \qquad (5.6.1)$$

The time-optimal control law for this sub-system is

$$u = -\text{sgn}(x_3) \qquad (5.6.2)$$

and the optimal sub-system settling time from an arbitrary initial sub-plant state x_3^A is given by

$$t_1 = |ax_3^A| = ax_3^A \text{ sgn}(x_3^A) \qquad (5.6.3)$$

Integrating the state equations

$$\begin{cases} \dot{x}_1 = x_2 \\ \dot{x}_2 = x_3 \\ \dot{x}_3 = \frac{u}{a} \end{cases} \qquad (5.6.4)$$

on the time optimal (switchless) trajectory to the sub-system origin yields

$$x_1(t_1)=x_1^B = x_1^A + x_2^A t_1 + x_3^A \frac{t_1^2}{2} - \frac{\text{sgn } x_3^A}{6a} t_1^3 \qquad (5.6.5)$$

$$x_2(t_1)=x_2^B = x_2^A + x_3^A t_1 - \frac{\text{sgn } x_3^A}{2a} t_1^2 \qquad (5.6.6)$$

which, from 5.6.3. on substituting for t_1 reduces to

$$x_1^B = x_1^A + ax_2^A x_3^A \text{ sgn}(x_3^A) + \frac{a^2(x_3^A)^3}{3} \qquad (5.6.7)$$

$$x_2^B = x_2^A + \frac{a(x_3^A)^2}{2} \text{ sgn } (x_3^A) \qquad (5.6.8)$$

Finally from 5.2.2, 5.5.4, 5.5.5 and omitting the superscript 'A', the sub-optimal control law may be written as

$$u(\underline{x}) = -\text{sgn}(\Gamma(x_1^B, x_2^B)) =$$
$$-\text{sgn } (x_1^B |x_1^B| + a(x_2^B)^3) \qquad (5.6.9)$$

or

$$u(\underline{x}) = -\text{sgn}\ (U\,|U| + -aV^3) \quad (5.6.10)$$

where from 5.6.5 and 5.6.6

$$\begin{cases} U = x_1{}^B = x_1 + \dfrac{a^2 x_3{}^2}{3} + a x_2 x_3\ \text{sgn}(x_3) \\ \\ V = x_2{}^B = x_2 + \dfrac{a x_3^2}{2}\ \text{sgn}(x_3) \end{cases} \quad (5.6.11)$$

The exact time-optimal control law for the triple integrator plant can be expressed as

$$\begin{cases} S = x_1 + \dfrac{a^2 x_3{}^3}{3} + a\ x_2\ x_3\ \text{sgn}\ (\phi_1) \quad (5.6.12) \\ \\ T = x_2 + \dfrac{a x_3^2}{2}\ \text{sgn}\ (\phi_1) \end{cases}$$

where $u(\underline{x}) = -\text{sgn}\ (S\,|S| + aT^3)$ (5.6.13)

Inspection of 5.6.12, 5.6.13 and 5.6.10, 5.6.11 confirms that the sub-optimal feedback control law derived from the sub-optimal predictive strategy corresponds closely to the time-optimal feedback control law: the switching functions differ only in the arguments of the signum functions of 5.6.12 and 5.6.11.

By analysing both strategies in a reduced state space (Fuller[10]) Ryan[31] verifies that the associated switching surfaces are in close agreement.

5.7 Experimental Procedures

The first stage of experimentation was executed on the analogue computer. The next stage was the conversion of the system equations for use on the minicomputer for hybrid simulation. In both stages the plant was simulated on the analogue computer and its form was identical to that of the previous three chapters. The final stage was the control of the DC motor by the minicomputer using the switching function $\phi(\underline{v})$, derived from the $\underline{v}$ transformed plant state-variables.

The implementation of the simple control Laws for a second-order plant (see Appendix A.14.1 for a description of the control equations on an analogue computer block diagram) follows the mechanization of equations A13.1.4 and A13.1.5 for any second-order plant under consideration.

For the second order plant $G_p(s) = \frac{K_p}{s(s+\alpha_p)}$ where $K_p(=\frac{1}{a})=1$ (nominal) and $\alpha_p = .1$, the $\underline{v}$ control equations are $v_1 = x_1$ and $v_2 = .\frac{2}{3} x_1 + x_2$, and the switching function $\phi(\underline{v})$ is $\phi(\underline{v}) = v_1 + \frac{1}{2} v_2 |v_2| = 0$.

For hybrid control, the program required to execute these $\underline{v}$ equations is simple and with the system block diagram is included in Appendix A14.2.

The third order plant (and triple integrator) control laws required some mathematical manipulations although the triple integrator plant merely required the direct mechanization of equations 5.6.10 and 5.6.11. Appendix A15 contains the manipulations and equations required to generate the control laws for a third-order plant $G_p(s) = \frac{K_p}{s(s^2+\alpha_p s+1)}$. The system block diagram is presented and the programme for the third-order plant $G_p(s)$.

The small DC motor was run with the programme written for a second-order plant and executed in exactly the same manner as for the fast model predictor controller described in chapter two. Figures 2.4.24 and 2.4.25 in chapter two also illustrate the motor response due to the $\underline{v}$ transformation method of control.

5.8 Simulation Results

Figures 5.8.1 to 5.8.4 depict the responses of a second-order plant to a reference step for variations in the plant gain parameter K_p and time constant $\frac{1}{\alpha_p}$. The plant has a transfer function $G_p(s) = \frac{K_p}{s(s+\alpha_p)}$ where $K_p = 1$ (nominal).

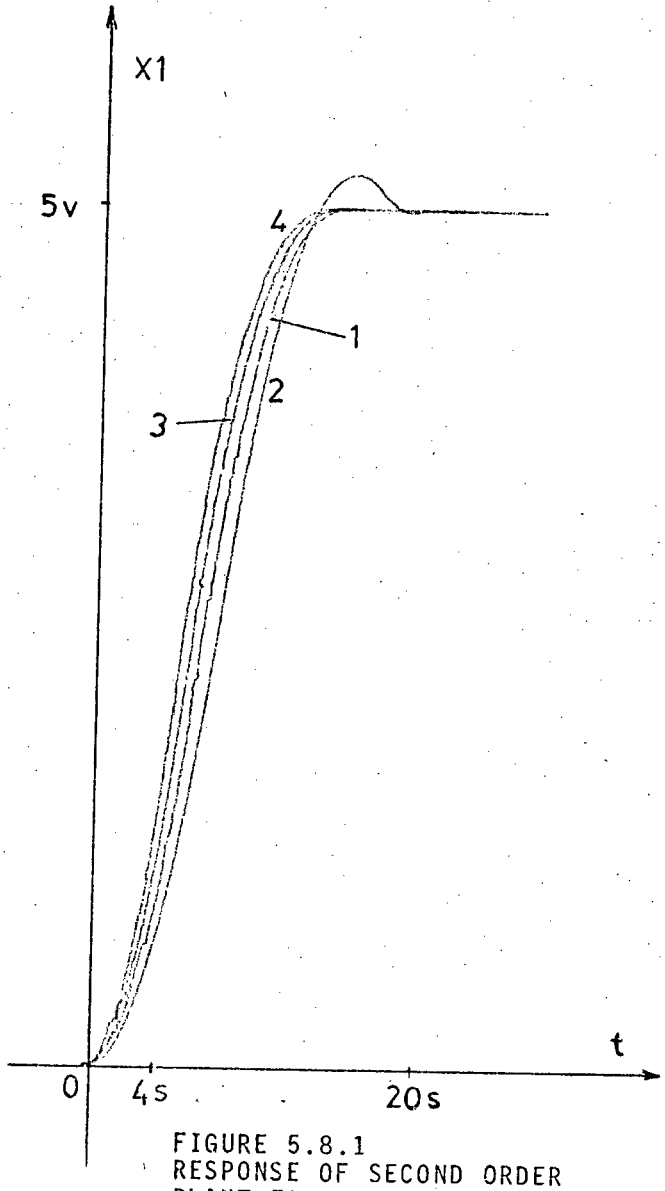

FIGURE 5.8.1
RESPONSE OF SECOND ORDER
PLANT FOR VARIATION IN K_p

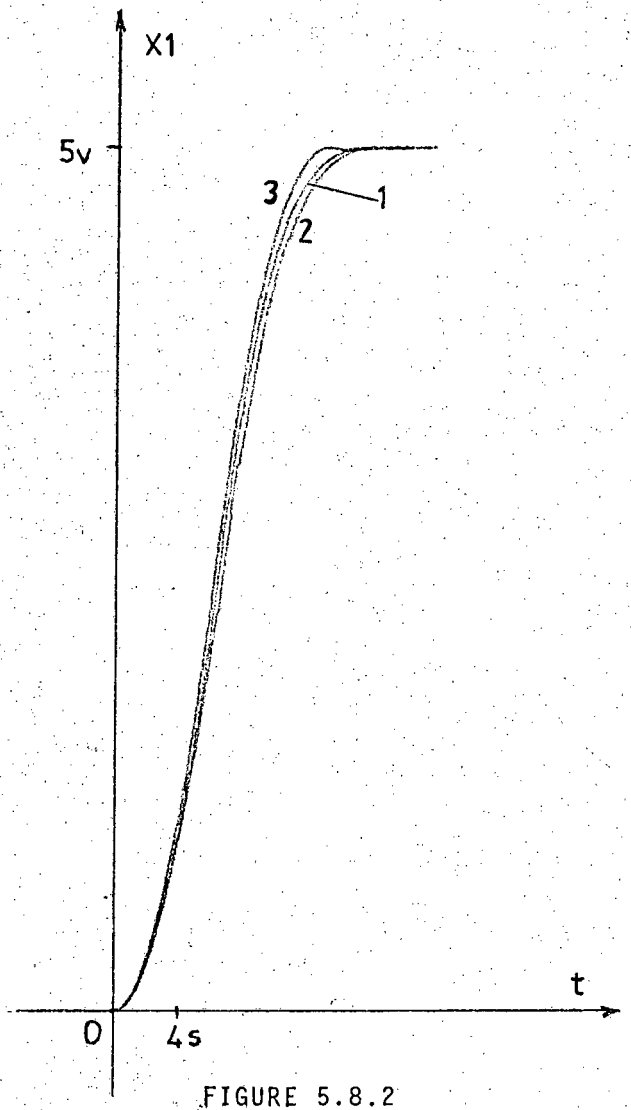

FIGURE 5.8.2
RESPONSE OF SECOND ORDER
PLANT FOR VARIATION IN α_p

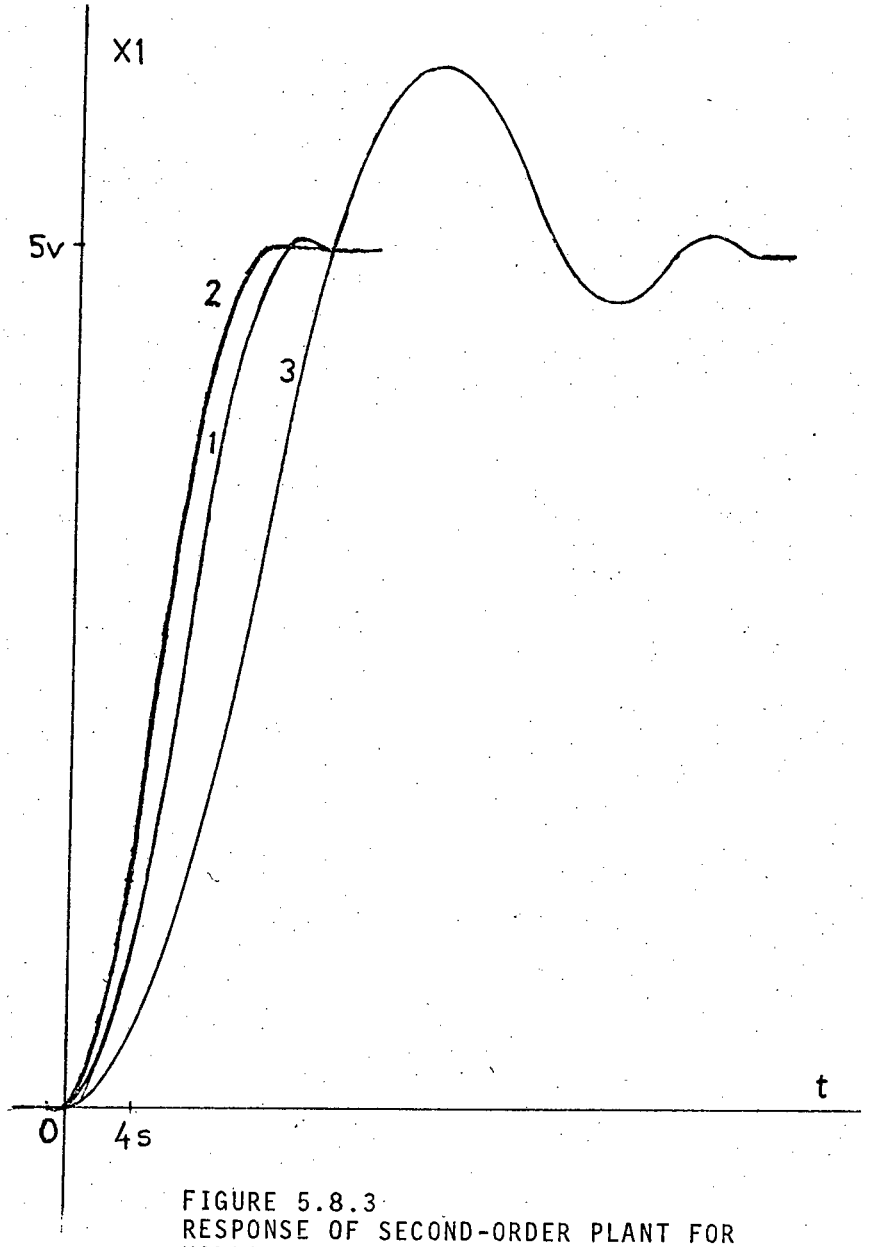

FIGURE 5.8.3
RESPONSE OF SECOND-ORDER PLANT FOR VARIATION IN K_p

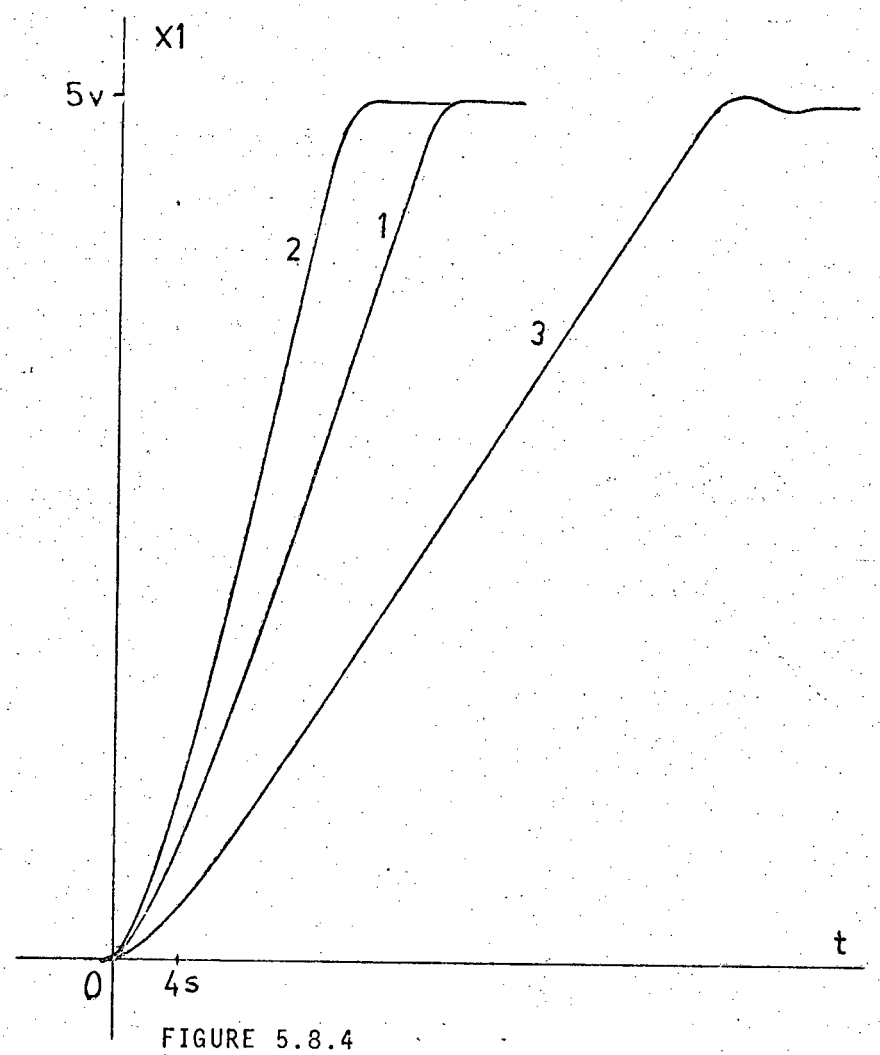

FIGURE 5.8.4
RESPONSE OF SECOND ORDER PLANT FOR VARIATION IN K_p

The curves of figures 5.8.1 and 5.8.2 depict the response of the analogue computer simulation of near-time optimal control using the nominal-$\underline{v}$ control transform method and where $K_p = 1$ and $\alpha_p = .1$ are the design values. The reference is a step of 5 volts.

For figure 5.8.1:

Curve No.	K_p	
1	1	(nominal design value)
2	.8	
3	1.2	
4	1.5	

and $\alpha_p = .1$

For figure 5.8.2

Curve No.	α_p	
1	.1	(nominal design value)
2	.2	
3	.05	

and $K_p = 1$

For variations of $K_p > K_{p(nom)}$ curves 3 and 4 remain remarkably close to the nominal, while for $K_p < K_{p(nom)}$ (curve 2) the ratio of the settling time to the nominal settling time is about 35% (if we compare this to the value obtained from figure 2.4.18 curve 3, the ratio is about 40% for a value of $\alpha_p = .5$).

The variation of α_p about the design value yields curves which hardly differ from the nominal design value. The curves in both figures demonstrate that for moderate plant parameter variations, the responses differ very little from the time-optimal response.

Two sets of curves for the second-order plant are submitted using the hybrid control facility. Figures 5.8.3. and 5.8.4 depict the responses of the second-order system for variation in K_p and α_p.

In figure 5.8.3

Curve No.	K_p	
1	1	(nominal design)
2	1.5	
3	.5	

and α_p = .1 (nominal design value).

And in figure 5.8.4

Curve No.	K_p
1	1
2	1.5
3	.5

and α_p = 1 (nominal design value)

For large variations in the ratio $\frac{b}{a}$ $\left(\frac{K_{p(nom)}}{K_p}\right)$ and for the two design values of α_p, the effect $\frac{b}{a} < 1$ yields a dead-beat type response. For $\frac{b}{a} > 1$ and $\alpha_p = .1$ a large overshoot occurs and the settling time is increased above the nominal by about 180%.

For $\alpha_p = 1$ and $\frac{b}{a} > 1$ the overshoot is small and the output merely takes a longer time to reach steady state as can be expected for reduced plant gain and for a large decrease in the plant time constant $\frac{1}{\alpha_p}$. Similarly for $\frac{b}{a} < 1$ the response is dead-beat and the time to reach steady state is reduced as the plant gain has been increased.

The simple algebraic structure of the control Laws (equations A 13.1.5 and A 13.1.8) yield a good degree of insensitivity to plant parameter variations, while the performance is close to optimal.

Figure 5.8.5. depicts the response of a triple integrator for a step initial condition for variations in K_p, K_p (nominal) = 1 and the step initial condition is 5 volts. The responses are:

Curve No.	K_p	
1	1	(nominal)
2	1.5	
3	.5	
4	.8	

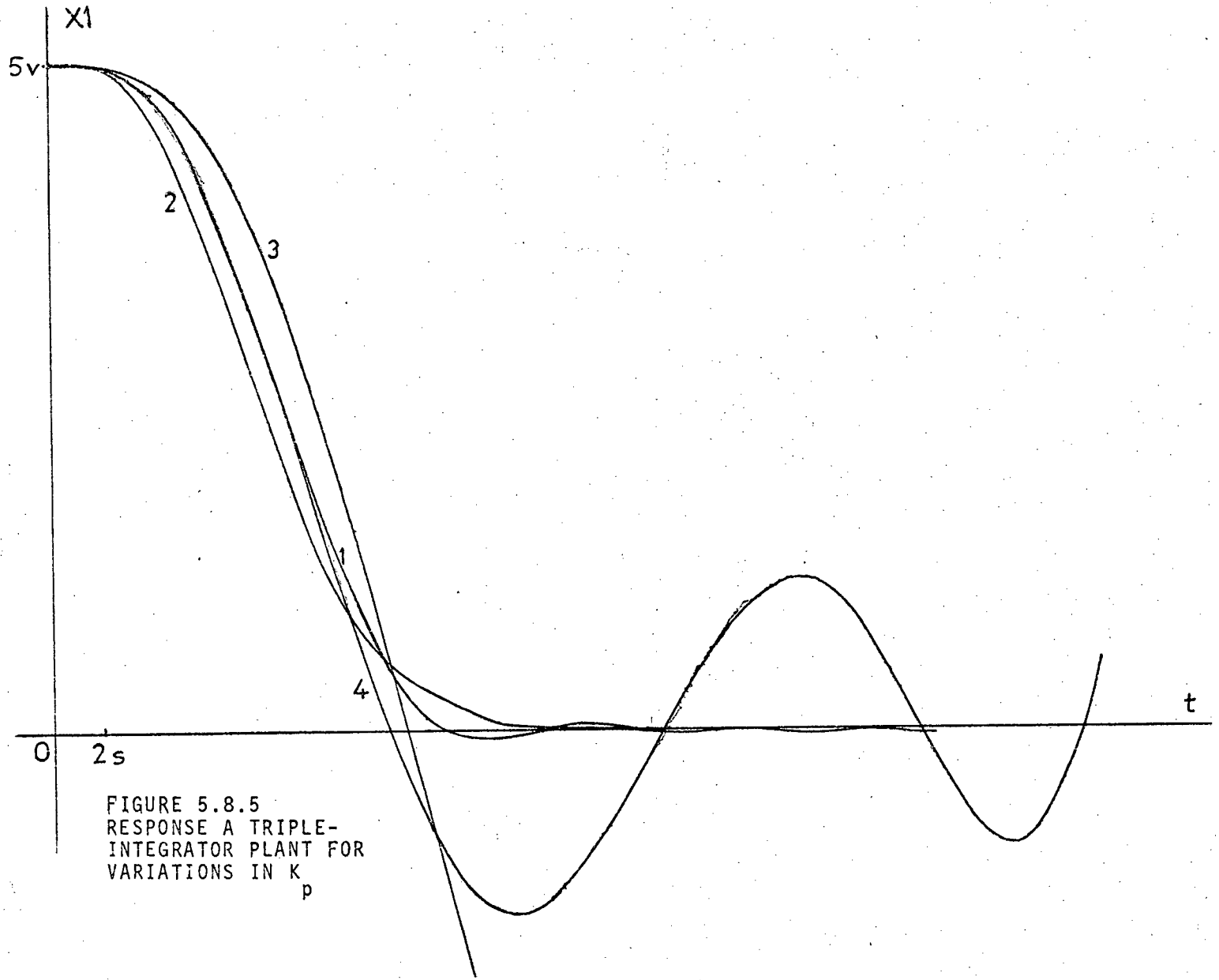

FIGURE 5.8.5
RESPONSE A TRIPLE-INTEGRATOR PLANT FOR VARIATIONS IN K_p

For $\frac{b}{a} < 1$ ($K_p = 1.5$) the response is dead-beat, and for $\frac{b}{a} > 1$ viz. $K_p = .5$ the plant goes unstable. For $K_p = .8$ there are large very lightly damped oscillations about the steady state. It is observed that the control laws are highly sensitive for any reduction in the nominal (design) plant gain.

Figures 5.8.6 and 5.8.7 represent the responses of a third-order plant with transfer function

$$G_p(s) = \frac{K_p}{s(s^2+\alpha_p ps+1)} \quad \text{where } K_p \ (=\tfrac{1}{a}) = 1 \text{ (nom)}$$

and $\alpha_p = .4$ (nominal design value), to a step initial condition for variation in α_p and with acceleration limiting (a non-linearity).

For figure 5.8.6. ($K_p = 1$)

Curve No.	α_p	
1	.4	(nominal design)
2	.2	
3	.6	
4	1	

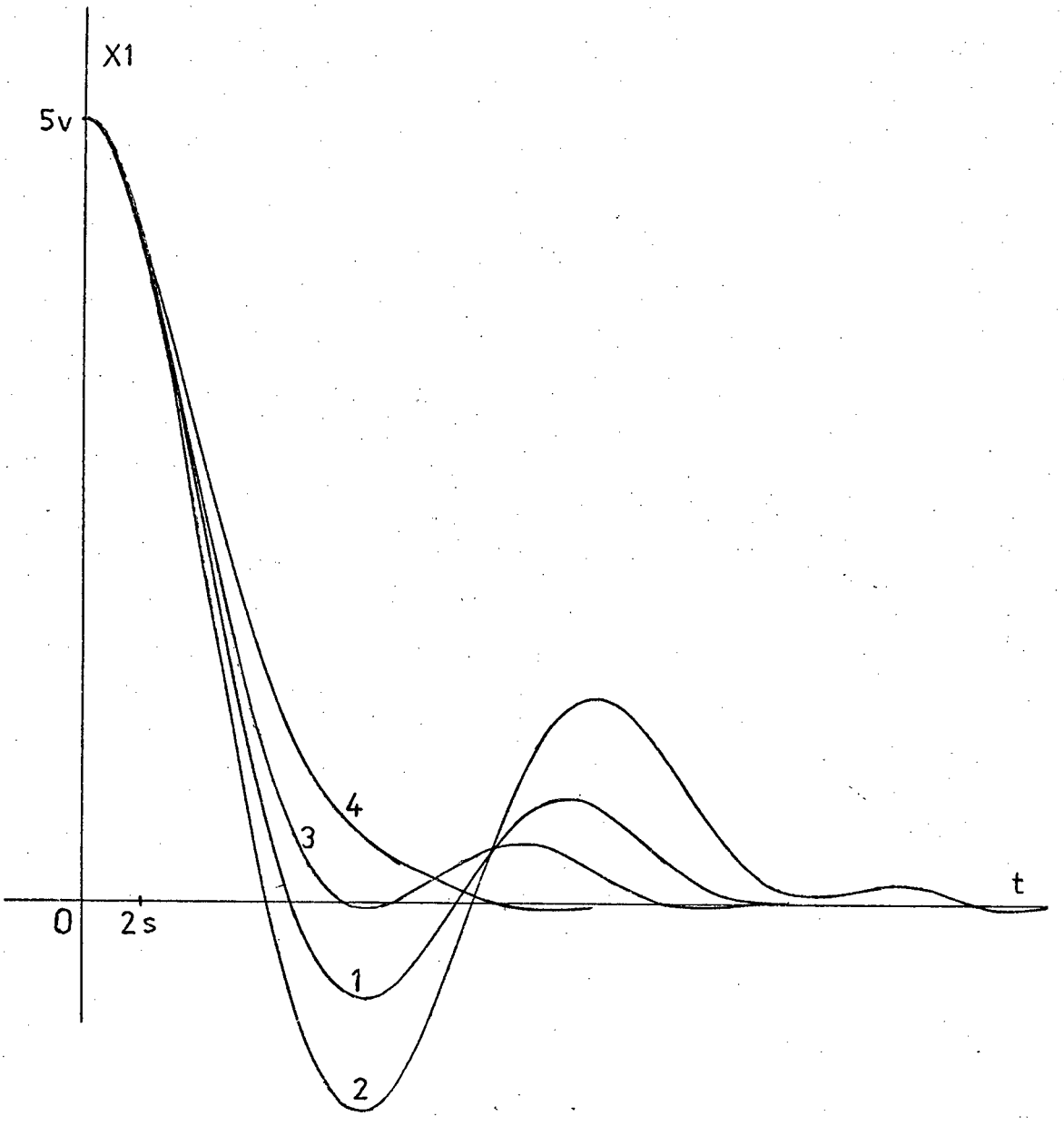

FIGURE 5.8.6
RESPONSE OF A THIRD-ORDER PLANT FOR VARIATIONS IN α_p

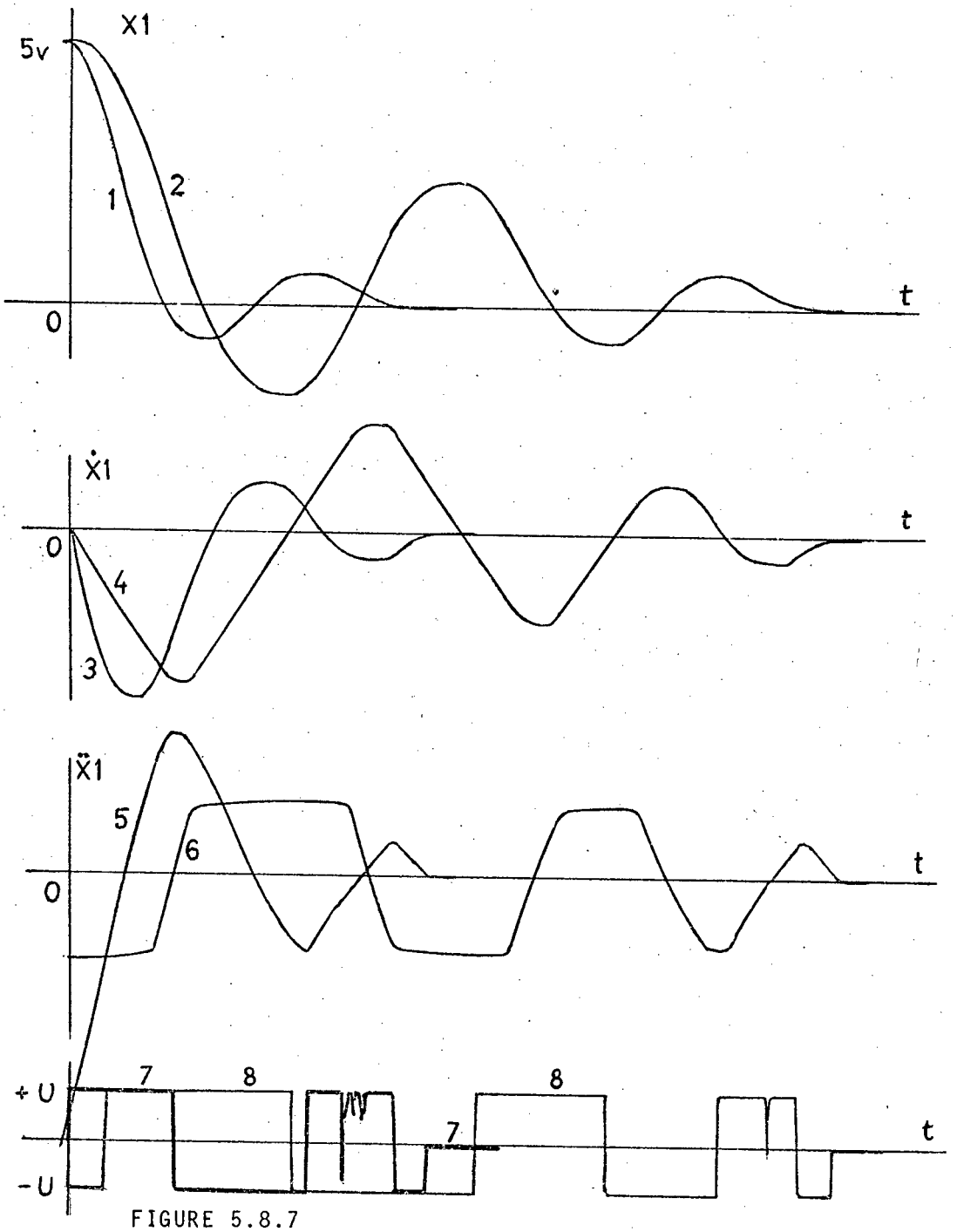

FIGURE 5.8.7
RESPONSE OF A THIRD-ORDER PLANT WITH AND WITHOUT ACCELERATION LIMITING

And for figure 5.8.7. ($K_p = 1, \alpha_p = .4$)

Curve No.

1 : Position response		
3 : Velocity response	No limit on acceleration	
5 : Acceleration response		
7 : Input signal		
2 : Position response		
4 : Velocity response		
6 : Acceleration response	With limit on acceleration ($\ddot{x}$ limit $\simeq .3\ \ddot{x}$)	
8 : Input signal		

In figure 5.8.6; increase in α_p resulted in a response with less overshoot and consequently reduced settling time as could be expected, in fact curve 4 yields a dead-beat type response. Although the $\underline{v}$ transformation method has been defined for plants with zero or real eigenvalues, the use of this method for complex eigenvalues is also quite successful expecially for plants with transfer function $G_p(s)$ above ($G_p(s)$ is an approximation to a DC motor with large inertial loads). However the correct choice of α_p (and K_p) for the control equations to yield a satisfactory response is still partially empirical.

Figure 5.8.7. demonstrates the effect of a non-linearity viz. limiting of the acceleration on the overall performance of a third-order plant. As can be observed the response is stable and comes to rest despite the several large overshoots. This test was repeated for $\alpha_p = 1$ as in figure 5.8.7. (although not included here) with a subsequent improvement in settling time.

In fact, figure 5.8.8 illustrates the response of $G_p(s)$ for the $\underline{v}$ transformation and adaptive relay control when $\alpha_p = .8$ (the design value for the $\underline{v}$ transformation was $\alpha_p = .4$) and $K_p = 1$.

The curves are:

Curve No.

1 :	Position response	Adaptive relay control
3 :	Velocity response	
5 :	Acceleration response	
2 :	Position response	$\underline{v}$ transformation control
4 :	Velocity response	
6 :	Acceleration response	

The performances are virtually identical but moreover the position response is of the 'dead-beat' type by merely increasing α_p in the transformation equations.

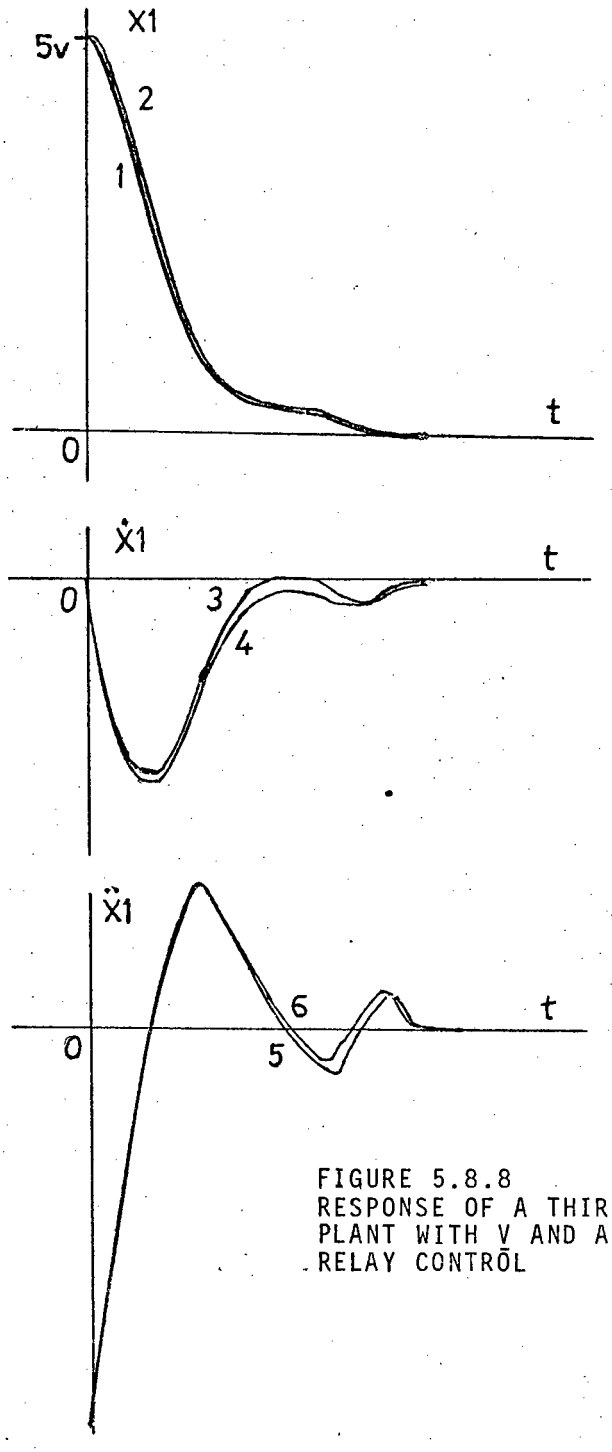

FIGURE 5.8.8
RESPONSE OF A THIRD-ORDER PLANT WITH V AND ADAPTIVE RELAY CONTROL

By careful selection and adjustment of the plant parameters for the $\underline{v}$ transformation equations it it possible to obtain satisfactory system performance for plants with complex eigenvalues and with the presence of non-linearities.

5.9 Summary of results and comments

The notion of the minimal number of drive reversals (the number of times the bang-bang input reverses sign) for minimal-time control was based upon plants with real negative eigenvalues. For plants with complex eigenvalues it can be stated (although not proved here) that if the co-state p, of the Hamiltonian has trigonometric or complex exponential terms (as it would for a plant with complex eigenvalues) then there is no limit theoretically, to the number of sign changes of p and therefore of $u^{*}(t)$, which may occur during an optimal transition.

However, assuming that the termination is accomplished in a finite time, the number of sign changes of p, and therefore of $u^{*}(t)$, is finite. The nominal $-\underline{v}$ transformation method applied to plants with non-positive real eigenvalues. For complex eigenvalues the nominal eigenvalue ratios are not defined. However the simulation

of a plant with complex eigenvalues, and with non-linearities yielded reasonable performance, with moderate overshoot and no sustained oscillations about the steady state. With careful tuning, a dead-beat type response can be achieved.

With regard to the calculations of U and V in Appendix A 15.1, it is important to note that the third-order plant with complex eigenvalues was approximated to by a plant with two real and equal eigenvalues. In this way the implementation of the nominal decomposed system could be achieved.

The response curves in figure 5.8.6. for variations in α_p indicate that although a design value of $\alpha_p = .4$ was selected, a value of $\alpha_p = 1$ set on the plant yielded the minimal settling time. This indicates however the difficulty of synthesizing a sub-optimal control function for a third order plant with complex eigenvalues (with a supposedly known value of α_p and K_p).

One of the primary improvements and advantages in this technique is the use of simple algebraic expressions for deriving the control laws, such that for second-order plants, maintain a near time-optimal response in

spite of plant parameter variations, viz. the control equations are to some degree insensitive to plant parameter variations. These expressions must be compared with the cumbersome and unwieldy exact time-optimal expressions involving exponentials and logarithms which also, are more sensitive about their nominal design parameters than the transformed algebraic expressions (see Appendix A6.2 and A6.5).

For third-order plants with complex eigenvalues this technique competes favourably with the adaptive relay control method, although knowledge concerning the plant parameters is essential to achieve satisfactory system performance.

Finally the DC motor was run with the programme written for a second-order plant as for the fast model controller in chapter two. Figures 2.4.24. and 2.4.25. illustrate also the motor response due to this method of control. Curve 1 in figure 2.4.24. and curve 2 in figure 2.4.25 are of the dead-beat type and represent angular position responses close to time-optimal. This method for motor position control offers up many practical possibilities especially as the hybrid simulation studies on a third order plant with complex eigenvalues appear very promising.

CHAPTER 6

CONCLUSION

The use of a fast model to predict the instants of change-over of the drive for a plant to achieve time-optimal control has been successfully demonstrated. This program, in fact, comprised certain developments and extensions and are listed below in five basic stages as well as certain reservations.

Stage 1 : The analogue computer simulation of a second-order fast model predictor for time-optimal control of a second-order plant (the second-order logic was also applied to third-and fourth-order plants).

Stage 2 : Hybrid simulation, where the fast model time-optimal trajectory equations are used to execute control for second-and third-order plants.

Stage 3 : The application of model reference, parameter identification and tracking scheme to maintain a closely matched plant to model pair and thereby ensure the time-optimal control action.

Stage 4 : The method of the adaptive relay control whereby the identification phase in stage 3 is eliminated

and a relatively simple sub-optimal control law was implemented. With the resulting plant response in some cases close to optimal.

Stage 5 : The method of the nominal-$\underline{y}$ transformed state variables, to replace the cumbersome and sensitive exact time-optimal equations used in Stage 2 for a set of simpler, less sensitive algebraic expressions in which the plant response is in some cases time-optimal.

The direct analogue simulation of Stage 1 successfully demonstrated the basis behind the objective and it was fairly satisfactory in providing control for second, third and fourth order plants, provided that the oscillations about the steady state for third and fourth order plants can be accommodated or the control is switched to an auxiliary strategy. The limitations in this method are the inherent delays, lags and drift in the analogue and electro mechanical elements which affect its ability to predict accurate control.

In order to improve upon the performance of the system, Stages 2 and 3 were logical steps. The introduction of a computerised fast or synthetic model (through the exact time-optimal trajectory equation) enabled the accuracy and repeatability of the control action to be greatly enhanced

while the addition of an identification scheme to the system radically improved the overall response in the presence of plant parameter variation. The computer program developed for the control of a second order plant was successfully applied to the position control of a small DC motor.

The time-optimal or near time-optimal control strategy for third-order (and higher order) plants followed in Stages 4 and 5. It was found however that the nominally time-optimal control systems were highly sensitive to parameter variation and in certain cases small deviations of the plant parameters increased the settling time while in some other cases caused instability.

In stage 4 a simple relay adaptive controller (which results in sliding motion) with a linear switching function has been applied with the resulting system response close to the time-optimal trajectory. A third-order plant with complex eigenvalues was also controlled by this method and its response was satisfactory for moderate variations in the plant parameters. A small DC motor was successfully controlled by this method and it appears that there exists a wide possible application of this strategy to systems with general higher order plants.

In Stage 5 a state variable transformation method, termed the nominal-$\underline{v}$ transformation control method, has been successfully applied to second-order plants. The relatively simple time-optimal control law for a double integrator plant has been applied to a range of more general second-order plants, with remarkably small deterioration of the optimal system performance. In this way, the difficulties inherent in synthesizing the logarithmic, exponential and other complicated functions of state variables which are present in the exact time-optimal control laws (where known) as in Stage 2 were avoided. It was also found that the simplified control laws were to some measure insensitive to plant parameter variation.

A sub-optimal predictive control strategy which is based on the time-optimal strategy for second-order systems is generalized for third-order (and higher order) systems. The sub-optimal strategy was simpler to implement than the exact time-optimal equation, and by direct application of this strategy to a third-order plant with complex eigenvalues, a satisfactory set of responses were achieved, although this method is based upon plants with negative real eigenvalues in simple ratios. The success attained by this method on a small DC motor indicated its use and application to general second and third order systems.

The advantages and disadvantages accrued to the stages described and tested, have been condensed in the following table :

Method of Control	Characteristics of Fast Model	Ease of Control Law Implementation	Sensitivity to Plant Parameter Variation	Performance w.r.t. Time-optimality
Analogue system using a fast model predictor based on relay sampling	Simulated directly (direct integration)	Relatively easy	Moderately Sensitive	The performance is sub-optimal unless tuning of the system is implemented
Hybrid system with the plant simulated on an analogue computer	Exact time-optimal equations of fast model executed on minicomputer	Moderately easy for a double integrator but complex for certain second-order plants	Highly sensitive	The performance is time-optimal or quasi-optimal provided plant and model are identically matched
Hybrid system with the plant and real-time model simulated on an analogue computer	Exact time-optimal equations of fast model and updating algorithm executed on minicomputer	Can be complex for certain second order systems	Largely insensitive provided the plant input does not slide	The performance is near time-optimal or quasi-optimal provided the plant and model remain closely matched
Hybrid system using adaptive relay control and plant simulated on an analogue computer	No fast model required	Control law is easy to implement as it is a linear function of the state variables	Relatively insensitive for second-order plants but moderately sensitive for third-order plants	The performance is sub-optimal but for certain cases is moderately close to optimal
Hybrid system using nominal-$\underline{v}$ transformation and plant simulated on an analogue computer	Fast model time-optimal equation is superceded by a simpler algebraic expression	Relatively easy	Moderately insensitive for second-and third order plants	The performance is near time optimal or quasi-optimal for second order systems but sub-optimal for third order systems

Further research is felt to be warrented in several fields as listed below:

1. The extension and development of the identification algorithm to accommodate fast reversals of the plant input for the hybrid adaptive system.

2. The problem of hidden state variables or the inability to measure a state variable, with the possible use of observer systems.

3. The investigation into the presence of noise and random disturbances in the input, measurement vectors and the sensitivity of the control laws.

4. The improvement of the y-transformation control laws for third- and fourth-order plants with complex eigenvalues.

Finally to provide an answer to the question as to which control method is deemed to be the best or most suitable, it can only be said that circumstances will dictate the appropriate technique. The system under consideration, the limits imposed by the environment, available finance, the design requirements of speed, accuracy, repeatability and reliability of performance will determine which method is to be ultimately selected.

REFERENCES

1. ZIEBOLZ, H and PAYNTER, H.M. ; 'Possibilities of a two-time scale computing system for control and simulation of dynamic systems', Proc. NEC, 9, 1954, pp 215-223.

2. ROZONOER, L.I.; 'L.S. Pontryagin maximum principle in the theory of optimum systems', Automatica and remote control, Vol. 20, Oct., Nov., Dec., 1959.

3. LANDAU, I.D.; 'A survey of model reference adaptive techniques - theory and applications', Automatica, Vol. 10, 1974, pp 353-379.

4. NARENDRA, K.S. and KUDVA, P.; 'Stable adaptive schemes for system identification and control - part 1', IEEE Trans. on SMC, Vol. SMC-4, No.6, 1974, pp 542-551.

5. ZINOBER, A.S.I.; 'Adaptive relay control of second-order systems', Int. J. Control, Vol. 21, No.1, 1975, pp 81-88.

6. RYAN, E.P.; 'Optimal and sub-optimal relay control by state-variable transformation', Int. J. Control, Vol. 22, No. 3, 1975, pp 329-362.

7. ZINOBER, A.S.I. and FULLER, A.T.; 'The sensitivity of nominally time-optimal control systems to parameter variation', Int. J. of control, Vol. 17, No. 4, 1973, pp 673-703.

8. RUBIN, O.; 'Design of bang-bang controllers', Symposium on control theory - S.A.C.A.C., Oct. 1975, pp 168-187.

9. McCAUSLAND, I.; 'Introduction to optimal control', John Wiley and Sons Inc., 1969.

10. FULLER, A.T.; 'Sub-optimal nonlinear controllers for relay and saturating control systems', Int. J. of Control, Vol 13, No. 3, 1971, pp 401-428.

11. WEISSENBERGER, S.; 'Stability boundry approximations for relay-control systems via a steepest ascent construction of Lyapunov functions', Journal of Basic Engineering, Trans. of the ASME, June 1966, pp 419-428.

12. BILLINGSLEY, J. and COALES, J.F.; 'Simple predictive controller for high-order systems', Proc. IEE, Vol. 115, No. 10, Oct. 1968, pp 1568-1576.

13. COALES, J.F. and NOTON, A.R.M.; 'An on-off servo mechanism with predicted change-over', Proc. IEE, Vol. 103B, 1956, pp 449-462.

14. CHESTNUT, H., SOLLECITO, W.E. and TROUTMAN, P.H.; 'Predictive control system application', Trans. AIEE, APPL. IND., 80, July 1961, pp 128-139.

15. ADEY, A.J., BILLINGSLEY, J. and COALES, J.F.; 'Predictive control of higher order systems', Proc. of the 3rd IFAC congress, session 40, June 1966, paper 40.F.

16. FALLSIDE, F. and THEDCHANAMOORTHY, N.; 'Predictive control using an adaptive fast model', Proc. IEE, Vol. 114, No. 11, Nov. 1967, pp 1761-1771.

17. ADAMS, P.G. and SCHOOLEY, A.T.; 'Ada-predictive control for a batch reaction', Instrumentation Technology, Jan. 1969, pp 57-62.

18. LEFKOWITZ, I. and ECKMAN, D.P.; 'Application and analysis of a computer control system', Journal of Basic Engineering, Trans. of the ASME, Dec. 1959, pp 569-577

19. SCHEIBER, L.S. and ELGERD,O.I.; 'A study of optimal switching of on-off type control systems through logic', Proc. of NEC, Vol. 18, 1962, pp 203-209.

20. ELGERD, O.I.; 'Hybrid computation - a means to study predictive control system behaviour', Proc. of IEEE Spring conf. New York, March 1964, pp 30-36.

21. RAE, W.G.; 'Fast model search control systems', Int. J. of Control, Vol. 6, 1967, pp 537-545.

22. KAUFMAN, H. and DERUSSO, P.M.; 'Stability analysis of predictive control systems', IEEE Trans. on AC, Vol. AC-11, No. 3, July 1966, pp 455-464.

23. NEHRIR, M.H.; 'A predictive controller for automatic voltage regulation of dc generators - a hybrid simulation study', IEEE Trans. on IECI, Vol. IECI-22, No. 1, Feb. 1975, pp 43-46.

24. ZINOBER, A.S.I.; 'Relay control of plants subject to parameter uncertainty', Ph.D. thesis, Cambridge University, Jan. 1974.

25. EVELEIGH, V.W.; 'Adaptive control and optimization techniques', McGraw-Hill, Inc., 1967.

26. GIBSON, J.E.; 'Nonlinear automatic control', McGraw-Hill, Inc., 1963.

27. PARKS, P.C.; 'Liapunov redesign of model reference adaptive control systems', IEEE Trans. on AC, Vol. AC-11, No. 3, July 1966, pp 362-367.

28. WINSOR, C.A. and ROY, R.J.. 'Design of model reference adaptive control systems by Liapunov's second method', IEEE Trans. on AC, Vol. AC-13, April 1968, p 204.

29. PHILLIPSON, P.H.; 'Design methods for model-reference adaptive systems', Proc. of the IME, Vol. 183, Pt. 1, No. 35, 1968-1969.

30. HANG, C. and PARKS, P.; 'Comparitive studies of model reference adaptive control systems', IEEE Trans. on AC, Vol AC-18, No. 5, Oct. 1973, pp 419-428.

31. RYAN, E.P.; 'A near-time-optimal control approach for third-and fourth order relay control systems', Int. J. Control, Vol. 23, No. 5, 1976, pp 741-774.

32. WIBERG, D.M.; 'State space and linear systems', Schaum's outline series, McGraw-Hill, Inc., 1971.

33. SCHEID, F.; 'Numerical analysis', Schaum's outline series, McGraw-Hill, Inc. 1968.

APPENDIX A1

DERIVATION OF THE HAMILTONIAN FORMULATION[9]

A quantity to be maximized or minimized, using the calculus of variations, is called a functional. A functional may be defined as a relationship by which we associate a definite real number with each function or curve belonging to a certain class. For example, the more general functional

$$J = \int_{x_0}^{x_1} f(x,y,y')dx \qquad (A1.1)$$

can be described where J = the value of the functional and f is some prescribed function of the arguments shown. It is required to find the curve $y(x)$ (the curve $y(x)$ will be restricted to the class of functions which are continuous and have continuous first derivations) joining two specified points (x_0, y_0) and (x_1, y_1) which makes J take on a maximum or minimum value.

The conditons which the function $y(x)$ must satisfy in order to make J take on its minimum value results in the equation

$$\frac{\partial f}{\partial y} = \frac{d}{dx}\left(\frac{\partial f}{\partial y'}\right) \qquad (A1.2)$$

where equation A1.2 is usually called the Euler-Lagrange equation. It is an ordinary differential equation whose

solution gives y as a function of x. Using the abbreviated notation

$f_y \triangleq \frac{\partial f}{\partial y}$, the E-L equation can be written in the form

$$f_y = \frac{df_{\dot{y}}}{dx} \qquad \text{(A1.3)}$$

It should be noted however that the E-L equation is only a necessary condition for a maximum or a minimum and further investigations might be required to test for a maximum or a minimum.

For several independent variables, we wish for example to find the two functions $x(t)$ and $y(t)$ which minimize a functional of the following form

$$J = \int_{t_0}^{t_1} f(t,x,\dot{x},y,\dot{y})\, dt \qquad \text{(A1.4)}$$

It turns out that the functions $x(t)$ and $y(t)$ must both satisfy the E-L equations; that is, the necessary conditions for an extreme value of J are the E-L equations

$$f_x = \frac{df_{\dot{x}}}{dt} \qquad \text{(A1.5)}$$

$$f_y = \frac{df_{\dot{y}}}{dt}$$

If, in addition, the right hand endpoint is variable, we also have a tranversality condition which may be expressed in the form (in many cases, the separate terms involved in the

tranversality condition will themselves be zero)

$$(f-\dot{x}f_{\dot{x}}-yf_{\dot{y}})dt + f_{\dot{x}}\,dx + f_{\dot{y}}\,dy)_1 = 0 \qquad (A1.6)$$

where the subscript 1 shows that this relationship is satisfied at the right-hand endpoint.

Extending this to n dependent variables, we find that the necessary conditions for an extreme value of

$$J = \int_{t_o}^{t_1} f(t,x_i,\dot{x}_1, \ldots, x_n, \dot{x}_n)\, dt$$

are

$$f_{x_i} = \frac{df_{\dot{x}_i}}{dt} \quad \text{for } i = 1,2,\ldots, n \qquad (A1.8)$$

If the right-hand endpoint is variable, we have in addition the transyersality condition

$$\left((f - \sum_{i=1}^{n} \dot{x}_i f_{\dot{x}_i})dt + \sum_{i=1}^{n} f_{\dot{x}_i}\, dx_i \right) = 0 \qquad (A1.9)$$

The tranversality conditions are really a generalization of the onthogonality conditions when dealing with the minimization of more general functionals, hence if the E-L equation is the differential equation which provides the solution in a general form, the transyersality conditions supply information concerning the boundry conditions of the problem.

Suppose instead of expressing the optimization problem in terms of the minimization of an integral of the form of

equation A1.7, the minimization is desired of the quantity defined by

$$J = g(t_1, x_1^1, x_2^1, \ldots, x_n^1) \qquad \text{(A1.10)}$$

subject to the auxiliary conditions

$$\phi_j (t, x_1, \dot{x}_1, \ldots, x_n, \dot{x}_n) = 0 \qquad \text{(A1.11)}$$

for $j = 1,2 \ldots, m < n$

This type of problem is known as the Mayer problem, whereas the problem in which an integral is to be minimized may be called the Lagrange problem, these two problems may be treated as alternative formulations of the same problem.

The method of solution of the Mayer problem is as follows The function F_m is formed defined by

$$F_m \triangleq \sum_{i=1}^{m} \lambda_i \phi_i \qquad \text{(A1.12)}$$

and solve the n+m E-L equations

$$F_{mx_i} = \frac{dF_{\dot{x}_i}}{dt} \quad (i = 1,2, \ldots,n) \qquad \text{(A1.13)}$$

$$\phi_j = F_{\lambda_j} = 0 \quad (j=1, \ldots, m) \qquad \text{(A1.14)}$$

Subject to the specified boundry conditions and the following transversality condition at the right-hand end point

$$\left(dg + \left(F_m - \sum_{i=1}^{n} \dot{x}_i F_{m\dot{x}_i}\right) dt + \sum_{i=1}^{n} F_{m\dot{x}_i} dx_i\right)_1 = 0 \qquad \text{(A1.15)}$$

For a system characterized by the vector differential equation

$$\dot{\underline{x}} = \underline{f}\ (\underline{x},\ \underline{u}) \qquad \text{(A1.16)}$$

where $\underline{x}$ is the vector with components $x_1, x_2, \ldots, x_n$ $\underline{f}$ is a vector with components $f_1, f_2, \ldots, f_n$ and $\underline{u}$ is the vector with components $u_1, u_2, \ldots, u_r$.

Suppose is desired to find the control input $\underline{u}(t)$ in the interval (t_0, t_1) which transfers the system state from $\underline{x}^0$ at time t_0 to $\underline{x}^1$ at time t_1 and gives a minimum value to the integral.

$$J = \int_{t_1}^{t_1} f_0\ (\underline{x},\ \underline{u})\ dt \qquad \text{(A1.17)}$$

This can be solved by formulating the problem in the Mayer form:

1. Introduce a new state variable x_0, characterised by the equation

$$\dot{x}_0 = f_0\ (\underline{x},\ \underline{u}) \qquad \text{(A1.18)}$$

2. Express the differential equations as constraining equations of the form

$$\phi_i = \dot{x}_i - f_i\ (\underline{x},\ \underline{u}) = 0 \qquad \text{(A1.19)}$$

for $i = 0, 1, 2, \ldots, n$

3. Form the function F, defined by

$$F \triangleq \sum_{i=0}^{n} \lambda_i \phi_i = \sum_{i=0}^{n} \lambda_i \left(\dot{x}_i - f_i (\underline{x}, \underline{u}) \right) \quad \text{(A1.20)}$$

4. Write the E-L equations for the dependent variables x_i, λ_i and u_j. These are

$$F_{x_i} = \frac{d}{dt} F_{\dot{x}_i} \quad (i = 0, 1, \ldots, n) \quad \text{(A1.21)}$$

$$F_{\lambda i} = \frac{d}{dt} F_{\dot{\lambda} i} = 0 \quad (i = 0, 1, \ldots, n) \quad \text{(A1.22)}$$

$$F_{u_j} = \frac{d}{dt} F_{\dot{u}_j} = 0 \quad (j = 1, \ldots, r) \quad \text{(A1.23)}$$

The quantities $F_{\dot{\lambda} i}$ and $F_{\dot{u}_j}$ are zero because F is not an explicit function of $\dot{\lambda}_i$ and $\dot{u}_j$.

The transversality condition, in this case may be written in the form

$$\left(x_0 + \left(F - \sum_{i=0}^{n} \dot{x}_i F_{\dot{x}_i} \right) dt + \sum_{i=0}^{n} F_{\dot{x}_i} \, dx_i \right)_1 = 0 \quad \text{(A1.24)}$$

The quantities $F_{\dot{u}_j}$ and $F_{\dot{\lambda} i}$ are all zero as before and need not be written in the transversality condition.

In order to relate the calculus of variations to the maximum principle, a function H is introduced (the Hamiltonian), defined by

$$H \triangleq \sum_{i=0}^{n} \lambda_i f_i (\underline{x}, \underline{u}) \quad \text{(A1.25)}$$

The quantity F can be written in the form

$$F = \sum_{i=0}^{n} \lambda_i \dot{x}_i - H \qquad \text{(A1.26)}$$

Expressing the three sets of the E-L equations A1.21 to A1.23 in terms of F as given by equation A1.26, yield respectively,

$$-\frac{\partial H}{\partial x_i} = \frac{d\lambda_i}{dt} \quad (i=0,1, \ldots, n) \qquad \text{(A1.27)}$$

$$\frac{dx_i}{dt} - \frac{\partial H}{\partial \lambda_i} = 0 \quad (i=0,1, \ldots, n) \qquad \text{(A1.28)}$$

$$\frac{\partial H}{\partial u_j} = 0 \qquad (j=1, \ldots, r) \qquad \text{(A1.29)}$$

The transversality condition for the Hamiltonian formulation of the problem is

$$\left(dx_0 - H\,dt + \sum_{i=0}^{n} \lambda_i\, dx_i \right)_1 = 0 \qquad \text{(A1.30)}$$

The problem can now be worked in terms of the Hamiltonian H, without using the function F.

APPENDIX A2

GENERAL CONSIDERATINS IN MINIMUM-TIME CONTROL OF LINEAR SYSTEMS

The problem of the double integrator is a special case of minimum time control of linear systems. Suppose we have a general linear system whose differential equations are written in the vector-matrix form

$$\dot{\underline{x}} = A\underline{x} + B\underline{u} \qquad \text{(A2.1)}$$

where A is an nxn constant matrix

B is an nxr constant matrix

$\underline{x}$ is an n vector

$\underline{u}$ is an r vector

The control vector $\underline{u}$ is required to lie in a specified closed bounded, convex region U.

Equation A2.1 may be written in the form

$$\dot{x}_i = \sum_{j=1}^{n} a_{ij} x_j + \sum_{k=1}^{r} b_{ik} u_k \quad (i=1,2,..,n) \qquad \text{(A2.2)}$$

The Hamiltonian H may be written as

$$H = \underline{p} \cdot A\underline{x} + \underline{p} \cdot B\underline{u} \qquad \text{(A2.3)}$$

which may also be written in the form

$$H = \sum_{i=1}^{n} \sum_{j=1}^{n} P_i a_{ij} x_j + \sum_{k=1}^{n} \sum_{l=1}^{r} P_k b_{kl} u_l \quad (A2.4)$$

The differential equations governing the behaviour of the p_i may be derived from equation A2.4 to be

$$\frac{dp_j}{dt} = -\frac{\partial H}{\partial x_j} = -\sum_{i=1}^{n} a_{ij} p_i \quad (j=1,..,n) \quad (A2.5)$$

In vector matrix form equations A2.5 may be written as

$$\frac{d\underline{p}}{dt} = -A^T \underline{p} \quad (A2.6)$$

where A^T is the transpose of A

Equation A2.6 is the adjoint equation corresponding to $\dot{\underline{x}} = A\underline{x}$.

The auxiliary variables p_i are sometimes referred to as the adjoint variables or the co-state variables.

From equation A2.3 it is seen that H reaches its maximum with respect to $\underline{u}$ when the second term on the right, $\underline{p} \cdot B\underline{u}$, is maximum. As this term is a linear function of $\underline{u}$, and as the control vector is required to lie in a closed, convex, bounded region U, the maximum value of $\underline{p} \cdot B\underline{u}$ will, unless this quantity identically zero, take on its maximum value when $\underline{u}$ is on the boundry of the admissible region and cannot have its maximum at any interior point.

APPENDIX A3

TRIPLE INTEGRATOR . MINIMAL TIME CONTROL

The differential equations governing the behaviour of the system in Figure A3.1 are

$$\frac{dx_1}{dt} = x_2$$

$$\frac{dx_2}{dt} = x_3 \qquad \text{(A3.1)}$$

$$\frac{dx_3}{dt} = \frac{u}{a} \qquad (a > 0 \text{ plant parameter})$$

We can write the Hamiltonian H, as defined in 1.3.6 as

$$H = \sum_{i=1}^{3} p_i f_i (\underline{x}, \underline{u})$$

$$\therefore H = p_1 x_2 + p_2 x_3 + p_3 \frac{u}{a} \qquad \text{(A3.2)}$$

The optimal value of u must be given by $u^* = \text{sgn } p_3$ (A3.3)

The differential equations governing the behaviour of the p variables are derived from equations 1.3.7

$$\frac{dp_i}{dt} = - \frac{\partial H}{\partial x_i} \quad i = 1,2,3$$

or $$\frac{dp_1}{dt} = 0$$

$$\frac{dp_2}{dt} = - p_1 \qquad \text{(A3.4)}$$

$$\frac{dp_3}{dt} = - p_2$$

$$\therefore \quad p_1 = c_1 \qquad \text{(A3.5)}$$

$$\therefore \quad p_2 = -c_1 t + c_2 \qquad \text{(A3.6)}$$

$$\text{and} \quad p_3 = \frac{c_1 t^2}{2} - c_2 t + c_3 \qquad \text{(A3.7)}$$

(c_1, c_2 and c_3 are constants)

p_3 can be expressed as

$$p_3 = \frac{c_1}{2}\left(t^2 - \frac{2c_2}{c_1} t + \frac{2c_3}{c_1}\right) \qquad \text{(A3.8)}$$

Since $u^* = \text{sgn } p_3$

$$\therefore \quad u^* = \text{sgn } \frac{c_1}{2}\left(t^2 - \frac{2c_2}{c_1} t + \frac{2c_3}{c_1}\right) \qquad \text{(A3.9)}$$

Since c_1 is a constant

$$u^* = \text{sgn}\left(t^2 - \frac{2c_2 t}{c_1} + \frac{2c_3}{c_1}\right)$$

$$\therefore \quad u^* = \text{sgn}\left(t - \frac{c_2}{c_1} - \frac{(c_2^2 - 2c_1c_3)^{\frac{1}{2}}}{c_1}\right)\left(t - \frac{c_2}{c_1} + \frac{(c_2^2 - 2c_1c_3)^{\frac{1}{2}}}{c_1}\right)$$

(A3.10)

We consider only values of $t > 0$ and real.

Equation A3.8 is a parabola in t and has the following forms as in Figure A3.2.

Figure A3.3. represents the optimal input u^* for $u^* = \text{sgn } p_3$ Curves A in both diagrams represents those values of p_3 and u^* for $c_1 > 0$ and curves B represent those values of p_3 and u^* for $c_1 < 0$.

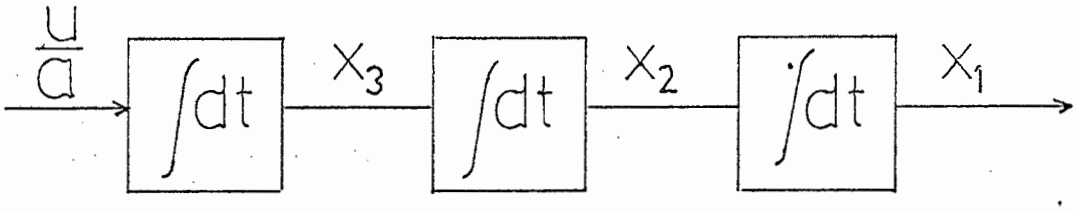

FIGURE A3.1 : A TRIPLE INTEGRATOR

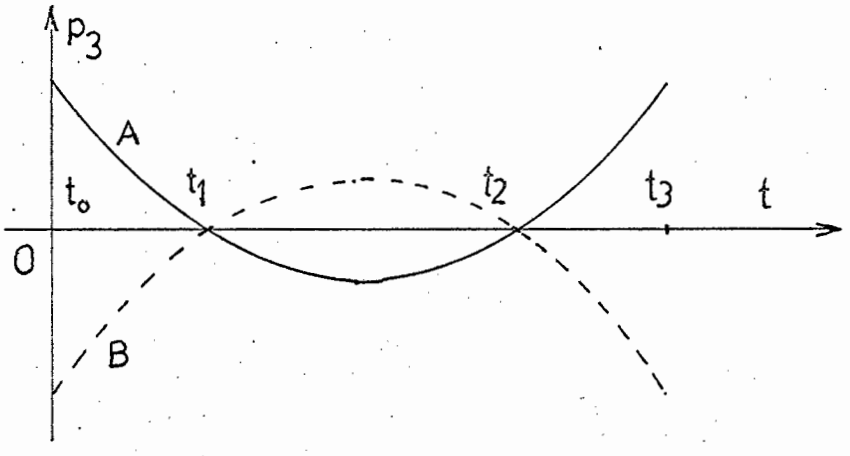

FIGURE A3.2 : CO-STATE p_3

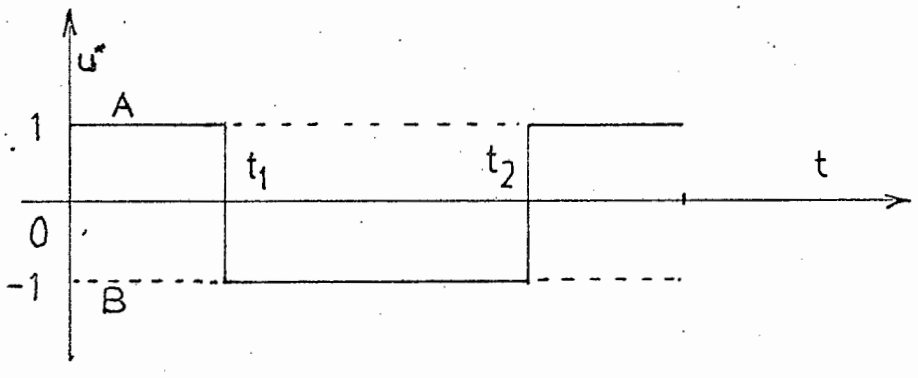

FIGURE A3.3 : CONTROL INPUT u^*

Pontryagin tells us that for a third order system we can expect the minimum of two switchings. It can be seen that they must be the switch-points t_1 and t_2 in Figure A3.3.

The time-optimal switching function[5] for the plant described by equations A3.1 is

$$u^* = -x_1 - \tfrac{1}{3}a^2x_3^3 - (ax_2x_3 + a^{\frac{1}{2}}(\tfrac{1}{2}ax_3^2 + x_2\,\mathrm{sgn}(x_2 + \tfrac{1}{2}ax_3|x_3|))^{3/2})\,\mathrm{sgn}(x_2 + \tfrac{1}{2}ax_3|x_3|)$$

provided the RHS $\neq 0$ (A3.11)

For state points such that the RHS of A3.11 is zero

$$u^* = -x_2 - \tfrac{1}{2}ax_3|x_3| \quad (x_2 + \tfrac{1}{2}ax_3|x_3| \neq 0) \quad \text{(A3.12)}$$

and

$$u^* = -x_3 \quad (x_2 + \tfrac{1}{2}ax_3|x_3| = 0) \quad \text{(A3.13)}$$

Finally by integrating equations A3.1 with respect to time we obtain

$$x_1(t) = x_1(0) + x_2(0)t + x_3(0)\frac{t^2}{2} + \frac{ut^3}{6a}$$

$$x_2(t) = x_2(0) + x_3(0)t + \frac{ut^2}{2a} \quad \text{(A3.14)}$$

$$x_3(t) = x_3(0) + \frac{ut}{a}$$

where $x_1(0)$, $x_2(0)$ and $x_3(0)$ are the initial corditions at $t = 0$

The complexity of the time optimal switching function

equation A3.11 and the manipulation of equations A3.14 involving t^3 are evident although the co-state p_3 indicates that at least two switchings are required to bring the system trajectory to its target. To achieve true time optimal response for a third order system in practice is extremely difficult and other strategies which are sub-optimal but more simpler and less sensitive are resorted to, as described in this thesis.

APPENDIX A4

THE DOUBLE INTEGRATOR PLANT

The plant trajectories are determined from

$$\dot{x}_1 = x_2$$
$$\dot{x}_2 = \frac{u}{b} \qquad (A4.1)$$

Integrating equations A4.1 with respect to time we obtain the trajectory equations as follows, for an interval during which $u(t)$ = constant = c

$$x_1(t) = x_1(t_0) + x_2(t_0)(t-t_0) + \tfrac{1}{2}\frac{c}{b}(t-t_0)^2$$
$$x_2(t) = x_2(t_0) + \frac{c}{b}(t-t_0)$$
$$t \geq t_0 \qquad (A4.2)$$

Eliminating time t from A4.2 we obtain

$$(x_2(t))^2 = (x_2(t_0))^2 + 2\frac{c}{b}(x_1(t)-x_1(t_0)) \qquad (A4.3)$$

The initial conditions $(x_1(0), x_2(0))$ are written as (x_1^0, x_2^0) and will be taken to lie in the region of the phase-plane $\phi(x_1^0, x_2^0, a) < 0$

The control is given by the equations:

$$u = \text{sgn } \phi \qquad (A4.4)$$
$$\phi = -x_1 - \tfrac{1}{2}ax_2|x_2| \quad (x_1+\tfrac{1}{2}ax_2|x_2| \neq 0) \qquad (A4.5)$$
$$\phi = -x_2 \quad (x_1+\tfrac{1}{2}ax_2|x_2| = 0) \qquad (A4.6)$$

Let the state point at the i th switch be (x_1^i, x_2^i). Let t_i be the time interval between the (i-1)th and the i th switch (i = 2,3,....).

Let t_1 be the time of the first switch.

Case (i) b = a

There is only one switching of the control (see Figure 1.5.1) because the time-optimal switching function is being used. The settling time is T_{aa} (see section 1.5) and satisfies

$$T_{aa} = t_1 + t_2 \qquad \text{(A4.7)}$$

Equations A4.2 yield at time t_1 and with b=a

$$x_1^1 = x_1^o + x_2^o\, t_1 - \frac{1}{2a}\, t_1^2 \qquad \text{(A4.8)}$$

$$x_2^1 = x_2^o - \frac{1}{a}\, t_1 \qquad \text{(A4.9)}$$

where u = - 1 and $t_o = 0$

Since (x_1^1, x_2^1) is on the switching curve A4.5 with $x_2^1 < 0$ (see Figure 1.5.1)

$$x_1^1 = \tfrac{1}{2}a\,(x_2^1)^2 \qquad \text{(A4.10)}$$

From A4.8, A4.9 and A4.10

$$t_1 = a(x_2^o - x_2^1) \qquad \text{(A4.11)}$$

and

$$x_2^1 = -(2ax_1^o + a^2(x_2^o)^2)^{\frac{1}{2}}\, 2^{-\frac{1}{2}}\, a^{-1} \qquad \text{(A4.12)}$$

Equations A4.2 yield at time $t_1 + t_2$, and with b = a,

$$x_2^2 = 0 = x_2^1 + \frac{1}{a}\, t_2 \qquad \text{(A4.13)}$$

(Since at t_2, $x_2^2 = 0$ and $t_o = 0$)

From A4.7, A4.11, A4.12 and A4.13

$$T_{aa} = ax_2^{\,o} + (2ax_1^{\,o} + a^2(x_2^{\,o})^2)^{\frac{1}{2}}\, 2^{\frac{1}{2}} \qquad \text{(A4.14)}$$

Case (ii) $b > a$

The settling time is

$$T_{ba} = t_1 + t_2 + t_3 + \ldots \qquad \text{(A4.15)}$$

From 4.2 t_1 satisfies

$$t_1 = b(x_2^{\,o} - x_1^{\,o}) \qquad \text{(A4.16)}$$

similarly the subsequent switch times (see Figure 1.5.2) satisfy

$$t_i = (-1)^i\, b(x_2^{\,i} - x_2^{\,i-1}) \quad (i=2,3,\ldots) \qquad \text{(A4.17)}$$

From A4.5 and A4.3 the first switch occurs at ($c = -1$)

$$x_2^{\,1} = -\left(\frac{2x_1^{\,o}}{b} + (x_2^{\,o})^2\right)^{\frac{1}{2}} \left(1 + \frac{a}{b}\right)^{-\frac{1}{2}} \qquad \text{(A4.18)}$$

Similarly the next switch occurs at

$$x_2^{\,2} = \frac{-2x_1^{\,1}}{b} + (x_2^{\,1})^2)^{\frac{1}{2}} \left(1 + \frac{a}{b}\right)^{-\frac{1}{2}} \qquad \text{(A4.19)}$$

or, since $x_1^{\,1} = \frac{1}{2}a(x_2^{\,1})^2$

$$x_2^{\,2} = -x_2^{\,1} \left(1 - \frac{a}{b}\right)^{\frac{1}{2}} \left(1 + \frac{a}{b}\right)^{-\frac{1}{2}} \qquad \text{(A4.20)}$$

Similarly

$$x_2^{\,i} = -x_2^{\,i-1} \left(1 - \frac{a}{b}\right)^{\frac{1}{2}} \left(1 + \frac{a}{b}\right)^{-\frac{1}{2}} = -\rho x_2^{\,i-1}, \text{ say } (i=2,3,\ldots) \qquad \text{(A4.21)}$$

i.e. the ratio of the values x_2 at successive switch points is the constant $(-\rho)$.

This result implies that the ratio of successive intervals t_i/t_{i-1} $(i > 2)$ is also a constant. In fact, from A4.17

$$\frac{t_i}{t_{i-1}} = -\frac{x_2^{\,i} - x_2^{\,i-1}}{x_2^{\,i-1} - x_2^{\,i-2}} = -\frac{x_2^{\,i}/x_2^{\,i-1} + 1}{1 - (x_2^{\,i-2}/x_2^{\,i-1})} \quad (A4.22)$$

$$= \frac{\rho + 1}{1 + \rho^{-1}} = \rho \ (< 1) \ (i = 3,4,\ldots) \quad (A4.23)$$

Thus $\sum_{i=2}^{\infty} t_i$ is a geometric series, so that the total settling time is finite.

From A4.15, A4.16 and A4.17

$$T_{ba} = b\,(x_2^{\,0} - 2x_2^{\,1} + 2x_2^{\,2} - 2x_2^{\,3} + \ldots) \quad (A4.24)$$

Substituting A4.21 into A4.24 we obtain

$$T_{ba} = b(x_2^{\,0} - 2x_2^{\,1}\,(1+\rho+\rho^2+\ldots)) \quad (A4.25)$$

$$= b(x_2^{\,0} - 2x_2^{\,1}\,(1-\rho)^{-1}) \quad (A4.26)$$

From A4.18, A4.21 and A4.26

$$T_{ba} = bx_2^{\,0} + (2bx_1^{\,0} + b^2(x_2^{\,0})^2)^{\frac{1}{2}}\, 2((1+\tfrac{a}{b})^{\frac{1}{2}} - (1-\tfrac{a}{b})^{\frac{1}{2}})^{-1} \quad (A4.27)$$

Case (iii) $b < a$

Zinober and Fuller[7] show that for $b < a$ every point of the switching surface of an n-integrator plant is a sliding point. The motion up to the first switching is as before. Thereafter the state slides along the switching curve to the phase-plane origin (see Figures 1.5.3 and 1.5.4).

If the duration of the sliding motion to the origin is t_2,

$$T_{ba} = t_1 + t_2 \qquad \text{(A4.28)}$$

From A4.2, with c = - 1

$$t_1 = b(x_2^0 - x_2^1) \qquad \text{(A4.29)}$$

Suppose the starting point satisfies

$$x_1^0 + \tfrac{1}{2}bx_2^0 \mid x_2^0 \mid \geq 0 \qquad \text{(A4.30)}$$

So that the sliding trajectory is below the x_1-axis (see Figure 1.5.3). During the sliding motion the trajectory followed is that of the time-optimal system with parameter a. Hence equations A4.2 apply, with $c = {}^{b}/_{a}$, and yield

$$t_2 = - ax_2^1 \qquad \text{(A4.31)}$$

From A4.28, A4.29 and A4.30

$$T_{ba} = b(x_2^0 - x_2^1) - ax_2^1 \qquad \text{(A4.32)}$$

Evaluation of x_2^1 from A4.18 (which still holds good for $b < a$) and substitution in A4.31 yields

$$T_{ba} = bx_2^0 + (2bx_1^0 + b^2(x_2^0)^2)^{\frac{1}{2}} (1+\tfrac{a}{b})^{\frac{1}{2}} \qquad \text{(A4.33)}$$

Similarly, for a starting point satisfying

$$x_1^0 + \tfrac{1}{2}bx_2^0 \mid x_2^0 \mid \leq 0 \qquad \text{(A4.34)}$$

for which the sliding trajectory is above the x_1-axis (see Figure 1.5.4) one finds

$$T_{ba} = bx_2^0 + (-2bx_1^0 - b^2(x_2^0)^2)^{\frac{1}{2}} (\tfrac{a}{b} - 1)^{\frac{1}{2}} \qquad \text{(A4.35)}$$

APPENDIX A5

GENERAL REMARKS CONCERNING THE USE OF LIAPUNOV'S DIRECT OR SECOND METHOD FOR STABILITY ANALYSIS

1. Stability in the sense of Liapunov

Conside a region ϵ (see Figure A5.1) in the state space enclosing an equilibrium point $\underline{x}_0$. The equilibrium point is stable provided that there is a region $s(\epsilon)$ contained within ϵ, such that any trajectory starting in the region s, say $\underline{x}(0)$ does not leave the region .

2. Asymptotic Stability

An equilibrium point is asymptotically stable, if, in addition to being stable in the sense of Liapunov, all trajectories approach the equilibrium point. This means that the variational solution $\underline{x}^*(t)$ approaches $\underline{0}$ as time $t \longrightarrow \infty$. This is the stability definition usually used in control system design when the region s includes the entire state-space and the definitions of Liapunov and asymptotic stability are said to apply in a global sense.

The second or direct method of Liapunov provides a means for determining the stability of a system without explicity solving for the trajectories in the state space and

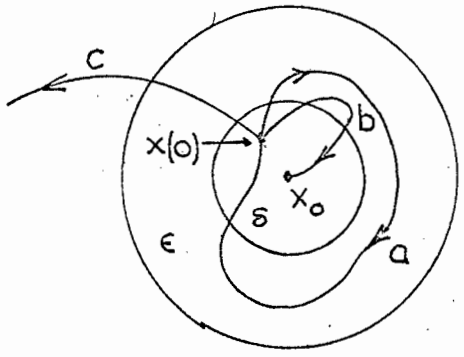

FIGURE A5.1 : STATE PLANE TRAJECTORIES INDICATING
a - LIAPUNOV STABILITY
b - ASYMPTOTIC STABILITY
c - INSTABILITY

hence the solution of the differential equation is not required. The procedure requires the selection of a scalar function $V(\underline{x})$, which is tested for the conditions that indicate stability. When $V(\underline{x})$ successfully meets these conditions, it is called a Liapunov function

3. Liapunov Asymptotic Stability

A system is asymtotically stable in the vicinity of the equilibrium point at the origin if there exists a scalar function $V(\underline{x})$ such that:

1. $V(\underline{x})$ is continuous and has continuous first partial derivatives in a region S around the origin
2. $V(\underline{x})$ $>$ 0 for $\underline{x} \neq 0$
3. $V(0) = 0$
4. $\dot{V}(\underline{x})$ $<$ 0 for $\underline{x} \neq 0$

Conditions 1 to 3 ensure that $V(\underline{x})$ is positive definite. Therefore $V(\underline{x}) = k$ is a closed surface within the region S. Condition 4 means that $\dot{V}(\underline{x})$ is negative definite and thus any trajectory in S crosses through the surface $V(\underline{x}) = k$ from the outside to the inside for all values of k. Therefore the trajectory converges on the origin where $V(0) = 0$.

4. Liapunov Global Asymptotic Stability

A system is globally asymptotically stable if there exists a scalar function $V(\underline{x})$ such that:

1. $V(\underline{x})$ is continuous and has continuous first partial derivatives in the entire state space
2. $V(\underline{x}) \quad 0$ for $\underline{x} \neq 0$
3. $V(0) = 0$
4. $V(\underline{x}) \longrightarrow \infty$ as $\|x\| \longrightarrow \infty$
5. $\dot{V}(\underline{x}) \leq 0$
6. Either $\dot{V}(x) \neq 0$ except at $\underline{x} = 0$ or any locus in the state space where $\dot{V}(\underline{x}) = 0$ is not a trajectory of the system.

Conditions 1 to 3 ensure that $V(\underline{x})$ is positive definite. Condition 4 is satisfied when $V(\underline{x})$ is positive definite i.e. it is closed in the entire state space. Conditions 5 and 6 mean that $V(\underline{x})$ is continuously decreasing along any trajectory in the entire plane and ensures that the system is asymptotically stable.

APPENDIX 6

FAST MODEL PREDICTIVE CONTROL

A6.1 Analogue Computer Simulation of a Fast Model Predictor System

In Figure A6.1.1 is a working diagram for simulating the behaviour of a double integrator plant using a fast model predictor.

Relay K1 is used for setting the initial conditions onto the fast model integrators. When K1 is unenergized the integrators are in the 'reset' mode i.e. the initial conditions from the plant are accepted. When K1 is energized the fast model integrators are in the 'operate' mode and prediction (integration) commences.

Relay K2 is used for applying the plant and model drive changeover. When K2 is energized the input to relay K1 is removed and K1 is energized hence the fast model is reset i.e. no prediction takes place. When K2 is not energized the signal actuating relay K1 is connected and prediction takes place.

Blocks 1, 2 and 3 are switches required to drive the relays (10 Volt, 20 ma). Blocks 4 and 5 are signum functions ($\pm$ 5 volt) and Blocks 6 and 7 are patching

FIGURE A 6.1.1
BLOCK DIAGRAM OF A DOUBLE INTEGRATOR
FAST MODEL PREDICTOR

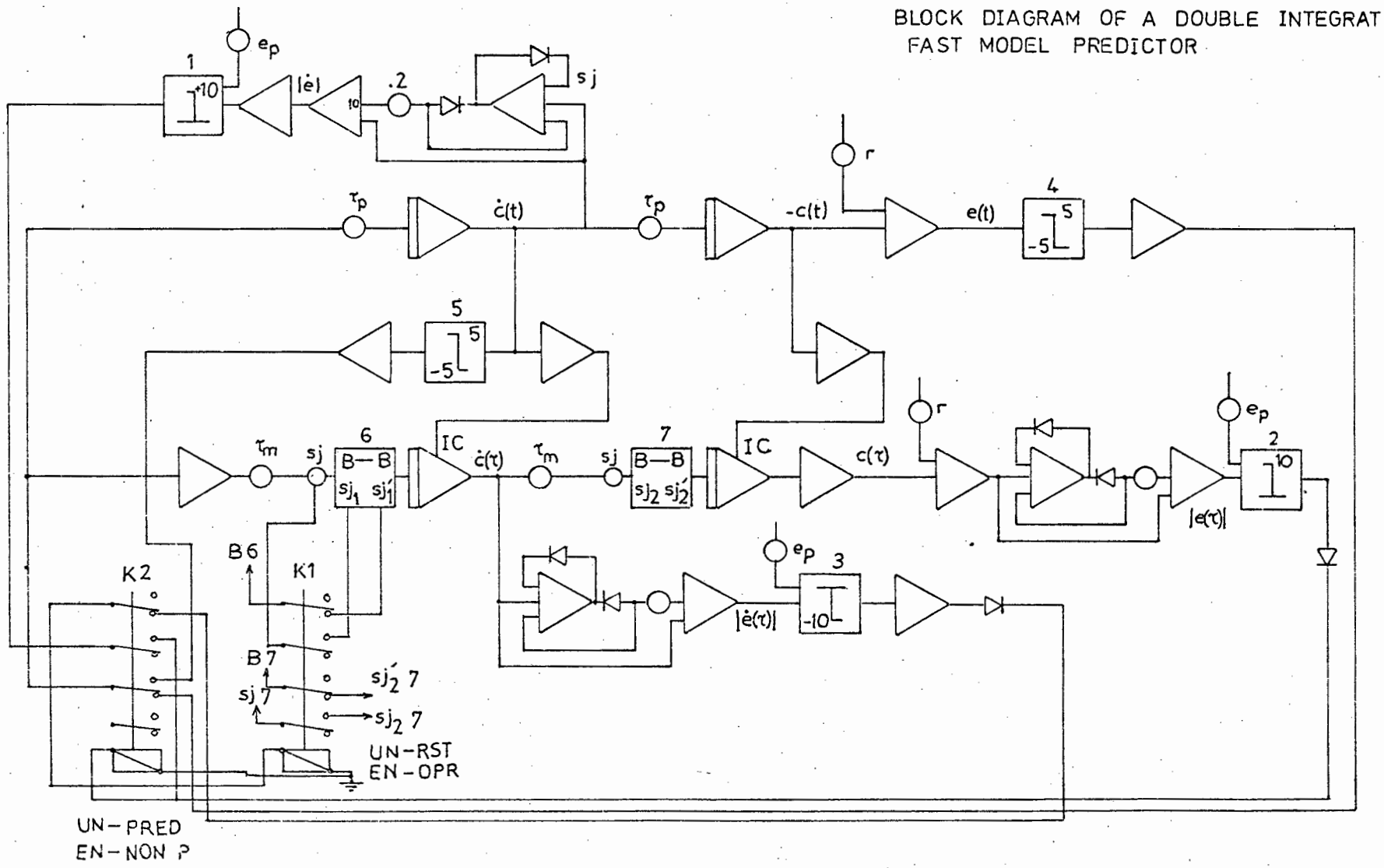

arrangements on the computer patch-panel to enable to integrators to be reset and operated by external means.

The potentiometers τ_p and τ_m are used to speed up or slow down the plant and fast model integration rates respectively.

The operation of the system is fairly straightforward. After depression of the computer OPR switch a step input r(t) is obtained from block 4 and this is applied to the inputs of the plant and model via K2. All integrators commence integration.

By virtue of its fast integration rate $\dot{e}(\tau)$ is driven to zero rapidly and at zero block 3 de-energizes K1 and the fast model is reset (to accept the current plant state). Since the predicted error $|e(\tau)|$ is still greater than zero, block 2 remains at zero and K2 remains unenergized.

The process iterates until $|e(\tau)|$ is less than a small bias e_p when block 2 provides drive for K2. K2 energizes and sgn $(\dot{e}(t))$ is obtained from block 5 which provides the correct polarity $(u(t) = -u(t))$ to the plant. K1 is de-energized and the fast model is reset (the use of sgn $(\dot{e}(t))$ for reverse polarity can be verified from observation of Figures 2.3.2 and 2.3.3 in section 2.3.1)

If the response is deadbeat the output limit cycles (no facility was used to set u(t)=0) or if there is overshoot (undershoot) the whole process is repeated once more as described in section 2.3.1.

Velocity limiting (saturation) was implemented by simply using diode limiters on the velocity integrators and is a standard procedure on analogue computers (see Figure A6.1.2)

A6.2 Digital Simulation of Second-order System

The plant (and fast model) used was an integrator and one lag. (see Figure A6.2.1)

Referring to Figure A6.2.1

$$\dot{x}_2 = (uK - \alpha x_2)\, K_1$$

Applying the Laplace transformation to A6.2.1 yields

$$sX_2(s) - x_2(0) = U(s)KK_1 - \alpha K_1 X_2(s)$$

$$\therefore X_2(s) = \frac{u(s)KK_1 + x_2(0)}{(s + \alpha K_1)} \qquad (U(s) = \frac{u}{s})$$

$$\therefore x_2(t) = \mathcal{L}^{-1}(X_2(s)) = \frac{Ku}{\alpha} - \frac{Ku}{\alpha}\, e^{-\alpha_1 K_1 t} + x_2(0) e^{-\alpha K_1 t} \qquad \text{(A6.2.2)}$$

Similarly $\dot{x}_1(t) = K_2 x_2(t)$

$$\therefore x_1(t) = \int \dot{x}_1(t)\, dt$$

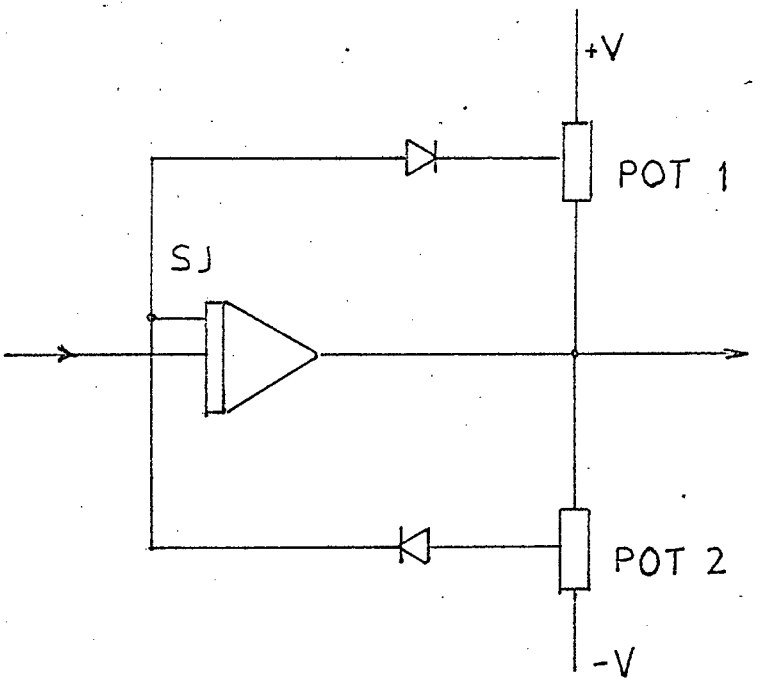

FIGURE A6.1.2 : LIMITING OR SATURATION SIMULATION

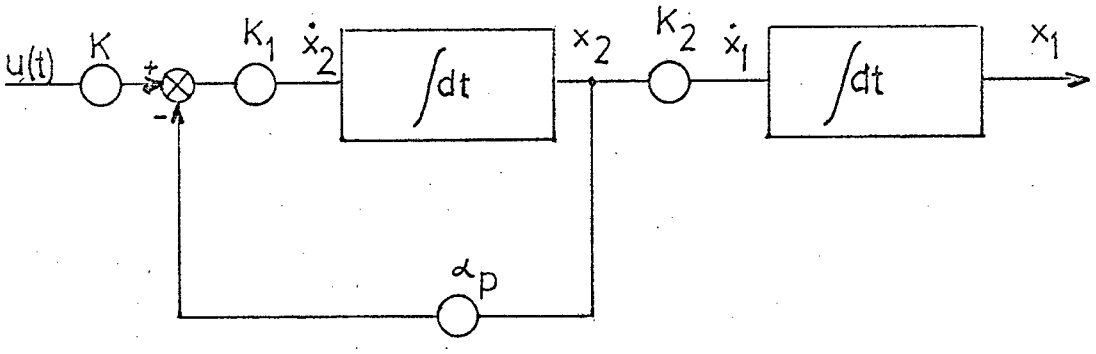

FIGURE A6.2.1 : BLOCK DIAGRAM OF SECOND ORDER PLANT ONE INTEGRATOR AND ONE LAG

K = PLANT GAIN PARAMETER

K_1, K_2 = INDIVIDUAL INTEGRATOR GAINS OR SCALING CONSTANTS

$\frac{1}{\alpha_p}$ = TIME CONSTANT

$$\therefore\ x_1(t)=x_1(0)+\frac{KK_2ut}{\alpha}-\frac{KK_2u}{K_1\alpha^2}\left(1-e^{-\alpha K_1 t}\right)+\frac{K_2}{K_1\alpha}x_2(0)\left(1-e^{-\alpha K_1 t}\right) \qquad \text{(A6.2.3)}$$

We wish to determine that value of t such that $x_2(t)=0$ or in other words the value of t where the trajectory crosses the abcissa.

In equation A6.2.2 we set $x_2(t)=0$

$$\therefore\ \frac{Ku}{\alpha}-\frac{Ku}{\alpha}e^{-\alpha K_1 t}+x_2(0)e^{-\alpha K_1 t}=0$$

$$\therefore\ e^{-\alpha K_1 t}=\frac{-\frac{Ku}{\alpha}}{-\frac{Ku}{\alpha}+x_2(0)}$$

and solving for t

$$t=\frac{1}{\alpha K_1}\ \mathrm{Ln}\left(1-\frac{\alpha x_2(0)}{Ku}\right) \qquad \text{(A6.2.4)}$$

and substituting into equation A6.2.3 yields

$$x_1(t_{ab})=x_1(0)+\frac{K_2\ Ku}{K_1\ \alpha^2}\ \mathrm{Ln}\left(1-\frac{x_2(0)\alpha}{Ku}+x_2(0)\ \frac{K_2}{K_1\alpha}\right) \qquad \text{(A6.2.5)}$$

where $x_1(0)$, $x_2(0)$ are some arbitrary initial conditions, $\alpha=\frac{1}{T}$ is the lag and $K=\frac{1}{a}=1$ is the nominal plant gain parameter. K_1 and K_2 are the individual integrator gains, these can be considered to be scaling factors to determine the integration rates and are entirely arbitrary.

A table for a double integrator is presented for the

ratio $(\frac{K_2}{K_1} \frac{1}{2u})$ where $(\frac{K_2}{K_1}) = \frac{50}{9}$ for various times 't', and such that x_1=5 and x_2=3 after t seconds (u=5).

t (seconds)	K_1	K_2
.1	6	33.333
.2	3	16.666
1	.6	3.333
5	.12	.666
10	.06	.333
50	.012	.0666

These particular values of K_1 and K_2 were originally selected to provide a suitable scale for x_1 and x_2 for the X-Y plotting in section 2.3.1. However variations in K_1 and K_2 do directly affect system performance and although K_1= K_2= 1 is an obvious choice, it is instructive to observe variations in K_1 and K_2.

Hence if a fast model to plant time-ratio is to be, say 50:1, then for a plant of t=5 seconds, τ = .1 seconds for the fast model is chosen. Therefore

K_1(plant) = ,12 K_2(plant) = .666

K_1(fast model)=6 K_2(fast model)= 33.333

The next step in implementing this program is straightforward. Equations A6.2.2 and A6.2.3 both define the plant and model dynamics (for the model we set K_3=K_1

and $K_4 = K_2$). Equation A6.2.5 defines the fast model trajectory during the prediction mode when we wish to establish the future error $e(\tau)$.

The programme is looped so that equation A6.2.5 is iterated until $e(\tau) \leq e_p (0 \leq e_p < 1)$ when reverse drive is applied ($u(t) = -u(t)$) to equations A5.2.2 and A6.2.3.

By incrementing t in the programme either the phase-plane representation can be called (via the 'call-point' facility in the Basic language depicted on the VDU) or the time-response curves may be called. Hence $x_2(t)$ is plotted against $x_1(t)$ for increasing t in steps of Δt or $x_1(t)$ is plotted against t in steps of Δt ($\Delta t = .002$ units).

Similarly it is quite easy to vary values of K, α, K_1 and K_2. Below is a programme used to generate the curves for the position response to a step reference. Standard 'Basic' was used throughout.

PROGRAMME FOR A SECOND ORDER PLANT FOR
POSITION RESPONSE WITH POSITIVE STEP REFERENCE

```
LIST
4  REM "FAST MODEL PREDICTION 4 QUAD CONTROL"
6  READ A,B
8  READ K1,K2,K3,K4
10  READ R
12  READ X0,Y0
14  READ V,U
16  DATA  1, 1
18  DATA  .12, .6666, 6, 33.3333
20  DATA  5
22  DATA  0, 0
24  DATA  5,-5
50  DEFFN G(T)=K2*Y0*( 1-EXP(-A*K1*T))/(K1*A)
55  DEFFN H(T)=U*K2*( 1-EXP(-A*K1*T))/(K1*A*A)
60  DEFFN I(T)=K2*U*T/A
65  DEFFN J(T1)=K4*Z2*( 1-EXP(-B*K3*T1))/(K3*B)
70  DEFFN L(T1)=U*K4*( 1-EXP(-B*K3*T1))/(K3*B*B)
75  DEFFN N(T1)=K4*U*T1/B
80  DEFFN A(T)=X0+FNI(T)-FNH(T)+FNG(T)
85  DEFFN B(T)=(V/A)*( 1-EXP(-A*K1*T))+Y0*EXP(-A*K1*T)
90  DEFFN C(T1)=Z1+FNN(T1)-FNL(T1)+FNJ(T1)
95  DEFFN D(T1)=(U/B)*( 1-EXP(-B*K3*T1))+Z2*EXP(-B*K3*T1)
100  LET T= 0
105  LET P1= 0
110  LET A1=FNA(T)
120  LET B1=FNB(T)
121  LET Q0=P1/ 10- .8
122  LET Q1=A1/ 4- .8
123  CALL  POINT,Q0,Q1
130  LET T1= 0
132  LET Z1=A1
134  LET Z2=B1
140  LET C1=FNC(T1)
150  LET D1=FND(T1)
160  IF ABS(R-C1)<= .1 THEN 220
170  IF ABS(-D1)<= .1 THEN 200
180  LET T1=T1+ 2.00000E-03
190  IF T1<= .2 THEN 140
191  GOTO 1500
200  LET T=T+ .1
205  LET P1=P1+ .1
210  IF T<= 30 THEN 110
211  GOTO 1500
220  LET V=-V
230  LET X0=A1
240  LET Y0=B1
250  LET T= 0
255  LET P2=P1
260  LET A2=FNA(T)
270  LET B2=FNB(T)
271  LET Q0=P2/ 10- .8
272  LET Q1=A2/ 4- .8
273  CALL  POINT,Q0,Q1
300  IF (R-A2)<= .1 THEN 338
310  IF (-B2)> 0 THEN 360
320  LET T=T+ .1
325  LET P2=P2+ .1
330  IF T<= 10 THEN 260
331  GOTO 1500
338  IF (-B2)> 0 THEN 344
340  LET T=T+ .1
341  LET P2=P2+ .1
342  IF T<= 10 THEN 260
343  GOTO 1500
344  IF (R-A2)<=-.1 THEN 640
350  GOTO 1500
360  LET V=-V
370  LET X0=A2
380  LET Y0=B2
390  LET T= 0
395  LET P3=P2
400  LET A3=FNA(T)
410  LET B3=FNB(T)
411  LET Q0=P3/ 10- .8
412  LET Q1=A3/ 4- .8
413  CALL  POINT,Q0,Q1
420  LET T1= 0
425  LET U=-5
426  LET Z1=A3
427  LET Z2=B3
430  LET C2=FNC(T1)
440  LET D2=FND(T1)
450  IF ABS(R-C2)<= .1 THEN 510
460  IF ABS(-D2)<= .1 THEN 490
470  LET T1=T1+ 2.00000E-03
480  IF T1<= .2 THEN 430
481  GOTO 1500
490  LET T=T+ .1
495  LET P3=P3+ .1
500  IF T<= 10 THEN 400
501  GOTO 1500
510  LET V=-5
520  LET X0=A3
530  LET Y0=B3
540  LET T= 0
545  LET P4=P3
550  LET A4=FNA(T)
560  LET B4=FNB(T)
561  LET Q0=P4/ 10- .8
562  LET Q1=A4/ 4- .8
563  CALL  POINT,Q0,Q1
590  IF (R-A4)<= .1 THEN 1500
600  IF (-B4)>=-.1 THEN 1500
610  LET T=T+ .1
615  LET P4=P4+ .1
```

```
620  IF T<= 10 THEN 550
621  GOTO 1500
640  LET V=V
650  LET X0=A2
660  LET Y0=B2
670  LET T= 0
675  LET P5=P2
680  LET A5=FNA(T)
690  LET B5=FNB(T)
691  LET Q0=P5/ 10- .8
692  LET Q1=A5/ 4- .8
693  CALL  POINT,Q0,Q1
700  LET T1= 0
701  LET U= 5
702  LET Z1=A5
703  LET Z2=B5
704  LET C3=FNC(T1)
705  LET D3=FND(T1)
706  IF ABS(R-C3)<= .1 THEN 730
707  IF ABS(-D3)<= .1 THEN 711
708  LET T1=T1+ 2.00000E-03
709  IF T1<= .2 THEN 704
710  GOTO 1500
711  LET T=T+ .1
715  LET P5=P5+ .1
720  IF T<= 10 THEN 680
721  GOTO 1500
730  LET V=-V
740  LET X0=A5
750  LET Y0=B5
760  LET T= 0
765  LET P6=P5
770  LET A6=FNA(T)
780  LET B6=FNB(T)
781  LET Q0=P6/ 10- .8
782  LET Q1=A6/ 4- .8
783  CALL  POINT,Q0,Q1
790  IF (R-A6)>=-.1 THEN 820
800  IF (-B6)< 0 THEN 860
810  GOTO 890
820  IF (-B6)< 0 THEN 850
830  LET T=T+ .1
835  LET P6=P6+ .1
840  IF T<= 10 THEN 770
850  IF (R-A6)>= .1 THEN 910
860  GOTO 1500
890  LET T=T+ .1
895  LET P6=P6+ .1
900  IF T<= 10 THEN 770
901  GOTO 1500
910  LET V=V
920  LET X0=A6
930  LET Y0=B6
940  LET T= 0
945  LET P7=P6
950  LET A7=FNA(T)
960  LET B7=FNB(T)
961  LET Q0=P7/ 10- .8
962  LET Q1=A7/ 4- .8
963  CALL  POINT,Q0,Q1
970  LET T1= 0
980  LET U=-5
990  LET Z1=A7
1000  LET Z2=B7
1010  LET C4=FNC(T1)
1020  LET D4=FND(T1)
1030  IF ABS(R-C4)<= .1 THEN 1090
1040  IF ABS(-D4)<= .1 THEN 1070
1050  LET T1=T1+ 2.00000E-03
1060  IF T1<= .2 THEN 1010
1061  GOTO 1500
1070  LET T=T+ .1
1075  LET P7=P7+ .1
1080  IF T<= 10 THEN 950
1081  GOTO 1500
1090  LET V=-V
1100  LET X0=A7
1110  LET Y0=B7
1120  LET T= 0
1125  LET P8=P7
1130  LET A8=FNA(T)
1140  LET B8=FNB(T)
1150  LET Q0=P8/ 10- .8
1151  LET Q1=A8/ 4- .8
1152  CALL  POINT,Q0,Q1
1153  CALL  POINT,Q1,Q2
1160  IF (R-A8)<= .1 THEN 1500
1170  IF (-B8)> 0 THEN 1500
1180  LET T=T+ .1
1185  LET P8=P8+ .1
1190  IF T<= 10 THEN 1130
1500  END
```

A6.3 Hybrid Control of a Second-order Plant using a Fast Model Predictor

The equations derived in Appendix A6.2 for the second order lag were used in the programme to synthesize the fast model (the time-optimal switching curve) and the switching decisions were based on those indicated in the flow charts of figures 2.3.1(b) and 2.3.3. This section of the programme is virtually identical to that of the digital simulation programme in Appendix A6.2.

However some means of command between the two computers had to be established and the existance of a 'Basic' sub-routine enabled the control of the A to D and D to A conventers to be easily implemented. Furthermore some means of synchronizing the start of both computer runs had to be arranged. This was easily done by using a spare 'diode-limited' integrator which upon depressing the OPR (operate) switch of the TR-48 provided a sense signal to the Varian 600i. The rise time of the sense signal was of the order of ten milliseconds which was negligible compared to the plant time constant (of the order of tens of seconds).

The analogue computer was patched as indicated in Figure 2.3.5, the plant gain parameter K_p could either be externally varied by a separate potentiometer or

changed internally in the programme. Similarly α_p, K_1 and K_2 could be changed by the potentiometer settings. K_m (fast model gain parameter), α_m(fast model lag), K_3 and K_4 were varied by merely changing these values in the program.

It must be noted the voltage conversion ranges were according to

+ 10 volts $\equiv$ + 2047 units and

- 10 volts $\equiv$ - 2047 units

Hence 1 unit $\equiv$ 4,89 millivolts. The resolution available on the DVM of the analogue computer is $\pm$ 10 millivolts, hence there is no real degredation of measurement accuracy of the state variables and the digitally derived input u(t), by the digital loop. The data capture time of the A to D channels is roughly 25 μs per channel and this time is insignificant when compared to the plant time constants.

At the termination of a computer run, i.e. when the plant trajectory had reached the error phase-plane origin*, the input u(t) was set to take on zero volts and the digital computer reverted back to the 'wait' mode ready for the new operate command, and hence the new sense signal. However the analogue computer had

to be manually reset.

For each computer run a permanent recording was done on an X-Y plotter with the X-axis(time axis) driven either internally or from an external source. However there was great difficulty in establishing an accurately calibrated time scale on the recordings owing to an unfortunate sporadic malfunction on the plotter.

However the (relative) ratio of the setting times of the nominal plant to a plant with overshoot was easily determined from the recordings.

Below is a program for control of a plant with one integrator and one lag.

* The trajectory does not in fact reach the origin. The computer is programmed to stop when the error is less than or is equal to a small positive number e_p.

A6.4 Direct Digital Control of a Small DC Motor

The motor used was a small teaching purpose device as well as several interfacing devices used with the motor system. These devices enabled the signals derived from the computer to be compatible with the signals required to drive the motor. The interfaces consisted of an

```
LIST
 10  READ K3,K4
 15  READ B
 20  READ P1
 25  READ P2
 30  DATA  3.00000E-02, .1666
 35  DATA  .1
 40  DATA  5.00000E-02
 45  DATA  5.00000E-02
 50  LET A4= 4
 60  CALL   ADC1,A4,S4
 70  IF S4> 20 THEN 90
 80  GOTO 60
 90  LET A0= 0
100  CALL   ADC1,A0,R
110  LET R=R* 10/ 2047
120  LET A1= 1
130  CALL   ADC1,A1,X1
140  LET X1=X1* 10/ 2047
150  LET V1= 0
160  LET V= 1024*SGN(R-X1)
170  CALL   DTOA,V1,V
180  LET A2= 2
190  LET U=-5
200  GOSUB 2000
205  LET V=-V
210  CALL   DTOA,V1,V
220  CALL   ADC1,A2,Y1
230  LET Y1=Y1* 10/ 2047
240  IF Y1<= 0 THEN 260
250  GOTO 220
260  CALL   ADC1,A1,X1
270  LET X1=X1* 10/ 2047
280  IF (R-X1)>P1 THEN 310
290  IF (R-X1+P1)>= 0 THEN 3000
300  GOTO 900
310  LET V=-V
320  CALL   DTOA,V1,V
330  LET U=-5
340  GOSUB 2000
350  LET V=-V
360  CALL   DTOA,V1,V
370  GOSUB 2100
380  IF (R-X1)>P1 THEN 400
390  GOTO 3000
400  LET V=-V
410  CALL   DTOA,V1,V
420  LET U=-5
430  GOSUB 2000
440  LET V=-V
450  CALL   DTOA,V1,V
460  GOSUB 2100
470  IF (R-X1)>P1 THEN 490
480  GOTO 3000
490  LET V=-V
500  CALL   DTOA,V1,V
510  LET U=-5
520  GOSUB 2000
530  LET V=-V
540  CALL   DTOA,V1,V
550  GOSUB 2100
560  IF (R-X1)>P1 THEN 580
570  GOTO 3000
580  LET V=-V
590  CALL   DTOA,V1,V
600  LET U=-5
610  GOSUB 2000
620  LET V=-V
630  CALL   DTOA,V1,V
640  GOSUB 2100
650  IF (R-X1)>P1 THEN 670
660  GOTO 3000
670  LET V=-V
680  CALL   DTOA,V1,V
690  LET U=-5
700  GOSUB 2000
710  LET V=-V
720  CALL   DTOA,V1,V
730  GOSUB 2100
740  IF (R-X1)>P1 THEN 760
750  GOTO 3000
760  LET V=-V
770  CALL   DTOA,V1,V
780  LET U=-5
790  GOSUB 2000
800  LET V=-V
810  CALL   DTOA,V1,V
820  GOSUB 2100
830  GOTO 3000
900  LET U= 5
910  GOSUB 2000
920  LET V=-V
930  CALL   DTOA,V1,V
940  GOSUB 2200
950  IF (R-X1)>P1 THEN 970
960  GOTO 3000
970  LET U=-5
980  GOSUB 2000
990  LET V=-V
1000  CALL   DTOA,V1,V
1010  GOSUB 2300
1020  IF (R-X1+P1)< 0 THEN 1040
1030  GOTO 3000
1040  LET U= 5
1050  GOSUB 2000
```

```
1050  LET U=-U
1070  CALL   DTOA,U1,U
1080  GOSUB 2200
1090  IF (R-X1)>P1 THEN 1110
1100  GOTO 3000
1110  LET U=-5
1120  GOSUB 2000
1130  LET U=-U
1140  CALL   DTOA,U1,U
1150  GOSUB 2300
1160  IF (R-X1+P1)< 0 THEN 1180
1170  GOTO 3000
1180  LET U= 5
1190  GOSUB 2000
1200  LET U=-U
1210  CALL   DTOA,U1,U
1220  GOSUB 2200
1230  IF (R-X1)>P1 THEN 1250
1240  GOTO 3000
1250  LET U=-5
1260  GOSUB 2000
1270  LET U=-U
1280  CALL   DTOA,U1,U
1290  GOSUB 2300
1300  GOTO 3000
2000  CALL   ADC1,A2,Y1
2010  LET Y0=Y1* 10/ 2047
2020  CALL   ADC1,A1,X1
2030  LET X0=X1* 10/ 2047
2040  LET C=(K4*U*LOG( 1-Y0*B/U))/(K3*B*B)+X0+(Y0*K4)/(K3*B)
2050  IF ABS(R-C)<=P2 THEN 2070
2060  GOTO 2000
2070  RETURN
2100  CALL   ADC1,A2,Y1
2110  LET Y1=Y1* 10/ 2047
2120  IF Y1<= 0 THEN 2140
2130  GOTO 2100
2140  CALL   ADC1,A1,X1
2150  LET X1=X1* 10/ 2047
2160  RETURN
2200  CALL   ADC1,A2,Y1
2210  LET Y1=Y1* 10/ 2047
2220  IF Y1>= 0 THEN 2240
2230  GOTO 2200
2240  CALL   ADC1,A1,X1
2250  LET X1=X1* 10/ 2047
2260  RETURN
2300  CALL   ADC1,A2,Y1
2310  LET Y1=Y1* 10/ 2047
2320  IF Y1<= 0 THEN 2340
2330  GOTO 2300
2340  CALL   ADC1,A1,X1
2350  LET X1=X1* 10/ 2047
2360  RETURN
3000  LET U= 0
3010  CALL   DTOA,U1,U
3020  LET A3= 3
3030  CALL   ADC1,A3,T1
3040  LET T1=T1* 10/ 2047
3050  CALL   ADC1,A1,X1
3060  LET X1=X1* 10/ 2047
3070  PRINT "R","X1","E1=R-X1","T1"
3080  PRINT R,X1,(R-X1),T1
3090  END
```

electronic relay, potentiometers and amplifiers normally used for the motor control.

In this way there was no danger of damaging the sensitive A to D and D to A circuits through overloading, current or voltage spikes. As an added precaution, the signals to the electronic relay and from the motor potentiometer and tacho-generator were passed through the inverting amplifiers and potentiometers of the TR-48 analogue computer as well as retaining the use of the 'sync' integrator for synchronization purposes.

To enable the motor output(position) to be recorded within a reasonable length of time, the motor shaft rotation was reduced through two gearboxes with a total reduction ratio of 960 to 1. There was however large backlash in the gears of the second gearbox.

Several other devices were included in the setup(see Figure A6.4.1). A relay K_1 was used to open the circuit between the electronic relay and the power amplifier of the motor, this was necessary when resetting the computers to prevent motor runaway. The X-Y plotter X-axis(time-axis) was driven from an integrator on the analogue computer as was the 'sync' signal. Hence by means of the OPR(operate)switch all the processes were synchronized.

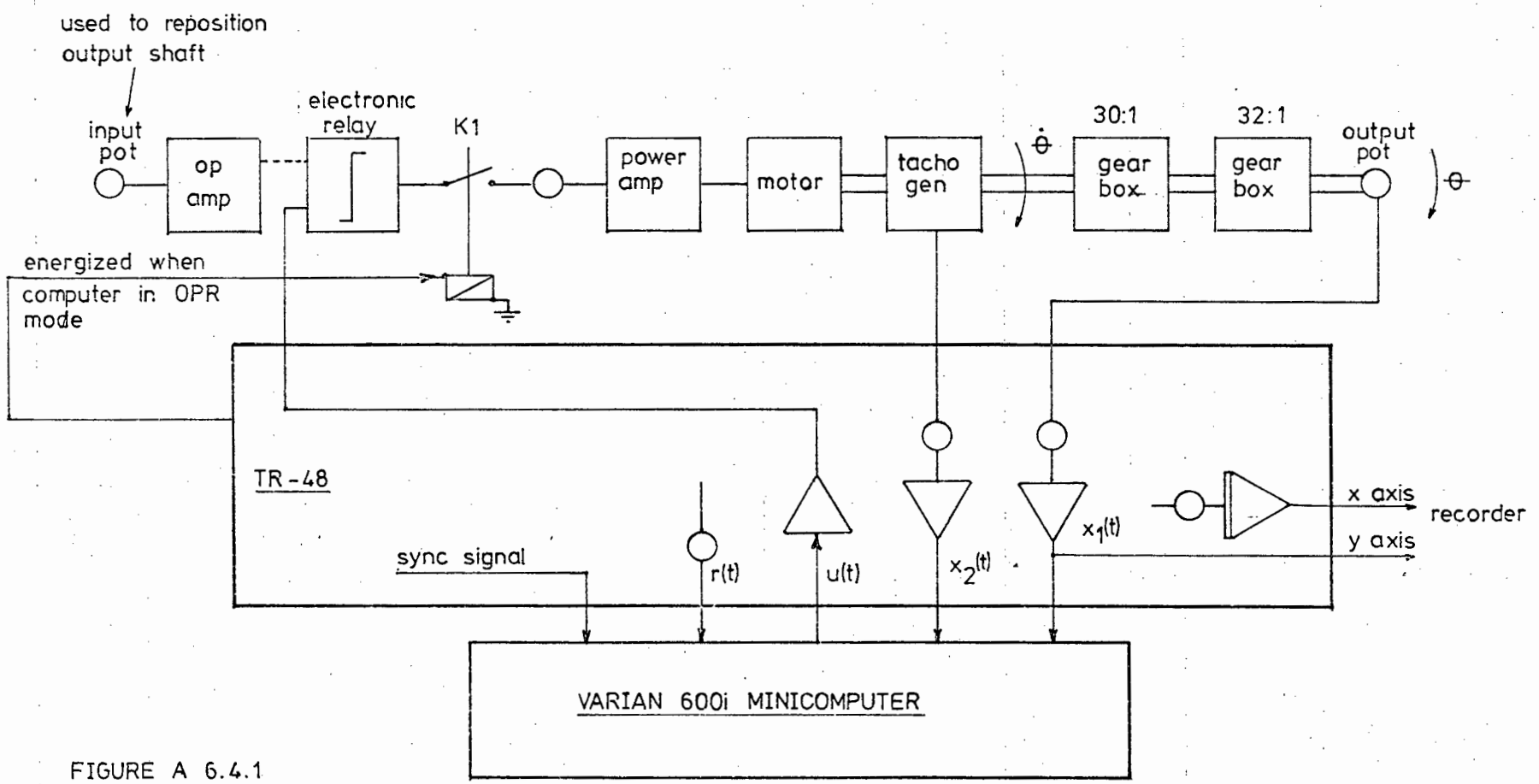

FIGURE A 6.4.1

FUNCTIONAL DIAGRAM OF DIRECT DIGITAL CONTROL
OF A DC MOTOR

A6.5 Derivation of the exact time-optimal expressions for a Second-order plant with two Lags

Consider Figure A6.5.1.

$$\dot{x}_1 = x_2 - \alpha_1 x_1 \qquad \text{(A6.5.1)}$$

$$\dot{x}_2 = Ku - \alpha_2 x_2 \qquad \text{(A6.5.2)}$$

The Laplace transformation of A6.5.2 yields

$$sx_2(s) - x_2(0) = U(s)K - \alpha_2 x_2(s)$$

$$\therefore \quad x_2(s) = \frac{Ku}{s(s+\alpha_2)} + \frac{x_2(0)}{(s+\alpha_2)} \quad \text{for } U(s) = \frac{u}{s} \qquad \text{(A6.5.3)}$$

$$x_2(t) = \mathcal{L}^{-1} x_2(s) = \frac{Ku}{\alpha_2} + e^{-\alpha_2 t}\left(x_2(0) - \frac{Ku}{\alpha_2}\right)$$

$$= x_2(0)e^{-\alpha_2 t} + \frac{Ku}{\alpha_2}(1-e^{-\alpha_2 t}) \qquad \text{(A6.5.4)}$$

The Laplace transformation of A6.5.1 yields

$$sx_1(s) - x_1(0) = x_2(s) - \alpha_1 x_1(s)$$

$$\therefore \quad x_1(s) = \frac{x_2(s)}{(s+\alpha_1)} + \frac{x_1(0)}{(s+\alpha_1)}$$

substituting for $x_2(s)$ from A6.5.3 yields

$$x_1(s) = \frac{Ku}{s(s+\alpha_1)(s+\alpha_2)} + \frac{x_2(0)}{(s+\alpha_1)(s+\alpha_2)} + \frac{x_1(0)}{(s+\alpha_1)} \qquad \text{(A6.5.5)}$$

$$\therefore \quad x_1(t) = \mathcal{L}^{-1} x_1(s)$$

$$= \frac{Ku}{\alpha_1\alpha_2}(1-e^{-\alpha_1 t}) + \left(\frac{x_2(0) - \frac{Ku}{\alpha_2}}{(\alpha_1 - \alpha_2)}\right)(e^{-\alpha_2 t} - e^{-\alpha_1 t}) \qquad \text{(A6.5.6)}$$

$$+ x_1(0)e^{-\alpha_1 t}$$

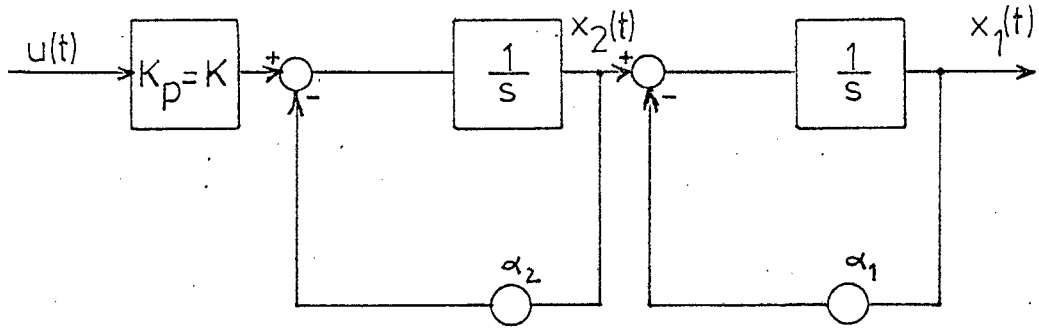

FIGURE A6.5.1 : SECOND-ORDER PLANT WITH TWO LAGS

$$\text{or } x_1(t)=\frac{Ku}{\alpha_1\alpha_2} + e^{-\alpha_1 t}\left(x_1(0)-\frac{Ku}{\alpha_1\alpha_2} - \frac{(\alpha_2 x_2(0)-Ku)}{\alpha_2(\alpha_1-\alpha_2)}\right)$$

$$+ e^{-\alpha_2 t}\left(\frac{\alpha_2 x_2(0)-Ku}{\alpha_2(\alpha_1-\alpha_2)}\right) \qquad \text{(A6.5.7)}$$

If we let $\alpha_1 = 0$, we have the one lag case as described in Appendix A6.2. This is easily observed by expanding the exponential in the first term of A6.5.6, cancelling the α_1's and setting $\alpha_1=0$ in the remaining terms.

The value of t when the trajectory crosses the abcissa, i.e. when velocity is zero is determined by $\dot{x}_1(t)=0$.

From A6.5.6

$$\frac{d}{dt}x_1(t) = \frac{Ku}{\alpha_1\alpha_2}1e^{-\alpha_1 t} + \frac{(x_2(0)-\frac{Ku}{\alpha_2})}{(\alpha_1-\alpha_2)}(-\alpha_2 e^{-\alpha_2 t}+\alpha_1 e^{-\alpha_1 t})$$

$$- x_1(0)\alpha_1 e^{-\alpha_1 t} = 0$$

$$\therefore e^{-\alpha_1 t}\left(\frac{Ku}{\alpha_2} - x_1(0)\alpha_1 + \frac{(x_2(0)-\frac{Ku}{\alpha_2})\alpha_1}{(\alpha_1-\alpha_2)} - e^{-\alpha_2 t}\right.$$

$$\left.\left(\frac{x_2(0)-\frac{Ku}{\alpha_2}}{\alpha_1-\alpha_2}\right)\alpha_2\right) = 0$$

$$\therefore \frac{e^{-\alpha_2 t}}{e^{-\alpha_1 t}} = \frac{\frac{Ku}{\alpha_2} - x_1(0)\alpha_1 + \frac{(x_2(0) - \frac{Ku}{\alpha_2})\alpha_1}{(\alpha_1 - \alpha_2)}}{\frac{(x_2(0) - \frac{Ku}{\alpha_2})\alpha_2}{(\alpha_1 - \alpha_2)}}$$

$$\therefore e^{t(\alpha_1 - \alpha_2)} = \frac{-x_1(0)\alpha_1(\alpha_1 - \alpha_2) + \alpha_1 x_2(0) - Ku}{\alpha_2 x_2(0) - Ku}$$

$$\therefore t = \frac{1}{(\alpha_1 - \alpha_2)} \text{ Ln } \left(\frac{\alpha_1 x_2(0) - Ku - x_1(0)\alpha_1(\alpha_1 - \alpha_2)}{\alpha_2 x_2(0) - Ku} \right) \quad \text{(A6.5.8)}$$

substituting equation A6.5.8 for t in equation A6.5.6 we obtain (t_{ab} = value of t where $\dot{x}_1 = 0$)

$$x_1(t_{ab}) = \frac{Ku}{\alpha_1 \alpha_2} \left(1 - e^{\frac{-\alpha_1}{\alpha_1 - \alpha_2} \cdot \text{Ln } W}\right) + \frac{(x_2(0) - \frac{Ku}{\alpha_2})}{(\alpha_1 - \alpha_2)}$$

$$\left(e^{\frac{-\alpha_2}{\alpha_1 - \alpha_2} \cdot \text{Ln } W} - e^{\frac{-\alpha_1}{\alpha_1 - \alpha_2} \text{ Ln } W}\right)$$

$$+ \; x_1(0)\, e^{\frac{-\alpha_1}{\alpha_1 - \alpha_2} \cdot \text{Ln } W}$$

$$\text{where } W = \frac{\alpha_1 x_2(0) - Ku - x_1(0)\alpha_1 (\alpha_1 - \alpha_2)}{\alpha_2 x_2(0) - Ku} \qquad \text{(A6.5.9)}$$

$x_1(t_{ab})$ can be slightly simplified to

$$x_1(t_{ab}) = \frac{Ku}{\alpha_1\alpha_2}\left(1 - W^{\frac{-\alpha_1}{\alpha_1-\alpha_2}}\right) + \left(\frac{x_2(0)-\frac{Ku}{\alpha_2}}{(\alpha_1-\alpha_2)}\right)\left(W^{\frac{-\alpha_2}{\alpha_1-\alpha_2}} - W^{\frac{-\alpha_1}{\alpha_1-\alpha_2}}\right) + x_1(0)\, W^{\frac{-\alpha_1}{\alpha_1-\alpha_2}} \qquad \text{(A6.5.10)}$$

Note in equation A6.5.10 $\alpha_1 \neq \alpha_2$. For $\alpha_1 = \alpha_2$ (two equal lags) the derivation of $x_1(t_{ab})$ has to be undertaken separately. Furthermore $x_2(0)\,\alpha_2 - Ku \neq 0$ in W or an indeterminate value will result, however if the logic conditions with respect to quadrants II and IV are adhered, $(x_2(0)\,\alpha_2 - Ku)$ will be different from zero provided α_2, $K > 0$.

For fast model prediction, the exact time-optimal trajectory are those values of $(x_1(0), x_2(0))$ such that $x_1(t_{ab}) \equiv 0$. Equation A6.5.10 is cumbersome and unwieldly as it contains several expressions in exponentials and logarithms. It also requires a great deal more processing time on the minicomputer than $x(t_{ab})$ in equation A6.2.5 for the single lag case.

APPENDIX A7

SUMMARY OF THE LIAPUNOV ADAPTIVE LAWS

A7.1 Adaptive Control of a plant described by a scalar differential equation.

Let the plant and model be described by the scalar differential equations.

$$\dot{x}_m = -a_m x_m + b_m u(t) \quad \text{model} \qquad (A7.1)$$

$$\dot{x}_p = -a_p(t) x_p + b_p(t) u(t) \quad \text{plant without controller} \qquad (A7.2)$$

In equations A7.1 and A7.2, a_m and b_m are known positive constants $a_p(t)$ and $b_p(t)$ represent the time varying parameters of the plant and $u(t)$ is the input to both plant and model (see Figure A7.1.1). To implement the adaptive control scheme, feedback and feedforward gains, $f(t)$ and $q(t)$ are introduced as follows:

$$\dot{x}_p = -(a_p(t) + b_p(t) f(t)) x_p + (b_p(t) q(t)) u \qquad (A7.3)$$

The aim of the adaptive procedure is to adjust $f(t)$ and $q(t)$ in such a manner that $(a_p(t)+b_p(t)f(t))$ and $(b_p(t)q(t))$ tend to a_m and b_m respectively.

Suppose $a_p(t)$ and $b_p(t)$ are constant but unknown.

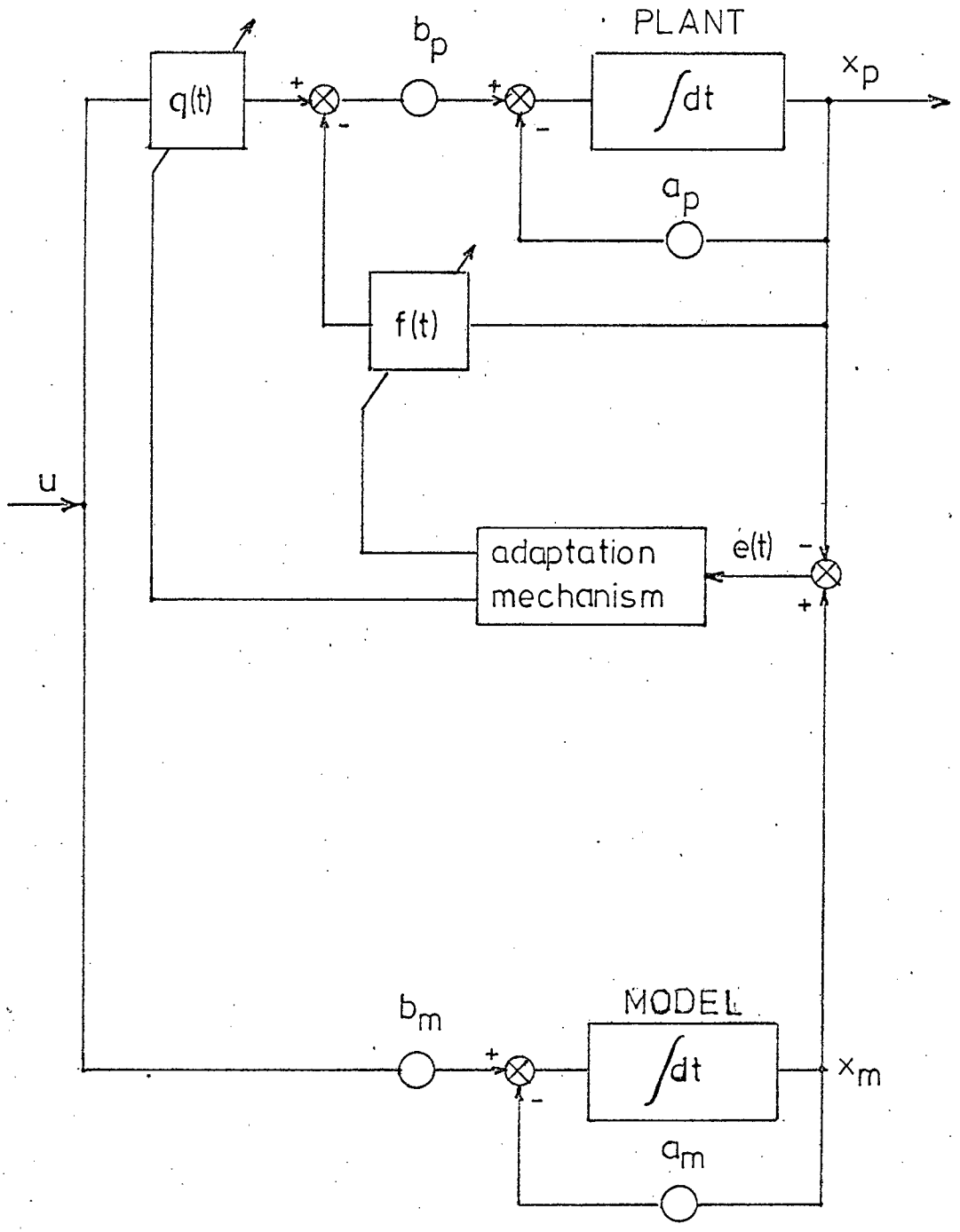

FIGURE A7.1.1 : ADAPTIVE CONTROL OF PLANT

The output error $e(t) \triangleq x_m(t) - x_p(t)$ satisfies the differential equation

$$\dot{e} = a_m e - (a_m - a_p - b_p f(t))x_p + (b_m - b_p q(t))u \qquad (A7.4)$$

The quantities $(a_m - a_p - b_p f(t))$ and $(b_m - b_p q(t))$ are errors in the parameters and are denoted by $\phi(t)$ and $\psi(t)$ respectively.

Hence

$$\dot{e} = a_m e - \phi x_p + \psi u \qquad (A7.5)$$

where $\phi(t) \triangleq (a_m - a_p - b_p f(t)) \qquad (A7.6)$

and $\psi(t) \triangleq (b_m - b_p q(t)) \qquad (A7.7)$

The objective is to adjust $f(t)$ and $q(t)$ so that as $t \rightarrow \infty$ $e(t) \rightarrow 0$, $\phi(t) \rightarrow 0$ and $\psi(t) \rightarrow 0$.

The differential equations for the dynamic controller are assumed to be of the form

$$\dot{f}(t) = g_1(x_m, x_p, u, f)$$

$$\dot{q}(t) = g_2(x_m, x_p, u, q) \qquad (A7.8)$$

or in terms of $\phi(t)$ and $\psi(t)$

$$\dot{\phi}(t) = k_1(x_m, x_p, u, f)$$

$$\dot{\psi}(t) = k_2(x_m, x_p, u, q) \qquad (A7.9)$$

The functions $k_1(\cdot)$ and $k_2(\cdot)$ or equivalently $g_1(\cdot)$ and $g_2(\cdot)$ specify the adaptive laws.

Equation A7.5 for the output error together with A7.9 for the parameter errors completely determine the error model of the system.

Let E denote the error space where the error vector $\underline{e} \in E$ is defined by

$$\underline{e}^T \triangleq (e, \phi, \psi)$$

The stability of the overall system must, then, be considered in E. The functions $k_1(\cdot)$ and $k_2(\cdot)$ are to be chosen such that the equilibrium state($e \equiv o$) of the overall system is asymptotically stable.

We consider as a candidate for the Liapunov function the quadratic form[4]:

$$V(\underline{e}) = \tfrac{1}{2}(b_p \operatorname{sgn}(b_p) e^2 + \frac{1}{\lambda_1}\phi^2 + \frac{1}{\lambda_2}\psi^2) \quad \lambda_1, \lambda_2 > 0 \quad \text{(A7.10)}$$

which is a positive definite function in E.

Differentiating V with respect to time and using A7.5 yields

$$\dot{V} = -b_p \text{sgn}(b_p) a_m e^2 + \phi \left(\frac{1}{\lambda_1} \dot{\phi} - b_p \text{sgn}(b_p) e x_p \right) + \left(\frac{1}{\lambda_2} \dot{\varphi} + b_p \text{ sgn}(b_p) e u \right) \qquad \text{(A7.11)}$$

Since the parameter errors $\phi(t)$ and $\varphi(t)$ are unknown and cannot be measured, the only manner in which $\dot{V}$ can be made negative semidefinite is to choose

$$\dot{\phi} = \lambda_1 (b_p \text{ sgn}(b_p)) \, e x_p$$

$$\dot{\varphi} = -\lambda_2 (b_p \text{ sgn}(b_p) e u \qquad \text{(A7.12)}$$

Since the control parameters are $f(t)$ and $q(t)$, for practical implementation, A7.12 has to be expressed in terms of $\dot{f}(t)$ and $\dot{q}(t)$. Since $\phi(t) = (a_m - a_p - b_p f(t))$ therefore $\dot{\phi}(t) = -b_p \dot{f}(t)$ and similarly for $\varphi(t)$, hence

$$\dot{f}(t) = -\lambda_1 \text{sgn}(b_p) e(t) x_p(t)$$

$$\dot{q}(t) = \lambda_2 \text{sgn}(b_p) e(t) u(t) \qquad \text{(A7.13)}$$

Equations A7.13 are the <u>adaptive updating laws</u>. The sign of b_p is assumed to be known to the designer for the implementation of these control laws; a not unrestrictive assumption.

The trajectories along which $\dot{V} \equiv 0$ or $e(t) \equiv 0$ along with equation A6.5 implies that

$$-\phi x_p + \varphi u \equiv 0 \qquad \text{(A7.14)}$$

One sufficient condition for this equation to have the trivial solutions $\phi=0$ and $\varphi = 0$ is that u be a signal with at least one frequency component (u= step function therefore presents no problem) and with this condition satisfied, the overall system is uniformly asymptotically stable.

A7.2 The Identification Scheme

Let the plant be described by the differential equation

$$\dot{x}_p = A_p x_p + B_p u \qquad \text{(A7.2.1)}$$

and the model used to track the plant parameters by

$$\dot{x}_m = C x_m + (A_m(t) - C)x_p + B_m(t) u \qquad \text{(A7.2.2)}$$

where C is a stable matrix and $A_m(t)$ and $B_m(t)$ are matrices with adjustable elements. The objective is to devise a scheme that dynamically adjusts these elements so that

$$\lim_{t \to \infty} A_m(t) = A_p$$

$$\lim_{t \to \infty} B_m(t) = B_p$$

$$\lim_{t \to \infty} (x_m(t) - x_p(t)) = \lim_{t \to \infty} e(t) = 0$$

The state error vector $e(t) \triangleq x_m - x_p$ satisfies the differential equation

$$\dot{e}(t) = Ce + \phi x_p + \varphi u \qquad \text{(A7.2.3)}$$

where the parameter error matrices are defined as

$$\phi \triangleq (A_m - A_p) \text{ and } \quad \psi \triangleq (B_m - B_p) \qquad \text{(A7.2.4)}$$

Stability is assured with the adaptive laws

$$\dot{\phi} = - \Gamma_1 P e x_p^T$$

$$\dot{\psi} = - \Gamma_2 P e u^T \qquad \text{(A7.2.5)}$$

where i) P,Q are positive definite symmetric matrices satisfying

$$C^T P + P C = - Q, \; Q = Q^T > 0 \qquad \text{(A7.2.6)}$$

and ii)

$$\Gamma_1 = \Gamma_1^T > 0, \; \Gamma_2 = \Gamma_2^T > 0 \qquad \text{(A7.2.7)}$$

For practical implementation, therefore, the identification laws are

$$\dot{A}_m(t) = - \Gamma_1 P e x_p^T \qquad \text{(A7.2.8)}$$

$$\dot{B}_m(t) = - \Gamma_2 P e u^T \qquad \text{(A7.2.9)}$$

Figure A7.1.1 is a description of the identification scheme provided the model and plant are interchanged.

The actual adjustment law used in this thesis was the law developed by Hang and Parks[30] and is identical to that of equation A7.2.9, except for an adaptive loop damping factor γ, which is zero in A7.2.9. It was found experimentally however that γ could take on the values $0 \leq \gamma < 1$ for satisfactory system performance.

As stated in section 3.2.3 only the model gain is considered and the adjustment applies only for the input matrix (see Figures A7.2.1 and A7.2.2 and note that Γ_2 is a scalar and gain factor in the adaptive loop.

The adjustement law is:

$$\dot{B}_m = \Gamma_2 e^T P b u + \gamma \frac{d}{dt}(\Gamma_2 e^T P b u) \qquad \text{(A7.2.10)}$$

Integrating both sides with respect to time yields

$$B_m = \int_{to}^{t} \Gamma_2 e^T P b u \, dt + \gamma \Gamma_2 e^T P b u \qquad \text{(A7.2.11)}$$

By using the nomenclature of Figure A7.2.1 equation A7.2.11 may be written as

$$K_v = \gamma \Gamma_2 e^T P b u + \int_{to}^{t} \Gamma_2 e^T P b u \, dt \qquad \text{(A7.2.12)}$$

Equation A7.2.12 is easily instrumented as in Figure 7.2.2.

As an example consider a second order plant and model with polynomical $g(s)= 1+s+s^2$, $K_p=1$ and $K_m= .4$. Hence we desire $K_v = .6$ such that $K_m+K_v=K_p$ and $C = A_m = A$ in equation A7.2.7.

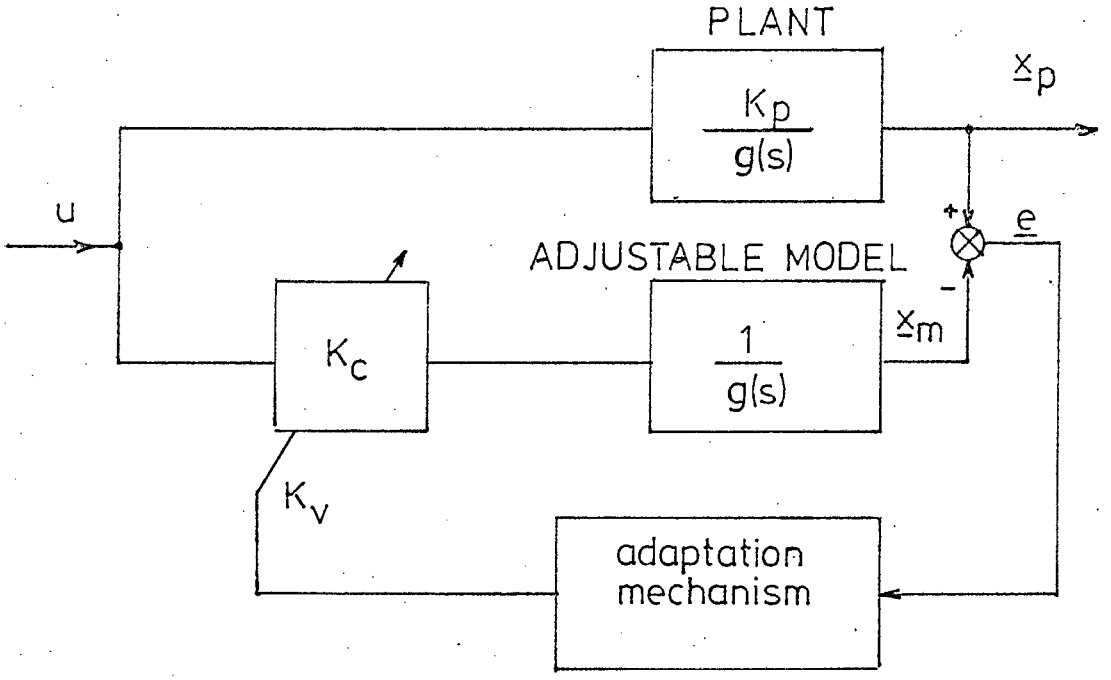

FIGURE A7.2.1 : PARAMETER IDENTIFICATION VIA AN ADJUSTABLE MODEL

K_p = ACTUAL PLANT PARAMETER

K_m = NOMINAL PLANT PARAMETER(INITIAL PARAMETER OF MODEL)

K_v = ADDITIONAL PARAMETER DETERMINED BY THE ADAPTIVE LOOP

K_c = (K_m+K) WHERE $K=f(K_v)$

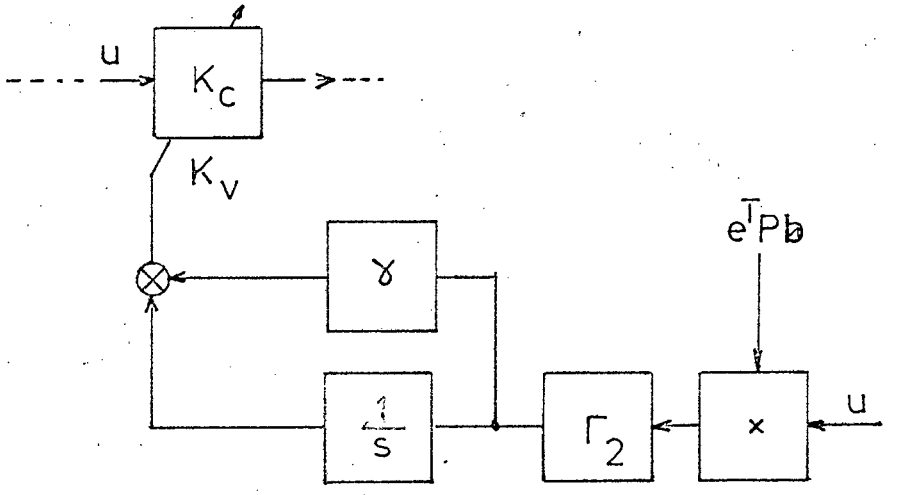

FIGURE A7.2.2 : ADAPTIVE LOOP $K_c = K_v + K_m$

We have from equation A7.2.7

$$A^T P + PA = -Q \qquad \text{(A7.2.13)}$$

$$P = \begin{bmatrix} p_{11} & p_{12} \\ p_{12} & p_{22} \end{bmatrix}, \quad A = \begin{bmatrix} 0 & 1 \\ -1 & -2 \end{bmatrix}, \quad b = \begin{bmatrix} 0 \\ 1 \end{bmatrix}$$

where $A = A_p$ and $b = B_p$ of equation A7.2.1. Generally we choose $Q = \begin{bmatrix} 2 & 0 \\ 0 & 2 \end{bmatrix}$

$$\text{Hence } A^T P = \begin{bmatrix} -p_{12} & -p_{22} \\ p_{11}-2p_{12} & p_{12}-2p_{22} \end{bmatrix}$$

$$\text{and } PA = \begin{bmatrix} -p_{12} & p_{11}-2p_{12} \\ -p_{22} & p_{12}-2p_{22} \end{bmatrix}$$

Therefore equating elements in A7.2.12 yields

$$P = \begin{bmatrix} 3 & 1 \\ 1 & 1 \end{bmatrix}$$

$$\text{Therefore } \underline{e}^T Pb = (e_1 \; e_2) \begin{bmatrix} 3 & 1 \\ 1 & 1 \end{bmatrix} \begin{bmatrix} 0 \\ 1 \end{bmatrix}$$

$$= e_1 + e_2 = e_1 + \dot{e}_1 \qquad \text{(A7.2.14)}$$

APPENDIX A8

ADAPTIVE HYBRID SIMULATON

A8.1 Hybrid Simulation. I

The trapezoidal rule is given by:

$$\int_{x_o}^{x_n} y(x)dx \simeq \frac{1}{2} h(y_o+2y_1+ \ldots + 2y_{n-1}+y_n) \quad (A8.1)$$

where h is the incremental interval and the y_i are the variables obtained after some manipulation from the plant and real-time model. n is the number of samples (or iterations) required for the integral to converge. x_o and x_n are limits which in this case is the plant run-time.

The truncation error is given as

$$t\ e \simeq -\frac{nh^3}{12}\ y^{(2)}(\epsilon) \quad (A8.2)$$

where $x_o < \epsilon < x_n$ and $y^{(2)}(\epsilon)$ is the second derivative of $y(x)$.

In the following program; G= γ , B = Γ_2 and H = h.
The integrand $y(x) = \Gamma_2\ r(e+\dot{e})$.

LIAPUNOV PARAMETER IDENTIFICATION PROGRAMME

```
LIST
1   REM "ADAPTIVE LOOP R=REF B=ADAP GAIN G=DAMP CONST"
2   REM "S5=SYNC SIGNAL H=INCR VAR"
3   REM "X1=X1M X2=X2M Y1=X1P Y2=X2P"
4   REM "N=NO OF ITERATIONS"
5   LET N= 10000
10   LET B= 5
15   LET G= .5
20   LET H= 5.00000E-02
25   LET D= 0
30   LET A0= 0
35   LET A1= 1
40   LET A2= 2
45   LET A3= 3
50   LET A4= 4
55   LET A5= 5
60   CALL    ADC1,A5,S5
65   IF S5> 20 THEN 75
70   GOTO 60
75   GOSUB 500
80   LET F4=H*F3/ 2
85   GOSUB 600
90   LET K0= 204.7*F7
95   CALL    DTOA,D,K0
100   FOR I= 1 TO N
105   GOSUB 500
110   LET F4=F4+H*F3
115   GOSUB 600
120   LET K0= 204.7*F7
125   CALL    DTOA,D,K0
130   NEXT I
135   PRINT F4,K0
500   CALL    ADC1,A0,R
505   LET R=R* 10/ 2047
510   CALL    ADC1,A1,X1
515   LET X1=X1* 10/ 2047
520   CALL    ADC1,A2,X2
525   LET X2=X2* 10/ 2047
530   CALL    ADC1,A3,Y1
535   LET Y1=Y1* 10/ 2047
540   CALL    ADC1,A4,Y2
545   LET Y2=Y2* 10/ 2047
550   LET E1=X1-Y1
555   LET E2=X2-Y2
560   LET F1=E1+E2
565   LET F2=R*F1
570   LET F3=B*F2
575   RETURN
600   LET F5=F3*G
605   LET F6=F5+F4
610   LET F7=R*F6
615   RETURN
650   END
```

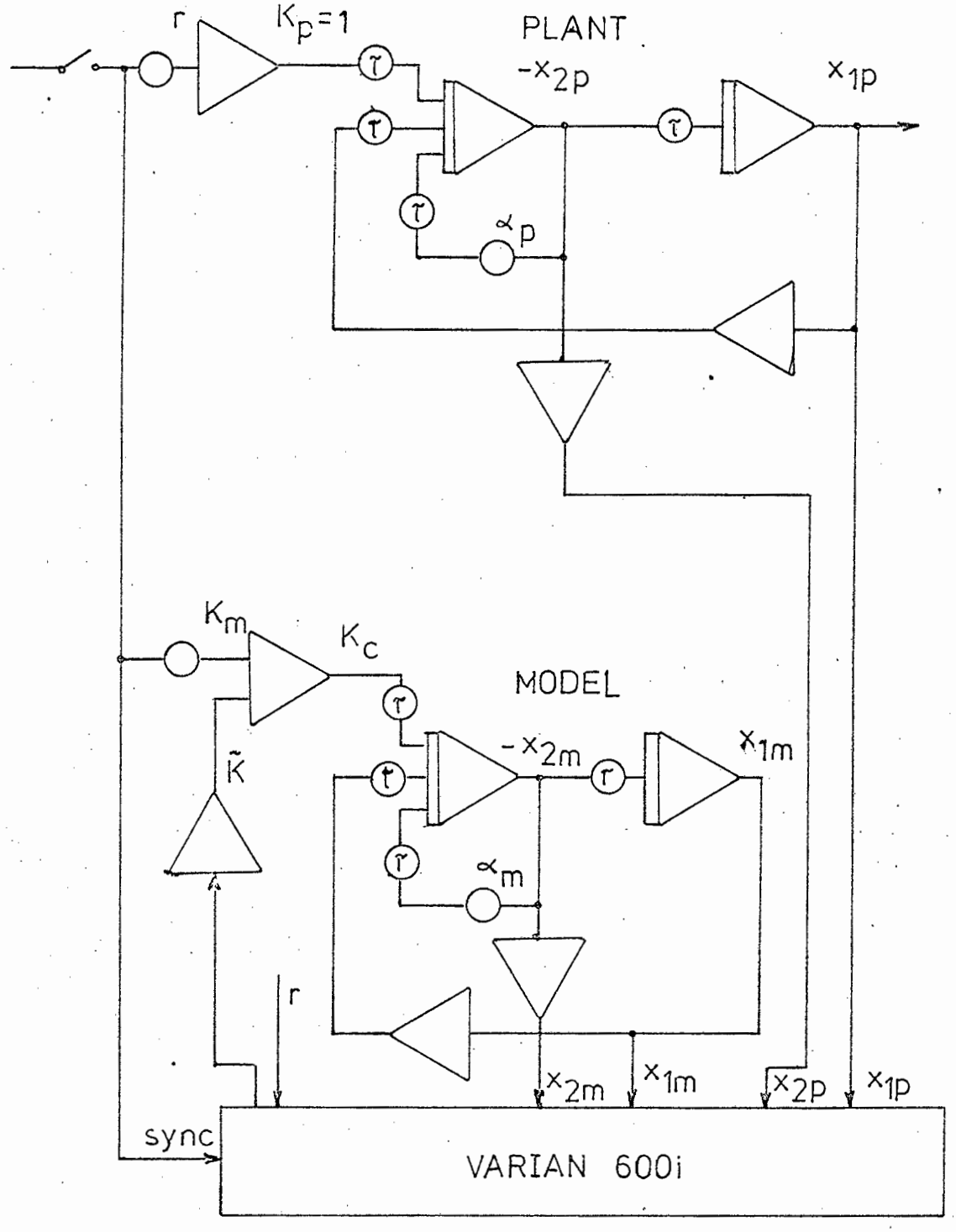

FIGURE A8.1.1 : HYBRID CONTROL FOR LIAPUNOV IDENTIFICATION SCHEME

τ = INTEGRATION-TIME SCALE FACTOR

α_p, α_m = PLANT AND MODEL DAMPING FACTOR

A8.2 Hybrid Simulation II

The program for the fast model predictor controller was modified to include the parameter identification algorithm. This was achieved by simply inserting the algorithm directly after the command for the correct plant (and real-time model) drive had been established. The prediction section commenced only after sufficient time had been allowed for the real-time model parameter to approach the plant parameter. Since the fast model trajectory equation is a function of its gain, this had to be updated once the real-time model gain parameter approached the plant gain parameter, and only after this updating, could the prediction phase commence.

After the point at which the state trajectory was switched to be driven to the origin, the parameter identification algorithm was recommenced to update the real-time model and fast model parameters (the input $u(t)$ had reversed in sign). At a point close to the origin, the plant vectors were sampled to determine their proximity to zero in order to apply the correct control strategy. Hence the sequence of operations may be listed as follows:

1. The correct drive polarity for the plant (and real-time model).

2. The implementation of the parameter identification scheme and the updating of the fast model gain parameter.
3. The prediction of the switch-point in the plant trajectory.
4. The recommencement of the scheme in 2.
5. The sampling of the state vectors in order to apply the correct strategy when close to the origin.

Below is a programme to achieve this method and Figure A8.2.1 illustrates the hybrid system.

ADAPTIVE PREDICTIVE CONTROL PROGRAMME

```
LIST
12  REM0 8
14  REM0 P1,P2
18  DATA   1
20  DATA  5.000000E-02, 5.000000E-02
22  LET L0= 1.4
24  LET H= 1.000000E-02
26  LET N= 100
28  LET G= 1
30  LET G1=  5
32  LET D1= 1
34  LET V1= 0
36  LET A0= 0
38  LET A1= 1
40  LET A2= 2
42  LET A3= 3
44  LET A4= 4
46  LET A5= 5
60  CALL    ADC1,A5,S5
70  IF S5> 20 THEN 100
80  GOTO 60
100  CALL    ADC1,A0,R
110  LET R=R* 10/ 2047
130  CALL    ADC1,A1,X1
140  LET X1=X1* 10/ 2047
160  LET U= 1024*SGN(R-X1)
170  CALL    DTOA,V1,V
180  GOSUB 4000
190  LET U=-5
200  GOSUB 2000
205  LET V=-V
210  CALL    DTOA,V1,V
212  LET L0=-1.4
215  GOSUB 4000
220  CALL    ADC1,A2,X2
230  LET X2=X2* 10/ 2047
240  IF X2<= 0 THEN 260
250  GOTO 220
260  CALL    ADC1,A1,X1
270  LET X1=X1* 10/ 2047
280  IF (R-X1)<P1 THEN 310
290  IF (R-X1+P1)>= 0 THEN 3000
300  GOTO 900
310  LET V=-V
320  CALL    DTOA,V1,V
330  LET U=-5
340  GOSUB 2000
350  LET V=-V
360  CALL    DTOA,V1,V
370  GOSUB 2100
380  IF (R-X1)>P1 THEN 400
390  GOTO 3000
400  LET V=-V
410  CALL    DTOA,V1,V
420  LET U=-5
430  GOSUB 2000
440  LET V=-V
450  CALL    DTOA,V1,V
460  GOSUB 2100
470  IF (R-X1)>P1 THEN 490
480  GOTO 3000
490  LET V=-V
500  CALL    DTOA,V1,V
510  LET U=-5
520  GOSUB 2000
530  LET V=-V
540  CALL    DTOA,V1,V
550  GOSUB 2100
560  IF (R-X1)>P1 THEN 580
570  GOTO 3000
580  LET U=-V
590  CALL    DTOA,V1,V
600  LET U=-5
610  GOSUB 2000
620  LET U=-V
630  CALL    DTOA,V1,V
640  GOSUB 2100
650  IF (R-X1)>P1 THEN 670
660  GOTO 3000
670  LET U=-V
680  CALL    DTOA,V1,V
690  LET U=-5
700  GOSUB 2000
710  LET U=-V
720  CALL    DTOA,V1,V
730  GOSUB 2100
740  IF (R-X1)>P1 THEN 760
750  GOTO 3000
760  LET U=-V
770  CALL    DTOA,V1,V
780  LET U=-5
790  GOSUB 2000
800  LET U=-V
810  CALL    DTOA,V1,V
820  GOSUB 2100
830  GOTO 3000
900  LET U= 5
910  GOSUB 2000
920  LET V=-V
930  CALL    DTOA,V1,V
940  GOSUB 2200
950  IF (R-X1)>P1 THEN 970
960  GOTO 3000
970  LET U=-5
980  GOSUB 2000
990  LET V=-V
1000  CALL    DTOA,V1,V
1010  GOSUB 2300
1020  IF (R-X1+P1)< 0 THEN 1040
1030  GOTO 3000
1040  LET U= 5
1050  GOSUB 2000
1060  LET V=-V
1070  CALL    DTOA,V1,V
1080  GOSUB 2200
1090  IF (R-X1)>P1 THEN 1110
1100  GOTO 3000
1110  LET U=-5
1120  GOSUB 2000
1130  LET V=-V
1140  CALL    DTOA,V1,V
1150  GOSUB 2300
1160  IF (R-X1+P1)< 0 THEN 1180
1170  GOTO 3000
1180  LET U= 5
1190  GOSUB 2000
1200  LET V=-V
1210  CALL    DTOA,V1,V
1220  GOSUB 2200
1230  IF (R-X1)>P1 THEN 1250
1240  GOTO 3000
1250  LET U=-5
1260  GOSUB 2000
1270  LET V=-V
1280  CALL    DTOA,V1,V
1290  GOSUB 2300
1300  GOTO 3000
2000  CALL    ADC1,A2,X2
2010  LET W2=X2* 10/ 2047
2020  CALL    ADC1,A1,X1
```

```
2030  LET W1=X1* 10/ 2047
2035  LET W3=A6* L0+L2)
2040  LET F=W3*U*LOG( 1-(W2*B/(U*W3)))/(B*B)+W1+W2/B
2045  IF ABS(R-F)<=P2 THEN 2070
2060  GOTO 2000
2070  RETURN
2100  CALL   ADC1,A2,Y1
2110  LET Y1=Y1* 10/ 2047
2120  IF Y1<= 0 THEN 2140
2130  GOTO 2100
2140  CALL   ADC1,A1,X1
2150  LET X1=X1* 10/ 2047
2160  RETURN
2200  CALL   ADC1,A2,Y1
2210  LET Y1=Y1* 10/ 2047
2220  IF Y1>= 0 THEN 2240
2230  GOTO 2200
2240  CALL   ADC1,A1,X1
2250  LET X1=X1* 10/ 2047
2260  RETURN
2300  CALL   ADC1,A2,Y1
2310  LET Y1=Y1* 10/ 2047
2320  IF Y1<= 0 THEN 2340
2330  GOTO 2300
2340  CALL   ADC1,A1,X1
2350  LET X1=X1* 10/ 2047
2360  RETURN
3000  LET U= 0
3010  CALL   DTOA,U1,U
3020  LET K0= 0
3030  CALL   DTOA,D1,K0
3040  GOTO 5000
4000  GOSUB 4140
4005  LET F4=H*F3/ 2
4010  GOSUB 4230
4020  LET L1=F7
4022  LET L2= .2*L1
4025  LET K0= 204.7*L1
4030  CALL   DTOA,D1,K0
4035  FOR I= 1 TO N
4040  GOSUB 4140
4045  LET F4=F4+H*F3
4050  GOSUB 4230
4055  LET L1=F7
4057  LET L2= .2*L1
4060  LET K0= 204.7*L1
4065  CALL   DTOA,D1,K0
4070  NEXT I
4075  RETURN
4140  CALL   ADC1,A1,X1
4155  LET X1=X1* 10/ 2047
4160  CALL   ADC1,A2,X2
4165  LET X2=X2* 10/ 2047
4170  CALL   ADC1,A3,Z1
4175  LET Z1=Z1* 10/ 2047
4180  CALL   ADC1,A4,Z2
4185  LET Z2=Z2* 10/ 2047
4190  LET E1=X1-Z1
4195  LET E2=X2-Z2
4200  LET F1=E1+E2
4205  LET F2= 5*F1*SGN(U)
4210  LET F3=G*F2
4215  RETURN
4230  LET F5=F3*G1
4235  LET F6=F5+F4
4240  LET F7= 5*F6*SGN(U)
4245  RETURN
5000  CALL   ADC1,A1,X1
5010  LET X1=X1* 10/ 2047
5020  PRINT "R","X1","EP=R-X1","L0+L2"
5030  PRINT R,X1,(R-X1),(L0+L2)
5040  END
```

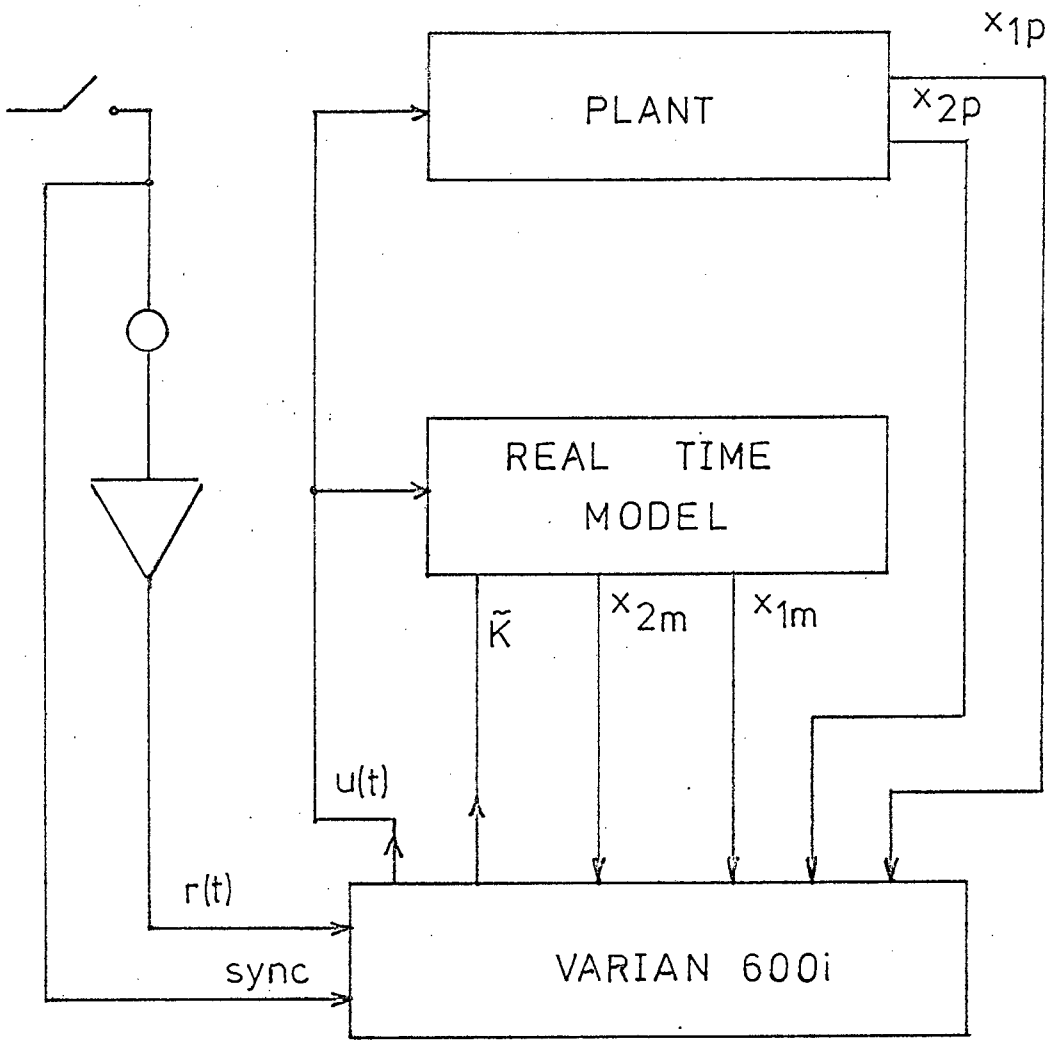

FIGURE A8.2.1 : DIAGRAM OF LIAPUNOV PARAMETER IDENTIFICATION METHOD FOR ADAPTIVE FAST MODEL PREDICTOR CONTROL

APPENDIX A9

THE MOTION OF A RELAY CONTROLLED SYSTEM

The system in Figure A9.1 may be described by an autonomous (no reference or reference is zero but with a set of initial conditions) vector differential equation of the form:

$\dot{\underline{x}} = F(\underline{x}) + B(\underline{x})\ \mathrm{sgn}(\phi\ (\underline{x})\ )$ but is modified to

$$\dot{\underline{x}} = A\underline{x} + B\ \mathrm{sgn}(\underline{d}^T\underline{x}) \qquad \text{(A9.1)}$$

where A = nxn matrix of constant coefficients

$\underline{d}$ = normal to the switching hyperplane

$\underline{x}$ = n dimensional state vector

B = nx1 matrix of constant coefficients

$\phi(\underline{x})$= continuous scalar function of $\underline{x}$

or $\phi(\underline{x})$ = switching function and $\phi(\underline{x})$ = 0 defining the switching surface.

$\underline{x}$ is represented in phase coordinates, i.e.

$x_{i+1} = \dot{x}_i \quad i= 1,2,3,\ldots, n-1$

Hence the DE takes on the canonical form

$$\text{sat}(\phi) = \begin{cases} +1 & \phi > {}^{1}/_{k} \\ k\phi & |\phi| \leq \frac{1}{k} \\ -1 & \phi < \frac{1}{k} \end{cases} \qquad \text{as } k \longrightarrow \infty$$

Solutions to A9.2 are usually well behaved everywhere except in the neighbourhood of $\phi = 0$ where their behaviour may be investigated by deriving the equations of motion in terms of ϕ.

We form the total time derivative of ϕ in terms of the switching surface gradient:-

$$\nabla\phi = \left(\frac{\partial\phi}{\partial x_1}, \frac{\partial\phi}{\partial x_2}, \ldots\ldots, \frac{\partial\phi}{\partial x_n}\right) \text{to obtain}$$

$$\dot{\phi} = \nabla\phi\,\dot{\underline{x}} = \nabla\phi\, A\underline{x} + \nabla\phi b\ \text{sgn}\ (\phi(\underline{x})) \qquad \text{(A9.3)}$$

For values of $\underline{x}$ satisfying the inequality

$$|\nabla\phi\, A\underline{x}| > |\nabla\phi b| \qquad |\text{sgn}\ \phi(\underline{x})|_{\max} = 1$$

$\dot{\phi}$ has the same sign on both sides of of the switching surface. Thus any value of ϕ in sgn ϕ of switching carries the state point across the surface. This is illustrated in Figure A9.2.

In order to ensure the uniqueness of $\dot{\underline{x}}$ for this motion, which we call regular switching, we arbitrarily define σ at $\phi = 0$ for $|\nabla\phi A\underline{x}| > |\nabla\phi b|$ to be + 1.

For those values of $\underline{x}$ which satisfy the relations

$$|\nabla\phi A\underline{x}| < |\nabla\phi b| \text{ or } |d^T A\underline{x}| < |d^T b|$$

and $\nabla\phi b < 0$ or $d^T b < 0$, yields $\dot{\phi}$ from equation A9.3 opposite in sign to ϕ and independent of its magnitude and this is constrained to be zero if $\phi = 0$, so that the motion is forced to continue on the switching surface once this surface is reached for as long as the equations

$$|\nabla\phi A\underline{x}| < |\nabla\phi b| \text{ and } \nabla\phi b < 0 \text{ hold.}$$

The orientation of the fan of tangent directions on the switching surface shows that only one of these tangent directions is allowable corresponding to a unique value of ϕ. This constrained motion is known as <u>chatter</u> or what is now termed <u>sliding motion</u>. This is illustrated in Figure A9.3.

The output of the relay, u, for a sliding trajectory may be determined by setting sgn ϕ = u and $\dot{\phi} = 0$ in equation A9.3 and solving for u this yields:

$$u = - \frac{\nabla\phi\, A\underline{x}}{\nabla\phi\, b} \qquad \text{(A9.4)}$$

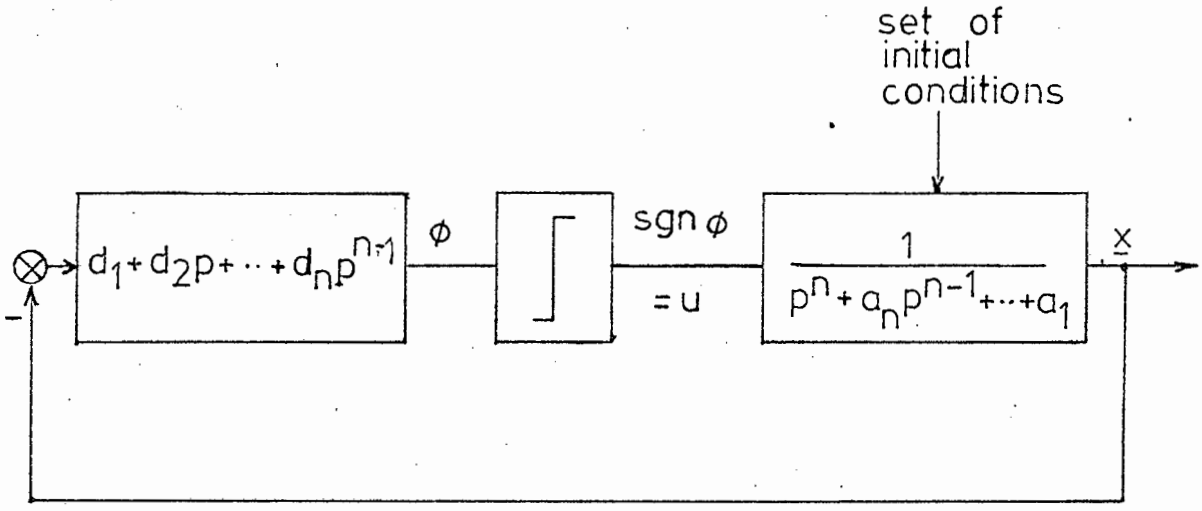

FIGURE A9.1 : BLOCK DIAGRAM OF RELAY-CONTROL SYSTEM WITH LINEAR PLANT AND SWITCHING

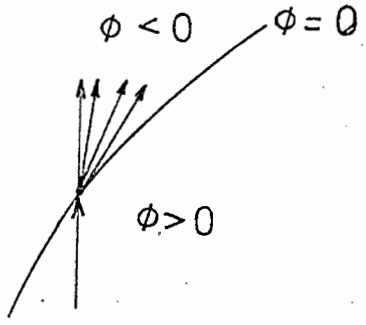

FIGURE A9.2 : TRAJECTORY DIRECTIONS AT ϕ=0 FOR REGULAR SWITCHING

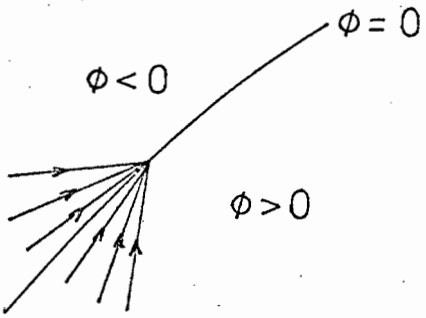

FIGURE A9.3 : TRAJECTORY DIRECTIONS AT ϕ=0 FOR SLIDING MOTION

The equation of motion for sliding may be expressed in first order form by substituting the expression for u from equation A9.4 in equation A9.3. Hence:

$$\dot{\underline{x}} = A\underline{x} - \frac{b \ \nabla\phi A\underline{x}}{\nabla\phi b} \qquad \text{(A9.5)}$$

or $\dot{\underline{x}} = [\, I - \frac{b \ \nabla\phi}{\nabla\phi \ b}]A\underline{x}$ on $\phi(\underline{x}) = 0$

$$\dot{\underline{x}} = [\, I - \frac{bd^T}{d^T b} \,]\, A\underline{x} = \hat{A}\underline{x} \qquad \text{(A9.6)}$$

Equation A9.6 is a linear equation.

If phase coordinates are used, sliding motions are described simply by the (n-1) order differential equations in x_1

i.e. $\phi(\underline{x}) = \phi\,(x_1, \dot{x}_1, \ , \ \ldots, \ x_1^{(n-1)}) = 0$ (A9.7)

The continuity condition on ϕ requires that it contains at most the (n-1) derivatives of x_1.

If in addition to $|\nabla\phi A\underline{x}| < |\nabla\phi b|$ and $\nabla\phi b > 0$ the trajectories intersecting the switching surface; points on this surface where this condition holds have been named 'starting points'.

If both $\nabla\phi A\underline{x}$ and $\nabla\phi b$ are zero, then $\ddot{\phi} = 0$ from equation A9.3 must be examined to determine motion in the neighbourhood of $\phi = 0$.

In conclusion the motions of the equation A9.3 based on sgn ϕ have solutions everywhere, and if $\nabla\phi b \leq 0$ (no starting points) trajectories proceed in well defined directions at every point in the state space.

APPENDIX A10

MODIFICATIONS TO THE BASIC STRATEGY

Consider the situation depicted in Figure A10.1. The trajectory ABCO results from an initial condition in the region

$$\begin{aligned} x_1(\varepsilon x_1+x_2) &< 0 \\ x_1(x_1+bx_2\,|x_2|\,) &> 0 \end{aligned} \qquad \text{(A10.1)}$$

The state trajectory does not approach the sliding boundry locus directly, but first moves towards the switching line

$$\varepsilon x_1+x_2 = 0 \qquad \text{(A10.2)}$$

From initial conditions in the region

$$\begin{aligned} x_1(x_1+\tfrac{1}{2}bx_2\,|x_2|\,) &> 0 \\ x_1(x_1+bx_2\,|x_2|\,) &< 0 \end{aligned} \qquad \text{(A10.3)}$$

we obtain the trajectory DEFGO. We see that the state trajectory crosses the sliding boundry locus at point E before reaching the switching line A10.2 at point F. The state then moves to point G on the sliding boundry locus and along this locus to the origin.

The respective alternative paths AB'CO from the initial conditions in the region A10.1 and DEGO from the initial conditions A10.2 result from a modified strategy. This modified strategy ensures that the state trajectory for initial conditions, through the state space, approaches the

sliding boundry locus directly and then remains on the locus. The time taken to reach the origin is greatly reduced.

The modified strategy also resets the control parameter q whenever a sudden disturbance gives rise to a new set of initial conditions.

The modified adaptive controller works in the following way: The control is given by

$$u = \text{sgn}(-qx_1-x_2) \quad q \geq 0 \qquad \text{(A10.4)}$$

and the switching line is from A10.4

$$qx_1+x_2 = 0 \qquad \text{(A10.5)}$$

For a state point in the second or fourth quadrants of the x_1-x_2 space i.e. the regions where

$$x_1x_2 < 0 \qquad \text{(A10.6)}$$

The modified adaptive controller carries out the following steps consecutively.

Step (i): The switching line is rotated until it passes through the current state point.

Step(ii): The controller tests for sliding at this point.

Step(iii): If sliding occurs the switch line is rotated further, to be just ahead of the state point (q is reset in accordance with equation 4.5.5)

Step (iv): If sliding does not occur, the switch line is kept fixed until sliding recurs (or until step(v) below causes step (i) to rotate the switch line)

Step(v) : An auxiliary switching line

$$Q\,x_1(t) + x_2(t) = 0 \qquad \text{(A10.7)}$$

is continuously rotated so as to pass through the state point $(x_1(t), x_2(t))$. If the inequality

$$q \leq Q < q(1+\epsilon) \qquad \text{(A10.8)}$$

does not hold, then we reset the value of the control parameter q to that of the auxiliary parameter Q

$$q = Q \qquad \text{(A10.9)}$$

i.e. rotate the switching line until it passes through the current state point (this initiates step (i)).

For state points in the quadrants where

$$x_1 x_2 \geq 0 \qquad \text{(A10.10)}$$

the time-optimal control is, for $x_2 \neq 0$

$$u = \text{sgn}\,(-x_2) \qquad \text{(A10.11)}$$

and for $x_2 = 0$

$$u = \text{sgn}\,(-x_1) \qquad \text{(A10.12)}$$

The adaptive strategy, steps (i) to (iv) and step(v), is not applied in this region; instead the optimal control A10.11 or A10.12 is used. The optimal control drives the state into the region

$$x_1 x_2 < 0 \qquad \text{(A10.13)}$$

from all points satisfying A10.10.

For a complete analysis of the modified control strategy see Zinober[5].

When the state space is bounded, the initial value of q can be increased as follows:

The parameter ε can then be chosen to be

$$= \frac{1}{b_{max} \, |x_2|_{max}} \qquad \text{(A10.14)}$$

where b_{max} is the maximum expected plant parameter and $|x_2|_{max}$ is the largest expected value of $|x_2|$.

Comparing A10.14 with 4.3.8 it is seen that the initial position of the switch line A10.2 lies wholly within the sliding region (see Figure A10.2).

The settling time from initial conditions in the regions A10.1 and A10.3 is considerably reduced as the time taken on the respective paths ABC and EFG See Figure A10.1 is lessened.

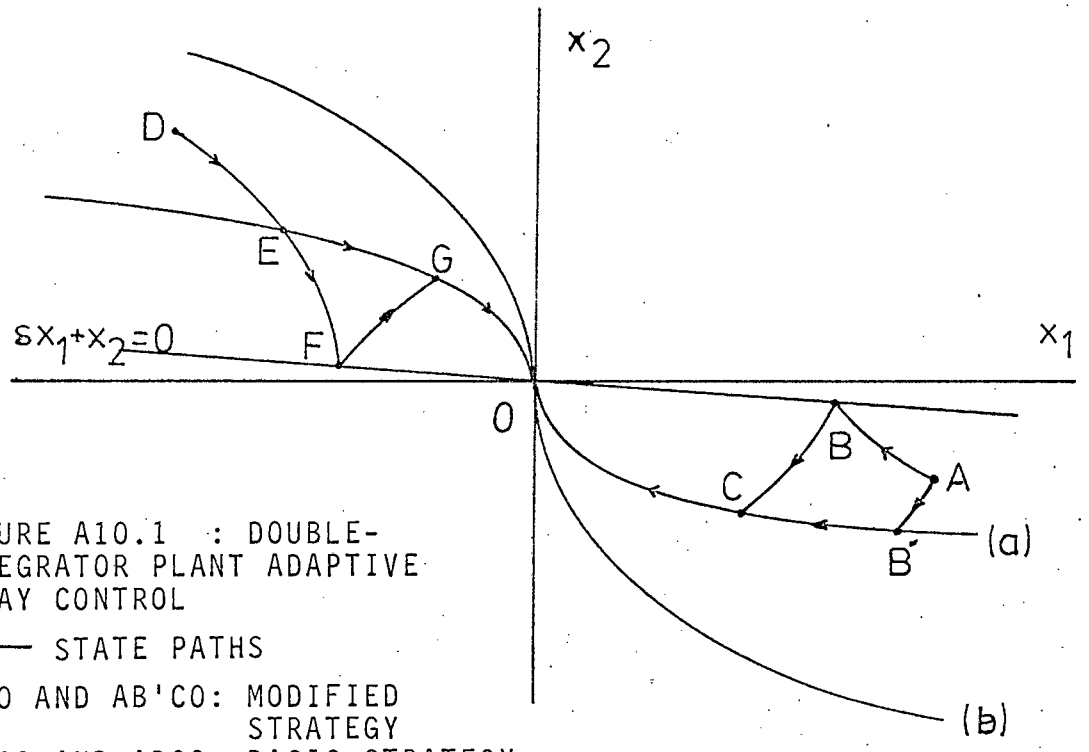

FIGURE A10.1 : DOUBLE-INTEGRATOR PLANT ADAPTIVE RELAY CONTROL

⟶ STATE PATHS

DEGO AND AB'CO: MODIFIED STRATEGY

DEFGO AND ABCO: BASIC STRATEGY

(a) $x_1+bx_2|x_2| = 0$

(b) $x_1+\frac{1}{2}bx_2|x_2| = 0$

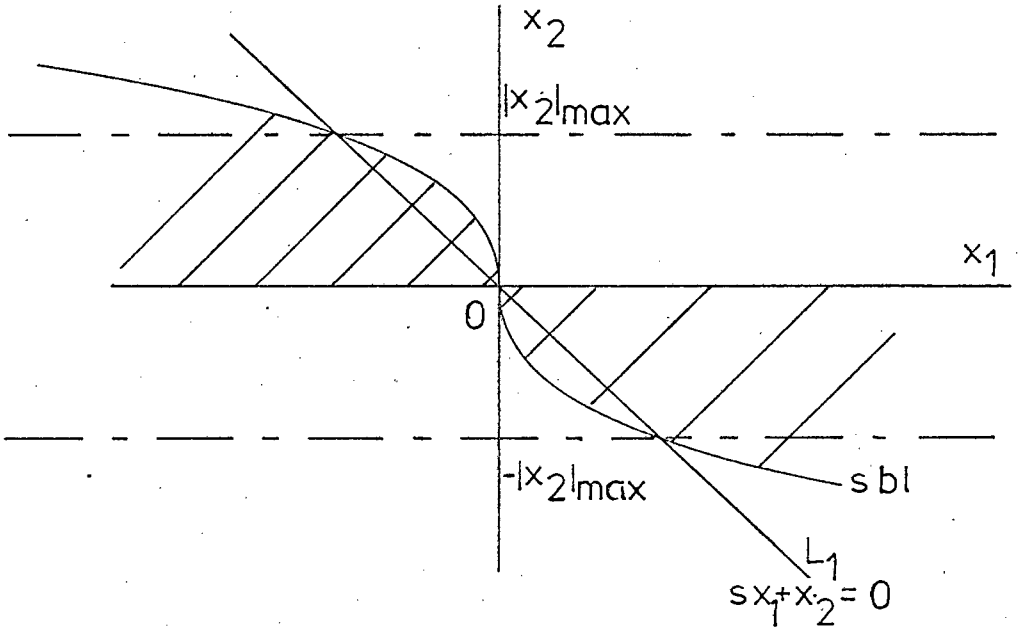

FIGURE A10.2 : BASIC ADAPTIVE CONTROL, DOUBLE INTEGRATOR PLANT

$$s = \frac{1}{b_{max}|x_2|_{max}}$$

Sliding Region 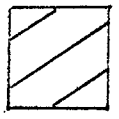

sbl - sliding boundry locus

APPENDIX A11

BASIC ADAPTIVE RELAY CONTROL STRATEGY OF TRIPLE-INTEGRATOR PLANTS

The triple-integrator plant is described by the equations:

$$\dot{x}_1 = x_2$$

$$\dot{x}_2 = x_3 \qquad \text{(A11.1)}$$

$$\dot{x}_3 = \frac{u}{b} \qquad (|u| \leq 1)$$

where the plant parameter b (= constant > 0) is assumed unknown or only partially known.

The basic adaptive controller has the linear switching function (see Figure A11.1).

$$u = \text{sgn}(-q^2 x_1 - 2dqx_2 - x_3) \qquad \text{(A11.2)}$$

$$(q > 0,\ d = \text{constant} \geq \tfrac{2}{3}2^{\frac{1}{2}})$$

and the switching plane is from A11.2

$$q^2 x_1 + 2dqx_2 + x_3 = 0 \qquad \text{(A11.3)}$$

At time, t=0, the control parameter q is set to the value

$$q = \varepsilon \qquad \text{(A11.4)}$$

Initially ε is small and the initial equation of the switching plane is, from A11.3 and A11.4

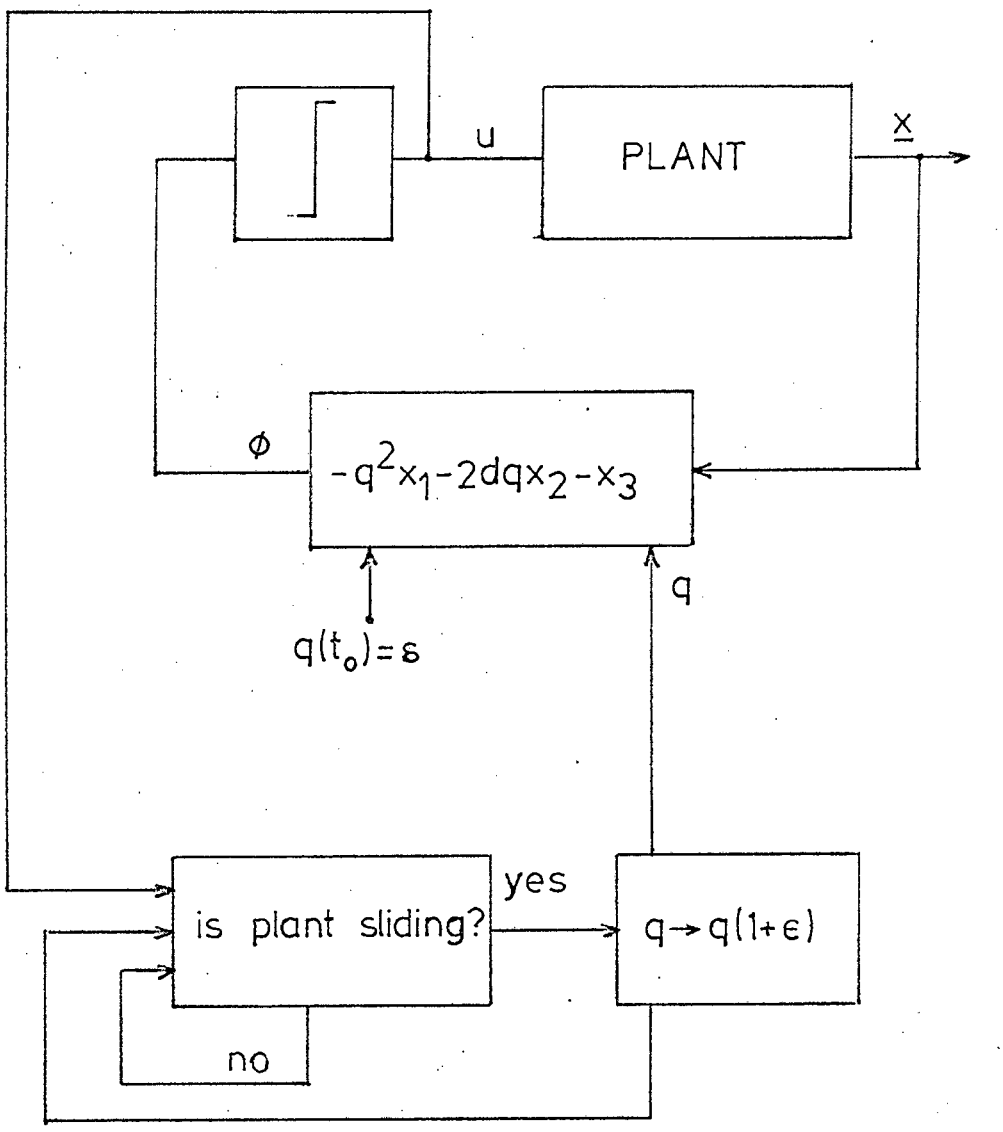

FIGURE A11.1 : BASIC ADAPTIVE CONTROL STRATEGY. THIRD ORDER PLANT

$\epsilon > 0 \quad s > 0$

$$\varsigma^2 x_1 + 2d\ \varsigma\ x_2 + x_3 = 0 \qquad \text{(A11.5)}$$

The parameter q is subsequently continually adjusted according to the following rule (the rule is identical to that of the second-order plant, except that we are rotating a plane and not a line):

If sliding motion occurs, the current switching plane is rotated to be just ahead of the state point, i.e. the control parameter is increased to the value

$$q(t+) = q(t)(1 + \epsilon) \quad (\epsilon > 0) \qquad \text{(A11.6)}$$

where ϵ is a small positive number.

There are several possible ways of rotating the plane (A11.3). By arbitrarily choosing the damping factor of the sliding motion d, to be constant (subject to the constraint $d \geq {}^{2}/_{3}\ 2^{\frac{1}{2}}$ we specify a particular mode of rotation. If the plant is not sliding on the current switch plane A11.3, the switch phase is kept fixed, i.e. the value of q remains unchanged. Ideally ς and ϵ are vanishingly small.

It can only be stated that the time taken to reach the origin is finite and the state trajectory approaches the state origin on a certain sliding boundry surface.

APPENDIX A12

ANALOGUE AND HYBRID ADAPTIVE RELAY CONTROL

A12.1 Analogue Computer Implementation of Adaptive Relay Control and Sliding Motion Detection

Figure A12.1.1 illustrates a block diagram of a double integrator plant. The operation of the sliding motion detector is as follows:

M_1 is a multiplier such that its output to an input u, is $\frac{u^2}{10} = 0.25$ provided $|u| = 5$.

For $|u| = 5$, the output of the summer S_2 is positive and the switch R_2 provides drive to the integrator I_3. Therefore $q(t)$ increases with time. As soon as a stage is reached where the state trajectory crosses the sliding boundry locus, sliding commences and $|u| < 5$. Hence $\frac{u^2}{10} < .25$ and the output of R_2 is switched to zero. This immediately holds the integrator I_3 at its current value of $q(t)$ (note the slew rate of the switching line is controlled by $\dot{q}_o$). The state trajectory then recrosses the sliding boundry locus and proceeds to the state origin along this locus.

The detection of sliding motion for the hybrid simulation (see A12.2) was modified as indicated in

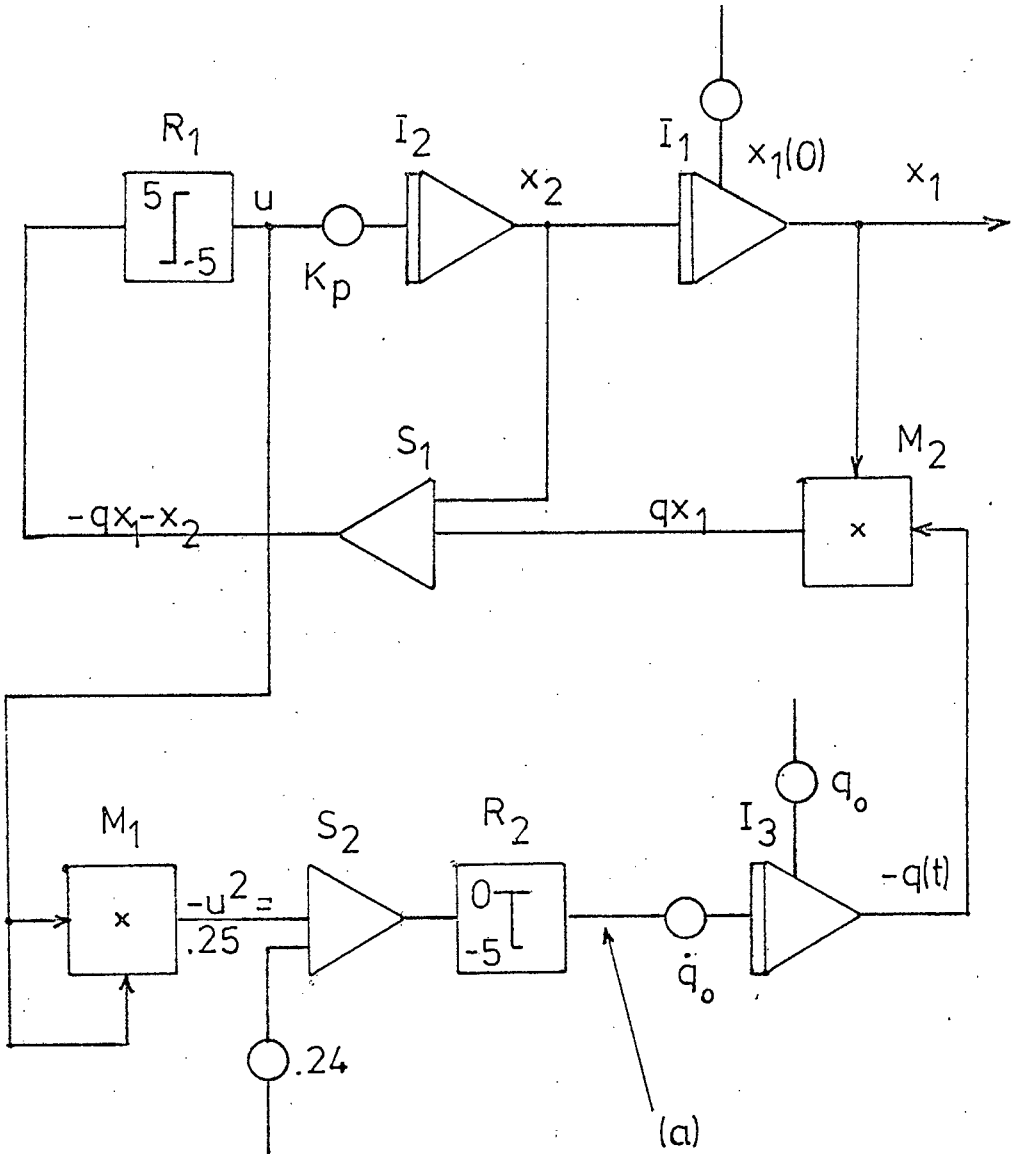

FIGURE A12.1.1 : BLOCK DIAGRAM OF A DOUBLE INTEGRATOR PLANT WITH ADAPTIVE RELAY CONTROL

(a) Output = 0 for $u^2 < .24$ or output =5 for $u^2 > .24$

Figure A12.1.2. Here a diode limited integrator is used (to prevent the amplifier from going into saturation) and the potentiometer P is normally set at unity as in (a). (b) Represents the rapid oscillations of sliding motion at the input to the integrator and (c) represents the output of the integrator. Since the output is an averaged or 'smoothed' input, sufficient time is available for the output of the integrator to be sampled and processed by the minicomputer.

A12.2 Diagram of Hybrid System and Programs for a Second and Third Order Plant

The block diagram for a second-order system is shown in Figure A12.2.1.

Below are the programs used in the hybrid simulation.

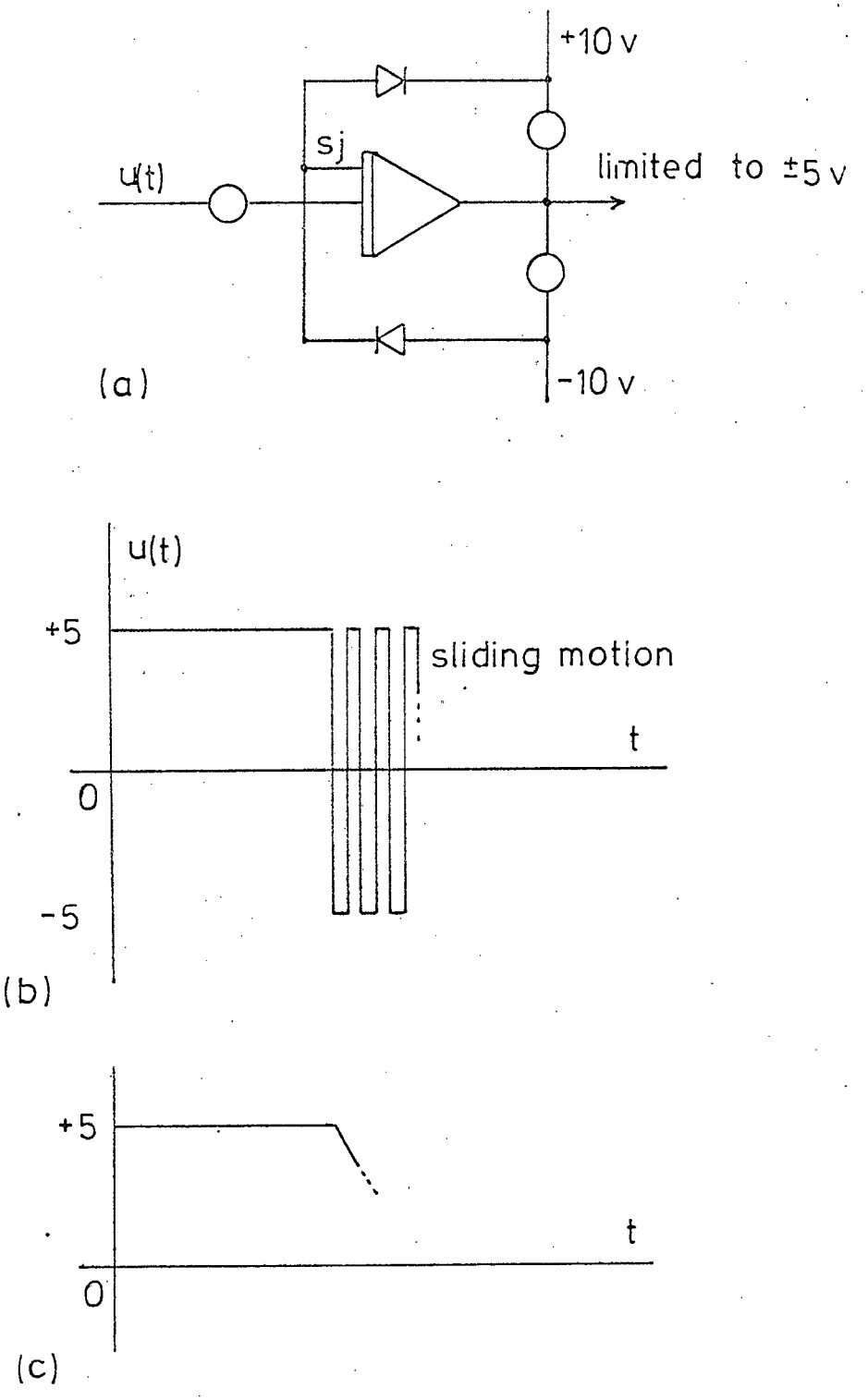

FIGURE A12.1.2 : SLIDING MOTION DETECTOR FOR HYBRID SIMULATION

(a) DIODE LIMITED INTEGRATOR(TO PREVENT SATURATION OF AMPLIFIER)
(b) INPUT TO INTEGRATOR
(c) OUTPUT OF INTEGRATOR

PROGRAMME FOR SECOND-ORDER PLANT WITH ADAPTIVE RELAY CONTROLLER

```
LIST
10  READ N1,N2
12  READ P1,P2
15  DATA  500, 1.00000E-05
17  DATA  1.00000E-02, 1.00000E-02
20  LET A4= 4
25  LET A3= 3
30  LET A2= 2
35  LET A1= 1
40  LET U0= 0
45  CALL   ADC1,A4,S4
46  IF S4> 20 THEN 50
47  GOTO 45
50  LET U1= 0
51  CALL   DTOA,U0,U1
54  LET Q= 0
55  FOR D= 1.00000E-02 TO N1 STEP N2
60  LET Q=Q+D
65  CALL   ADC1,A1,X1
70  LET X1=X1* 10/ 2047
75  CALL   ADC1,A2,X2
80  LET X2=X2* 10/ 2047
82  IF ABS(X1)<=P1 THEN 200
85  LET V=Q*X1+X2
90  LET U1= 1024*SGN(-V)
95  CALL   DTOA,U0,U1
100  CALL   ADC1,A3,U2
105  LET U2=U2* 10/ 2047
110  LET U3=U2*U2
115  IF U3< 23 THEN 100
120  NEXT D
125  GOTO 210
200  IF ABS(X2)<=P2 THEN 210
205  GOTO 85
210  LET U1= 0
215  CALL   DTOA,U0,U1
220  END
235  CALL   DTOA,U0,U1
240  END
```

PROGRAMME FOR THIRD-ORDER PLANT WITH ADAPTIVE RELAY CONTROLLER

```
LIST
10   READ N1,N2
12   READ P1,P2
15   DATA  500, 1.00000E-06
17   DATA  1.00000E-02, 1.00000E-02
20   LET A4= 4
25   LET A3= 3
30   LET A2= 2
35   LET A1= 1
40   LET U0= 0
42   LET A0= 0
45   CALL    ADC1,A4,S4
46   IF S4> 20 THEN 50
47   GOTO 45
50   LET U1= 0
51   CALL    DTOA,U0,U1
54   LET Q= 0
55   FOR D= 1.00000E-02 TO N1 STEP N2
60   LET Q=Q+D
62   CALL    ADC1,A3,X3
63   LET X3=X3* 10/ 2047
65   CALL    ADC1,A1,X1
70   LET X1=X1* 10/ 2047
75   CALL    ADC1,A2,X2
80   LET X2=X2* 10/ 2047
82   IF ABS(X1)<=P1 THEN 200
85   LET V=Q*Q*X1+ 2*Q*X2+X3
90   LET U1= 1024*SGN(-V)
93   CALL    DTOA,U0,U1
100   CALL    ADC1,A0,U2
103   LET U2=U2* 10/ 2047
110   LET U3=U2*U2
115   IF U3< 23 THEN 100
120   NEXT D
125   GOTO 210
200   IF ABS(X2)<=P2 THEN 210
205   GOTO 85
210   LET U1= 0
215   CALL    DTOA,U0,U1
220   END
235   CALL    DTOA,U0,U1
240   END
```

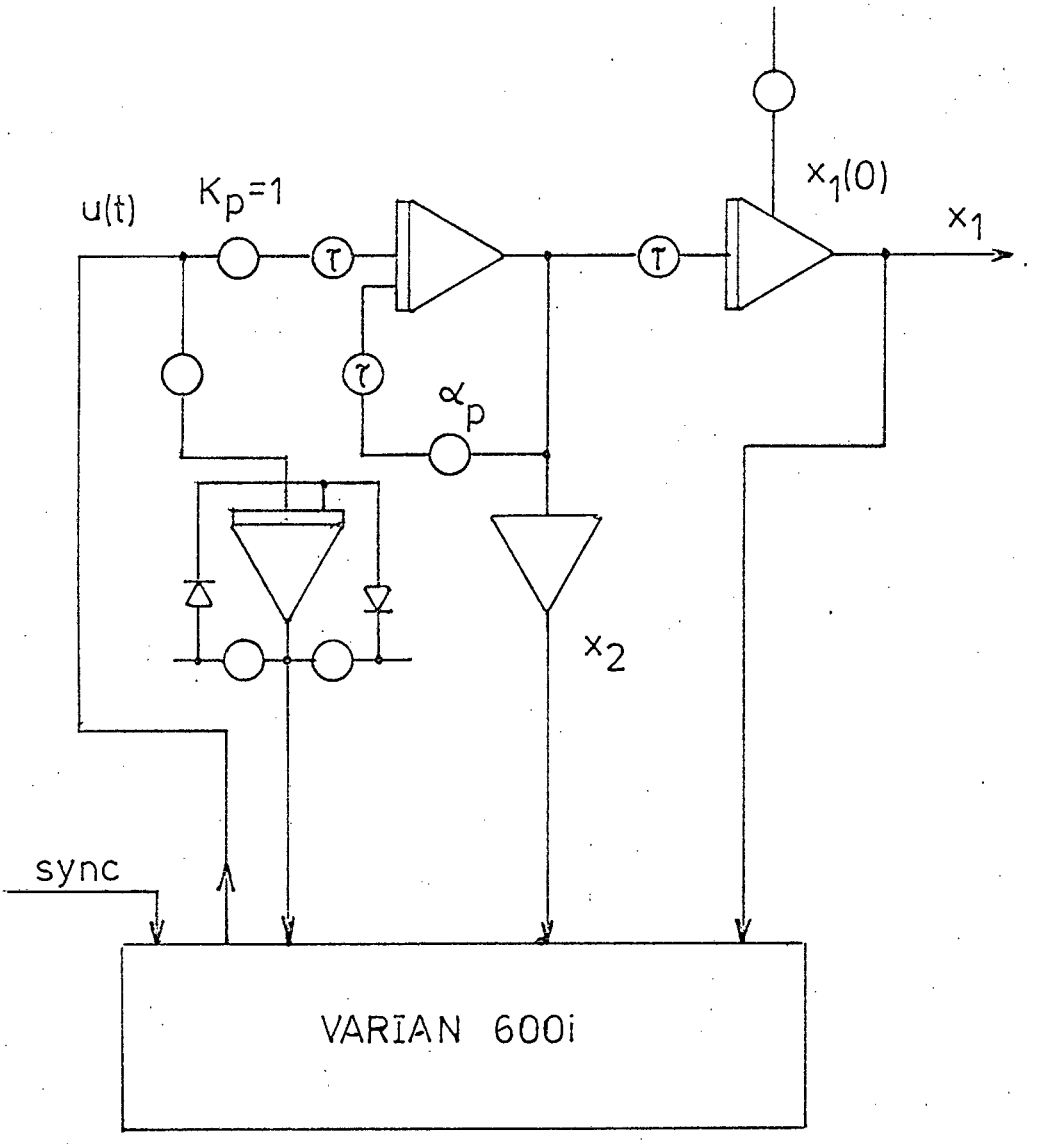

FIGURE A12.2.1 : BLOCK DIAGRAM OF SECOND-ORDER SYSTEM FOR ADAPTIVE RELAY HYBRID CONTROL

NOTE: τ IS A SCALE FACTOR FOR THE INTEGRATORS

APPENDIX A13

SECOND ORDER NOMINAL-$\underline{v}$ CONTROL SYSTEMS

A13.1 Properties of Second Order Nominal-$\underline{v}$ Control Systems

The eigenvalues λ_1, λ_2 of the matrix A are assumed real and non-positive. We can assume the eigenvalue ordering $0 \geq \lambda_2 \geq \lambda_1$ (λ is -ve) (A13.1.1)

The eigenvalue ratio α is defined as

$$\alpha = \frac{\lambda_1}{\lambda_2} \qquad \text{(A13.1.2)}$$

which with A13.1.1 implies that $\alpha \geq 1$.

In terms of the $\underline{x}$ state vector, the system equation is

$$\begin{bmatrix} \dot{x}_1 \\ \dot{x}_2 \end{bmatrix} = \begin{bmatrix} 0 & 1 \\ -\frac{\lambda_1^2}{\alpha} & \lambda_1\left(\frac{\alpha+1}{\alpha}\right) \end{bmatrix} \begin{bmatrix} x_1 \\ x_2 \end{bmatrix} + \begin{bmatrix} 0 \\ \frac{1}{a} \end{bmatrix} u \qquad \text{(A13.1.3)}$$

Application of the nominal-$\underline{v}$ control method yields, from 5.4.7 and 5.4.3 nominal eigenvalues satisfying

$$\lambda_{2(nom)} = \lambda_c = \frac{1}{3}(\lambda_1 + \lambda_2) = \frac{\lambda_1}{3}\left(\frac{\alpha+1}{\alpha}\right) \qquad \text{(A13.1.4)}$$

$$\lambda_{1(nom)} = 2\lambda_c = \frac{2}{3}(\lambda_1 + \lambda_2) = \frac{2\lambda_1}{3}\left(\frac{\alpha+1}{\alpha}\right)$$

For the nominal system, the transformation from the $\underline{x}$ to the $\underline{v}$ state vector (i.e. the nominal-$\underline{v}$ state transformation) is, from 5.4.10 and 5.4.12.

$$v_1 = x_1$$

$$v_2 = \frac{-2\lambda_1}{3}\left(\frac{\alpha+1}{\alpha}\right) x_1 + x_2 \qquad \text{(A13.1.5)}$$

i.e. $\underline{v} = T_{(nom)}\,\underline{x}$

In terms of the nominal $\underline{v}$ state vector the system equation is

$$\dot{\underline{v}} = T_{(nom)}\, A\, T^{-1}_{(nom)}\, \underline{v} + T_{(nom)}\, Bu \qquad \text{(A13.1.6)}$$

which from A13.1.3 and A13.1.5, may be shown to be

$$\begin{bmatrix} \dot{v}_1 \\ \dot{v}_2 \end{bmatrix} = \begin{bmatrix} \frac{2\lambda_1}{3}\left(\frac{\alpha+1}{\alpha}\right) & 1 \\ \frac{\lambda_1^2}{9\alpha^2}(\alpha-2)(2\alpha-1) & \frac{\lambda_1}{3}\left(\frac{\alpha+1}{\alpha}\right) \end{bmatrix} \begin{bmatrix} v_1 \\ v_2 \end{bmatrix} + \begin{bmatrix} 0 \\ \frac{1}{a} \end{bmatrix} u \qquad \text{(A13.1.7)}$$

The nominal-$\underline{v}$ control law may now be written the same form as that of the double integrator plant, viz.

$$u = u(\underline{v}) = -\text{sgn}\left(v_1 + \frac{a}{2} v_2 \,|v_2|\right) \qquad \text{(A13.1.8)}$$

when (a) $\lambda_1 = \lambda_2 = 0$ (the double integrator plant)

and

(b) $\lambda_1 = 2\lambda_2$ (when $\alpha = 2$) equation A13.1.8 represents the exact time optimal control law. In other cases the control is sub optimal and the nominal-$\underline{v}$ control system has the following properties (see Ryan[6] for a detailed analysis).

1. For all admissible values of $\alpha < 2$ the nominal-$\underline{v}$ switching curve is composed entirely of regular switch points
2. For all values of $\alpha > 2$ a sliding segment bounded by

$$|v_1| = |x_1| = \frac{18\alpha^2}{\alpha\lambda_1^2(\alpha-2)(2\alpha-1)}$$ exists on the nominal-$\underline{v}$ switching curve. Points of the switching curve interior to this segment are sliding points, all exterior points being regular switch points.
3. Forvalues of $\alpha > 2$ all state trajectories reach and remain on the sliding segment of the nominal-$\underline{v}$ switching curve after at most one regular switch.
4. For values of $\alpha > 2$ the Time T to the state origin from an arbitrary point (v_1^o, v_2^o) on the sliding segment of the nominal-$\underline{v}$ switching curve is given by

$$T = \frac{-3\alpha}{\lambda_1(\alpha+1)} \text{ Ln } \left(1 - \frac{\alpha\lambda_1(\alpha+1)}{3\alpha} |v_2^o|\right) \quad \text{(A13.1.9)}$$

(For an account of regular switching and sliding motion see Appendix A9).

From property 1 it may be established that, for admissible values of $\alpha < 2$ (i.e. $1 \leq \alpha \leq 2$), the state point follows a regular switching trajectory to the state origin with successive switches alternating between the second and fourth quadrants of the $\underline{x}$ state plane. Ryan[6] has showed that this overshoot motion

is highly damped and in general, the state point may be regarded as having reached the origin after the second of the theoretical infinity of switches.

From properties 2,3 and 4 it may be concluded that, under nominal-$\underline{v}$ control, the time to the origin from all initial states is finite for values of $\alpha > 2$. Every state trajectory terminates in a sliding path to the origin (with the exception of switchless trajectories, originating at points on the exact time-optimal switching curve, which follow a P or N path to the state origin and are thus precisely time-optimal trajectories)

This sliding path corresponds to a time-optimal path for the nominal system since the state point is constrained to remain on the nominal-$\underline{v}$ switching curve (i.e. the time-optimal switching curve for the nominal system).

Note: Trajectories in the state space having $u = +1$ are termed P-trajectories and similarly trajectories described with $u = -1$ are termed N-trajectories. Since $u = \text{sgn } \phi$, P-trajectories lie in that region of the state space where $\phi > 0$ and N-trajectories lie in the sub space $\phi < 0$.

A13.2 Examples of second order nominal-$\underline{y}$ control.

From A13.1.2 the state equations may be written as

$$\frac{dx_1}{dt} = x_2$$

$$\frac{dx_2}{dt} = -\frac{\lambda_1^2}{\alpha} x_1 + \lambda_1 \left(\frac{\alpha+1}{\alpha}\right) x_2 + \frac{u}{a} \qquad \text{(A13.2.1)}$$

Defining the set of normalized variables

$$t' = -\lambda_1 t; \quad x_1' = \lambda_1^2 a x_1; \quad x_2' = -\lambda_1 a x_2 \qquad \text{(A13.2.2)}$$

on substituting in A13.2.1 the normalized system equations become

$$\frac{dx_1'}{dt'} = x_2'$$

$$\frac{dx_2'}{dt'} = \frac{-x_1'}{\alpha} - x_2' \left(\frac{\alpha+1}{\alpha}\right) + u \qquad \text{(A13.2.3)}$$

Equations A13.2.3 imply that the transfer function between the scalar input u and the normalized output variable x_1' is given by

$$G(s) = \frac{1}{(s+1)(s+\frac{1}{\alpha})} \qquad \text{(A13.2.4)}$$

For the integrator plus lag plant the normalized form of A13.2.4 is assumed and the superscript ($'$) is omitted, also for the integrator plus lag $\alpha = \infty$. Hence for the integrator plus lag, the normalized values $\lambda_1 = -1$; $\lambda_2 = 0$; $a = 1$ are assumed (see equations A13.1.2 and A13.1.3) i.e. the plant transfer function is

$$G(s) = \frac{1}{s(s+1)} \qquad (A13.2.5)$$

The time-optimal switching curve, consisting of P and N paths heading to the state origin, may be shown to satisfy (see Appendix A6.2)

$$x_1 + x_2 - \mathrm{sgn}(x_2)\,\mathrm{Ln}(1+|x_2|) = 0 \qquad (A13.2.6)$$

Applying the nominal-$\underline{v}$ control method, from A1.4 the nominal eigenvalues are

$$\lambda_{1(nom)} = 2\lambda_c = -2/3$$
$$\lambda_{2(nom)} = \lambda_c = -1/3 \qquad (A13.2.7)$$

From A13.1.5 the nominal-$\underline{v}$ variables are given by

$$v_1 = x_1 \; ; \; v_2 = 2/3\, x_1 + x_2 \qquad (A13.2.8)$$

and from A1.8, the nominal-$\underline{v}$ switching curve satisfies

$$v_1 + \tfrac{1}{2} v_2 |v_2| = 0 \qquad (A13.2.9)$$

Through the implementation of equation A13.2.9, the difficulty in synthesizing the logarithmic function of A13.2.6 may be avoided.

For the double-pole plant (two lags) $\alpha = 1$, the normalized values $\lambda_1 = -1$; $\lambda_2 = -1$; $a = 1$ are assumed, i.e. the plant transfer function is

$$G(s) = \frac{1}{(s+1)^2} \qquad (A13.2.10)$$

The time-optimal switching curve for this plant may be shown to satisfy

$$\mathrm{sgn}(x_1+x_2).(1+|x_1+x_2|).\mathrm{Ln}(1+|x_1+x_2|)-x_2 = 0 \qquad \text{(A13.2.11)}$$

Application of the nominal-$\underline{v}$ control method yields, from A13.1.4, nominal eigenvalues

$$\lambda_{1(nom)} = 2\lambda_c = -4/3$$

$$\lambda_{2(nom)} = \lambda_c = -2/3 \qquad \text{(A13.2.12)}$$

From A13.1.5, the nominal-$\underline{v}$ state variables are

$$v_1 = x_1; \quad v_2 = 4/3\, x_1 + x_2 \qquad \text{(A13.2.13)}$$

and again, the nominal-$\underline{v}$ switching curve satisfies

$$v_1 + \tfrac{1}{2} v_2 |v_2| = 0 \qquad \text{(A13.2.14)}$$

Thus again equation A13.2.11 can be superceded by a set of simpler functions, viz that of equations A13.2.13.

APPENDIX A14

ANALOGUE AND HYBRID V CONTROL

A14.1 V Control equations and analogue computer block diagram.

The transfer function of the second order-plant used is

$$G_p(s) = \frac{1}{s(s+.1)} \qquad \text{(A14.1.1)}$$

Hence the eigenvalues are $\lambda_1 = -.1$ and $\lambda_2 = 0$.

From equations A13.1.4

$$\lambda_{2(nom)} = \lambda_c = 1/3\ (-.1+0) = -.1/3 \qquad \text{(A14.1.2)}$$

$$\lambda_{1(nom)} = 2\lambda_c = 2/3(-.1+0) = -.2/3$$

$$\text{therefore } \alpha_{nom} = \frac{-.2/3}{-.1/3} = 2 \qquad \text{(A14.1.3)}$$

therefore from equations A13.1.5

$$v_1 = x_1$$

$$v_2 = -2/3\ (-\tfrac{.2}{3})(\tfrac{2+1}{2})\ x_1 + x_2$$

$$\therefore v_2 = \tfrac{.2}{3}\ x_1 + x_2 \qquad \text{(A14.1.4)}$$

The drive signal u is given by equation A13.1.8 and is

$$u = u(\underline{v}) = -\operatorname{sgn}(v_1 + \tfrac{1}{2}\ v_2\ |v_2|) \qquad \text{(A14.1.5)}$$

where v_1 and v_2 are the equations A14.1.4.

The block diagram for a second order plant with the above control equations is illustrated in Figure A14.1.1

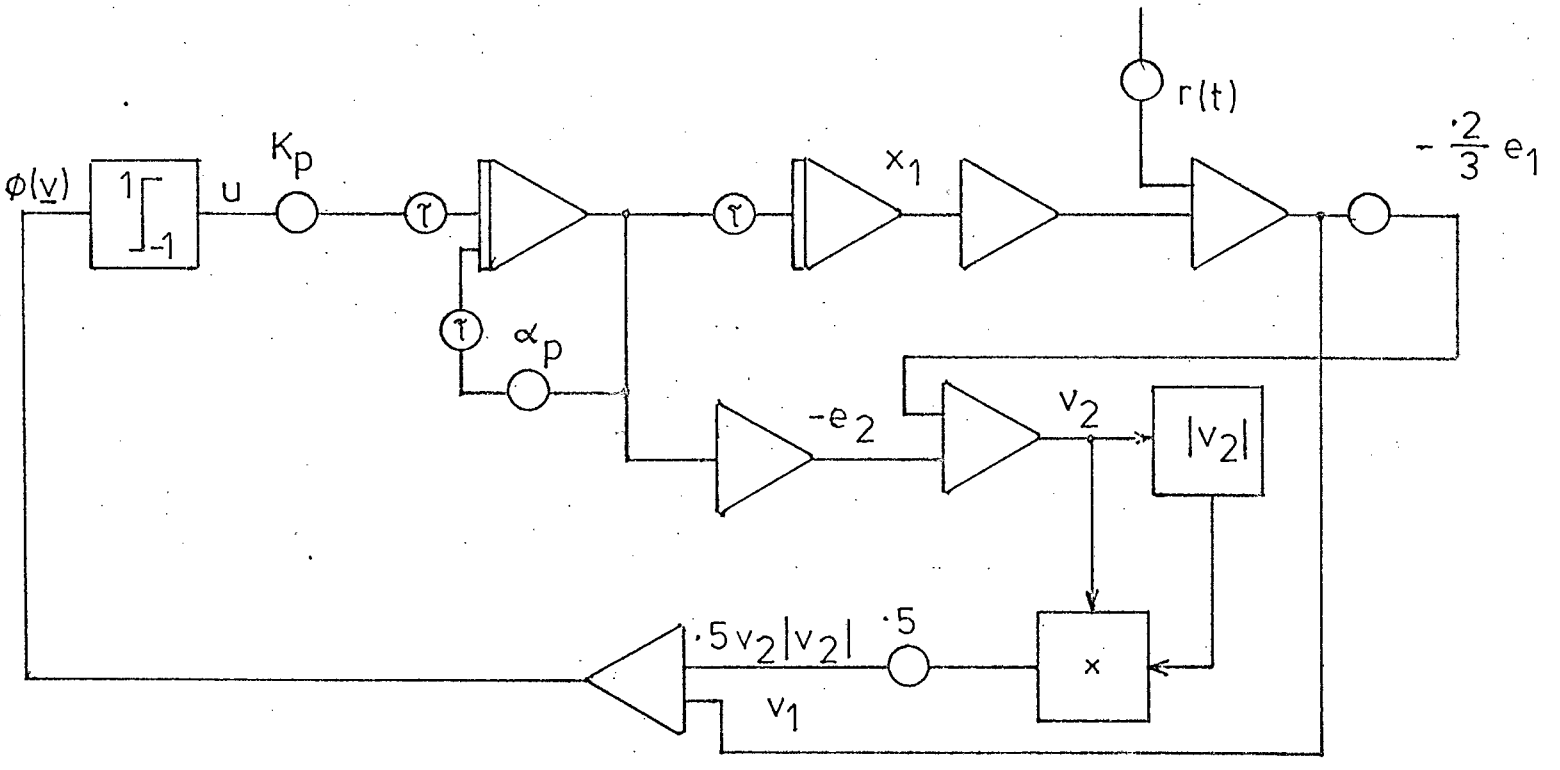

FIGURE A14.1.1 : ANALOGUE COMPUTER BLOCK DIAGRAM OF THE $\underline{V}$ TRANSFORMATION CONTROL

Note: The error and error rate state-variables are used, as the reference is not an 'initial condition' but an external reference step function.

A14.2 Program for hybrid control of a second-order plant and system block diagram.

Below is a program for the hybrid control of a second-order plant.

HYBRID CONTROL OF A SECOND ORDER PLANT WITH
V TRANSFORMATION CONTROL EQUATIONS

```
LIST
10  LET P1= 1.00000E-02
15  LET P2= 1.00000E-02
25  LET A1= 1
30  LET A2= 2
35  LET A3= 3
40  LET A0= 0
45  LET U1= 0
50  CALL    ADC1,A3,S3
55  IF S3> 20 THEN 100
60  GOTO 50
100  CALL    ADC1,A1,X1
105  LET X1=X1* 10/ 2047
110  CALL    ADC1,A2,X2
115  LET X2=X2* 10/ 2047
120  LET V1=X1
125  LET V2=X2+X1* 2/ 30
130  LET W2=ABS(V2)
135  LET U=-1024*SGN(V1+V2*W2/ 2)
140  CALL    DTOA,U1,U
145  IF ABS(X1)<=P1 THEN 155
150  GOTO 100
155  IF ABS(X2)<=P2 THEN 200
160  GOTO 100
200  LET U= 0
205  CALL    DTOA,U1,U
210  CALL    ADC1,A1,X1
215  LET X1=X1* 10/ 2047
220  CALL    ADC1,A0,T
225  LET T=T* 10/ 2047
230  LET T1=T/ 5.00000E-02
235  PRINT X1,T1
240  END
```

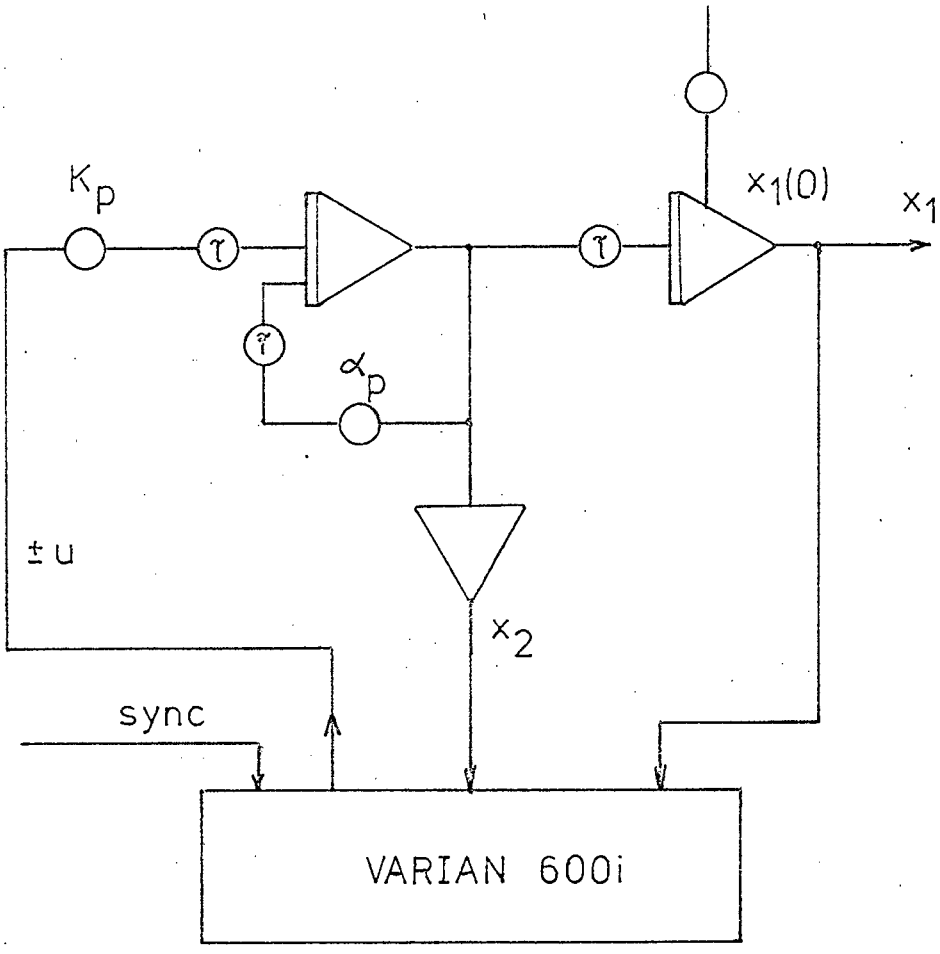

FIGURE A14.2.1 : BLOCK DIAGRAM OF HYBRID SECOND-ORDER SYSTEM

APPENDIX A15

THIRD-ORDER HYBRID V CONTROL

A15.1 The derivation of the control law equations for a third-order plant.

The plant considered has a transfer function

$$G_p(s) = \frac{K_p}{s(s^2+\alpha_p s+1)} \qquad \text{(A15.1.1)}$$

when $K_p = \frac{1}{a} = 1$ (nominal) and $0 < \alpha_p < 1$.

From equations 5.4.10 and 5.4.13

$\underline{v} = T_{nom}\,\underline{x}$ and

$$T_{nom} = \begin{bmatrix} 1 & 0 & 0 \\ -\lambda_{1(nom)} & 1 & 0 \\ \lambda_{1(nom)}\,\lambda_{2(nom)} & -(\lambda_{1(nom)}+\lambda_{2(nom)}) & 1 \end{bmatrix} \qquad \text{(A15.1.2)}$$

For a step input $\frac{u}{s}$, the system equations can be written as

$$\begin{bmatrix} \dot{x}_1 \\ \dot{x}_2 \\ \dot{x}_3 \end{bmatrix} = \begin{bmatrix} 0 & 1 & 0 \\ 0 & 0 & 1 \\ 0 & -1 & -\alpha_p \end{bmatrix} \begin{bmatrix} x_1 \\ x_2 \\ x_3 \end{bmatrix} + \begin{bmatrix} 0 \\ 0 \\ K_p \end{bmatrix} u \qquad \text{(A15.1.3)}$$

The eigenvalues of A15.1.3 are merely

$$\lambda(\lambda^2 + \alpha_p \lambda + 1) = 0 \quad \text{or}$$

$$\lambda_3 = 0,\ \lambda_2 = \frac{-\alpha_p}{2} + j\,(1-\frac{\alpha_p^2}{4})^{\frac{1}{2}},\quad \lambda_1 = \frac{-\alpha_p}{2} - j\,(1-\frac{\alpha_p^2}{4})^{\frac{1}{2}}$$

We select $\alpha_p = .4$; hence

$\lambda_3 = 0,\ \lambda_2 = -.2+j.98,\ \lambda_1 = -.2-j.98$

Step 1. We assume a nominal plant with nominal eigenvalues satisfying (from equations 5.4.7 and 5.4.8)

$\lambda_i = (4-i)\,\lambda_c \quad i=1,2,3 \quad \lambda_c = \text{constant} > 0$

$$\text{i.e. } \lambda_{1(nom)} = 3\lambda_c$$
$$\lambda_{2(nom)} = 2\lambda_c \qquad \text{(A15.1.4)}$$
$$\lambda_{3(nom)} = \lambda_c$$

Step 2. Sum of the eigenvalues = sum of actual eigenvalues

$$\sum_{i=1}^{3} \lambda_{i(nom)} = \sum_{i=1}^{3} \lambda_i$$

$$\text{i.e. } \lambda_c = \frac{1}{6}(\lambda_1 + \lambda_2 + \lambda_3) \qquad \text{(A15.1.5)}$$

Step 3. The implementing on the actual system the sub-optimal control law of the nominal series decomposed system ; $u = -\text{sgn}(\phi(\underline{v})$ (identical to that of

$\dot{x}_1 = x_2$, $\dot{x}_2 = x_3$ and $\dot{x}_3 = u/a$, and see Figure A15.1.1)

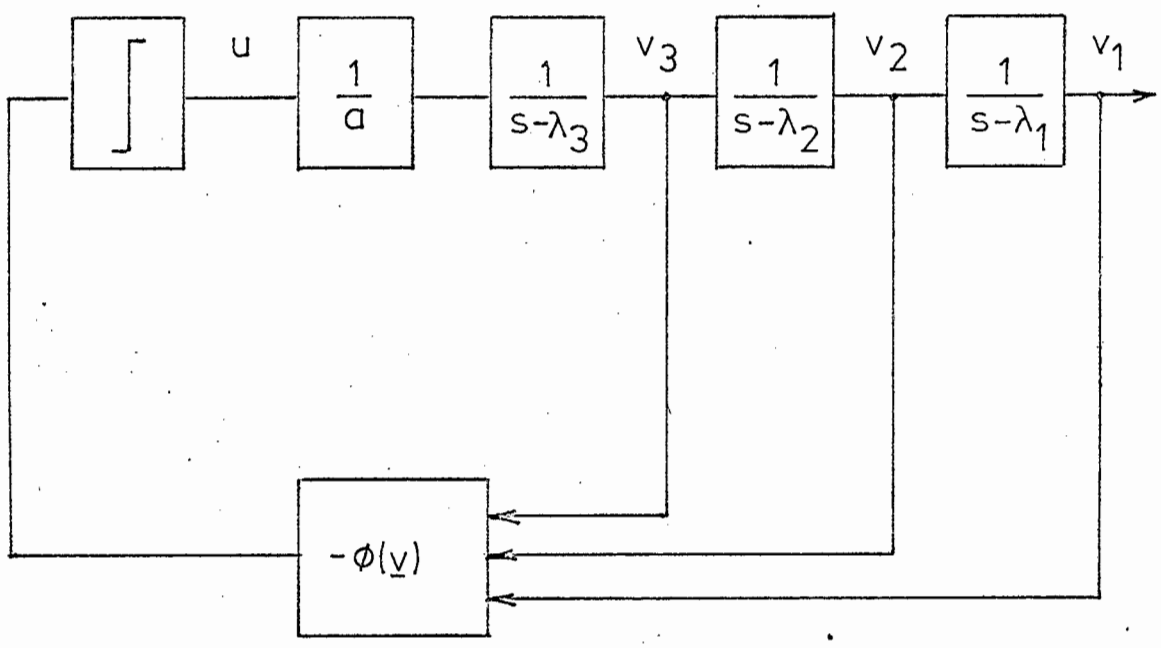

FIGURE 15.1.1 : SERIES DECOMPOSITION FOR A THIRD-ORDER PLANT

Step 4. Let $\underline{v} = T_{nom}\,\underline{x}$ where T_{nom} = A15.1.2

$$\text{Hence } T = \begin{bmatrix} 1 & 0 & 0 \\ -3\lambda_c & 1 & 0 \\ 6\lambda_c^2 & -5\lambda_c & 1 \end{bmatrix} \qquad \text{(A15.1.6)}$$

$$\text{Hence } \lambda_c = \frac{1}{6}\,(0-.2+j\ .98-.2-j\ .98)$$

$$= -\frac{.4}{6} = -\ .067$$

Hence

$$\lambda_{1(nom)} = 3\,\lambda_c = -.201$$

$$\lambda_{2(nom)} = 2\,\lambda_c = -.134$$

$$\lambda_{3(nom)} = \lambda_c = -.067$$

and from equation A15.1.6

$$\underline{v} = \begin{bmatrix} 1 & 0 & 0 \\ .201 & 1 & 0 \\ .0268 & .335 & 1 \end{bmatrix}$$

therefore $v_1 = x_1$

$$v_2 = .201\ x_1 + x_2$$

$$v_3 = .0268\ x_1 + .335\ x_2 + x_3 \qquad \text{(A15.1.7)}$$

The control input $u(\underline{v}) = -\text{sgn}\,(\phi(\underline{v}))$

$$= -\text{sgn}(U\,|\,U\,| + a\,V^3) \qquad \text{(A15.1.8)}$$

where $\frac{1}{a} = K_p = 1$ (nominal)

and $U = v_1 + a^2\,\frac{v_3^3}{3} + a v_2\,v_3\,\text{sgn}(v_3)$

$$V = v_2 + \frac{a v_3^2}{2}\text{sgn}\,(v_3) \qquad \text{(A15.1.9)}$$

and v_1, v_2 and v_3 take on the values of x_1, x_2 and x_3 in equations A15.1.7. In other words the plant states are sampled regularly and are transformed into the $\underline{v}$ variables by the steps 1 to 4. The control input is then given by equations A15.1.8 and A15.1.9.

A15.2 Program and block diagram for a third-order system.

Below is a program for $\underline{v}$ transformation control of a third order plant for a step initial condition. The block diagram follows on the next page.

PROGRAMME FOR THE CONTROL OF A THIRD-ORDER PLANT
USING THE V TRANSFORMED VARIABLES

```
LIST
 3  LET A= 1
 10  LET P= 5.00000E-02
 20  LET A1= 1
 25  LET A2= 2
 30  LET A3= 3
 35  LET A4= 4
 40  LET U0= 0
 45  CALL    ADC1,A4,S4
 50  IF S4> 20 THEN 60
 55  GOTO 45
 60  CALL    ADC1,A1,X1
 65  LET X1=X1* 10/ 2047
 70  CALL    ADC1,A2,X2
 75  LET X2=X2* 10/ 2047
 80  CALL    ADC1,A3,X3
 85  LET X3=X3* 10/ 2047
 90  LET W1= 2.68000E-02*X1+ .335*X2+X3
 95  LET W2=W1*W1
 100  LET W3=W2*W1
 105  LET W4=  .201*X1+X2
 110  LET U1=X1+(A*A*W3/ 3)+A*W4*W1*SGN(W1)
 115  LET U2=W4+A*W2*SGN(W1)/ 2
 120  LET U3=ABS(U1)
 125  LET U4=U2*U2*U2
 130  LET U=-204.7*SGN((U1*U3)+(A*U4))
 140  CALL    DTOA,U0,U
 145  IF ABS(X1)<=P THEN 155
 150  GOTO 60
 155  IF ABS(X2)<=P THEN 165
 160  GOTO 60
 165  IF ABS(X3)<=P THEN 180
 170  GOTO 60
 180  LET U= 0
 185  CALL    DTOA,U0,U

 190  PRINT X1,X2,X3
 200  END
```

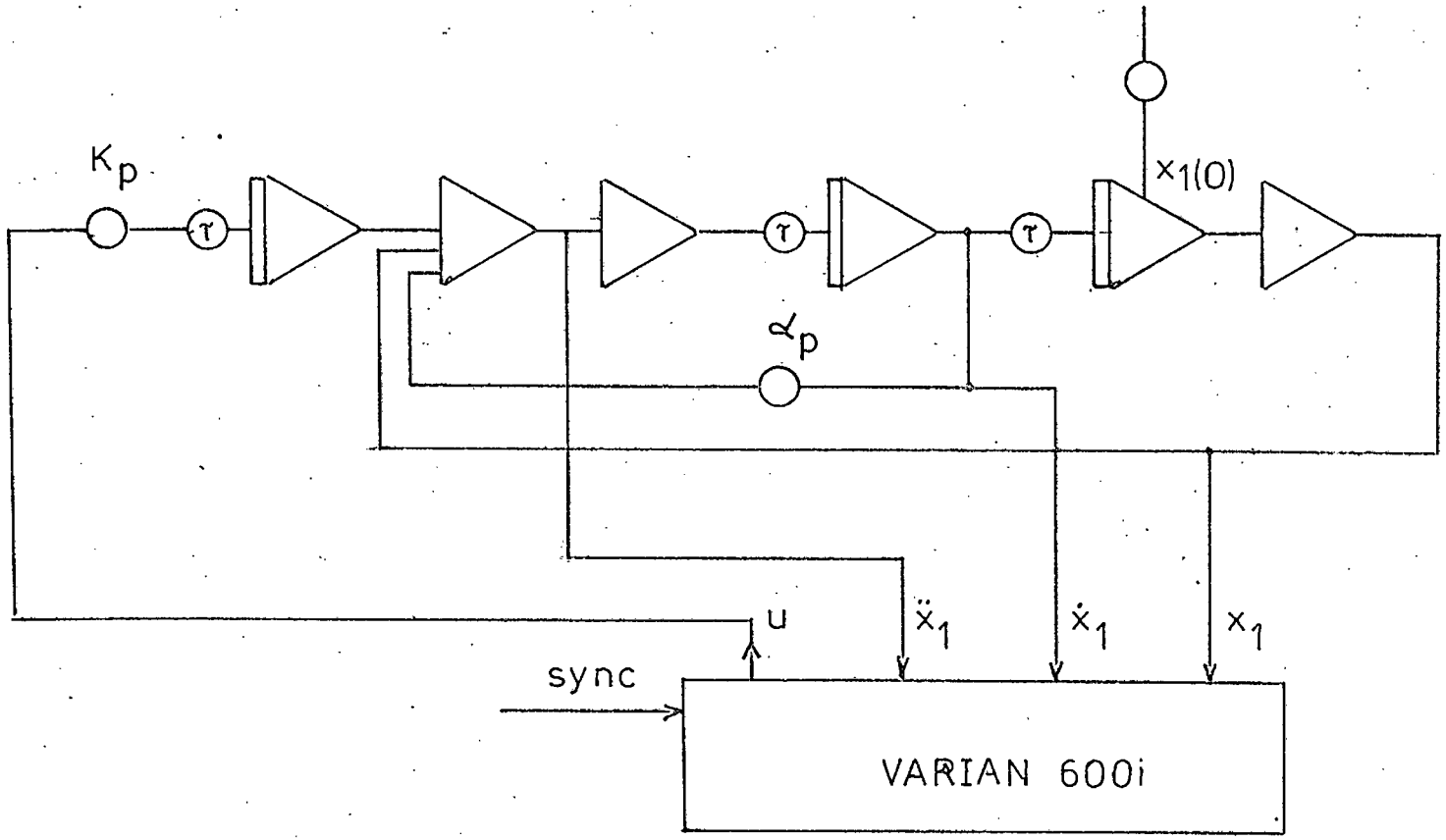

FIGURE 15.2.1 : BLOCK DIAGRAM OF THIRD-ORDER SYSTEM WHERE $G_p(s) = \frac{K_p}{s(s^2+\alpha_p s+1)}$. τ IS A SCALING FACTOR FOR THE RATE OF INTEGRATION